

# **Drug delivery to the bone-implant interface: Functional hydroxyapatite surfaces and particles**

Dissertation to obtain the Degree of Doctor of Natural Sciences  
(Dr. rer. nat.)

from the Faculty of Chemistry and Pharmacy  
of the University of Regensburg



Presented by  
**Andrea Schüssele**  
from Waldkirch-Buchholz  
2006



Promotionsgesuch eingereicht am:	31.08.2006
Die Arbeit wurde angeleitet von:	Prof. Dr. A. Göpferich
Mündliche Prüfung am:	02.11.2006
Prüfungsausschuss:	Prof. Dr. S. Elz Prof. Dr. A. Göpferich Prof. Dr. G. Franz Prof. Dr. N. Korber

---

**IM**  **POSSIBLE**

---

## Table of contents

<b>Chapter 1</b>	Introduction and Goals of the Thesis .....	1
<b>Chapter 2</b>	Surface modifications of Hydroxyapatite ceramics to modulate cell adhesion and improve tissue generation.....	23
<b>Chapter 3</b>	Labeling of lysozyme and BMP-2 with <sup>125</sup> Iodine for the characterization of surface modification methods.....	35
<b>Chapter 4</b>	Adsorption and immobilization of lysozyme on PEGylated HA ceramic surfaces .....	53
<b>Chapter 5</b>	A novel method for protein immobilization on HA ceramic surfaces using bisphosphonates .....	81
<b>Chapter 6</b>	Pamidronate-based surface modification of hydroxyapatite particles: Adsorption and co-precipitation.....	109
<b>Chapter 7</b>	Confocal microscopy for monitoring particle uptake and distribution in a three-dimensional cell culture model.....	131
<b>Chapter 8</b>	Summary and Conclusions .....	151
<b>Appendices</b>	Abbreviations..... Curriculum vitae..... List of publications..... Acknowledgements.....	167 160 161 164

---



# **Chapter 1**

## **Introduction and Goals of the Thesis**

## **1. Bone, implant failure and the significance of the bone-implant interface**

In recent years, implant materials have gained growing importance in all areas of medicine [1]. The placement of endosseous implants has improved the quality of life for millions of people [2]. It is estimated that over 500,000 total joint replacements, primarily hips and knees, and between 100,000 and 300,000 dental implants are used each year in the United States [2]. The success of endosseous implants depends on acquiring and retaining stable fixation of the device in the surrounding bone. Load bearing implants in orthopedics have to sustain complex mechanical loads without failure under rather corrosive environmental conditions. Furthermore, permanent implants, e.g. joint prostheses or dental implants, which are designed for service throughout the lifetime of the patient, have to bond tightly to the surrounding bone [3]. Unfortunately, the current average lifetime of an orthopedic implant is only 15 years [1]. Stable fixation largely depends on obtaining intimate apposition of bone to the implant, a fact that has lead to renewed focus on biomimetic surface coatings [1]. Biomimetic materials are capable of eliciting specific cellular responses and directing new tissue formation mediated by biomolecular recognition [4]. Biomimetic cell carriers are one of the key strategies applied for bone tissue engineering [5;6]. Bone tissue engineering concepts have focused on two approaches: the use of three-dimensional matrices as cell-free conduits to guide bone ingrowth from the surrounding bone or as carriers for seeded cells for in vitro or in vivo bone formation [7]. The fabrication of materials to provide appropriate scaffolding that is conducive to cell attachment and maintenance of cell function is a key strategy [5]. To achieve an increase in the lifetime of permanent implants requires investigating and understanding the remodeling properties of the bone, the implant materials, and the bone-implant interface structure.

### **1.1. Bone**

In order to use the potential of biomimesis in the design of cell carriers for bone tissue engineering, the basic principles of structure and development of the skeleton have to be studied [8]. The knowledge of bone physiology has continuously increased in recent years. A complete review is beyond the scope of this thesis, but can be found in [9]. The following facts are of significance for a better understanding of the chapters ahead: The composition of bone varies with age, anatomical location, general health, and nutritional status. In general, bone mineral accounts for 50-70% of adult bone, the organic matrix, mainly collagen, for about 20-40%, water for about 5-10% and lipids for about 1-5% by volume [10]. Bone mineral is mostly in the form of hydroxyapatite  $[\text{Ca}_{10}(\text{PO}_4)_6(\text{OH})_2]$ , which provides rigidity and strength for skeletal and load-bearing functions. The hydroxyapatite in bone consists of small crystals



(about 20 nm) and contains impurities, including carbonate and magnesium [10;11]. The adult skeleton consists 80% of compact (or cortical) bone, which contains channel systems for nerve fibers and blood vessels, and 20% of trabecular (or spongy) bone, which is filled with bone marrow. Mature bone is termed lamellar bone and consists of both of trabecular and compact bone, while new bone, which is formed e.g. during fracture repair, is woven bone. Woven bone is a relatively disorganized array of collagen and mineralization patterns, which becomes lamellar bone through the process of remodeling [10;11].

As bone is a living tissue, the biological response to implanted materials is a key factor to improve the osseointegration process. This biological response can be influenced by stimulating the four different cell types found in bone: osteoblasts, osteocytes, bone lining cells and osteoclasts [9;12]. Osteoblasts are responsible for the formation and organization of the extracellular matrix of bone and its subsequent mineralization [12]. Osteoblasts express relatively high amounts of alkaline phosphatase, which plays a role in bone mineralization and represents an early marker of osteoblastic differentiation [13]. Osteoclasts, which are large multinucleated cells, cause bone resorption [12;14]. Osteocytes are derived from osteoblasts and are involved in the transduction of mechanical stimulus into biochemical signals, thereby orchestrating bone remodelling and tissue repair [12]. Bone lining cells are inactive cells that cover bone surfaces and undergo neither bone formation nor resorption [12].

## **1.2. Significance of the bone implant interface**

When attempting to regenerate bone via the conduction of bone into biomaterials [7], the conduit material is implanted adjacent to bone tissue. Cells from the tissue begin to invade and populate the material, lay down new matrix, and eventually form new bone. Following implantation of a biomaterial in bone, events analogous to those that occur during fracture healing will occur, including the formation of a hematoma between bone and implant as a scaffold for the infiltration of cells [2;15]. A short overview is given in Fig. 1, adopted from [2]: First proteins from blood and other tissue fluids will adsorb to the surface (a) mediating adhesion of cells such as inflammatory and connective tissue cells (b). These cells stimulate the invasion of osteoprogenitor cells that will differentiate to osteoblastic cells by exposure to adequate growth factors (c). These osteoblastic cells are capable of forming new bone (d). With time, the newly formed bone will be remodeled by osteoclasts to mature, lamellar bone, which further stabilizes the implant (e).

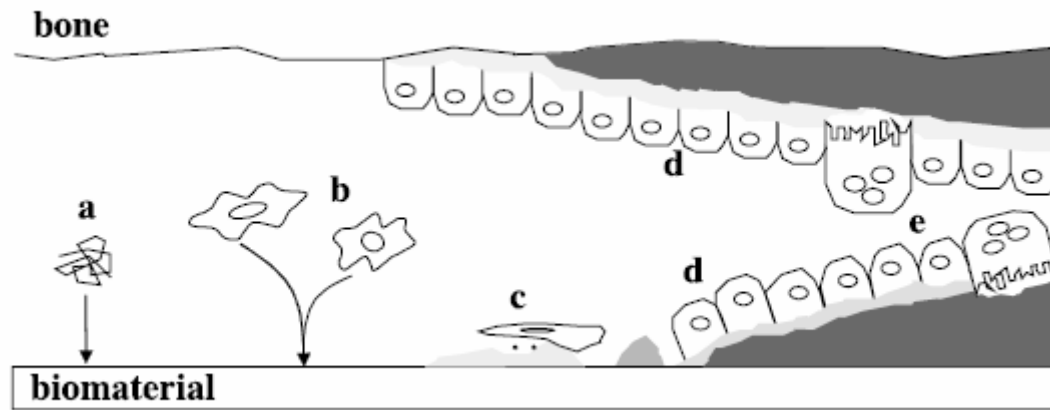


*Fig. 1: Schematic representation of the events occurring at the bone-implant interface. **a:** Protein adsorption from blood and tissue fluids. **b:** Inflammatory and connective tissue cells approach the implant. **c:** Formation of an afibrillar mineralized layer and adhesion of osteogenic cells. **d:** Bone deposition on both the bone and the implant surfaces. **e:** Remodelling of newly formed bone by osteoclasts (adopted with modifications from [2]).*

The response of the host to the implant material ideally culminates in an intimate apposition of bone to the biomaterial. Two crucial steps have been identified for this intimate contact to occur and additionally minimize conditions that would lead to the formation of a fibrous capsule: first, the adhesion of the desired type of cells, mediated by adsorbed proteins [16] and, second, the recruitment of osteogenic cells and their differentiation to osteoblasts by adequate cytokines [2].

The strategy applied in this thesis intended to create biomaterial surfaces suitable for specific stimulation of cells when implanted into bony tissue. In the following, a short review of key factors for the control of cell-biomaterial interactions at the bone-implant interface is given.

### 1.3. Hydroxyapatite as biomaterial for bone replacement

One important strategy to decrease the rate of implant failure would be to use biomaterials with similar mechanical properties to bone [5]. Current therapies for bony defects include the autologous bone graft, which is still the gold-standard, although it has its anatomical limitations and carries a risk of infection [5]. Despite the wide use of biodegradable polymers and hydrogels as cell carriers for the engineering of bone and cartilage [17], they are not suitable for application in load-bearing sites due to their lack of mechanical competence. Natural and synthetic ceramic materials provide an acceptable alternative for medical purposes [8;18]. By the mid-1980s ceramic materials had reached clinical use in a variety of orthopedic and dental applications [19]. Different types of bioceramics, including calcium phosphates, alumina, and bioactive glasses, are reviewed and classified with focus on the type of attachment to bone in [20]. Bioactive ceramics, such as hydroxyapatite (HA), tricalcium phosphate (TCP), and certain compositions of silicate and phosphate glasses (bioactive glasses) react with physiological fluids and through cellular activity to form

tenacious bonds to hard tissue [20]. Synthetic hydroxyapatite ceramics began to be routinely used as porous implants [19], powders, and coatings on metallic prostheses to provide bioactive fixation [21-23]. The presence of sparingly soluble HA led to osteoconduction, a tissue response in which bone grew along the coating and formed a mechanically strong interface responsible for the long-term reliability of the implant [20]. Enhanced protein adsorption relative to other hard-tissue replacement materials is considered responsible for the good osseointegration properties of HA ceramics [24]. The variety of degradation rates of calcium phosphate ceramics in vivo broadens the spectrum of applications even further [25]. To summarize, synthetic hydroxyapatite is a biocompatible, bioactive and osteoconductive material that comprises sufficient mechanical strength for application in load-bearing sites [19] and resembles the inorganic phase of bone [26]. Solid discs (Fig. 2) provided by the Friedrich-Baur-Research-Institute for Biomaterials (Bayreuth, Germany) were used as models for our studies on surface modification methods to gain control of the events at the bone-implant interface.

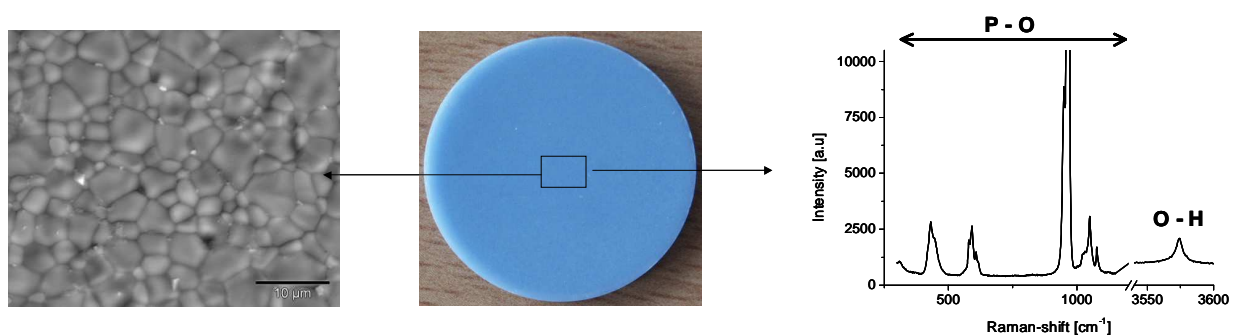


*Fig. 2: Hydroxyapatite ceramic disc, manufactured by the Friedrich-Baur Research Institute for biomaterials (Bayreuth, Germany). From left to right: SEM image of the surface of a disc, photo and  $\mu$ -Raman spectrum of the surface. The discs were used as model surfaces for the investigation of surface modification methods.*

#### 1.4. Strategies to influence bone cell response to biomaterials

The development of biomaterials for tissue engineering applications has recently focused on the design of biomimetic materials that are capable of eliciting specific cellular responses [4]. As outlined above, the integration of materials into bone tissue takes place at the material-tissue interface and is often determined by initial cell and substrate interactions [4]. This is also true for biomimetic materials. The quality of interaction is greatly influenced by the surface properties of the implant materials [27]. A promising strategy is to combine hydroxyapatite surfaces that comprise osteoconductive properties with cell-specific signals to control and improve the osseointegration of implants [15;28]; this is an approach that requires knowledge about the signals capable of influencing cellular response to a material.

#### 1.4.1. Roughness of implant surfaces

The cell response to a material surface is strongly influenced by the roughness of the surface [29]. However, general trends on the influence of surface roughness on cell adhesion, proliferation, or differentiation can hardly be extracted from literature [30;31]. Divergent results are reported for cell response to surface roughness that may be explained by a strong dependency on the particular material, the type of cell, and the culture conditions.

#### 1.4.2. Cell adhesion and enhancement of osteogenesis by RGD peptides

In general, cell adhesion to biomaterials is mediated by integrins, heterodimeric transmembrane cell receptors comprised of non-covalently bound  $\alpha$ - and  $\beta$ - subunits, which selectively bind to different extracellular matrix (ECM) proteins and are often cell type specific [32]. Since the identification of the tripeptide sequence arginine-glycine-aspartic acid (RGD) as the integrin binding site of ECM proteins such as fibronectin [33], a plethora of small peptide analogues has been synthesized and applied for surface coatings in order to enhance osteoblast adhesion to orthopedic biomaterials [34;35]. In addition to the stimulation of osteoblast adhesion, RGD coated biomaterials promoted cell proliferation as well as bone formation [36]. RGD coating of hydroxyapatite by adsorption [37;38] or covalent binding [35;39] significantly improved cell attachment and osteogenesis of various cell types.

#### 1.4.3. Stimulation of bone formation: growth factors

Bone contains a variety of growth factors that are capable of stimulating both cell proliferation and osteoblastic differentiation [40]. Therefore, various growth factors have been supplemented to bone cell cultures in order to investigate their influence on osteogenesis [5]. Classes of growth factors that are produced by osteoblasts include transforming growth factor- $\beta$  (TGF- $\beta$ ), bone morphogenetic proteins (BMPs), insulin-like growth factors (IGFs) and fibroblast growth factors (FGFs) [40]. TGF- $\beta$  is involved in the stimulation of collagen I production, the main component of the ECM of bone. However, its effects on matrix mineralization and differentiation of osteoblastic progenitor cells are conflicting, depending on the cell type, the differentiation state, and the culture conditions [41;42]. IGFs present the most abundant growth factors produced by osteoblasts and are involved in bone formation as well as resorption [40]. FGFs stimulate osteoblast proliferation and promote bone growth [40]. Furthermore, they play key roles during physiological and pathological conditions, such as wound healing, skeletal repair, neovascularization, and tumor growth [40].

The BMPs were discovered in the late 1960s when evidence surfaced that the implantation of demineralized bone at ectopic sites caused an induction of extrasketal bone development [43]. To date, more than 15 BMPs have been identified [44]. All of the BMPs, except BMP-1, belong to the TGF- $\beta$  superfamily and share significant sequence homology in the carboxy-terminal region with a conserved pattern of seven cysteine residues [40]. BMPs

are strongly involved in tissue morphogenesis and regeneration [45] and therefore have strong therapeutic potential [46].

#### 1.4.4. Bone Morphogenetic Protein-2 (BMP-2)

Among the members of the TGF- $\beta$  superfamily, BMP-2 has gained the most interest as a prominent factor for osteoblastic differentiation and bone repair [47]. BMP-2 up-regulates differentiation in pre-existing osteoblasts and additionally induces the commitment of a variety of cell types, including mesenchymal cells, to the osteoblastic pathway [47;48]. To utilize these effects following surgery, a product containing BMP-2 has recently gained approval by the authorities: Induct Os<sup>®</sup> (Wyeth Pharma), an implantable collagen sponge loaded with BMP-2.

BMP-2 is a disulfide-linked homodimeric protein, whose structure, mechanisms of action, receptor binding, and therapeutic potential for bone repair and regeneration have been extensively investigated [46;49-52]. BMP-2 signaling requires binding to cell surface receptors, which consist of two types of receptor serine/threonine-kinases [52]. The concept of localized delivery of BMP-2 to the bone-implant interface was implemented by adsorbing BMP-2 to implant materials in a variety of in vivo approaches in different animal models [53-57]. Adsorbed BMP-2 successfully stimulated osseointegration and new bone formation compared to non-biomimetic implant surfaces in these studies. The cellular response, however, is highly dependent on the duration of exposure to BMP-2 [58]. Therefore, covalent immobilization of BMP-2 at the bone-implant interface is expected to further improve osseointegration compared to adsorbed factor [59].

#### 1.4.5. Inhibition of bone resorption

As mentioned before, in addition to the bone-forming osteoblasts, osteoclasts have an equally important role in the formation of the skeleton and regulation of its mass [14]. Among others, parathyroid hormone and 1,25-dihydroxyvitamin D<sub>3</sub> are osteoclastogenic agents that are involved in the stimulation of osteoclastic differentiation and the regulation of bone resorption [14]. An imbalance in skeletal turnover leads to osteoporosis, a disease that is currently treated by suppressing osteoclast formation with estrogen and suppressing osteoclast activity with calcitonin and bisphosphonates [28].

Bisphosphonates are currently the most important class of anti-resorptive agents used in the treatment of metabolic bone diseases, including tumor-associated osteolysis and hypercalcemia, Paget's disease, and osteoporosis [60]. Bisphosphonates are pyrophosphate analogues in which the oxygen bridge has been replaced by a carbon atom with various side chains (Fig. 3) [28].

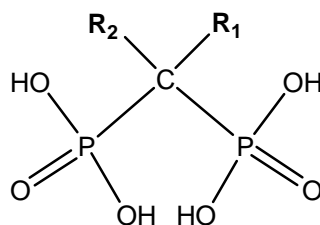


Fig. 3: General structure of a geminal bisphosphonate.  $R_1$  being  $-H$ ,  $-OH$ ,  $-NH_2$  or  $-Cl$ .

Their cellular and molecular mechanisms of action on osteoclasts depends on the structure of the respective derivative [60]: After internalization to osteoclastic cells, the simple bisphosphonates (BPs), such as clodronate and etidronate, are metabolized to methylene-containing analogues of ATP that exhibit cytotoxic effects on osteoclasts [61]. The nitrogen-containing bisphosphonates (N-BPs), such as pamidronate and alendronate, interact with the mevalonate-pathway as inhibitors of the farnesyl diphosphate synthase, thus limiting the production of cholesterol and isoprenoids [61]. However, bisphosphonate action seems not to be limited to osteoclasts. Further pharmacological actions of bisphosphonates including effects on osteoblastic differentiation in vitro and in vivo have been reported [62-64].

### 1.5. Drug immobilization on hydroxyapatite surfaces

Calcium phosphate cements, including hydroxyapatite, have been successfully employed as drug delivery systems, delivering adsorbed or incorporated substances such as antibiotics, analgesics, and anti-inflammatory drugs to the skeleton [65;66]. In general, hydroxyapatite exhibits a strong ability to adsorb proteins [67;68]. However, to provide a controlled and sustainable influence on cell behavior over that of soluble or slowly released proteins or drugs it seems beneficial to develop biomaterial surfaces with covalently immobilized ligands [59;69;70]. One of the reasons may be that the activity of proteins immobilized on solid surfaces, including glass, plastics, and polymer films, exceeds that of adsorbed or soluble protein [71-74].

#### 1.5.1 Current approaches for covalent and adsorptive binding to hydroxyapatite

So far, only a few attempts to covalently immobilize biomolecules on the surface of HA particles or implant materials have been reported. One approach primarily used to bond polymers to the inorganic HA in composite materials by grafting hexamethylene diisocyanate to the HA surface has also been used to immobilize drugs on HA surfaces [75-78]. A second approach introduced amine groups on the surface through aminosilanization. The aminosilanization procedure is well-established for glass, silica, metal, and metal oxide materials [79-84] and has been employed for HA ceramic particles [85]. Particles modified with aminopropyl-triethoxysilane were determined to be non-toxic to a variety of cells in a biocompatibility screening [86]. Furthermore, silanized hydroxyapatite was used for the immobilization of RGD peptides and promoted cell adhesion and differentiation [39;87]. Other

approaches for surface functionalization utilize compounds comprising strong adsorptive binding to hydroxyapatite surfaces: Compounds such as phosphates [88], amino acids [89], polyglutamate motifs [90], and polyelectrolytes, such as polyacids [38], have been utilized to create a platform for covalent binding of growth factors and RGD peptides in order to stimulate cells.

#### 1.5.2 Bisphosphonates: adsorption to hydroxyapatite and targeting to bone

Among other bone bonding motifs [91], bisphosphonates (Fig. 3) are a class of substances characterized by a high affinity for bone and hydroxyapatite [92;93]. The capacity of bisphosphonates to accumulate in bone is a consequence of their high affinity to hydroxyapatite due to bi- or tridentate interactions depending on the structure of the respective derivative [94]. The phosphonic acids and the functions in position  $R_1$  (Fig. 4; if -OH or -NH<sub>2</sub>) are involved in the formation of bonds to hydroxyapatite [95]. The influence of the chemical structure of bisphosphonate derivatives on the bone binding affinity and additionally on the growth of hydroxyapatite crystals are reviewed in [93]. This strong affinity is utilized to immobilize bisphosphonates on inorganic material surfaces aiming to stimulate cells at the bone-implant interface, which, in the case of pamidronate and ibandronate, improved the osseointegration in vivo and stimulated the osteoblastic differentiation in vitro [96-98].

Much more common and established is the use of bisphosphonates in drug targeting to bone. Due to their pharmacokinetic properties [99], bisphosphonates are ideal candidates for targeting to bone and calcified tissues, which has been demonstrated by the development of bone-targeted drug delivery systems, such as bisphosphonate-conjugated proteins [100-103].

## 2. Drug targeting and tissue distribution of nanoparticles

Drug targeting is of particular interest in the field of cancer chemotherapy, as it can increase anti-tumor efficacy and restrict the delivery of the chemotherapeutic agents to the tumor site while reducing systemic side effects [104;105]. This is also true for bone tissue for which numerous malignancies are known that are hard to treat. Here, targeting concepts including bisphosphonates, tetracyclines and polyaminoacids are employed [91;103]. Furthermore, bisphosphonates have been proven to be effective in the treatment of malignant skeletal diseases characterized by enhanced osteoclastic bone resorption [106].

Current research areas in drug targeting include the development of carriers to allow alternative dosing routes, new therapeutic targets, such as blood vessels, and targeted therapeutics that are more specific in their activity [107]. One strategy is to associate antitumor drugs with colloidal nanoparticles prepared from degradable polymers in order to overcome non-cellular and cellular mechanisms of drug resistance and to increase the selectivity of drugs towards cancer cells while reducing their toxicity towards healthy tissues [105].

Targeting can be achieved either passively, as a result of physical or chemical characteristics of the carrier ("passive targeting"), or actively, by specifically including a recognition moiety into the carrier ("active targeting") [108]. Nanoscale devices (100 nm or below) carrying chemotherapeutic drugs can extravasate from blood vessels and even diffuse through the tissue and enter tumor cells [109]. Intravenously injected nanoparticles accumulate in cancerous tissue, which can be explained by a passive diffusion or convection across the leaky, hyperpermeable tumor vasculature [105]. The defective vasculature, a result of rapid vascularization, coupled with poor lymphatic drainage allows for an enhanced permeation and retention effect (EPR), a critical advantage of colloidal carrier based therapies [107]. However, the usefulness of conventional nanoparticles is limited by their massive capture by macrophages of the mononuclear phagocyte system (MPS), which can be avoided by the use of hydrophilic coatings ("stealth™ particles") [105].

Active, tumor-specific targeting uses strategies that exploit differences between malignant and healthy cells: inactive drugs that are activated in cancerous cells by specific mechanisms ("prodrugs") [107] or selective ligands for cell-specific receptors [108]. A variety of targeting motifs have been successfully used including antibodies interacting with tumor-specific antigens, folate-conjugated systems, vascular endothelial growth factor (VEGF) for targeting tumor neovasculature, and galactosamine for liver-cell targeting [110-116].

Furthermore, improvements in the delivery of selected drugs were achieved by incorporating them into nanoparticles, such as overcoming solubility restrictions for poorly soluble drugs (paclitaxel), avoiding toxic side effects (doxorubicin), and prolonging circulation in the



bloodstream for substances with short half-lives (5-fluorouracil) [107]. Once the particles have successfully been deposited in the tumor, they kill cancer cells by releasing their drugs and function as a stationary source, depending on the characteristics of the tumor type, carrier, and incorporated drug [109], leading to higher local drug concentrations compared to drugs applied as solutions [117].

## 2.1. Multicellular tumor spheroids – an in vitro tumor model

The factors influencing drug transport through tissues are of key interest for the development of delivery strategies to tumors [117]. In addition to mathematical simulations of drug transport processes [118;119], in vitro models for tumors are providing a rapid alternative to investigate drug distribution and transport limitations in a three-dimensional cellular context [117;120;121]. The models used for in vitro investigation of tumor growth, anticancer drug effects, and drug distribution include in vitro cultivated tumor biopsies, multilayered post-confluent cell cultures, and multicellular tumor spheroids (MCTS) [120-124].

3D cultures can mimic the specific biochemical and morphological features found in the corresponding tissue in vivo. In comparison to conventional cultures, cells in the 3D environment resemble the in vivo situation more closely with regard to the gene expression and biological behavior of the cells [123]. The multicellular tumor spheroids (MCTS) provide an excellent model, as they are easily prepared from a variety of cell lines [125], are tunable in size within a certain range, and have a well defined geometry [122;123].

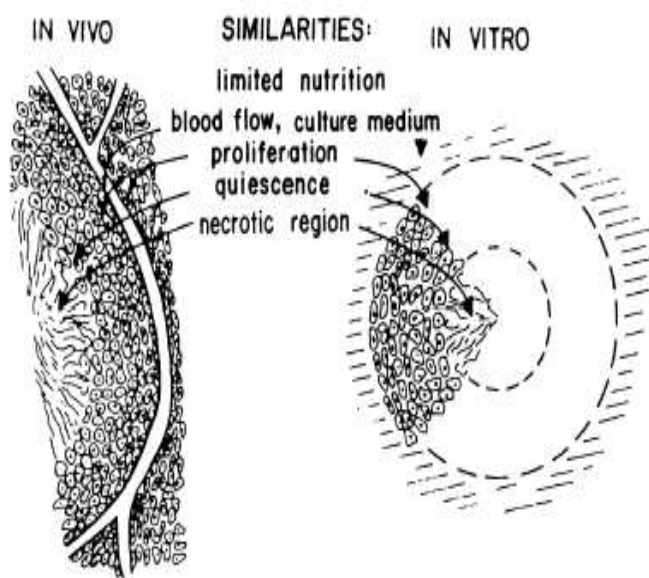


*Fig. 4: Schematic presentation of the similarities of a tumor (in vivo) and a spheroid (in vitro) [120].*

Additionally, tumor characteristics, such as limited nutrition supply in the avascular state, can be perfectly mimicked by the spheroid model (Fig. 4) [120], in contrast to a monolayer culture in vitro [122]. Their ease of preparation makes the spheroids suitable for high throughput

screening approaches in drug testing [124]. In addition to the rapid screening of new anticancer drugs, the spheroid model allows for the investigation of novel particulate drug delivery systems. Their distribution and retention in the tumor model can be investigated by means of confocal microscopy, allowing for observations of particles in intact, living spheroids and the determination of particle distribution throughout the cell aggregates (Fig. 5).

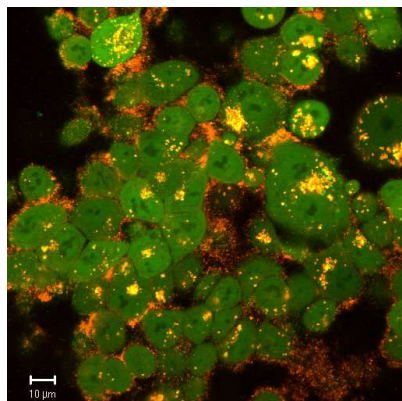


*Fig. 5: Confocal image of GFP-expressing tumor cells (HCT-116) in a spheroid with extracellular fluorescent nanoparticles (orange) and intracellular nanoparticles (yellow).*

### 3. Goals of the Thesis

To control the events at the bone-implant interface by selective adhesion and direct stimulation of cells is still a great challenge. The focus of the first part of this thesis was to develop and characterize methods for the immobilization of cell stimulating factors on hydroxyapatite surfaces, intending to create functionalized surfaces of solid hydroxyapatite discs or particles (Fig. 6).

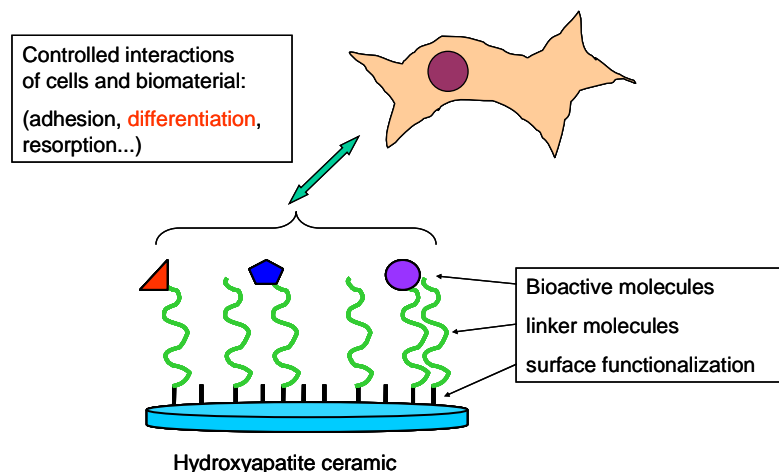


Fig. 6: Immobilization of bioactive molecules in order to control the interactions with cells.

To achieve specific interactions between a surface and cells by attaching adhesion peptides to a surface, it is a prerequisite to suppress unspecific cell adhesion by the creation of inert surfaces [29]. Therefore, we grafted poly(ethylene glycol) (PEG) to ceramic discs that were activated for further conjugation steps by the well-established aminosilanization procedure [85]. The synthesis of a suitable PEG derivative (PEG acetaldehyde) was adopted from the literature. PEG-modified hydroxyapatite surfaces were characterized by contact angle measurements and X-ray photoelectron spectroscopy (XPS). Cell adhesion was studied by using rat marrow stromal cells (rMSC) (**Chapter 2**).

The next objective was to establish a method to assess the efficacy of protein attachment to surfaces by various immobilization procedures. In order to detect very low levels of protein on the surfaces, we used proteins labeled with radioisotopes. We identified lysozyme as suitable model protein due to similarities in its physico-chemical characteristics compared to some growth factors, such as BMPs [126], and the well-known mechanism of enzymatic action [127] and analytics thereof [128]. A radiolabeling procedure with  $^{125}\text{I}$  was established for lysozyme and a procedure from the literature was employed to label BMP-2. Products were characterized with a focus on structural fragmentation due to the labeling procedure and the adsorption of lysozyme to ceramic discs was studied (**Chapter 3**).

Tethering cytokines to the material surface via PEG is a common principle to enhance stability and biological performance of the respective biomolecules [72]. Therefore, a further

challenge was to immobilize a protein on the silanized ceramic discs employing PEG acetaldehyde of varying molecular weights as homobifunctional spacers. The potential of PEG-grafted ceramic discs to suppress the adsorption of lysozyme was explored and the impact of the immobilization method on the stability of the attached protein was determined by assessing the enzymatic activity of lysozyme (**Chapter 4**).

Although immobilization by PEG spacers seemed to be promising with regard to the stability of the attached proteins, immobilization on the surface by smaller spacers might be favorable due to the ease of preparation and amount of attached growth factor. Therefore, we evaluated the aminosilanization procedure in combination with carbodiimide coupling chemistry in order to immobilize proteins on the surface of HA ceramic discs. In addition to the silanization procedure, a novel method for the creation of functional groups on HA ceramic surfaces using the aminobisphosphonates alendronate and pamidronate as anchoring molecules was evaluated. Lysozyme was used to assess the amount of immobilized protein and the impact of coupling chemistry on enzymatic activity. The potential of immobilized BMP-2 for the stimulation of cells was then investigated by the effects on the osteoblastic differentiation of C2C12 mouse myoblasts (**Chapter 5**).

To gain a deeper insight into the bisphosphonate-mediated surface functionalization, an adsorption study of the bisphosphonate pamidronate on hydroxyapatite powder particles was performed. Through these experiments, we intended to determine the type of adsorption and the suitability of surface immobilized bisphosphonate as anchoring molecule for further conjugation steps. In order to control the amount of attached molecules, we determined the number of surface amine groups and the range of concentration dependency. In addition, the precipitation of calcium phosphate in the presence of pamidronate was evaluated as alternative route to obtain functionalized particles (**Chapter 6**).

In addition to their usefulness in surface functionalization, bisphosphonates are interesting tools for drug targeting to bone and calcified tissues, due to their pharmacokinetic characteristics. Drug targeting is of particular interest in the treatment of cancer. Therefore, in a second part of the thesis, the interactions of fluorescent model nanoparticles with a three-dimensional cell culture model were investigated by means of confocal laser scanning microscopy. The objective was to establish a method for the rapid determination of uptake and distribution of particles as models for drug carriers inside a three-dimensional cell context as an alternative to the conventional time-consuming cryo-sections (**Chapter 7**).

## 4. References

- [1] Buchanan, J. M. (2005): "Sixteen year review of hydroxyapatite ceramic coated hip implants - a clinical and histological evaluation"; *Key Engineering Materials* (284-286) p.1049-1052
- [2] Puleo, D. A. (2004): "Bone-implant interface"; *Encyclopedia of Biomaterials and Biomedical Engineering* (1) p.190-198; Marcel Dekker, Inc., New York
- [3] Triffitt, J. (2002): "Osteogenic stem cells and orthopedic engineering: summary and update"; *Journal of Biomedical Materials Research* p.384-389
- [4] Shin, H., Jo, S., and Mikos, A. G. (2003): "Biomimetic materials for tissue engineering"; *Biomaterials* (24) p.4353-4364
- [5] Rose, F. R. and Oreffo, R. O. C. (2002): "Bone Tissue Engineering: Hope vs Hype"; *Biochemical and Biophysical Research Communications* (292) p.1-7
- [6] Langer, R. and Vacanti, J. P. (1993): "Tissue engineering"; *Science* (260) p.920-926
- [7] Crane, G. M., Ishaug, S. L., and Mikos, A. G. (1996): "Bone tissue engineering"; *Nature Medicine* (1) p.1322-1324
- [8] Green, D., Walsh, D., Mann, S., and Oreffo, R. O. C. (2002): "The potential of biomimesis in bone tissue engineering: lessons from the design and synthesis of invertebrate skeletons"; *Bone* (30) p.810-815
- [9] Marks, S. and Odgren, P. R. (2002): "Structure and development of the skeleton"; in "Principles of bone biology" (Bilezikian, J., Raisz, L., and Rodan, G. A.; Eds.), Academic press, San Diego, CA
- [10] Shea, J. E. and Miller, S. C. (2005): "Skeletal function and structure: implications for tissue-targeted therapeutics"; *Advanced Drug Delivery Reviews* (57) p.945-957
- [11] Marks, S. and Hermey, D. (1996): "The structure and development of bone"; in "Principles of bone biology" (Bilezikian, J., Raisz, L., and Rodan, G. A.; Eds.), Academic Press, San Diego, CA
- [12] Manolagas, S. C. (2000): "Birth and death of bone cells: basic regulatory mechanisms and implications for the pathogenesis and treatment of osteoporosis"; *Endocrine Reviews* (21) p.115-137
- [13] Henthorn, P. (1996): "Alkaline Phosphatase"; in "Principles of bone biology" (Bilezikian, J., Raisz, L., and Rodan, G. A.; Eds.), Academic Press, San Diego, CA
- [14] Teitelbaum, S. L. (2000): "Bone resorption by osteoclasts"; *Science* (289) p.1504-1508
- [15] Puleo, D. A. and Nanci, A. (1999): "Understanding and controlling the bone-implant interface"; *Biomaterials* (20) p.2311-2321
- [16] Wilson, C. J., Clegg, R. E., Leavesley, D. I., and Pearcy, M. J. (2005): "Mediation of biomaterial-cell interactions by adsorbed proteins: A review"; *Tissue Engineering* (11) p.1-18
- [17] Hutmacher, D. W. (2000): "Scaffolds in tissue engineering bone and cartilage"; *Biomaterials* (21) p.2529-2543
- [18] Joschek, S., Nies.B., Krotz, R., and Gopferich, A. (2000): "Chemical and physicochemical characterization of porous hydroxyapatite ceramics made of natural bone"; *Biomaterials* (21) p.1645-1658
- [19] Hench, L. L. and Polak, J. M. (2002): "Third-generation biomedical materials"; *Science* (295) p.1014-1017
- [20] Hench, L. L. (1991): "Bioceramics: From concept to clinic"; *Journal of the American Ceramic Society* (74) p.1487-1510
- [21] Wang, M. (2003): "Developing bioactive composite materials for tissue replacement"; *Biomaterials* (24) p.2133-2151
- [22] Boccaccini, A. R. and Blaker, J. J. (2005): "Bioactive composite materials for tissue engineering scaffolds"; *Expert Review of Medical Devices* (2) p.303-317
- [23] Lewis, G. (2000): "Hydroxyapatite-coated bioalloy surfaces: Current status and future challenges"; *Bio-Medical Materials and Engineering* (10) p.157-188

- [24] Kilpadi, K. L., Chang, P. L., and Bellis, S. L. (2002): "Hydroxylapatite binds more serum proteins, purified integrins, and osteoblast precursor cells than titanium or steel"; *Journal of Biomedical Materials Research* (57) p.258-267
- [25] Lu, J., Deschamps, M., Dejou, J., Koubi, G., Hardouin, P., Lemaitre, J., and Proust, J.-P. (2002): "The biodegradation mechanism of calcium phosphate biomaterials in bone"; *Journal of Biomedical Materials Research* p.408-412
- [26] Leventouri, T. (2006): "Synthetic and biological hydroxyapatites: Crystal structure questions"; *Biomaterials* (27) p.3339-3342
- [27] Altankov, G., Thom, V., Groth, T., Jankova, K., Jonsson, G., and Ulbricht, M. (2000): "Modulating the biocompatibility of polymer surfaces with poly(ethylene glycol): effect of fibronectin"; *Journal of Biomedical Materials Research* (52) p.219-230
- [28] Rodan, G. A. and Martin, T. J. (2000): "Therapeutic approaches to bone diseases"; *Science* (289) p.1508-1514
- [29] Castner, D. G. and Ratner, B. D. (2002): "Biomedical surface science: Foundations to frontiers"; *Surface Science* (500) p.28-60
- [30] Deligianni, D. D., Katsala, N. D., Koutsoukos, P. G., and Missirlis, Y. F. (2001): "Effect of surface roughness of hydroxyapatite on human bone marrow cell adhesion, proliferation, differentiation and detachment strength"; *Biomaterials* (22) p.87-96
- [31] Campoccia, D., Arciola, C. R., Cervellati, M., Maltarello, M. C., and Montanaro, L. (2003): "In vitro behaviour of bone marrow-derived mesenchymal cells cultured on fluorohydroxyapatite-coated substrata with different roughness"; *Biomaterials* (24) p.587-596
- [32] Lieb, E., Hacker, M., Tessmar, J., Kunz-Schughart, L. A., Fiedler, J., Dahmen, C., Hersel, U., Kessler, H., Schulz, M. B., and Goepferich, A. (2005): "Mediating specific cell adhesion to low-adhesive diblock copolymers by instant modification with cyclic RGD peptides"; *Biomaterials* (26) p.2333-2341
- [33] Ruoslahti, E. (1996): "RGD and other recognition sequences for integrins"; *Annual Review of Cell and Developmental Biology* (12) p.697-715
- [34] Anselme, K. (2000): "Osteoblast adhesion on biomaterials"; *Biomaterials* (21) p.667-681
- [35] Hersel, U., Dahmen, C., and Kessler, H. (2003): "RGD modified polymers: biomaterials for stimulated cell adhesion and beyond"; *Biomaterials* (24) p.4385-4415
- [36] Kantlehner, M., Kessler, H., and et al (2000): "Surface Coating with Cyclic RGD Peptides stimulates Osteoblast Adhesion and Proliferation as well as bone formation"; *Chemistry and Biochemistry* (1) p.107-114
- [37] Sawyer, A. A., Hennessy, K. M., and Bellis, S. L. (2005): "Regulation of mesenchymal stem cell attachment and spreading on hydroxyapatite by RGD peptides and adsorbed serum proteins"; *Biomaterials* (26) p.1467-1475
- [38] Itoh, D., Yoneda, S., Kuroda, S., Kondo, H., Umezawa, A., Ohya, K., Ohyama, T., and Kasugai, S. (2002): "Enhancement of osteogenesis on hydroxyapatite surface coated with synthetic peptide (EEEEEEPRGDT) in vitro"; *Journal of Biomedical Materials Research* (62) p.292-298
- [39] Durrieu, M. C., Pallu, S., Guillemot, F., Bareille, R., Amedee, J., Baquey, C., Labrugere, C., and Dard, M. (2004): "Grafting RGD containing peptides onto hydroxyapatite to promote osteoblastic cells adhesion"; *Journal of Materials Science: Materials in Medicine* (15) p.779-786
- [40] Qin, X. and others (2001): "Bone growth factors"; in "Osteoporosis" (Marcus, R., Feldman, D., and Kelsey, J.; Eds.), Academic Press, San Diego, CA
- [41] Lieb, E., Vogel, T., Milz, S., Dauner, M., and Schulz, M. B. (2004): "Effects of Transforming Growth Factor b1 on bonelike tissue formation in three-dimensional cell culture II: Osteoblastic differentiation"; *Tissue Engineering* (10) p.1414-1425
- [42] Lieb, E., Milz, S., Vogel, T., Hacker, M., Dauner, M., and Schulz, M. B. (2004): "Effects of Transforming Growth Factor b1 on bonelike tissue formation in three-

- dimensional cell culture I: Culture conditions and tissue formation"; *Tissue Engineering* (10) p.1399-1413
- [43] Urist, M. R. (1965): "Bone formation by autoinduction"; *Science* (150) p.893-899
  - [44] de Groot, K. (1998): "Carriers that concentrate native bone morphogenetic protein in vivo"; *Tissue Engineering* (4) p.337-341
  - [45] Ripamonti, U. and Duneas, N. (1998): "Tissue morphogenesis and regeneration by bone morphogenetic proteins"; *Plastic and Reconstructive Surgery* (101) p.227-239
  - [46] Kirker-Head, C. A. (2000): "Potential applications and delivery strategies for bone morphogenetic proteins"; *Advanced Drug Delivery Reviews* (43) p.65-92
  - [47] Chen, D., Zhao, M., and Mundy, G. R. (2004): "Bone Morphogenetic Proteins"; *Growth Factors* (22) p.233-241
  - [48] Rosen, V., Cox, K., and Hattersley, G. (1996): "Bone Morphogenetic Proteins"; in "Principles in bone biology" (Bilezikian, J., Raisz, L., and Rodan, G. A.; Eds.), Academic Press, San Diego, CA
  - [49] Sakou, T. (1998): "Bone Morphogenetic Proteins: From Basic Studies to Clinical Approaches"; *Bone* (22) p.591-603
  - [50] Tabata, Y. (2003): "Tissue regeneration based on growth factor release"; *Tissue Engineering* (9) p.S5-S15
  - [51] Sebald, W., Nickel, J., Zhang, J. L., and Mueller, T. D. (2004): "Molecular recognition in bone morphogenetic protein (BMP)/receptor interaction"; *Biological Chemistry* (385) p.697-710
  - [52] Nickel, J., Dreyer, M. K., Kirsch, T., and Sebald, W. "The crystal structure of the BMP-2:BMPr-1A complex and the generation of BMP-2 antagonists"; *Journal of Bone and Joint Surgery* (83-A Suppl 1) p.S7-14
  - [53] Jennissen, H. (2002): "Method for immobilizing mediator molecule on inorganic and metal implant material"; PCT Application WO99/26674
  - [54] Jennissen, H. P. (2002): "Accelerated and improved osteointegration of implants biocoated with bone morphogenetic protein 2 (BMP-2)"; *Annals of the New York Academy of Sciences* (961) p.139-142
  - [55] Jennissen, H. P., Chatzinikolaidou, M., and Rumpf, H. (2001): "Method for producing bioactive surfaces on prosthetic implants using bone morphogenic proteins"; PCT Application 2001-DE2893
  - [56] Voggenreiter, G., Hartl, K., Assenmacher, S., Chatzinikolaidou, M., Rumpf, H. M., and Jennissen, H. P. (2001): "Assessment of the biological activity of chemically immobilized rhBMP-2 on titanium surfaces in vivo"; *Materialwissenschaft und Werkstofftechnik* (32) p.942-948
  - [57] Wiemann, M., Jennissen, H. P., Rumpf, H., Winkler, L., Chatzinikolaidou, M., Schmitz, I., and Bingmann, D. (2002): "A reporter-cell assay for the detection of BMP-2 immobilized on porous and nonporous materials"; *Journal of Biomedical Materials Research* (62) p.119-127
  - [58] Puleo, D. A. "Dependence of mesenchymal cell responses on duration of exposure to bone morphogenetic protein-2 in vitro"; *Journal of Cellular Physiology* (173) p.93-101
  - [59] Luginbuehl, V., Meinel, L., Merkle, H. P., and Gander, B. (2004): "Localized delivery of growth factors for bone repair"; *European Journal of Pharmaceutics and Biopharmaceutics* (58) p.197-208
  - [60] Rogers, M. J., Gordon, S., Benford, H. L., Coxon, F. P., Luckman, S. P., Monkkonen, J., and Frith, J. C. (2000): "Cellular and molecular mechanisms of action of bisphosphonates"; *Cancer* (88) p.2961-2978
  - [61] Rogers, M. J. (2004): "From Molds and Macrophages to Mevalonate: A decade of progress in understanding the molecular mode of action of bisphosphonates"; *Calcified Tissue International* (75) p.451-461
  - [62] Giuliani, N., Pedrazzoni, M., Negri, G., Passeri, G., Impicciatore, M., and Girasole, G. (1998): "Bisphosphonates stimulate formation of osteoblast precursors and mineralized nodules in murine and human bone marrow cultures in vitro and promote early osteoblastogenesis in young and aged mice in vivo"; *Bone* (22) p.455-461

- [63] Ganguli, A., Henderson, C., Grant, M. H., Meikle, S. T., Lloyd, A. W., and Goldie, I. (2002): "The interactions of bisphosphonates in solution and as coatings on hydroxyapatite with osteoblasts"; *Journal of Materials Science: Materials in Medicine* (13) p.923-931
- [64] Reinholz, G. G., Getz, B., Pederson, L., Sanders, E. S., Subramaniam, M., Ingle, J. N., and Spelsberg, T. C. (2000): "Bisphosphonates directly regulate cell proliferation, differentiation, and gene expression in human osteoblasts"; *Cancer Research* (60) p.6001-6007
- [65] Ginebra, M. P., Traykova, T., and Planell, J. A. (2006): "Calcium phosphate cements as bone drug delivery systems: A review"; *Journal of Controlled Release* (113) p.102-110
- [66] Jain, A. K. and Panchagnula, R. (2000): "Skeletal drug delivery systems"; *International Journal of Pharmaceutics* (206) p.1-12
- [67] Rosengren, A., Pavlovic, E., Oscarsson, S., Krajewski, A., Ravaglioli, A., and Piancastelli, A. (2002): "Plasma protein adsorption pattern on characterized ceramic biomaterials"; *Biomaterials* (23) p.1237-1247
- [68] Rosengren, A., Oscarsson, S., Mazzocchi, M., Krajewski, A., and Ravaglioli, A. (2003): "Protein adsorption onto two bioactive glass-ceramics"; *Biomaterials* (24) p.147-155
- [69] Backer, M. V., Patel, V., Jehning, B. T., Claffey, K. P., and Backer, J. M. (2006): "Surface immobilization of active vascular endothelial growth factor via a cysteine-containing tag"; *Biomaterials* (27) p.5452-5458
- [70] Vasita, R. and Katti, D. S. (2006): "Growth factor-delivery systems for tissue engineering: a materials perspective"; *Expert Review of Medical Devices* (3) p.29-47
- [71] Groll, J., Amirgoulova, E. V., Ameringer, T., Heyes, C. D., Roecker, C., Nienhaus, G. U., and Moeller, M. (2004): "Biofunctionalized, ultrathin coatings of cross-linked star-shaped poly(ethylene oxide) allow reversible folding of immobilized proteins"; *Journal of the American Chemical Society* (126) p.4234-4239
- [72] Kuhl, P. R. and Griffith-Cima, L. G. (1996): "Tethered epidermal growth factor as a paradigm for growth factor-induced stimulation from the solid phase." *Nature Medicine* (2) p.1022-1027
- [73] Ito, Y. (1998): "Tissue engineering by immobilized growth factors"; *Materials Science and Engineering: C* (6) p.267-274
- [74] Otsuka, H., Nagasaki, Y., and Kataoka, K. (2004): "Characterization of aldehyde-PEG tethered surfaces: Influence of PEG chain length on the specific biorecognition"; *Langmuir* (20) p.11285-11287
- [75] Liu, Q., de Wijn, J. R., and van Blitterswijk, C. A. (1998): "A study on the grafting reaction of isocyanates with hydroxyapatite filler particles"; *Journal of Biomedical Materials Research* (40) p.358-364
- [76] Liu, Q., de Wijn, J. R., de Groot, K., and van Blitterswijk, C. A. (1998): "Surface modification of nano-apatite by grafting organic polymer"; *Biomaterials* (19) p.1067-1072
- [77] Dong, G., Sun, J.-S., Yao, C.-H., Jiang, G.-J., Huang, C.-W., and Lin, F.-H. (2001): "A study on grafting and characterization of HMDI-modified calcium hydrogenphosphate"; *Biomaterials* (22) p.3179-3189
- [78] Liu, Q., de Wijn, J. R., and van Blitterswijk, C. A. (1998): "Composite biomaterials with chemical bonding between hydroxyapatite filler particles and PEG/PBT copolymer matrix"; *Journal of Biomedical Materials Research* (40) p.490-497
- [79] Weetall, H. H. (1976): "Covalent coupling methods for inorganic support materials"; *Methods in Enzymology* (44) p.134-148
- [80] Puleo, D. A. (1995): "Activity of enzyme immobilized on silanized Co-Cr-Mo"; *Journal of Biomedical Materials Research* (29) p.951-957
- [81] Van Der Voort, P. and Vansant, E. F. (1997): "Modification of the silica surface with aminosilanes"; *Polish Journal of Chemistry* (71) p.550-567



- [82] Halliwell, C. M. and Cass, A. E. G. (2001): "A factorial analysis of silanization conditions for the immobilization of oligonucleotides on glass surfaces"; *Analytical Chemistry* (73) p.2476-2483
- [83] Wojcik, S. M. and Puleo, D. A. (1997): "Biochemical surface modification of Ti-6Al-4V for the delivery of protein to the cell-biomaterial interface"; *Biomedical Sciences Instrumentation* (33) p.166-171
- [84] Bruening, C. and Grobe, J. (1995): "Aldehyde-functionalized ethoxysilanes as new enzyme immobilization reagents"; *Journal of the Chemical Society, Chemical Communications* p.2323-2324
- [85] Furuzono, T., Sonoda, K., and Tanaka, J. (2001): "A hydroxyapatite coating covalently linked onto a silicone implant material"; *Journal of Biomedical Materials Research* (56) p.9-16
- [86] Dupraz, A. M. P., Meer, S. A. T., de Wijn, J. R., and Goedemoed, J. H. (1996): "Biocompatibility screening of silane-treated hydroxyapatite powders, for use as filler in resorbable composites"; *Journal of Materials Science: Materials in Medicine* (7) p.731-738
- [87] Balasundaram, G., Sato, M., and Webster, T. J. (2006): "Using hydroxyapatite nanoparticles and decreased crystallinity to promote osteoblast adhesion similar to functionalizing with RGD"; *Biomaterials* (27) p.2798-2805
- [88] Meyer, J., Nies, B., Dard, M., Hoelzemann, G., Kessler, H., Kantlehner, M., Hersel, U., Gibson, C., and Sulyok, G. (2001): "Peptide and peptide mimetic conjugates with integrin-inhibitor properties and usage for the integration of prosthetic materials"; 2001-EP8932
- [89] Matsumoto, T., Okazaki, M., Inoue, M., Hamada, Y., Taira, M., and Takahashi, J. (2000): "Crystallinity and solubility characteristics of hydroxyapatite adsorbed amino acid"; *Biomaterials* (23) p.2241-2247
- [90] Sawyer, A. A., Weeks, D. M., Kelpke, S. S., McCracken, M. S., and Bellis, S. L. (2005): "The effect of the addition of a polyglutamate motif to RGD on peptide tethering to hydroxyapatite and the promotion of mesenchymal stem cell adhesion"; *Biomaterials* (26) p.7046-7056
- [91] Roberts, M. J. and Kozlowski, A. (2001): "Hydroxyapatite-targeting poly(ethylene glycol) and related polymers, their preparation and biologically active conjugates"; 2001-US32566
- [92] Leu, C. T., Luegmayr, E., Freedman, L. P., Rodan, G. A., and Reszka, A. A. (2006): "Relative binding affinities of bisphosphonates for human bone and relationship to antiresorptive efficacy"; *Bone* (38) p.628-636
- [93] Papapoulos, S. E. (2006): "Bisphosphonate actions: Physical chemistry revisited"; *Bone* (38) p.613-616
- [94] Grossmann, G., Grossmann, A., Ohms, G., Breuer, E., Chen, R., Golomb, G., Cohen, H., Hagele, G., and Classen, R. (2000): "Solid-state NMR of bisphosphonates adsorbed on hydroxyapatite"; *Magnetic Resonance in Chemistry* (38) p.11-16
- [95] Cohen, H., Solomon, V., Alferiev, I. S., Breuer, E., Ornoy, A., Patlas, N., Eidelman, N., Hagele, G., and Golomb, G. (1998): "Bisphosphonates and tetracycline: experimental models for their evaluation in calcium-related disorders"; *Pharmaceutical Research* (15) p.606-613
- [96] Tengvall, P., Skoglund, B., Askendal, A., and Aspenberg, P. (2004): "Surface immobilized bisphosphonate improves stainless-steel screw fixation in rats"; *Biomaterials* (25) p.2133-2138
- [97] Yoshinari, M., Oda, Y., Ueki, H., and Yokose, S. (2001): "Immobilization of bisphosphonates on surface modified titanium"; *Biomaterials* (22) p.709-715
- [98] Kajiwar, H., Yamaza, T., Yoshinari, M., Goto, T., Iyama, S., Atsuta, I., Kido, M. A., and Tanaka, T. (2005): "The bisphosphonate pamidronate on the surface of titanium stimulates bone formation around tibial implants in rats"; *Biomaterials* (26) p.581-587
- [99] Lin, J. H. (1996): "Bisphosphonates: A review of their pharmacokinetic properties"; *Bone* (18) p.75-85

- [100] Uludag, H., Kousinioris, N., Gao, T., and Kantoci, D. (2000): "Bisphosphonate Conjugation to Proteins as a Means To Impart Bone Affinity"; *Biotechnology Progress* (16) p.258-267
- [101] Hirabayashi, H. and Fujisaki, J. (2003): "Bone-specific drug delivery systems: Approaches via chemical modification of bone-seeking agents"; *Clinical Pharmacokinetics* (42) p.1319-1330
- [102] Uludag, H. and Yang, J. (2002): "Targeting systemically administered proteins to bone by bisphosphonate conjugation"; *Biotechnology Progress* (18) p.604-611
- [103] Wang, D., Miller, S., Sima, M., Kopeckova, P., and Kopecek, J. (2003): "Synthesis and evaluation of water-soluble polymeric bone-targeted drug delivery systems"; *Bioconjugate Chemistry* (14) p.853-859
- [104] Moses, M. A., Brem, H., and Langer, R. (2003): "Advancing the field of drug delivery: Taking aim at cancer"; *Cancer Cell* (4) p.337-341
- [105] Brigger, I., Dubernet, C., and Couvreur, P. (2002): "Nanoparticles in cancer therapy and diagnosis"; *Advanced Drug Delivery Reviews* (54) p.631-651
- [106] Clezardin, P. (2005): "Anti-tumour activity of zoledronic acid"; *Cancer Treatment Reviews* (31) p.S1-S8
- [107] Brannon-Peppas, L. and Blanchette, J. O. (2004): "Nanoparticle and targeted systems for cancer therapy"; *Advanced Drug Delivery Reviews* (56) p.1649-1659
- [108] Satchi-Fainaro, R., Duncan, R., and Barnes, C. (2006): "Polymer therapeutics for cancer: Current status and future challenges"; (193) p.1-65
- [109] Sinek, J., Frieboes, H., Zheng, X., and Cristini, V. (2004): "Two-dimensional chemotherapy simulations demonstrate fundamental transport and tumor response limitations involving nanoparticles"; *Biomedical Microdevices* (6) p.297-309
- [110] Steinhauser, I., Spaenkuch, B., Strebhardt, K., and Langer, K. (2006): "Trastuzumab-modified nanoparticles: Optimisation of preparation and uptake in cancer cells"; *Biomaterials* (27) p.4975-4983
- [111] Dixit, V., Van den Bossche, J., Sherman, D. M., Thompson, D. H., and Andres, R. P. (2006): "Synthesis and grafting of thioctic Acid-PEG-folate conjugates onto Au nanoparticles for selective targeting of folate receptor-positive tumor cells"; *Bioconjugate Chemistry* (17) p.603-609
- [112] Liang, H. F., Chen, S. C., Chen, M. C., Lee, P. W., Chen, C. T., and Sung, H. W. (2006): "Paclitaxel-loaded poly(g-glutamic acid)-poly(lactide) nanoparticles as a targeted drug delivery system against cultured HepG2 cells"; *Bioconjugate Chemistry* (17) p.291-299
- [113] Stevens, P. J., Sekido, M., and Lee, R. J. (2004): "A folate receptor-targeted lipid nanoparticle formulation for a lipophilic paclitaxel prodrug"; *Pharmaceutical Research* (21) p.2153-2157
- [114] Farokhzad, O. C., Jon, S., Khademhosseini, A., Tran, T. N., LaVan, D. A., and Langer, R. (2004): "Nanoparticle-aptamer bioconjugates: A new approach for targeting prostate cancer cells"; *Cancer Research* (64) p.7668-7672
- [115] Sahoo, S. K., Ma, W., and Labhasetwar, V. (2004): "Efficacy of transferrin-conjugated paclitaxel-loaded nanoparticles in a murine model of prostate cancer"; *International Journal of Cancer* (112) p.335-340
- [116] Hattori, Y. and Maitani, Y. (2004): "Enhanced in vitro DNA transfection efficiency by novel folate-linked nanoparticles in human prostate cancer and oral cancer"; *Journal of Controlled Release* (97) p.173-183
- [117] Lankelma, J. (2002): "Tissue transport of anti-cancer drugs"; *Current Pharmaceutical Design* (8) p.1987-1993
- [118] Lankelma, J., Fernandez Luque, R., Dekker, H., Schinkel, W., and Pinedo, H. M. (2000): "A mathematical model of drug transport in human breast cancer"; *Microvascular Research* (59) p.149-161
- [119] Ward, J. P. and King, J. R. (2003): "Mathematical modelling of drug transport in tumour multicell spheroids and monolayer cultures"; *Mathematical Biosciences* (181) p.177-207
- [120] Padron, J. M., van der Wilt, C. L., Smid, K., Smitskamp-Wilms, E., Backus, H. H. J., Pizao, P. E., Giaccone, G., and Peters, G. J. (2000): "The multilayered

- postconfluent cell culture as a model for drug screening"; *Critical Reviews in Oncology/Hematology* (36) p.141-157
- [121] O'Connor, K. C. (1999): "Three-dimensional cultures of prostatic cells: Tissue models for the development of novel anti-cancer therapies"; *Pharmaceutical Research* (16) p.486-493
- [122] Mueller-Klieser, W. "Tumor biology and experimental therapeutics"; *Critical Reviews in Oncology/Hematology* (36) p.123-139
- [123] Mueller-Klieser, W. (1997): "Three-dimensional cell cultures: from molecular mechanisms to clinical applications"; *American Journal of Physiology* (273) p.C1109-C1123
- [124] Kunz-Schughart, L. A., Freyer, J. P., Hofstaedter, F., and Ebner, R. (2004): "The use of 3-D cultures for high-throughput screening: the multicellular spheroid model"; *Journal of Biomolecular Screening* (9) p.273-285
- [125] Santini, M. T. and Rainaldi, G. (1999): "Three-dimensional spheroid model in tumor biology"; *Pathobiology* (67) p.148-157
- [126] Puleo, D. A., Kissling, R. A., and Sheu, M.-S. (2002): "A technique to immobilize bioactive proteins, including bone morphogenetic protein-4 (BMP-4), on titanium alloy"; *Biomaterials* (23) p.2079-2087
- [127] Chipman, D. M. and Sharon, N. (1969): "Mechanism of lysozyme action"; *Science* (165) p.454-465
- [128] Klaeger, A. J., Cevallos, V., Sherman, M. D., Whitcher, J. P., and Stephens, R. S. (1999): "Clinical application of a homogeneous colorimetric assay for tear lysozyme"; *Ocular Immunology and Inflammation* (7) p.7-15



# **Chapter 2**

## **Surface modification of Hydroxyapatite ceramics to modulate cell adhesion and improve tissue generation**

A. Schuessele<sup>1</sup>, B.Volk<sup>1,3</sup>, H. Mayr<sup>2</sup>, T. Blunk<sup>1</sup>, M. B. Schulz<sup>1,3</sup>, A. Goeperich<sup>1</sup>

<sup>1</sup>Department of Pharmaceutical Technology, University of Regensburg,, Germany

<sup>2</sup>Friedrich-Baur-Research Institute for Biomaterials, D-95440 Bayreuth, Germany

<sup>3</sup>Inst. for Pharm. Sciences, Pharm. Technology, Karl-Franzens-University, Graz, Austria

Proceedings of the 9<sup>th</sup> Conference on Ceramics, Cells and Tissues

“Chemistry and Microstructure, the Role for Ceramics”

Editors: A. Ravaglioli, A. Krajewski, ISTEC-CNR, Faenza, Italy, 2005, p. 87-94

## 1. Introduction

Hydroxyapatite ceramics are suitable bone replacement materials, as they resemble the natural inorganic phase of bone and provide adequate mechanical strength. Coatings of metal implants with hydroxyapatite (HA) enhanced bone integration in vivo [1-4] and hydroxyapatite culture surfaces improved the differentiation of rat marrow stromal cells to osteoblasts when compared to titanium and glass-ceramic in vitro [5].

A promising strategy to improve the osseointegration of biomaterials in general is to control the interactions at the bone-implant interface by using surface modifications, such as adhesive peptides, to promote the adhesion of osteoprogenitor cells, or the local delivery of growth factors, to stimulate cell differentiation and enhance healing and fixation.

Beneficial effects on the osseointegration have been reported when therapeutic proteins, such as BMP-2 and TGF- $\beta$  [6], were simply adsorbed to the surface of implant materials. Due to the short biological half-life and lack of long-term stability of proteins, controlled release devices have been developed to provide suitable release kinetics for prolonged stimulation [7]. But, considering the therapeutic potential of those factors and their lack of tissue selectivity, the covalent immobilization of the proteins would offer better control of the amount and distribution of the proteins delivered to the bone-implant interface and prevent uncontrolled desorption [8].

Compared to the numerous studies dealing with surface modifications of metal and metal oxide implants, only few approaches have been explored for the modification of the surface properties of hydroxyapatite by means of covalent bonding: Hydroxyapatite powder particles have been conjugated to polymers to form composite materials by either using organic isocyanates, e.g. hexamethylenediisocyanate (HMDI) [9-12], or silane coupling agents [13;14]. Both methods use the hydroxyl groups present at the surface for covalent bonding. The silane coupling method has major advantages compared to the isocyanate method: Due to the formation of silane layers, the number of functional groups that can be introduced is not limited by the number of hydroxyl groups present at the surface. Biocompatibility screening of silane-treated hydroxyapatite powders revealed no toxic effects of the silane layers [15]. Recently, adhesive peptides (RGD) were successfully immobilized at the surface of porous hydroxyapatite cylinders after treatment with aminopropyltriethoxysilane (APTES), promoting increased cell attachment over 24h compared to pure hydroxyapatite surfaces [16].

When growth factors are immobilized, it is crucial to prevent conformational changes during grafting reactions and to retain the biological activity of the proteins. Covalent bonding by the use of suitable spacer molecules, such as poly(ethylene glycol) (PEG), would lead to increased stability and to a potentiated and prolonged in vivo response, which has been demonstrated for TGF- $\beta$ 2 [17]. Additionally, PEG-grafted surfaces have been reported to

improve the stability of adsorbed fibronectin, thus promoting cell adhesion and spreading [18]. Furthermore, complete shielding of a surface by dense PEG layers would lead to the suppression of unspecific protein adsorption and cell adhesion [19] and may, thus, allow for controlled interactions with the molecules immobilized at the terminal ends of the PEG chains.

Therefore, as a first step, it was our goal to modify the surface properties of hydroxyapatite ceramic discs, as a model system, by aminosilanisation and subsequently to attach PEG. Methoxy-terminated PEG-acetaldehyde (MPEGAc) was used as a model compound for conjugation to the surface. The silanized discs were grafted with Methoxy-terminated PEG (MPEG) of varying molecular weight and the resulting surfaces were characterized by contact angle measurements and X-ray photoelectron spectroscopy (XPS). The impact of the chemical surface modifications on cell adhesion was investigated using rat marrow stromal cells (rMSC).

## 2. Materials and Methods

### 2.1. Materials

The ceramic discs were prepared from a commercially available powder (Merck, Germany), as follows: the powder was heat-treated at 700 °C to reduce the specific surface and then added to a butanolic solution of waxes, PEG 400 and 1,4-butanediol (binder and humidity storage for granulation and pressing). The suspension was stirred and subsequently dried in a rotary evaporator. The powder was sieved to < 500 µm and granulated in a tubular mixer. The resulting granulate was uniaxially pressed at 80 MPa. The so obtained discs (30 mm diameter and approx. 2 mm thickness) were sintered at 1300 °C for 1 hour in air with a heating rate of 450 K/h. The ceramic discs had a density of 99 % of the theoretical density and consisted of pure phase HA.

Aminopropyltriethoxysilane (APTES) was purchased from Aldrich and freshly distilled prior to use. Methoxy-terminated PEGs of varying molecular weights ( $M_w$ =750, 2000 and 5000 Da) were purchased from Sigma.

### 2.2. Polymer synthesis

Methoxy-terminated PEG acetaldehyde diethylacetal was synthesized following a procedure of Bentley et al. to provide a stable intermediate [20]. The polymers were characterized by  $^1\text{H}$ -NMR spectroscopy and gel permeation chromatography (GPC).

### 2.3. Surface modification

HA ceramic discs were washed with ethanol immediately before use. The aminosilanisation of the discs was performed in dry toluene. The reaction was performed in an argon atmosphere and APTES was used at a concentration of 1.5%. After 4h, the samples were thoroughly rinsed with toluene and chloroform. The density of amino groups on the discs was determined to be approximately 1 nmol/cm<sup>2</sup>, using a colorimetric method described by Puleo et al. [21].

MPEG acetaldehyde diethylacetals were hydrolyzed to the corresponding acetaldehydes in 0.1N hydrochloric acid at 50°C. The polymers were conjugated to the silanized ceramic discs by reductive amination in a 0.1M sodium tetraborate solution at pH=9.3 (Fig. 1). The polymers were used in 1000-fold molar excess relative to the amino groups present on the surface. The discs were rinsed with distilled water and dried.



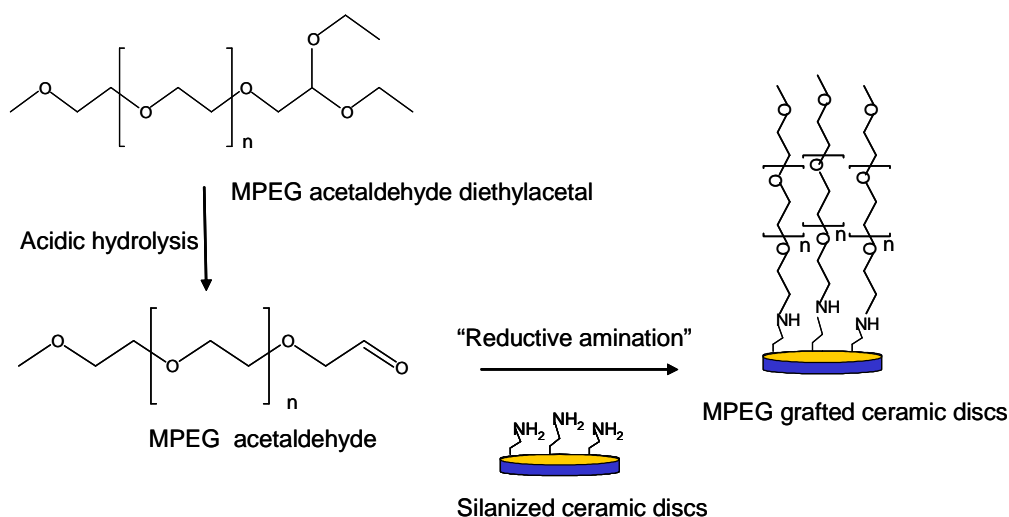


*Fig. 1: Surface modification of HA ceramic discs: Grafting of MPEG acetaldehyde to aminosilanized ceramic discs by “reductive amination”.*

## 2.4. Surface characterization

Contact angle measurements were carried out on an optical contact angle device (OCA 20; dataphysics, Filderstadt; Germany). Three discs of each modification were analyzed by seeding drops of 2  $\mu$ l of distilled water on five different points on each disc.

The XPS measurements were performed on a Phi 5700 XPS system (Physical electronics, Ismaning; Germany) using an Al  $K_{\alpha}$  source. For each sample, a survey scan was carried out with a step-size of 0.8 eV and the excited photoelectrons were analyzed at a take-off angle of 90° relative to the surface.

## 2.5. Cell adhesion study

Rat bone marrow was isolated from the femur and tibia of 6 weeks old (150-200g) male Sprague-Dawley rats following a protocol from Dobson et al. [22]. Freshly isolated bone marrow cells were resuspended in primary medium (10% FCS, 1% Penicillin/Streptomycin, 0.5% L-glutamine and minimal essential medium, alpha modification). The cells were left to adhere for 3 days before non-adherent cells were removed and the adherent cells were further cultured in humidified atmosphere with 5% CO<sub>2</sub> at 37°C. On day 7 or 8 after isolation (80% confluency) the cells were trypsinized, resuspended in medium supplemented with 10% serum and seeded at a density of 10,000 cells /cm<sup>2</sup> on the discs, which corresponds to 20% confluency. After incubation for 3h, unattached cells were removed by rinsing with PBS. Adherent cells were fluorescently stained with Calcein AM (Biotium, Hayward, USA). For cell number assessment, photographs over the entire diameter were taken using a 4-fold magnification and the cells were counted either manually or using the ImageJ program (<http://rsb.info.nih.gov/ij/>, version 1.31).

### 3. Results and Discussion

#### 3.1. Polymer synthesis

We synthesized MPEG acetaldehyde diethylacetal as a stable derivative that can be stored and easily hydrolysed to the corresponding acetaldehyde immediately before use. Using the chosen synthesis route, more than 80% of the hydroxyl groups became acetals, as determined by integration of the respective signals in the  $^1\text{H}$ -NMR-spectra (Tab. 1). The acetal group was completely cleaved by acidic hydrolysis to result in the respective acetaldehyde, as analyzed by  $^1\text{H}$ -NMR-spectroscopy according to [20] (data not shown).

POLYMER	YIELD [%]	ACETAL GROUPS [%] ( $^1\text{H}$ -NMR spectroscopy)
MPEG Acetal, $M_w = 750$ Da	25	87
MPEG Acetal, $M_w = 2000$ Da	50	83
MPEG Acetal, $M_w = 5000$ Da	87	88

*Tab. 1: MPEG derivatives; the content of acetal groups was determined to be more than 80% for the 3 MPEG acetaldehyde diethylacetals used in this study.*

GPC analysis of the polymers prior to and after derivatization revealed no major changes in chain length due to cleavage, oxidation or the formation of dimers (Fig. 2). The slight increase in molecular weight due to the conjugation of the acetaldehyde diethylacetal groups to the polymer chains caused a shorter retention time on the GPC column. For the low molecular weight derivative (MPEG 750), this effect is clearly visible (Fig. 2A). For MPEG 2000 only a minor difference in retention time was observed (Fig. 2B), while the relative increase in molecular weight after the reaction was too small in the case of MPEG 5000 to result in a shorter retention time on the column (Fig. 2C).

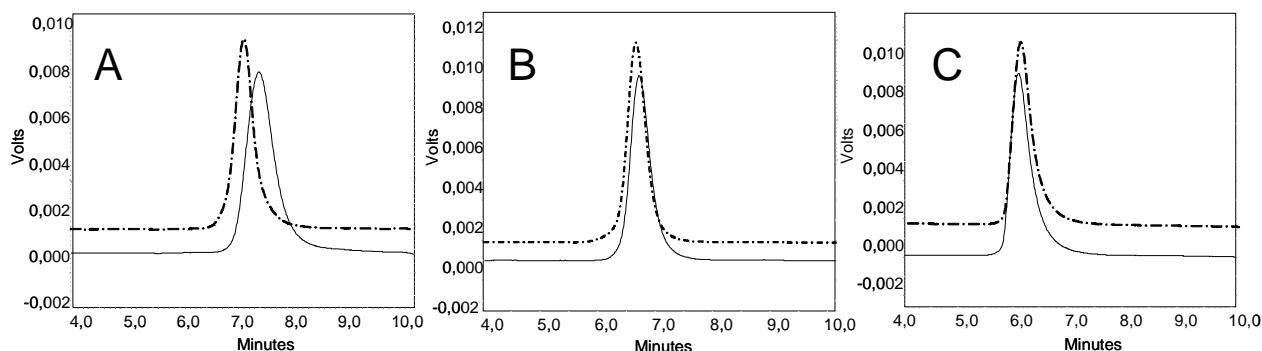


Fig. 2: GPC chromatograms of methoxy-poly(ethylene glycol) ( $M_w=750$  [A], 2000 [B] and 5000 Da [C]) and the respective acetaldehyde diethylacetal derivatives. The black lines correspond to MPEG prior to synthesis and the dotted line to the corresponding acetaldehyde diethylacetal.

### 3.2. Surface characterization

#### 3.2.6. Contact angle

The contact angle measurements of unmodified and PEGylated ceramics revealed differences in hydrophobicity (Fig. 3). The formation of a hydrophobic aminosilane layer at the ceramic surface caused the contact angle between water and the discs to increase significantly from  $35^\circ$  to  $65^\circ$ . When attaching MPEGAc, a hydrophilic polymer, to the amino groups on the surface of the ceramic, the surfaces performed differently depending on the molecular weight of the attached polymer. Following grafting of the 750 and 2000 Da derivatives, contact angle values similar to the silanized surface were measured ( $65^\circ$ ). The polymer chains - although hydrophilic - were not capable of changing the hydrophobic character of the surface caused by the silane layer. In contrast, binding of the 5000 Da polymer resulted in a significantly lower contact angle measurement ( $47^\circ$ ), that is, the longer polymer chains of MPEG 5000 were capable of changing the hydrophobic character of the aminosilanized discs.

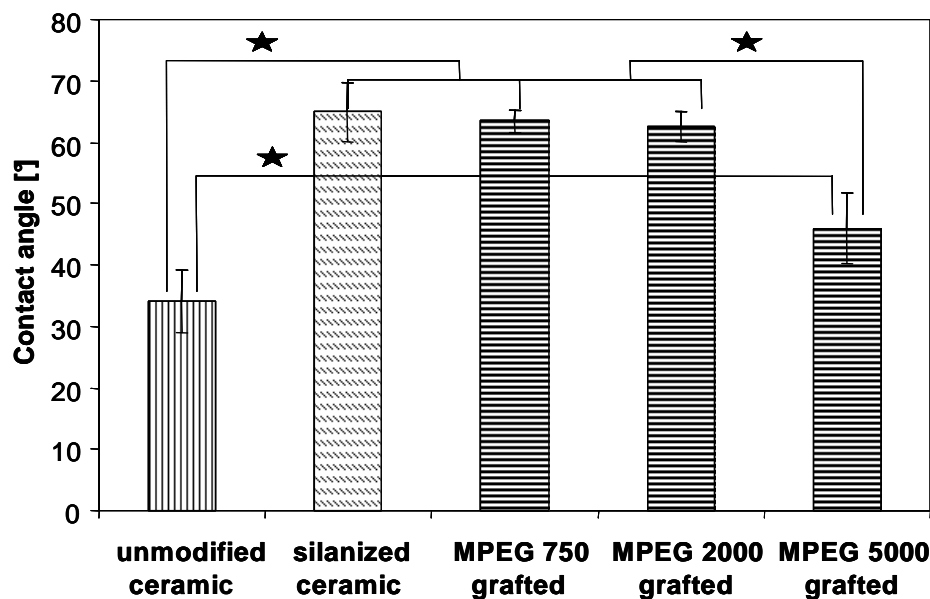


Fig. 3: Contact angles of modified and unmodified ceramic discs. Significant differences ( $p < 0.05$ ) between the groups were marked with ★.

### 3.2.7. X-ray photoelectron spectroscopy (XPS)

To characterize the modified discs more precisely, the elemental composition of the uppermost surface layers was determined by XPS (Tab. 2). All surfaces contained the elements Ca, P, O, C, Si and N in varying amounts. The Ca/P ratio obtained for the unmodified ceramic discs was 1.8, which is close to the theoretical ratio for hydroxyapatite (1.67). After the silanization, the content of Si and N increased due to the formation of the silane layer.

When comparing the unmodified and modified ceramic discs, the calcium content in the uppermost surface layers decreased after surface grafting with APTES and the respective MPEGAcS. Initially, the uppermost layers contained 14.7 % Ca (unmodified ceramic), which was reduced with increasing PEG chain length to 7.7 % for MPEG 5000-grafted ceramic), indicating a gradually progressive coverage of the surfaces. When looking at the O/C ratio of the MPEG-grafted discs, a shift towards the theoretical O/C ratio of a pure PEG surface occurred with increasing molecular weight of the attached polymer chains, indicating again that the thickness of the created MPEG-layer was linked to the molecular weight of the respective polymer.

These data also demonstrate that the MPEG coatings were thinner than the XPS probe depth (10nm), as the elements present only in the pure ceramic surface, such as Ca and P, were still detected.

Sample	% O	% C	% Si	% N	% Ca	% P	O/C
Unmodified ceramic	49.2	21.8	0.9	1.1	14.7	8.3	2.3
Silanized ceramic	39.3	38.2	3.4	2.2	10.0	6.9	1.0
MPEG-750 grafted ceramic	44.9	30.8	2.9	1.7	11.0	8.0	1.5
MPEG-2000 grafted ceramic	40.2	39.4	1.8	1.9	9.5	7.0	1.0
MPEG-5000 grafted ceramic	32.0	50.0	3.0	1.5	7.7	5.8	0.6
PEG (theoretical)	34	66					0.5

Tab. 2: Elemental composition of the uppermost surface layers determined by XPS survey scans and O/C ratio calculated from the data.

### 3.3 Cell adhesion study

Rat marrow stromal cells (rMSC) were seeded onto discs modified with MPEG 750 and MPEG 5000 to investigate whether the surface modifications had any impact on the adhesion behavior of cells. Again, the discs performed differently depending on the molecular weight of the attached MPEG derivative (Fig. 4).

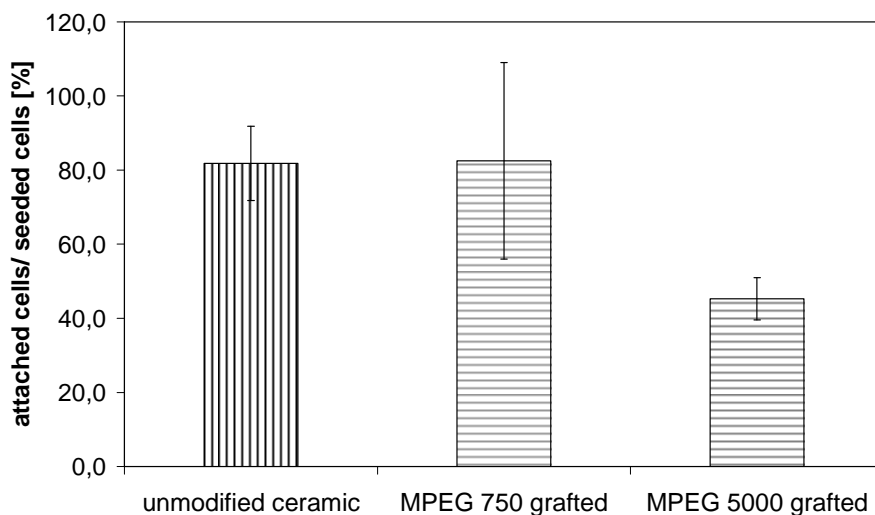


Fig. 4: Adhesion of rat marrow stromal cells on unmodified ceramic discs and PEGylated ceramic discs. The values represent the number of attached cells/seeded cells.

After 3h, 80% of the initially seeded cells adhered to the unmodified ceramic discs. The cell adhesion to surfaces grafted with 750 Da MPEG chains remained unchanged. In contrast, only 43% of cells adhered to the surface coated with 5000 Da MPEG. This indicated that more effective surface shielding was achieved using the derivative of higher molecular weight.

In our model system, which was based on introducing a certain density of amino groups at the surface and varying the molecular weight of the attached polymer, the characteristics of the resulting surfaces were dependent on the molecular weight of the grafted MPEG derivative. Thus, low molecular weight PEG would be a suitable spacer molecule for protein attachment in cases where interactions with the surface of the material are desired. When the avoidance of non-specific interactions between cells and material is preferable, complete shielding from unspecific protein adsorption would be necessary. For this purpose, a higher molecular weight PEG could be a suitable spacer. A more densely packed PEG layer could potentially be created by varying the reaction conditions for reductive amination [23].

## **4. Conclusion**

The surfaces of hydroxyapatite ceramic discs were successfully modified by using APTES to create an amino group-containing layer. MPEG derivatives of varying molecular weights were synthesized and covalently attached to the amino groups present at the surface. The MPEG-grafted surfaces performed differently with regard to hydrophobicity and adhesion of rMSCs, dependent on the molecular weight of the respective polymer. This represents the first step towards covalent bonding of proteins by the application of PEG as a spacer molecule. Methods for the immobilization of proteins by using bifunctional PEGs are under investigation.

## **Acknowledgements**

This work was financially supported by the Bayerische Forschungsförderung (ForTePro).

## 5. References

- [1] Vasudev, D. V., Ricci, J. L., Sabatino, C., Li, P., and Parsons, R. (2004): "In vivo evaluation of a biomimetic apatite coating grown on titanium surfaces"; *Journal of Biomedical Materials Research* (69A) p.629-636
- [2] Stephenson, P. K., Freeman, M. A., Revell, P. A., Germain, J., Tuke, M., and Pirie, C. J. (1991): "The effect of hydroxyapatite coating on ingrowth of bone into cavities in an implant"; *Journal of Arthroplasty* (6) p.51-58
- [3] Cook, S. D., Thomas, K. A., Dalton, J. E., Volkman, T. K., Whitecloud, T. S., and Kay, J. F. (1992): "Hydroxylapatite coating of porous implants improves bone ingrowth and interface attachment strength"; *Journal of Biomedical Materials Research* (26) p.989-1001
- [4] Geesink, R. G., de Groot, K., and Klein, C. P. (1988): "Bonding of bone to apatite-coated implants"; *Journal of Bone and Joint Surgery*. British volume (70) p.17-22
- [5] Ozawa, S. and Kasugai, S. (1996): "Evaluation of implant materials (hydroxyapatite, glass-ceramics, titanium) in rat bone marrow stromal cell culture"; *Biomaterials* (17) p.23-29
- [6] Chen, R. R. and Mooney, D. J. (2003): "Polymeric Growth Factor Delivery Strategies for Tissue Engineering"; *Pharmaceutical Research* (20) p.1103-1112
- [7] Luginbuehl, V., Meinel, L., Merkle, H. P., and Gander, B. (2004): "Localized delivery of growth factors for bone repair"; *European Journal of Pharmaceutics and Biopharmaceutics* (58) p.197-208
- [8] Puleo, D. A. and Nanci, A. (1999): "Understanding and controlling the bone-implant interface"; *Biomaterials* (20) p.2311-2321
- [9] Dong, G., Sun, J.-S., Yao, C.-H., Jiang, G.-J., Huang, C.-W., and Lin, F.-H. (2001): "A study on grafting and characterization of HMDI-modified calcium hydrogenphosphate"; *Biomaterials* (22) p.3179-3189
- [10] Liu, Q., de Wijn, J. R., and van Blitterswijk, C. A. (1998): "A study on the grafting reaction of isocyanates with hydroxyapatite filler particles"; *Journal of Biomedical Materials Research* (40) p.358-364
- [11] Liu, Q., de Wijn, J. R., de Groot, K., and van Blitterswijk, C. A. (1998): "Surface modification of nano-apatite by grafting organic polymer"; *Biomaterials* (19) p.1067-1072
- [12] Liu, Q., de Wijn, J. R., and van Blitterswijk, C. A. (1998): "Composite biomaterials with chemical bonding between hydroxyapatite filler particles and PEG/PBT copolymer matrix"; *Journal of Biomedical Materials Research* (40) p.490-497
- [13] Furuzono, T., Sonoda, K., and Tanaka, J. (2001): "A hydroxyapatite coating covalently linked onto a silicone implant material"; *Journal of Biomedical Materials Research* (56) p.9-16
- [14] Deb, S., Wang, M., Tanner, K. E., and Bonfield, W. (1996): "Hydroxyapatite-polyethylene composites: effect of grafting and surface treatment of hydroxyapatite"; *Journal of Materials Science: Materials in Medicine* (7) p.191-193
- [15] Dupraz, A. M. P., Meer, S. A. T., de Wijn, J. R., and Goedemoed, J. H. (1996): "Biocompatibility screening of silane-treated hydroxyapatite powders, for use as filler in resorbable composites"; *Journal of Materials Science: Materials in Medicine* (7) p.731-738
- [16] Durrieu, M. C., Pallu, S., Guillemot, F., Bareille, R., Amedee, J., Baquey, C., Labrugere, C., and Dard, M. (2004): "Grafting RGD containing peptides onto hydroxyapatite to promote osteoblastic cells adhesion"; *Journal of Materials Science: Materials in Medicine* (15) p.779-786
- [17] Bentz, H., Schroeder, J. A., and Estridge, T. D. (1998): "Improved local delivery of TGF- $\beta$ 2 by binding to injectable fibrillar collagen via difunctional polyethylene glycol"; *Journal of Biomedical Materials Research* (39) p.539-548
- [18] Altankov, G., Thom, V., Groth, T., Jankova, K., Jonsson, G., and Ulbricht, M. (2000): "Modulating the biocompatibility of polymer surfaces with poly(ethylene glycol): effect of fibronectin"; *Journal of Biomedical Materials Research* (52) p.219-230

- [19] Kingshott, P. and Griesser, H. J. (1999): "Surfaces that resist bioadhesion"; *Current Opinion in Solid State and Materials Science* (4) p.403-412
- [20] Bentley, M. D., Roberts, M. J., and Harris, J. M. (1998): "Reductive Amination Using Polyethylene glycol Acetaldehyde Hydrate Generated in Situ: Applications to Chitosan and Lysozyme"; *Journal of Pharmaceutical Sciences* (87) p.1446-1449
- [21] Puleo, D. A. (1995): "Activity of enzyme immobilized on silanized Co-Cr-Mo"; *Journal of Biomedical Materials Research* (29) p.951-957
- [22] Dobson, K. R., Reading, L., Haberey, M., Marine, X., and Scutt, A. (1999): "Centrifugal isolation of bone marrow from bone: an improved method for the recovery and quantitation of bone marrow osteoprogenitor cells from rat tibiae and femuræ"; *Calcified Tissue International* (65) p.411-413
- [23] Kingshott, P., Thissen, H., and Griesser, H. J. (2002): "Effects of cloud point grafting, chain length and density of PEG layers on competitive adsorption of ocular proteins"; *Biomaterials* (23) p.2043-2056



# **Chapter 3**

## **Labeling of lysozyme and BMP-2 with $^{125}$ Iodine for the characterization of protein immobilization methods**

A. Schuessele<sup>1</sup>, A. Goeperich<sup>1</sup>

<sup>1</sup>Department of Pharmaceutical Technology, University of Regensburg, Germany

**Abstract**

Aiming for immobilization of proteins on the surface of hydroxyapatite (HA) ceramic discs analytical methods were searched to determine even trace amounts of protein and compare different surface modification strategies with regard to their efficacy in protein immobilization. The use of radiolabeled compounds provides a possibility to overcome the detection limits of other established methods and additionally gather quantitative information. Therefore, the goal was to establish a procedure for radioactive labeling of lysozyme and BMP-2 using the chloramine-T method. In “cold” experiments, the iodination was determined to be successful for lysozyme without affecting protein integrity. In contrast, BMP-2 was either destroyed by the oxidizing agent chloramine-T or lost in the preparation process due to strong adsorption to reaction vessels or the column used for purification. Lysozyme was then radiolabeled, purified to result in a specific activity > 95 %, and an adsorption study on HA ceramic discs was carried out. In our study, dependent on the concentration of the feed solution 0.1 – 1 µg of lysozyme adsorbed to the ceramic discs. The protein mass per disc was reduced to 0.05 - 0.1 µg after washing the discs with a surfactant. Significant differences were determined. For lysozyme, the demonstrated procedure will be suitable for the investigation of protein immobilization, while for BMP-2 alternative methods have to be established.

## 1. Introduction

Localized delivery of growth factors to the bone-implant interface is a promising strategy to improve healing and fixation of implants in the surrounding tissue [1]. For some growth factor, such as BMP-2, deposited on a surface or released from a delivery device, the amount and release kinetics are of particular interest as the cellular response is strongly dependent on the dose of growth factor and the duration of exposure [2].

To characterize surface modifications such as protein adsorption and immobilization several methods are described in literature. Surface roughness and orientation of macromolecules such as proteins on a surface can be investigated by atomic force microscopy (AFM) [3]. Using X-ray photoelectron spectroscopy (XPS) information about the elemental composition of the uppermost layers of a surface can be obtained [4]. Proteins adsorbed or attached to a surface can be identified by means of Time-of-flight secondary ion mass spectroscopy (ToF-SimS) [5]. While all these methods provide excellent qualitative data, they are not suited for quantifying the amount of protein present on a materials surface. Although some authors were successful in using protein assays such as the BCA assay for the detection of surface immobilized proteins [6], the protein amount on some surfaces is below the detection limit of the method. An alternative method to analyze even traces of protein is provided by radiolabeled compounds that can be prepared by a variety of well-established methods using isotopes, such as  $^{14}\text{C}$ ,  $^{125}\text{I}$  or  $^3\text{H}$  [7]. In order to use the primary amines of the proteins for covalent attachment to the surface, methods such as the Bolton-Hunter-method or the  $^{14}\text{C}$ -methylation, were not appropriate for our purposes and therefore the chloramine-T method was chosen [7]. By the chloramine-T method aromatic rings of tyrosine and histidine residues are halogenated. For the proteins that were intended to be immobilized on the ceramic surfaces, lysozyme and bone morphogenetic protein-2 (BMP-2) [8], radiolabeling with the chloramine-T method is described in literature [9-11].

To assure that lysozyme and BMP-2 were not affected by the procedure, the reaction was first carried out under “cold” conditions with the non radioactive isotope  $^{126}\text{I}$  and the product was characterized by high performance liquid chromatography combined with mass spectrometry (HPLC-MS) for lysozyme and matrix assisted laser desorption/ionization time of flight mass spectroscopy (MALDI-ToF) for BMP-2. The objective was to establish a procedure that would allow for quantitative analysis of proteins on the surface of ceramic discs and furthermore for comparison of different techniques for protein immobilization.

## **2. Materials and Methods**

### **2.1. Materials**

Sodium hydrogen phosphate, sodium dihydrogen phosphate, trichloroacetic acid, lysozyme (50.000 units/mg) and sinapic acid were bought from Sigma-Aldrich (Steinheim, Germany). 0.1 M hydrochloric acid, potassium chloride (KI) and chloramine-T were purchased from Merck (Darmstadt, Germany). <sup>125</sup>Iodide - as alkaline solution of NaI (37 MBq/ml) - and PD 10 columns were purchased from Amersham Biosciences (Freiburg, Germany). Sodium dodecylsulfate (SDS) and phosphate-buffered saline (PBS) were obtained from Invitrogen (Karlsruhe, Germany). Acetonitrile for high performance liquid chromatography (HPLC) was purchased from Mallinckrodt Baker (Griesheim, Germany). Bone Morphogenetic Protein-2 (BMP-2) was produced by Scil Proteins (Halle, Germany). Water was of double distilled quality. Hydroxyapatite (HA) ceramic discs were provided by the Friedrich-Baur-Research Institute for Biomaterials (Bayreuth, Germany). The ceramic discs had a density of 99 % of the theoretical density and consisted of phase pure, crystalline hydroxyapatite (HA). All reagents were of analytical grade and used as received unless otherwise noted. To reduce protein adsorption, all materials (glass vials, eppendorf cups) in contact with protein solution has been pre-treated with Sigmacote™ (Sigma-Aldrich, Steinheim, Germany) following manufacturer's instructions.

### **2.2. Iodination of lysozyme**

#### **2.2.1. Iodination of lysozyme**

Lysozyme was labeled using the chloramine-T method. To establish the procedure of radiolabeling, iodide (KI) and lysozyme were used in different stoichiometric relations (1:1, 3:1, 5:1 and 1:100; the last being the conditions for radiolabelling as a content of 0.1 % of labeled product allows for quantitative analysis). For the preparation of a 1 mg/ml lysozyme solution 2 µl of an aqueous KI solution were added to 1 ml of a 1 mg/ml solution of lysozyme in PBS. After the addition of 100 µl of a 0.2 mg/ml chloramine-T solution, the mixture was shaken for 10 min. In order to stop the reaction, 100 µl of a 4 mg/ml sodium metabisulfite solution was mixed and shaken with the lysozyme solution for 2 min.

#### **2.2.2. Purification of labeled protein: Size exclusion chromatography (SEC)**

The resulting solution was purified using a PD-10 column, Sephadex G-25 M (Amersham Biosciences, Uppsala, Sweden) and lysozyme was eluted using a phosphate-buffered saline (PBS) pH 7.4. Different sample volumes were used to determine the elution method resulting in the highest protein concentration after SEC. Fractions of 1 ml were collected and the protein concentration was determined by UV-spectroscopy at 274 nm (Uvikon 941, Kroton Inc., Munich, Germany). To assure that the fractions were free of iodide, 2-3 drops of

a silver nitrate solution were added to aliquots of the fractions and the precipitate was checked for the presence of yellow silver iodide.

### 2.2.3. High performance liquid chromatography coupled with mass spectrometry (HPLC-MS)

For HPLC-MS analysis, samples were analyzed using an Agilent 1100 HPLC system with degasser, binary pump, autosampler, column oven and diode array detector (all from Agilent, Waldbronn, Germany), coupled with a TSQ7000 mass spectrometer (ThermoQuest, San Jose, CA, USA) with API2-source (capillary temperature: 300 °C, spray voltage: 4 kV). A mixture of 68 % solvent A (acetonitrile + 0.1 % TFA) and 32 % solvent B (distilled water + 0.1 % TFA) served as a mobile phase at a flow rate of 0.2 ml/min for 20 min. For the next 4 min a linear gradient of 32-95 % solvent B in solvent A was carried out and for additional 4 min the content of B in A was decreased to 32 % again and kept constant for further 2 min. 30 µl of the samples were separated using a C18 reversed phase analytical column (Jupiter, 2 mm X 250 mm) from Phenomenex (Aschaffenburg, Germany). The XCALIBUR® software package (ThermoQuest, San Jose, CA, USA) was used for data acquisition and analysis.

## 2.3. Iodination of BMP-2

### 2.3.1. Iodination of BMP-2

The iodination of BMP-2 was carried out as described by Yamamoto et al. [9]. <sup>126</sup>I was used as non radioactive isotope to analyze if BMP-2 was destroyed by the reaction procedure. 4 µl of an aqueous KI solution (5 mg/ml) were added to 90 µl of BMP-2 solution (5 mg/ml) in 5 mM glutamic acid, 2.5 wt% glycine, 0.5 wt% sucrose, and 0.01 wt% Tween 80 (pH 4.5). Then, 0.2 mg/ml of chloramine-T in 0.5 M potassium phosphate-buffered solution (pH 7.5) containing 0.5 M sodium chloride (100 µl) was added to the solution mixture. After agitation at room temperature for 2 min, 100 µl of phosphate-buffered saline solution (PBS, pH 7.4) containing 0.4 mg of sodium metabisulfate were added to the reaction solution to stop the iodination.

### 2.3.2. Purification of labeled protein: Anion exchange chromatography

The reaction mixture was passed through an anionic-exchange column (Dowex 1 X 8, mesh size 200-400, packed in 2.5 ml syringe) to remove the uncoupled, free I molecules from the I-labeled BMP-2. Fractions of 0.5 ml were collected and analyzed by UV-spectroscopy at 278 nm (Uvikon 941, Kroton Inst., Munich, Germany). The column chromatography was first carried out with lysozyme (100 µl of a lysozyme solution (5 mg/ml) + 100 µl of the chloramine-T solution + 100 µl of sodium metabisulfite solution) to determine the protein rich fractions and then BMP-2 after the reaction with Iodine was passed through a column.

### 2.3.3. Characterization of labeled protein: MALDI-ToF

The spectra were recorded on a HP G2030A MALDI-ToF MS system (HP G 2025A MALDI-ToF MS spectrometer from Hewlett Packard, Germany).

1 ml of a BMP-2 solution in 10 mM hydrochloric acid (1 mg/ml) and 3 ml of freshly prepared solution of sinapic acid in a mixture of 70% (v/v) acetonitrile and 30% (v/v) methanol (10 mg/ml) were mixed and dropcasted as one layer onto the MALDI sample target. For the fractions of the column chromatography, BMP-2 samples were freeze dried and dissolved in 10 mM hydrochloric acid to a concentration of 1 mg/ml before mixed with 3 volumes of freshly prepared solution of sinapic acid in a mixture of 70% (v/v) acetonitrile and 30% (v/v) methanol (10 mg/ml).

## 2.4. Adsorption of $^{125}\text{I}$ -lysozyme to hydroxyapatite ceramic discs

### 2.4.1. Radioiodination of lysozyme

For the preparation of a 1 mg/ml lysozyme solution 2.00  $\mu\text{l}$   $\text{Na}^{125}\text{I}$  (1.5-2 MBq) were added to 1 ml of a 1 mg/ml solution of lysozyme in PBS. After the addition of 100  $\mu\text{l}$  of a 0.2 mg/ml chloramine-T solution, the mixture was shaken for 10 min. In order to stop the reaction, 100  $\mu\text{l}$  of a 4 mg/ml sodium metabisulfite solution were mixed and shaken with the lysozyme solution for 2 min. The reaction mixture was passed through a PD-10 column and eluted with PBS. Fractions of 1 ml were collected and checked for  $\gamma$ -ray activity using a NaI(Tl)-Scintillation-Detector (Ortec, Oak Ridge, USA) calibrated with a  $^{137}\text{Cs}$  standard source (Amersham Biosciences, Freiburg, Germany). The GammaVision-32 software package (Version 5.2; Ortec, Oak Ridge, USA) was used for data analysis. The fraction of highest protein concentration (Fraction "4", 4<sup>th</sup> ml of eluent), was used for the adsorption experiments.

### 2.4.2. Determination of specific protein bound radioactivity

25  $\mu\text{l}$  of the protein rich fractions (3, 4 and 5) were diluted with 2 ml of water and submitted to scintillation to determine the total activity of the samples (100 %). In order to determine the protein bound activity, 50  $\mu\text{l}$  of the protein rich fractions (3, 4 and 5) were precipitated in Eppendorf cups in 1 ml of a solution of 10 % trichloroacetic acid and left on ice for 30 min. The precipitates were separated by centrifugation and 500  $\mu\text{l}$  of the supernatant were diluted with 1.5 ml water and submitted to scintillation. The activity measured here was due to free, non-protein bound activity. Values of specific protein bound activity were calculated as  $100 - x$  %, whereas 100 % is the activity of the protein solution and  $x$  encodes the activity of the supernatant after precipitation of the proteins.

### 2.4.3. Adsorption and washing procedure

To establish a washing procedure to distinguish between reversibly bound protein and "immobilized" protein, hydroxyapatite ceramic discs ( $n=3$ ) were incubated with 2 ml of a

solution of 10 µg/ml  $^{125}\text{I}$ -lysozyme over night. Samples were washed 5 times with 2 ml of water or 2 ml of a solution of 1 % SDS in PBS. The washing solutions were analyzed for  $\gamma$ -ray activity and the samples were measured after all 5 washing steps had been performed.

#### 2.4.4. Adsorption of $^{125}\text{I}$ -lysozyme to HA ceramic discs

Hydroxyapatite ceramic discs (n=3) were immersed in 2 ml PBS buffer containing varying amounts of  $^{125}\text{I}$ -lysozyme (1, 10, 25, 50 µg) and left to adsorb overnight. The ceramic samples were first washed with water, activity was determined and in a second step washed with a solution of 1 % SDS in PBS and activity was determined again (Fig. 1) to distinguish between weakly bound and irreversibly adsorbed lysozyme. A standard curve was prepared using different dilutions of labeled lysozyme according to [12].

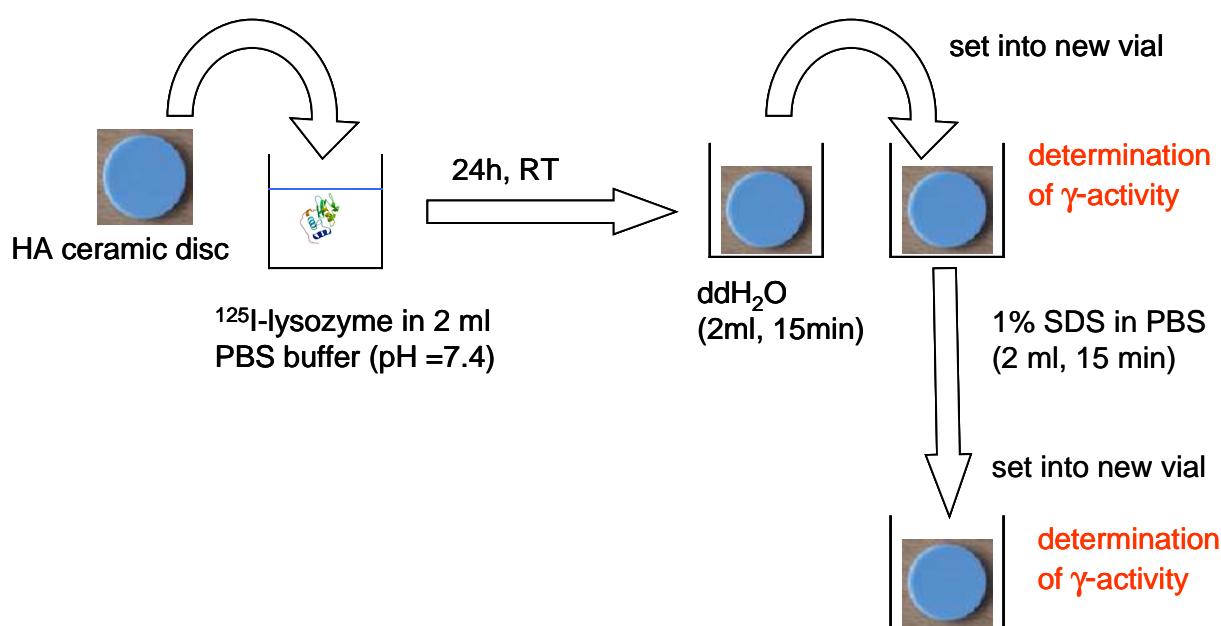


Fig. 1: Schematic setup for the adsorption experiments of  $^{125}\text{I}$ - lysozyme on HA ceramic discs using different concentrations of  $^{125}\text{I}$ -lysozyme.

### 3. Results

#### 3.1. Iodination of lysozyme

To separate iodinated protein from free iodide after labeling of lysozyme, a size exclusion chromatography (SEC) procedure was established. Different sample volumes were used in order to obtain a concentrated protein solution, ideally with the complete lysozyme in one fraction. The fractions collected after SEC were analyzed by UV-spectroscopy for absorption at 278 nm. The preparation method using 1 ml of sample volume resulted in the highest protein concentration in one fraction (fraction 4, Fig. 2). Consequently, to obtain even more concentrated protein solutions less sample volume has to be used. Unfortunately, this was not possible due to poor solubility of lysozyme in the reaction buffer. Therefore, the elution procedure with 1 ml of sample volume and fraction 4 were used for further experiments.

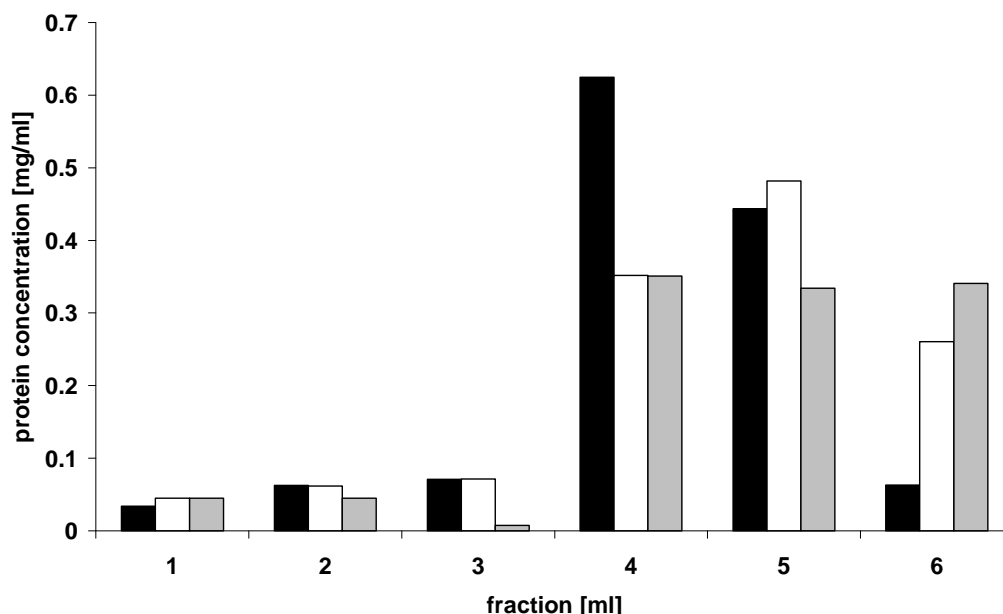
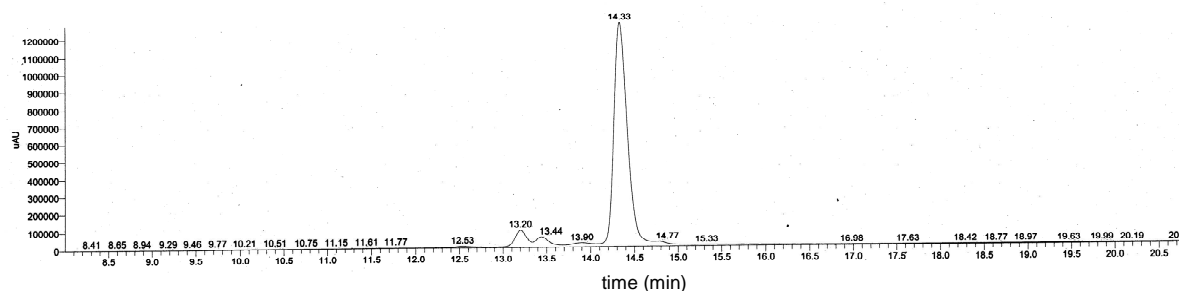


Fig. 2: SEC of lysozyme with starting with different sample volumes: 1 ml (■), 2 ml (□) and 3 ml (▒). Fractions of 1 ml were collected and the content of lysozyme was determined by UV-spectroscopy at 278 nm.

After SEC, iodinated lysozyme in fraction 4 was analyzed with focus on changes in molecular weight due to the substitution of  $^1\text{H}$  by  $^{125}\text{I}$  or fragmentation. As 0.1 % of radiolabeled lysozyme per total protein would be enough for the detection of proteins on ceramic surfaces, lysozyme was iodinated in a ratio of 1:1000 and the product was characterized by HPLC-MS (Fig. 3). The spectrum displayed only signals of molecule ions corresponding to the mass of unmodified lysozyme (2385.8 Da for the 5+ and 2862.7 Da for the 4+ adduct) (Fig. 3) due to the detection limits of the HPLC-MS method. Fragments due to oxidation were not detected.



a)



b)

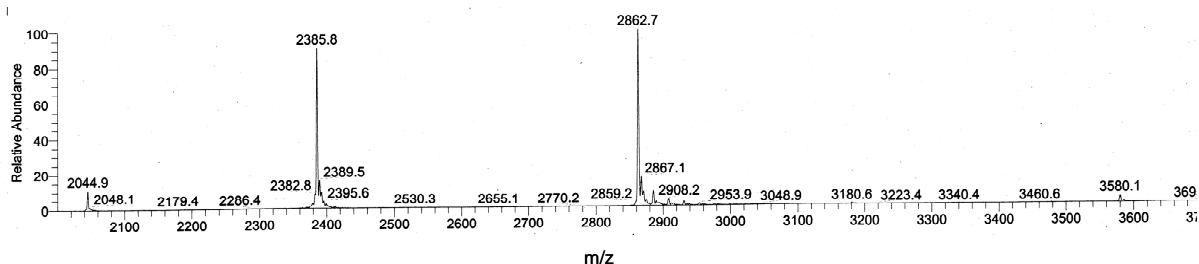
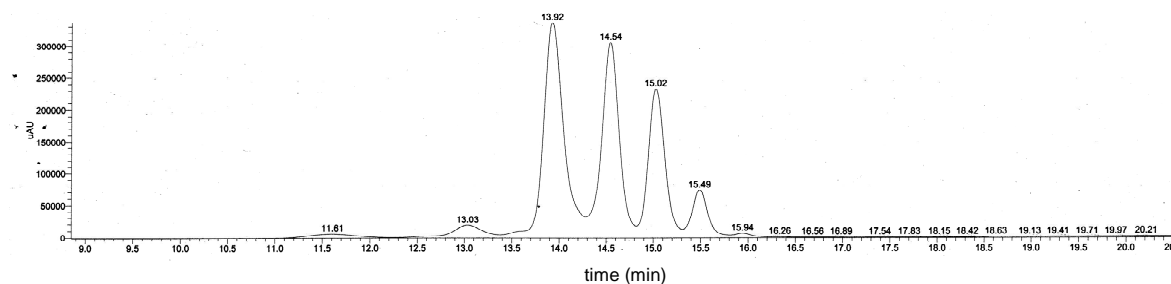


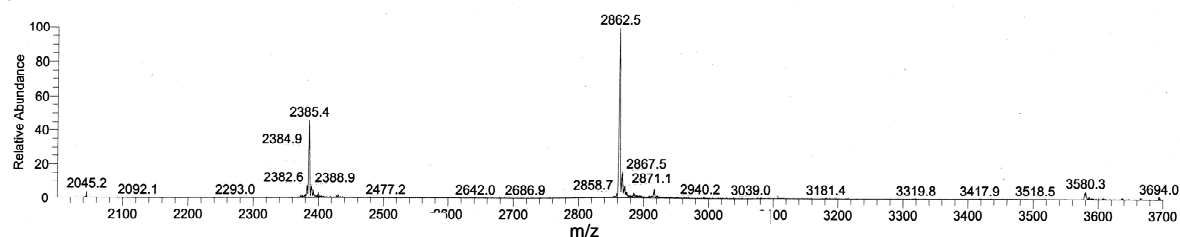
*Fig. 3: HPLC-MS of iodinated lysozyme (ratio 1000:1): a) HPLC chromatogram, UV-detector (274 nm) b) mass spectrum of the main peak (retention time 14:33 min) displaying masses of a 4+ lysozyme and 5+ lysozyme.*

To investigate if the reaction would happen in general an excess of iodide was used in a stoichiometric ratio of iodide to lysozyme of 5:1. The product of this reaction was purified by SEC and fraction 4 was analyzed by HPLC-MS (Fig. 4). In the HPLC-chromatogram (Fig. 4 a), 4 separate peaks with retention times varying from 13 to 16 min were found. The mass of the substances of each peak were analyzed and revealed that peak 1 corresponded to mono-iodinated lysozyme (Fig. 4 b), peak 2 corresponded to double-iodinated lysozyme (Fig. 4 c), peak 3 corresponded to lysozyme with three iodine per molecule (Fig. 4 d), and peak 4 corresponded to a mixture of lysozyme with three or four iodine per molecule (Fig. 4 e). Again signals of lower molecular weight fragments were not detected. Although the results are not exactly quantitative, the single-iodinated lysozyme seems to be the main product obtained according to the HPLC-chromatogram.

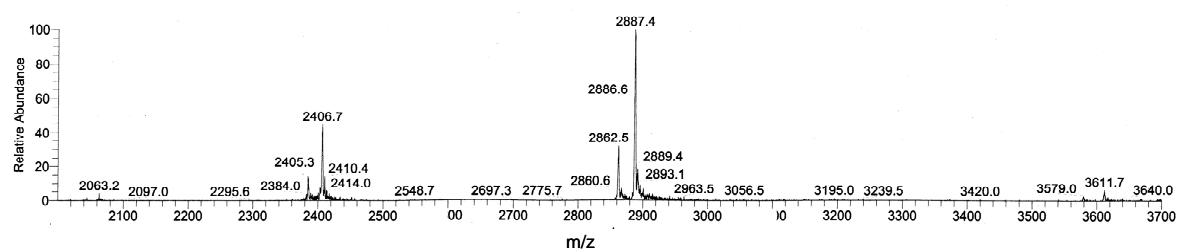
a)



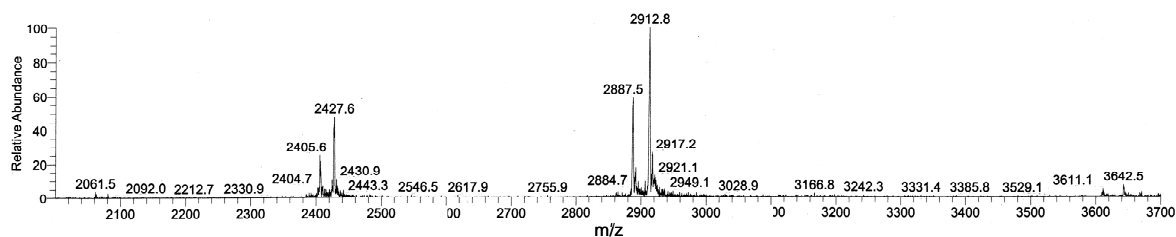
b)



c)



d)



e)

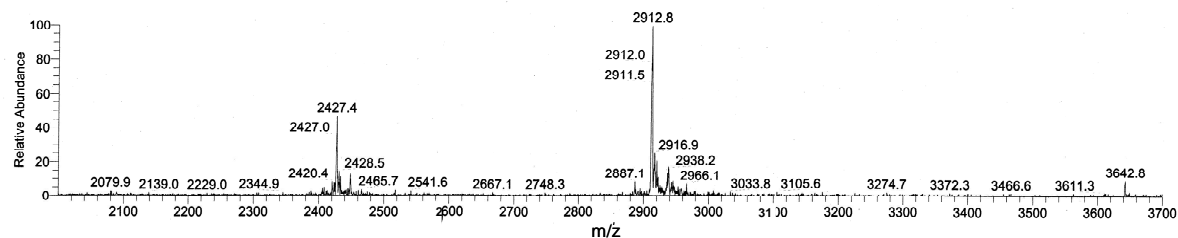


Fig. 4: HPLC-MS of iodinated lysozyme (ratio 1:5): **a)** HPLC chromatogram, UV-detector (274 nm); **b)-e)** mass spectra of peaks 1 to 4 displaying masses of 4-fold and 5-fold charged lysozyme substituted with 1-4 iodines.

### 3.2. Iodination of BMP-2

The iodination of BMP-2 was performed as described in the literature [9]. BMP-2 was separated from free iodide using anion exchange chromatography. Lysozyme was used as a control in advance to determine the protein containing fractions. Fractions of 0.5 ml were collected. For lysozyme three protein rich fractions were detected by UV-spectroscopy (2, 2.5 and 3). The total amount of lysozyme in fraction 1 to 5 corresponds to 97 % of protein amount that was submitted to the column. For BMP-2 less than 30 % of the total protein amount were eluted from the column as quantified by UV-spectroscopy.

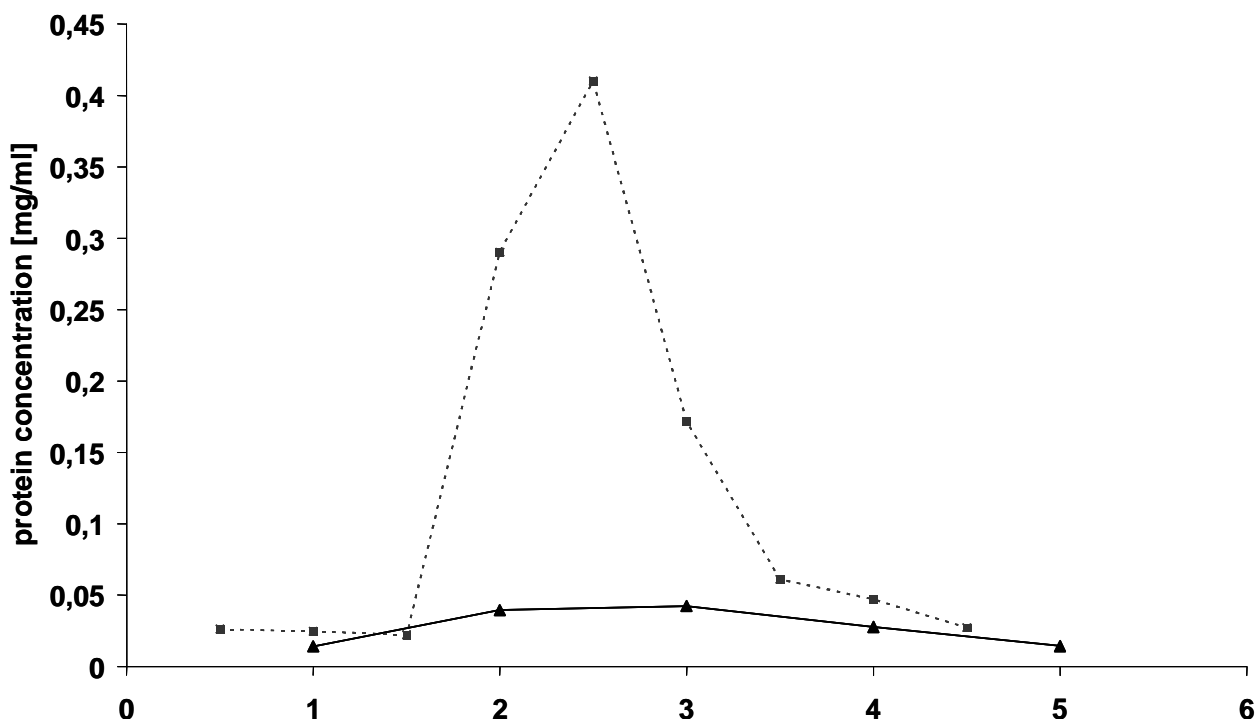
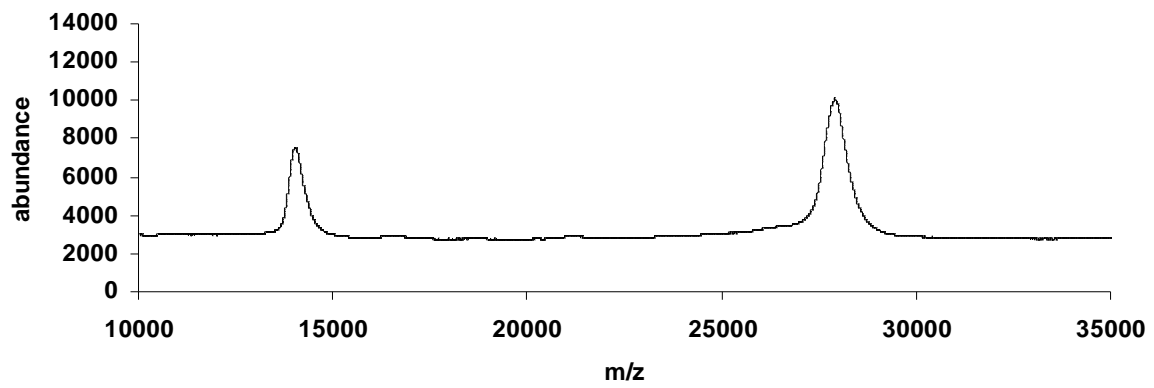


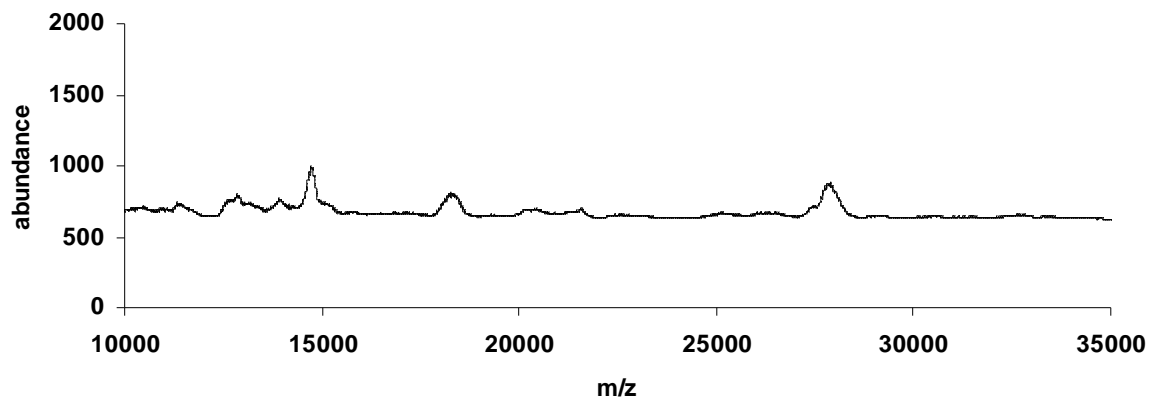
Fig. 5: Protein concentration in the fractions after anion exchange chromatography: while lysozyme showed a clear elution profile with three protein rich fractions (· · ■ · ·), BMP-2 was hardly eluted from the column (—▲—).

MALDI-ToF analysis was carried out to assess changes in the molecular mass of the protein caused by the labeling procedure (Fig. 6). First, the spectrum of native BMP-2 was prepared displaying two peaks of the masses of 14059 and 27952 Da which correspond to a subunit of BMP-2 and to the dimeric, disulfide-linked BMP-2, respectively (Fig. 6 a). Fraction 2 and 3 collected after anion exchange chromatography were investigated by MALDI-ToF. In these fractions, hardly any signals were detected (Fig. 6 b, c) as indicated by the low abundance. Furthermore, in fraction 2 (Fig. 6 b) small signal of the mass of native BMP-2 were detected among other signals that were probably fragments, while in fraction 3 (Fig. 6 c) a signal of the mass of native BMP-2 was not found, suggesting that the protein was destroyed by the labeling procedure.

a)



b)



c)

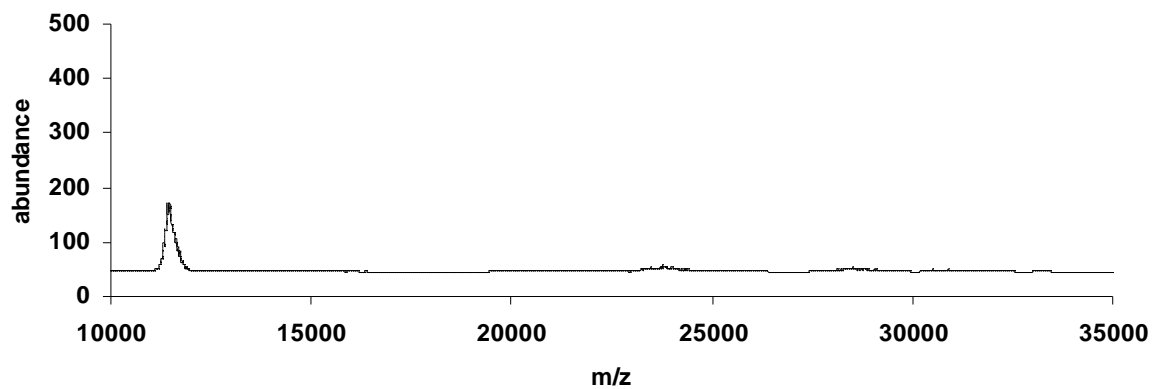


Fig. 6: MALDI-ToF analysis of a) native BMP-2 b) fraction 2 and c) fraction 3 after anion exchange chromatography.

### 3.3. Radioiodination of lysozyme and adsorption to ceramic discs

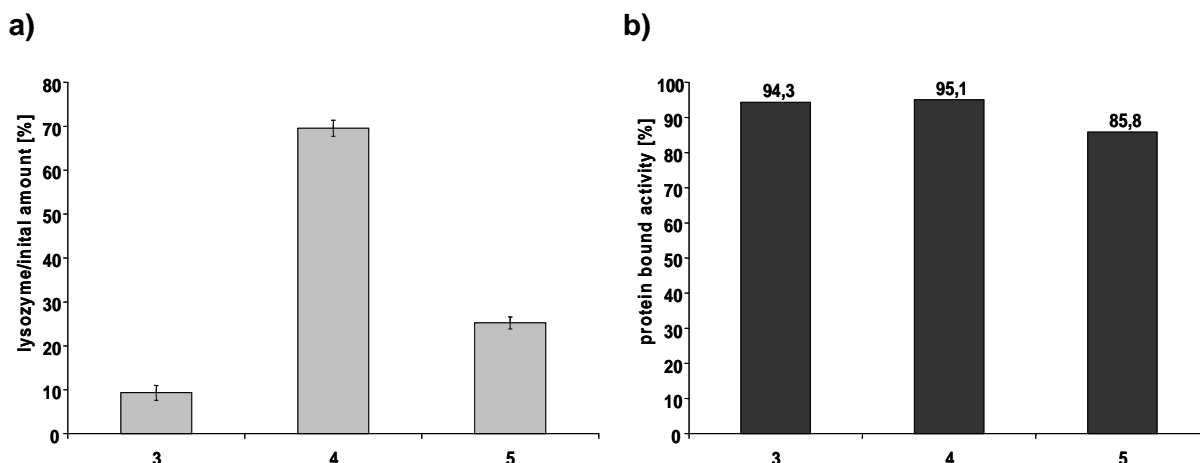
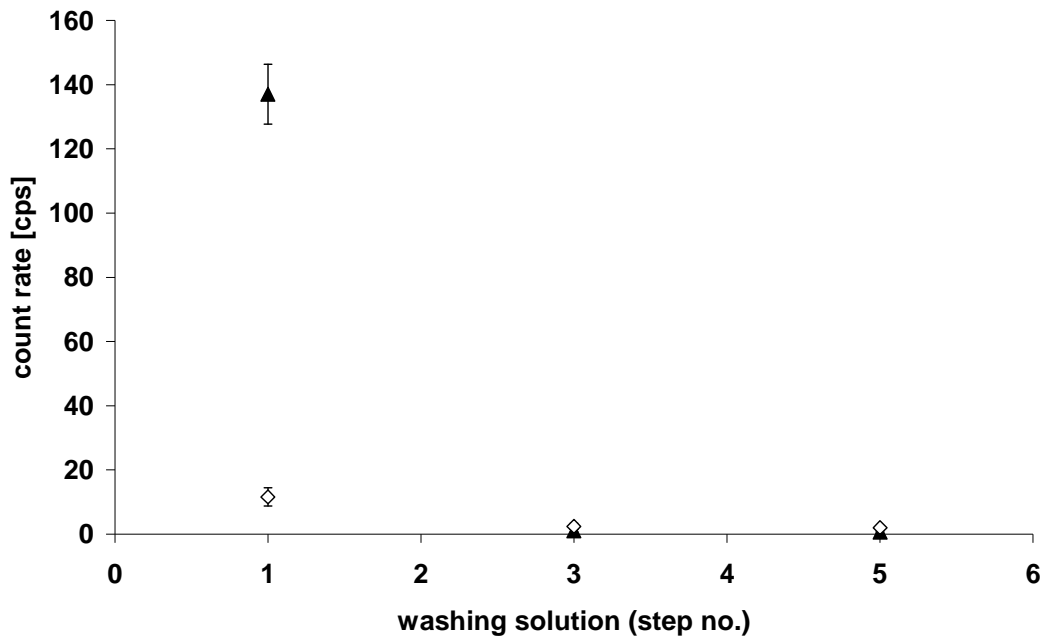


Fig. 7: a) Relative protein content determined by UV-spectroscopy in the protein rich fractions after size exclusion chromatography. Fraction 4 contains 70 % of total protein. b) Specific, protein bound activity of the protein rich fraction (3.-5. ml) after passing the reaction mixture through a SEC-column.

Intending to use the protein in fraction 4 of the size exclusion chromatography the concentration of the protein rich fractions was determined by quantitative UV-spectroscopy and the protein content was calculated. The fraction 4 was a solution of 700 µg/ml lysozyme (Fig. 7 a). Lysozyme was then labeled with  $^{125}\text{I}$  and the specific “protein bound” activity of lysozyme in the protein rich fractions 3-5 was determined. Precipitation of the labeled protein revealed that at least 95 % of the  $\gamma$ -activity in fraction 4 was protein bound (Fig. 7 b).

The fraction 4 was used at different dilutions for studying the adsorption of lysozyme to hydroxyapatite ceramic discs: Ceramic discs were immersed in a protein solution (5 µg/ml) and adsorbed over night. On the next day the samples were washed 5 times, one half of the samples with distilled water, the other half with 1 % SDS in PBS (Fig. 8 a). The washing solutions were analyzed for  $\gamma$ -ray activity: In the first washing step, the SDS solution contained 10 fold more activity indicating a higher amount of protein that was washed off. In the following washing steps, the SDS solution contained less activity than water. The remaining  $\gamma$ -activity on the ceramic samples that had been washed 5 times was determined (Fig. 8 b). Washing with water led to a significantly higher activity, indicating that a higher amount of labeled lysozyme remained on the discs.

a)



b)

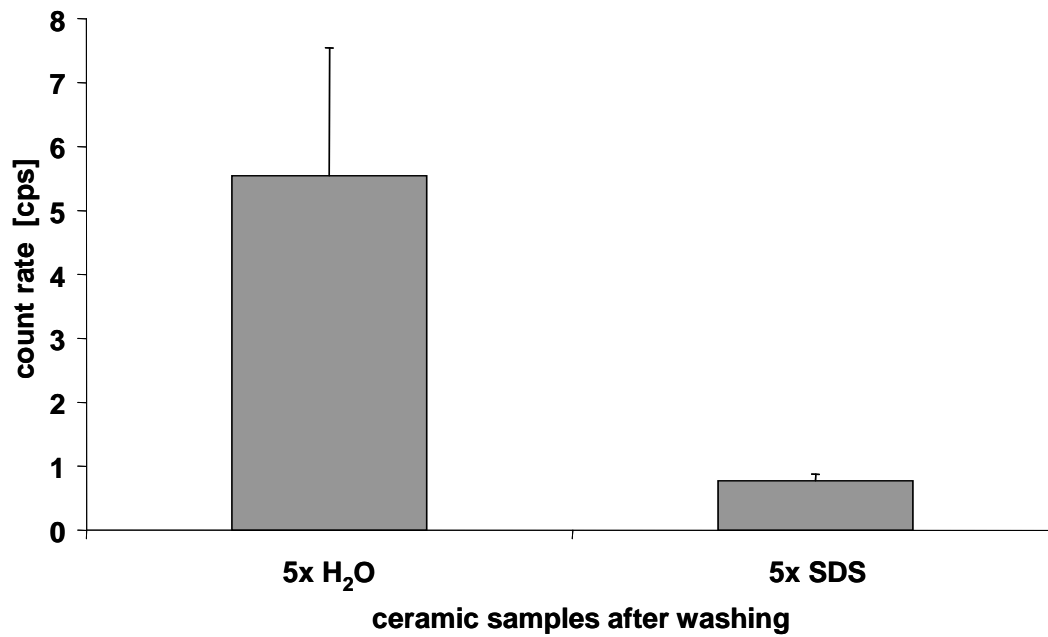


Fig. 8: Investigation of a washing protocol for protein coated ceramic samples ( $n=3$ ):  
**a)** activity in the washing solutions determined at step 1, 3 and 5 after washing the samples with 1 % SDS in PBS (▲) and ddH<sub>2</sub>O (◇).  
**b)** activity on ceramic samples after 5 washing steps performed with H<sub>2</sub>O and 1 % SDS.

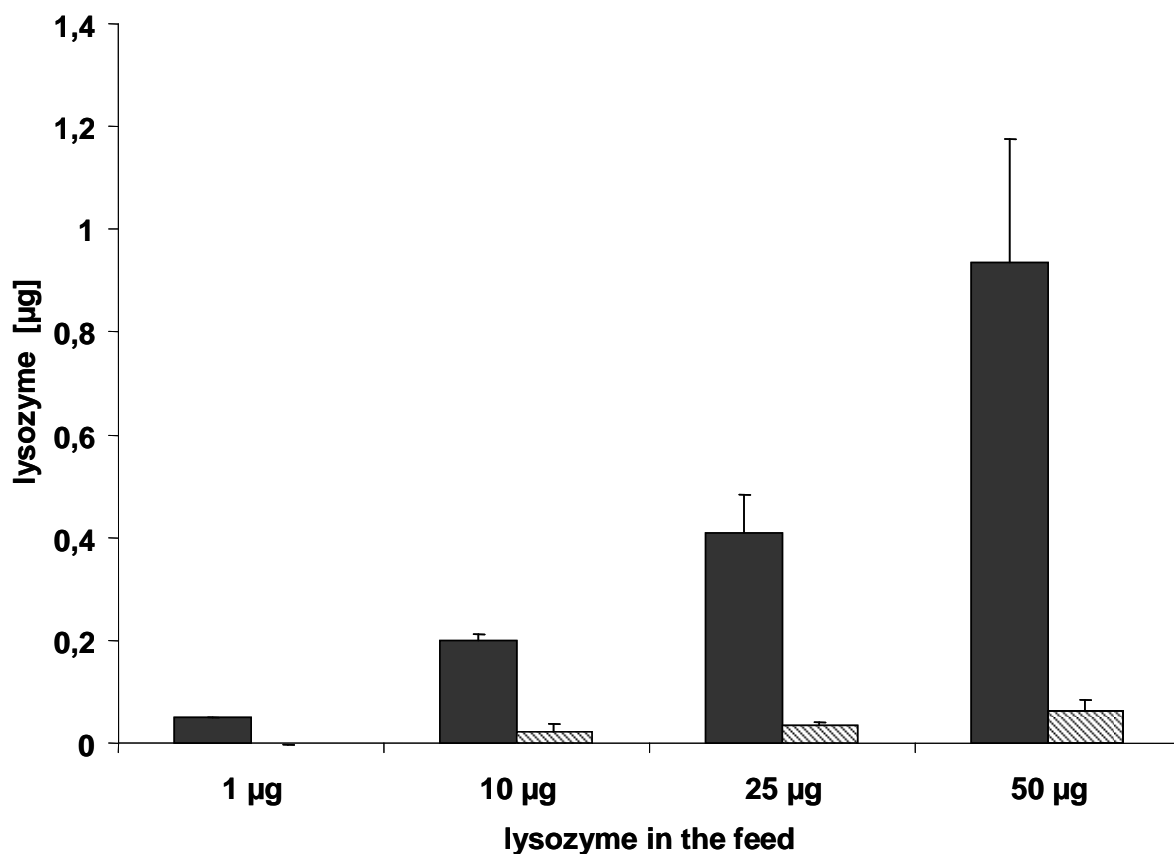


Fig. 9: Amount of lysozyme adsorbed to HA ceramic discs ( $n=3$ ) after washing the samples with 2 ml of ddH<sub>2</sub>O (■) and 1 % SDS in PBS (▨).

The adsorption of lysozyme on HA ceramic surfaces from solutions with different protein concentration resulted in different amounts of protein on the ceramic discs (Fig. 9). The amount ranged from 0.1 to 1 µg per ceramic sample. After washing the samples with a solution of 1 % SDS in PBS the amount of protein was decreased to 50 -100 ng per sample for all experimental groups. Differences between the experimental groups after SDS washing were not significant.

## 4. Discussion

The radioactive labeling of lysozyme and BMP-2 was intended to provide a method suitable for the detection of trace amounts of the proteins on the surfaces and for the characterization of surface modification methods with regard to their efficacy in retaining the protein on the ceramic surfaces.

Iodination of lysozyme by the chloramine-T method resulted in iodinated protein with different degrees of iodination. A maximum degree of substitution of 4 iodines per lysozyme molecule was found reflecting the 3 tyrosine residues and 1 histidine residue per protein molecule as possible targets for iodination. Labeling lysozyme in a ratio of protein to iodide of 1000:1 iodinated product was not detectable by HPLC-MS analysis, but the results assured that the protein was not affected by the oxidation reaction as no degradation products were detected. Using  $^{125}\text{I}$  for labeling a purification protocol was established resulting in a concentrated solution of  $^{125}\text{I}$ -lysozyme with a specific protein bound activity of > 95 %.

Although the method for labeling of BMP-2 derives from the literature the protein was obviously destroyed by the procedure, probably due to oxidation by chloramine-T. Therefore alternative methods have to be established for the investigation of surface immobilized BMP-2, such as the indirect determination of active BMP-2 by the use of cells that respond to BMP-2 by the expression of a specific marker in a dose-dependent manner [13;14].

For further characterization of the adsorption of  $^{125}\text{I}$ -lysozyme to the ceramic surfaces a washing procedure was established to distinguish between weakly and strongly adsorbed protein. Using distilled water the washing solution contained only 7 % of the activity that could be removed by washing the samples with 1 % SDS in PBS. This profound difference occurred only in the first washing step while in the following steps significant differences between water and SDS were not detected. After treating the ceramic samples 5 times with water a significantly higher amount of activity remained compared to samples treated 5 times with SDS. Therefore it was assumed that by treating the samples with distilled water only weakly bound protein could be removed while by washing with SDS strongly adsorbed lysozyme was removed. Therefore, the following experimental set up was chosen for further characterizations of protein adsorption: Ceramic discs with adsorbed protein were washed with water and the  $\gamma$ -activity was counted. Then the samples were washed with SDS and  $\gamma$ -activity was counted again.

$^{125}\text{I}$ -lysozyme adsorbed to the ceramic discs in a concentration dependent manner. However, after rinsing the samples with SDS the remaining mass of lysozyme on the samples did not differ significantly. This indicates that lysozyme adsorbs to the surface of HA ceramic discs, but can almost completely be removed by a surfactant, which can probably be utilized to distinguish adsorbed protein from chemically immobilized protein. This would allow for the evaluation of different procedures for the immobilization of proteins.



## 5. Conclusion

Radiolabeling of lysozyme with  $^{125}\text{I}$ iodine was successful without destroying the protein. By using the labeled compound quantitative measurements of protein on the surface of HA ceramic discs was possible. A washing procedure to distinguish between reversibly bound and strongly adsorbed lysozyme was established. This experimental set up allows for investigation and comparison of different methods for protein immobilization on the surfaces. Labeling of BMP-2 with the chloramine-T method was not successful in contrast to reports in the literature.

## 6. References

- [1] Luginbuehl, V., Meinel, L., Merkle, H. P., and Gander, B. (2004): "Localized delivery of growth factors for bone repair"; *European Journal of Pharmaceutics and Biopharmaceutics* (58) p.197-208
- [2] Puleo, D. A. "Dependence of mesenchymal cell responses on duration of exposure to bone morphogenetic protein-2 in vitro"; *Journal of Cellular Physiology* (173) p.93-101
- [3] Castner, D. G. and Ratner, B. D. (2002): "Biomedical surface science: Foundations to frontiers"; *Surface Science* (500) p.28-60
- [4] Kasemo, B. (2002): "Biological surface science"; *Surface Science* (500) p.656-677
- [5] Wagner, M. S., Shen, M., Horbett, T. A., and Castner, D. G. (2003): "Quantitative time-of-flight secondary ion mass spectrometry for the characterization of multicomponent adsorbed protein films"; *Applied Surface Science* (203-204) p.704-709
- [6] Puleo, D. A., Kissling, R. A., and Sheu, M.-S. (2002): "A technique to immobilize bioactive proteins, including bone morphogenetic protein-4 (BMP-4), on titanium alloy"; *Biomaterials* (23) p.2079-2087
- [7] Slater, R. J. (2002): "Radioisotopes in Biology"; Oxford University Press, 307p.
- [8] Chen, D., Zhao, M., and Mundy, G. R. "Bone morphogenetic proteins"; *Growth factors* (22) p.233-241
- [9] Yamamoto, M., Takahashi, Y., and Tabata, Y. (2003): "Controlled release by biodegradable hydrogels enhances the ectopic bone formation of bone morphogenetic protein"; *Biomaterials* (24) p.4375-4383
- [10] Gittens, S. A., Bagnall, K., Matyas, J. R., Lobenberg, R., and Uludag, H. (2004): "Imparting bone mineral affinity to osteogenic proteins through heparin-bisphosphonate conjugates"; *Journal of Controlled Release* (98) p.255-268
- [11] Tejedor, F. and Ballesta, J. P. G. (1982): "Iodination of biological samples without loss of functional activity"; *Analytical Biochemistry* (127) p.143-149
- [12] Kreke, M. R., Badami, A. S., Brady, J. B., Michael Akers, R., and Goldstein, A. S. (2005): "Modulation of protein adsorption and cell adhesion by poly(allylamine hydrochloride) heparin films"; *Biomaterials* (26) p.2975-2981
- [13] Katagiri, T., Yamaguchi, A., Komaki, M., Abe, E., Takahashi, N., Ikeda, T., Rosen, V., Wozney, J. M., Fujisawa-Sehara, A., and Suda, T. (1994): "Bone morphogenetic protein-2 converts the differentiation pathway of C2C12 myoblasts into the osteoblast lineage"; *Journal of Cell Biology* (127) p.1755-1766
- [14] Wiemann, M., Jennissen, H. P., Rumpf, H., Winkler, L., Chatzinikolaidou, M., Schmitz, I., and Bingmann, D. (2002): "A reporter-cell assay for the detection of BMP-2 immobilized on porous and nonporous materials"; *Journal of Biomedical Materials Research* (62) p.119-127

# **Chapter 4**

## **Adsorption and immobilization of lysozyme on PEGylated hydroxyapatite ceramic surfaces**

To be submitted to “Journal of Colloid and Interface Science”

A. Schuessele<sup>1</sup>, H. Mayr<sup>2</sup>, M.B. Schulz<sup>3</sup>, A. Goepferich<sup>1</sup>

<sup>1</sup>Department of Pharmaceutical Technology, University of Regensburg, Germany

<sup>2</sup>Friedrich-Baur-Research Institute for Biomaterials, Bayreuth, Germany

<sup>3</sup>Inst. for Pharm. Sciences, Pharm. Technology, Karl-Franzens-University, Graz, Austria

**Abstract**

A promising strategy to control the osseointegration of biomaterials such as hydroxyapatite (HA) ceramics is the local delivery of growth factors to the bone-implant interface. However, when simply adsorbing the factors to the surfaces, uncontrolled desorption may occur and unspecific protein adsorption may mask the cytokines thus limiting the control of cell stimulation. These limitations may be overcome by tethering cytokines to a surface by the use of poly(ethylene) glycol (PEG). Therefore, hydroxyapatite surfaces were modified by silanization and subsequent attaching of PEG. The adsorption of lysozyme to PEG monomethylether-grafted surfaces was investigated and PEG acetaldehyde was used for covalent attachment of the protein. Surfaces were characterized by contact angle measurements and X-ray photoelectron spectroscopy. PEGylation did not suppress the adsorption of lysozyme to the ceramic surfaces: nitrogen content on surfaces after protein adsorption was 5 to 7 % of the chemical composition and significant differences between PEGgrafted and unmodified ceramics were not determined. The amount of adsorbed and attached protein was determined using radiolabeled lysozyme: By immobilization, 90 ng of lysozyme were deposited compared to 30 ng that adsorbed to pure HA surfaces. The enzymatic activity of lysozyme on the discs was not affected by covalent attachment.

## 1. Introduction

Surface design of biomaterials for implants plays a fundamental role in biology and medicine, as the surface properties of a material determine its interactions with the biological environment [1]. Grafting poly(ethylene glycol) (PEG) onto a surface is probably the most common method towards controlling protein adsorption and consequently cell response [2]. In most cases PEGylation is used to reduce protein adsorption intending to achieve specific interactions of cells with material [3]. Contradictory results are reported in the literature concerning the optimal length and density of PEG chains for effective “surface shielding”. Relatively short PEG chains ( $M_w = 750\text{-}2000$  Da) have been found to provide full resistance to bioadhesion whereas other studies emphasize the need for long chains ( $>10000$  Da) or branched polymer structures [4-6]. Not only the type of PEG but also size and charge of the particular protein influence the shielding efficacy [7]. Attaching linear PEG molecules, the chain density on a surface was reported to be more important than chain length [8-10]. So, for every particular combination of surface type, PEG derivative and grafting reaction, the optimal reaction conditions have to be determined. Besides complete shielding, PEG-grafted biomaterials exhibited additional advantages: intermediate interfacial PEG densities were shown to enhance cell adhesion [11], to improve the acceptance of hydrophobic materials by cells [12] and poly(ethylene glycol)-poly(lactic acid) (PEG-PLA) diblock copolymers promoted the osteoblastic differentiation of marrow stromal cells [13]. Tethering cytokines to material surfaces is another application of PEG towards preserving stability and enhancing biological efficacy [14] by avoiding direct contact with a material's surface which might lead to reduced activity [15]. Despite the promising potential of this strategy, until now few studies have investigated the covalent immobilization of growth factors or proteins via PEG spacers to materials. TGF- $\beta$ 2, TGF- $\beta$ 1 and bFGF were tethered to collagen or acrylate hydrogels with retention of their biological activity [16-18]. Concerning solid surfaces, EGF tethered to glass slides retained its biological activity in contrast to adsorbed EGF [19]. Defined interactions of cells and biomaterial are of particular importance for the events at the bone-implant interface in order to achieve rapid healing and long-term fixation [20] which is favored by hydroxyapatite coatings [21] and localized delivery of growth factors [22]. Combining hydroxyapatite surfaces that would allow for specific interactions with cells via chemically immobilized growth factors would be a promising strategy to control and improve the osseointegration of implants. Unfortunately, there are no reports in the literature if the PEG tethering strategy can be used to modify HA surfaces as well. Therefore, we modified HA ceramic surfaces by aminosilanization and subsequent attachment of linear PEGacetaldehyde monomethylether and investigated their potential to prevent unspecific adsorption of proteins. To allow for the immobilization of proteins PEG acetaldehyde was chosen as homobifunctional derivative. Lysozyme served as a model protein to investigate the suitability for protein attachment.



## 2. Materials and Methods

### 2.1. Materials

Hydroxyapatite (HA) ceramic discs were provided by the Friedrich-Baur-Research Institute for Biomaterials (Bayreuth, Germany). The discs had a density of 99 % of the theoretical density and consisted of crystalline, phase pure HA. The discs were 12 mm in diameter and 2 mm thick.

Aminopropyltriethoxysilane (APTES) was purchased from Sigma-Aldrich (Steinheim, Germany) and freshly distilled prior to use. Toluene was purchased from Merck (Darmstadt, Germany) and dried by azeotropic distillation prior to use. Ethanol, sodium hydrogen phosphate, sodium dihydrogen phosphate, sodium cyanoborohydride, sodium citrate, lysozyme (50.000 units/mg), polyethylene glycol (PEG) of molecular weight (2000, 4000 Da; denoted as PEG 2k and PEG 4k) and polyethylene glycol monomethylether (mPEG) (750, 2000 and 5000 Da) were bought from Sigma-Aldrich (Steinheim, Germany). 0.1 M hydrochloric acid, sodium tetra borate decahydrate, sodium carbonate and chloramine T were purchased from Merck (Darmstadt, Germany). Alkaline solution of Na<sup>125</sup>I (37 MBq/ml) and PD-10 columns were purchased from Amersham Biosciences (Freiburg, Germany). Sodium dodecylsulfate (SDS) and phosphate-buffered saline (PBS) were purchased from Invitrogen (Karlsruhe, Germany). P-nitrophenyl penta-N-acetyl- $\beta$ -chitopentaoside (PNP-(GlcNAC)<sub>5</sub>) was purchased from Seikagaku Corp. (Tokyo, Japan).  $\beta$ -N-acetylglucosaminidase from Jack Beans was purchased from Sigma-Aldrich (Steinheim, Germany). Deuterated solvents for NMR-spectroscopy, chloroform, dimethylene sulfoxid (CDCl<sub>3</sub>, DMSO-d<sub>6</sub>) were obtained from Deutero GmbH (Kastellaun, Germany). All reagents were of analytical grade and used as received unless something different is stated.

### 2.2. Surface modification of HA ceramics

#### 2.2.4. Aminosilanization

HA ceramic discs were washed with 5 ml ethanol immediately prior to use. The aminosilanization of the discs was carried out in dry toluene. Briefly, 12 ceramic discs (diameter 12 mm) were placed in a three-necked glass reaction vessel with flat bottom (diameter 10 cm). 40 ml of dry toluene were added and the temperature was increased to 120° C. Freshly distilled aminopropyltriethoxysilane (APTES) was then added to result in a 1.5% (v/v) concentration and the reaction was held at 120° C for 4 hours in argon atmosphere (Argon 4.6, Linde AG, Pullach, Germany). After 4 hours, the samples were thoroughly rinsed with 3 ml toluene and 3 ml chloroform and dried under vacuum.

#### 2.2.5. Synthesis of PEG acetaldehyde diethylacetal and mPEG acetaldehyde diethylacetal

PEG acetaldehyde diethylacetal was synthesized following a procedure of Bentley et al. as a stable intermediate that could be stored and hydrolyzed to gain the corresponding aldehyde

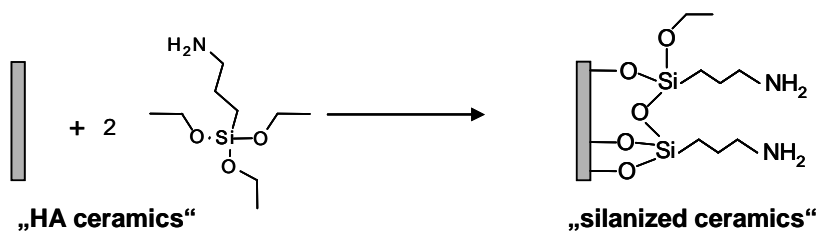
immediately before the attachment to the surface [23]. The polymers were characterized by  $^1\text{H}$ -NMR spectroscopy. The  $^1\text{H}$ -NMR spectra were recorded after dissolving 10-20 mg polymer in  $\text{CDCl}_3$  or  $\text{d}_6$ -DMSO on Avance 300 NMR-spectrometer (Bruker, Rheinstetten, Germany). The spectra displayed the characteristic PEG backbone absorption at 3.51 ppm and the ethyl triplet absorption at 1.11 ppm and the acetal triplet at 4.55 ppm. Integration of the acetal triplet relative to the PEG backbone peak allowed for the determination of the degree of substitution of several preparations of PEG acetaldehyde diethylacetal to be 80-95%.

#### 2.2.6. Stability of PEG acetaldehydes under conditions for protein attachment

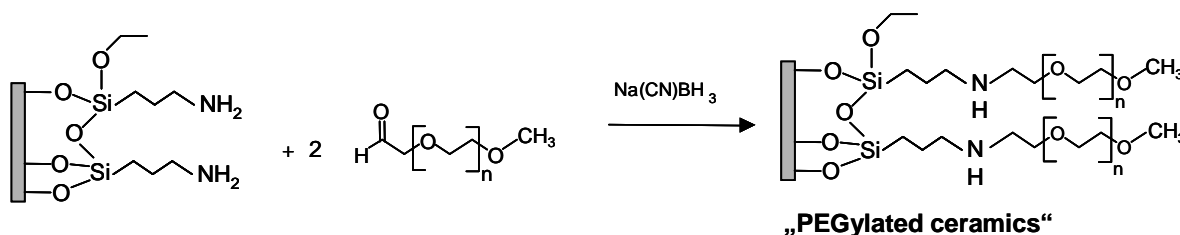
PEG acetaldehydes were prepared by heating a stirred solution of the respective PEG acetaldehyde diethylacetal in aqueous HCl (0.1 M; pH 1) at 50°C for 20 min as described in [23]. In a typical experiment, 250 - 500 mg PEG-derivative and 10 ml of hydrochloric acid were used. After cooling to room temperature, the pH was carefully adjusted to 6 by drop wise adding of 5% aqueous sodium bicarbonate to the rapidly stirred solution. The resulting solution was saturated with NaCl and extracted with methylene chloride (3x). The extract was dried over  $\text{Na}_2\text{SO}_4$  and filtered, and the filtrate was evaporated under vacuum to a final volume of 10 ml. Addition of cold ethyl ether precipitated the PEG derivative which was collected by vacuum filtration and dried under vacuum at room temperature. The degree of substitution was determined by  $^1\text{H}$ -NMR spectroscopy in  $\text{CDCl}_3$  using TMS as standard. The  $^1\text{H}$ -NMR spectra displayed the characteristic PEG backbone absorption at 3.51 ppm and the aldehyde singlett at 9.57 ppm. To assess the stability of the aldehyde under surface grafting conditions, mPEG acetaldehyde was stirred in sodium tetraborate solution (0.1 M; pH 9.3) over night in the presence of sodium cyanoborohydride. The  $^1\text{H}$ -NMR spectra were recorded on a Avance 300 NMR-spectrometer (Bruker, Rheinstetten, Germany).



- Aminosilanization of HA ceramic discs in toluene (120°C, argon atm.)



- Reaction with PEG monomethylether acetaldehyde (mPEG) in borate-buffer (0.1 M, pH 9.3)



*Scheme 1: Surface functionalization and grafting of mPEG acetaldehyde to silanized HA ceramic discs.*

#### 2.2.7. Attaching of PEG acetaldehydes to the surface

mPEG acetaldehyde diethylacetals and PEG acetaldehyde diethylacetals were hydrolyzed to the corresponding acetaldehydes in 0.1 M hydrochloric acid at 50°C. The polymers were conjugated to the silanized ceramic discs by reductive amination in a 0.1 M sodium tetraborate solution at pH=9.3 (scheme 1). For the reaction conditions a protocol from the literature was followed [24]. The polymers were used in 100-fold molar excess relative to the amino groups present on the surface. The discs were rinsed with distilled water and dried under vacuum.

### 2.3. X-ray photoelectron spectroscopy

The surface composition of the ceramic discs before and after adsorption of lysozyme was determined by X-ray photoelectron spectroscopy (XPS) on a Phi 5700 XPS system (Physical electronics, Ismaning, Germany) using an  $Al_{K\alpha}$  source. Increase in nitrogen content in the uppermost surface layers was considered as a measure of lysozyme adsorption when compared to the composition of the respective surface before immersion into a protein solution. A more detailed description can be found in [25].

### 2.4. Radioactive labeling of lysozyme with $^{125}I$

Lysozyme was labeled using the chloramine T method. In the following, the preparation of a 1 mg/ml lysozyme solution is exemplarily described. 2.00  $\mu$ l  $Na^{125}I$  (1.5-2 MBq) were added to 1 ml of a 1 mg/ml solution of lysozyme in PBS. After the addition of 100  $\mu$ l of a 0.2 mg/ml chloramine T solution, the mixture was shaken for 10 min. In order to stop the reaction, 100  $\mu$ l of a 4 mg/ml sodium metabisulfite solution was mixed and shaken with the lysozyme

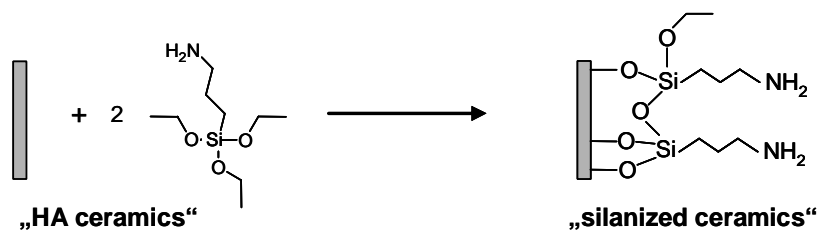
solution for 2 min. Products and educts were separated on a PD-10 column and lysozyme was eluted using a phosphate-buffered saline (PBS) pH 7.4. The resulting solution was a 700 µg/ml lysozyme solution in PBS, pH 7.4, with a specific protein bound activity > 95%, which was used at different dilutions for all adsorption and binding experiments.

## **2.5. Adsorption and immobilization of lysozyme at HA ceramic surfaces**

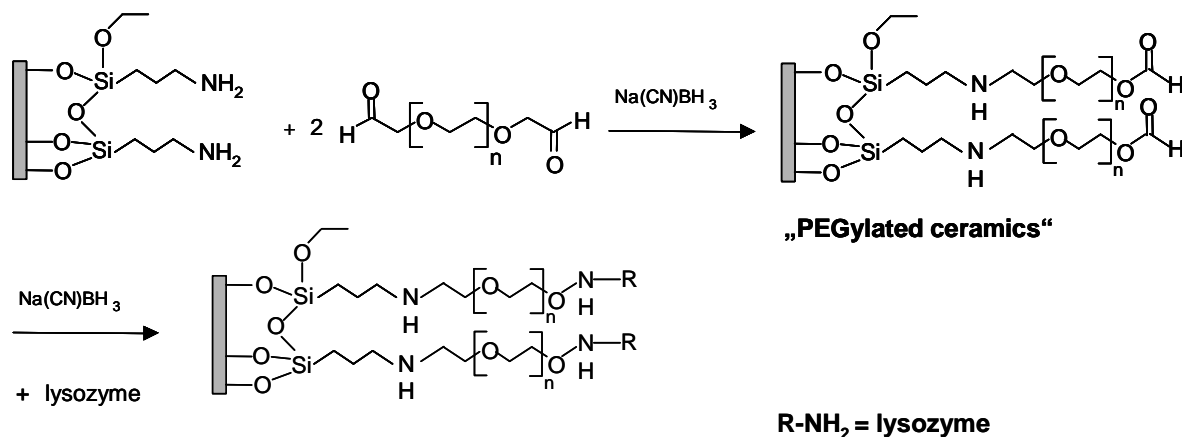
The adsorption experiments were carried out with mPEG grafted ceramic discs that were prepared as described in 2.2.4. Modified ceramic samples (n=3) were immersed in 2 ml of an aqueous solution of lysozyme (100 µg/ml). The protein was allowed to adsorb overnight to assure completed adsorption. Then discs were washed with 2 ml water to remove non-adsorbed protein and dried under vacuum.

The immobilization of <sup>125</sup>I-lysozyme to PEGylated ceramic discs was performed in sodium tetra borate solution (0.1 M; pH 9.3) (scheme 2). The protein was used in a concentration of 10 µg/ml. The covalent binding of lysozyme and PEG acetaldehyde was carried out in the presence of sodium cyanoborohydride to result in a stable secondary amine. HA ceramics, silanized ceramics and PEGgrafted ceramics without sodium cyanoborohydride served as control groups to distinguish between adsorbed and immobilized lysozyme. Samples (n=3) were immersed in protein solution over night. Discs were first washed with water and in a second step, washed with 1 % sodium dodecylsulfate in PBS to determine the amount of irreversibly attached protein. After each washing step, samples were submitted to scintillation to determine the amount of protein that was present on the surface. The samples were placed in polyvials (Zinsser Analytik, Frankfurt, Germany) and submitted to scintillation using a NaI(Tl)-Scintillation-Detector (Ortec, Oak Ridge, USA). The GammaVision-32 software package (Version 5.2, Ortec, Oak Ridge, USA) was used for data analysis.

- Aminosilanization of HA ceramic discs in toluene (120°C, argon atm.)



- Reaction with PEG acetaldehyde (DPEG) and lysozyme in borate-buffer (0.1 M, pH 9.3)



Scheme 2: Surface modification: attachment of PEG acetaldehyde and subsequent binding of proteins (i.e. lysozyme) covalently to the surface.

## 2.6. Enzymatic activity of lysozyme

The enzymatic activity of lysozyme at the surface of the discs was assessed by a method described by Klaeger et al. [26]. The discs were immersed in a lysozyme solution (10 µg/ml) overnight to allow for complete adsorption and immobilization. The reaction conditions were as described in 2.4 using non-labeled lysozyme. The enzymatic activity was assessed by the coupled reaction of lysozyme and β-N-acetylglucosaminidase to remove the sugar residues from (PNP-(GlcNAC)<sub>5</sub>) resulting in free p-nitrophenol. Samples were incubated at 37°C and allowed to react for 5 hours until a considerable amount of the substrate was cleaved. A standard curve was performed and the amount of released p-nitrophenolat was measured by a micro plate reader (CS 9301, Shimadzu) at 405 nm.

## 2.7. Contact angle measurements

To assess changes in surface wettability, water contact angles of the surfaces were measured before protein adsorption and immobilization and after the subsequent washing steps. The measurements were performed on OCA 15 (dataphysics, Filderstadt, Germany), using the sessile drop method with 1 µl drops of ddH<sub>2</sub>O.

**2.8. Statistical analysis**

All measurements were collected (n=3) and expressed as means  $\pm$  standard deviation (SD). Single factor analysis of variance (ANOVA) was used in conjunction with a multiple comparison test (Tukey test) to assess the statistical significance.

### **3. Results**

The first part of the study investigated the adsorption behavior of the model protein lysozyme to unmodified and mPEGgrafted ceramic discs. As first step of surface modifications, the HA ceramic discs were aminosilanized to allow for further conjugation steps and subsequently, mPEG acetaldehydes of varying molecular weights were grafted to the amino groups by the formation of a schiff base followed by reduction of the intermediate resulting in a secondary amine (Scheme 1).

#### **3.1. Adsorption of lysozyme on mPEG grafted ceramic discs**

The protein resistance of mPEG grafted ceramic discs was investigated using lysozyme as a model protein. mPEG of molecular weight of 750 to 5000 Da were attached to the surfaces. In order to investigate the chemical composition of the surfaces prior to and after protein adsorption XPS-survey scans were recorded (Fig. 1 a-e). After silanization, a signal from nitrogen was detected on the samples indicated by a small peak at 400 eV in the inserted spectra (Fig. 1 b) that was not present on untreated ceramics (Fig. 1 a). The signal was still present after grafting mPEGs of varying molecular weight (Fig. 1 c, d and e). While on HA ceramic discs prior to surface modification, the nitrogen content was below 1%, on silanized ceramics, the mean nitrogen content increased to 2.3% of atomic composition and decreased again after PEGgrafting by all three PEG chain lengths to 1.3 - 1.8%. Although there is a tendency that the longer PEG chains reduce the nitrogen content of the uppermost surface layers, a quantitative interpretation of the results is difficult as all these values are below the limit for exact analysis.

After adsorption of lysozyme, the N 1s signal was strongly increased in all experimental groups, which indicates adsorption of the protein to the surfaces (Fig. 2 a-e). The atomic concentration of nitrogen was ranging from 5 to 8% of total elemental composition. This indicates that none of the PEG derivatives was capable to suppress the adsorption of lysozyme completely.

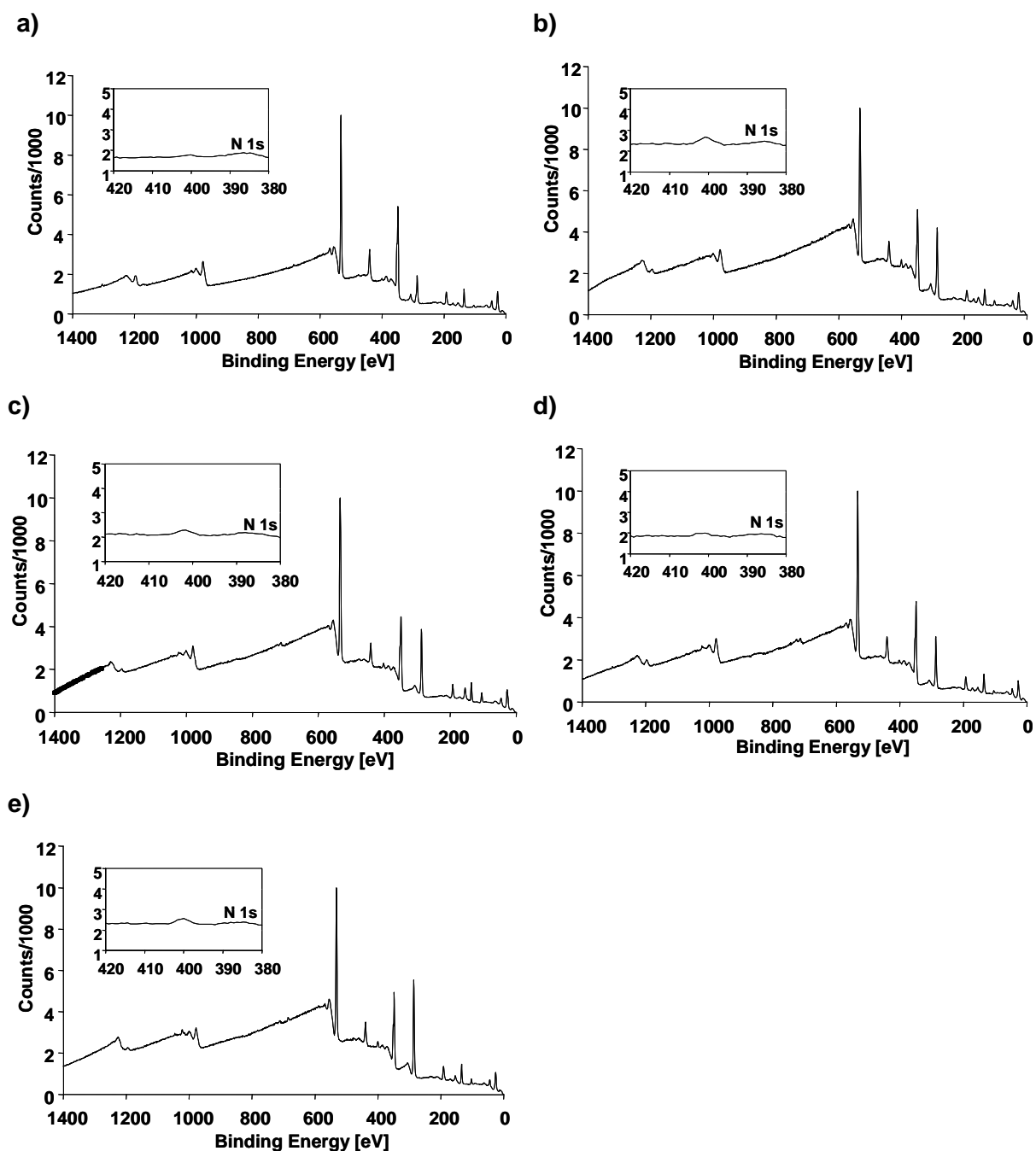
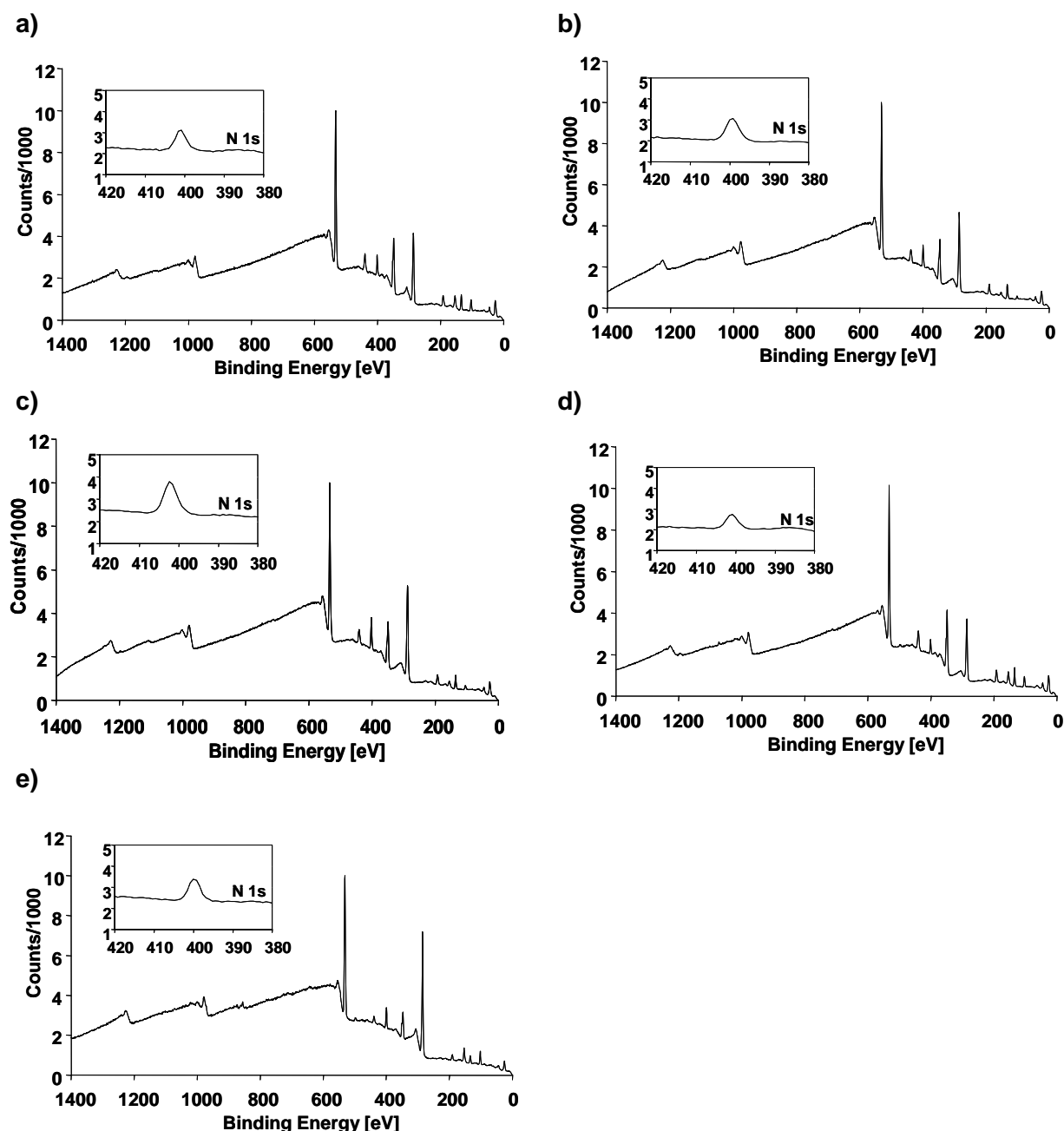


Fig. 1: XPS survey scans of pure surfaces prior to protein adsorption: **a)** HA ceramic **b)** silanized ceramic **c)** mPEG 750 **d)** mPEG 2000 and **e)** mPEG 5000 grafted ceramic. The peak at binding energies of 550 eV corresponds to the O 1s electron, while the peaks at 350 and 450 eV correspond to the Ca 2p, 400 eV to the N 1s, 250 eV to the C 1s, 200 and 150 eV to the P 2p and 175 and 125 eV to the Si 2p electrons, respectively. Inserted spectra show the nitrogen signal (N 1s) as a measure of protein adsorption at high resolution.



*Fig. 2: XPS survey scans of discs after protein adsorption: **a)** HA ceramics **b)** silanized ceramics **c)** mPEG 750 **d)** mPEG 2000 and **e)** mPEG 5000. The peak at binding energies of 550 eV corresponds to the O 1s electron, while the peaks at 350 and 450 eV correspond to the Ca 2p, 400 eV to the N 1s, 250 eV to the C 1s, 200 and 150 eV to the P 2p and 175 and 125 eV to the Si 2p electrons, respectively. Inserted spectra show the nitrogen signal (N 1s) as a measure of protein adsorption at high resolution.*

A quantitative comparison of protein adsorption assessed by nitrogen content in the uppermost surface layers was carried out for the untreated ceramic as well as mPEG 750 and mPEG 5000 coated samples (Fig. 3). The nitrogen content is significantly increased by the adsorption of lysozyme but a significant difference between ceramics treated with different PEG chain lengths after protein adsorption was not detected.

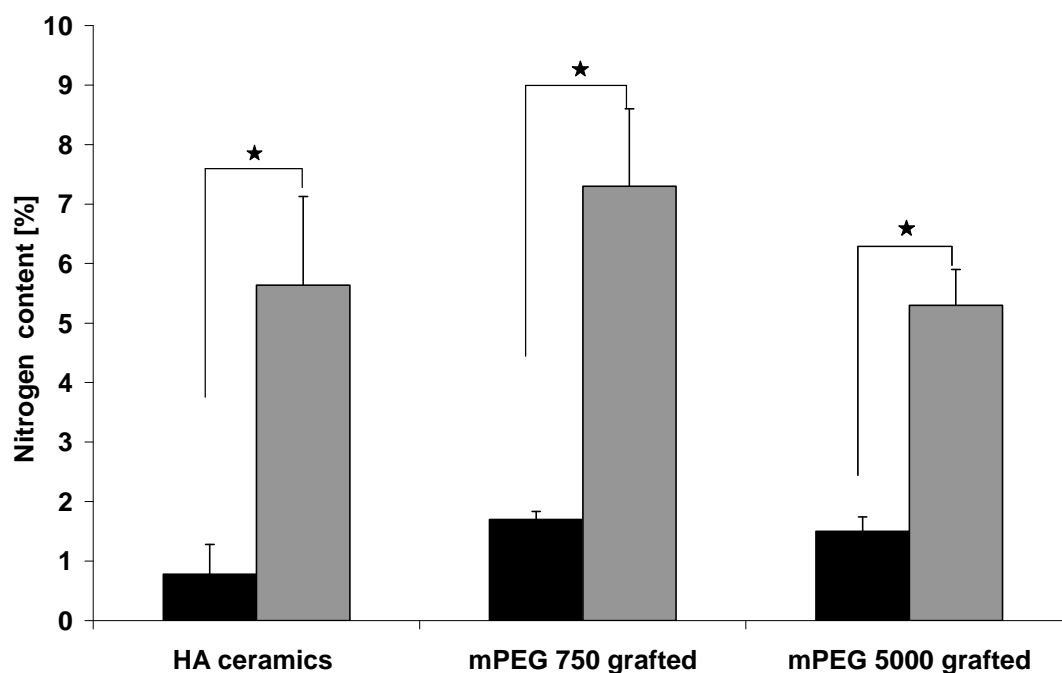


Fig. 3: Percentage of nitrogen in the atomic composition of the uppermost surface layers on the respective surfaces before (■) and after (□) protein adsorption as determined by XPS survey scans. At all the surfaces, a significant increase in nitrogen content was found after immersion in a solution of lysozyme, but none of the PEGylated ceramic discs was suitable to suppress protein adsorption completely. ★ indicates significant differences ( $n=3$ ;  $p<0.05$ ).

### 3.2. Suitability for protein attachment: stability of PEG acetaldehydes under protein grafting conditions

In order to prove whether PEG acetaldehyde was suitable for covalent binding of proteins after attachment to the surface, the stability of the aldehyde-function under surface grafting conditions was assessed by  $^1\text{H}$ -NMR-spectroscopy. For these experiments mPEG (2000 Da) was chosen as a model compound. The methylether singlet ( $\delta = 3.41$  ppm) served as internal standard for the integration of the signals. Fig. 4 shows the  $^1\text{H}$ -NMR spectrum of mPEG acetaldehyde diethylacetal after synthesis. By integration of signal 2 to signal 5 a degree of substitution of 80% was determined.



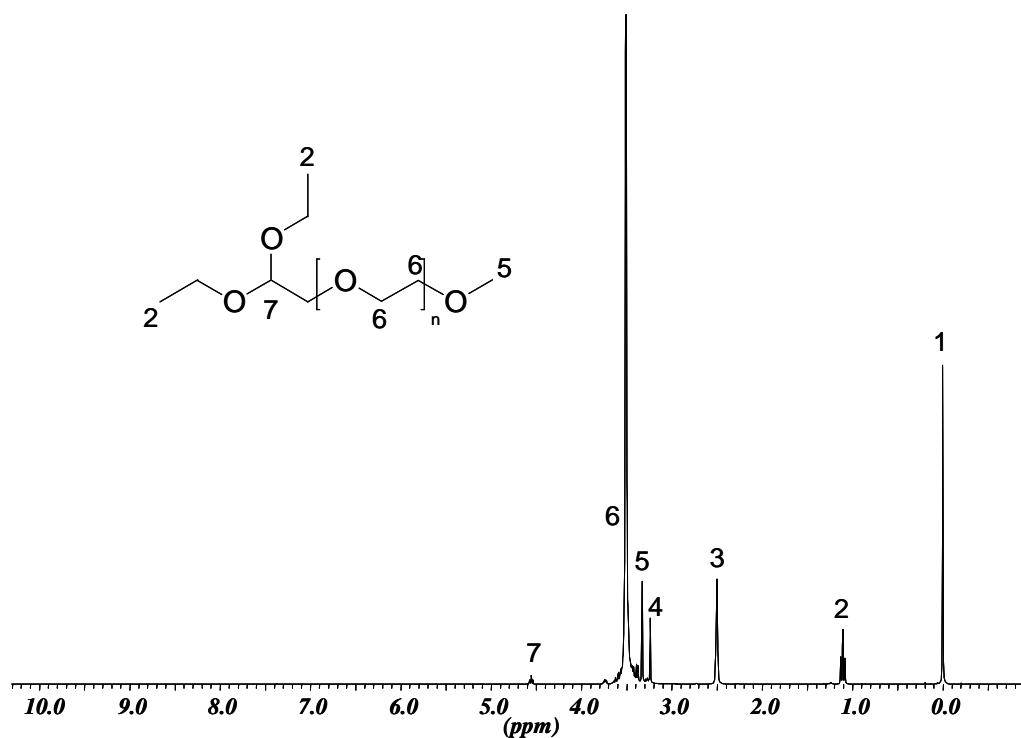


Fig. 4: <sup>1</sup>H-NMR spectrum of mPEG acetaldehyde diethylacetal monomethylether). Peaks 3 and 4 are due to solvent residues (DMSO and water, respectively).

After acidic hydrolysis, mPEG acetaldehyde diethylacetal was converted to the corresponding acetaldehyde as indicated by the typical singlet signal of the aldehyde proton 6 (Fig. 5 a). A degree of substitution of 72 % was determined by integration of the peaks for the aldehyde singlet ( $\delta = 9.57$  ppm) relative to the methylether singlet ( $\delta = 3.41$  ppm). Hydrolysis was not completed as a residue of the diethylacetal was observed ( $\delta = 1.11$  ppm, indicated by arrow).

Spectrum 5 b was recorded after stirring a mPEG acetaldehyde solution at pH 9.3 overnight in the presence of sodium cyanoborohydride (Fig. 5 b). The spectrum clearly displays the aldehyde singlet at 9.57 ppm. Peak integration revealed a content of mPEG acetaldehyde of 80 %. The increase in degree of conversion could be explained by completed hydrolysis after stirring over night. Additional peaks, despite the solvent residues, indicating the formation of by-products or destruction of the compound were not detected.

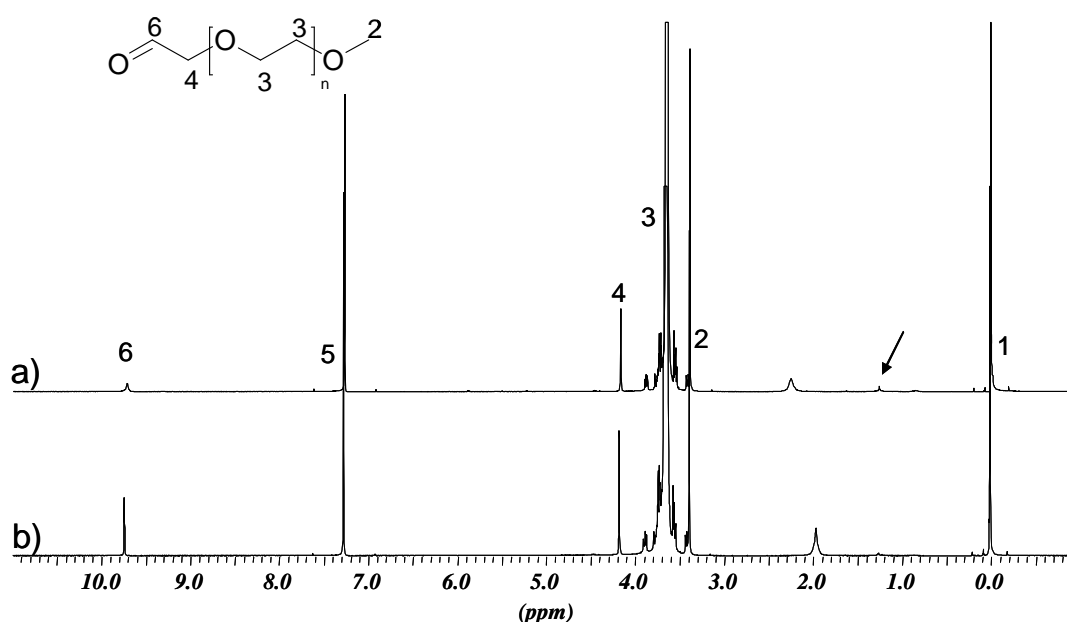


Fig. 5:  $^1\text{H}$ -NMR spectra of mPEG acetaldehyde: after hydrolysis (B) and after stirring under surface attachment conditions (C). The signal at 9.57 ppm is characteristic for the aldehyde proton (6) as well as signal 4 which corresponds to the C-atom next to the aldehyde functional group. Peak 5 is the solvent residual peak ( $\text{CDCl}_3$ ).

### 3.3. Immobilization of lysozyme using PEG acetaldehyde as spacer molecule

The XPS results clearly showed that the adsorption of the model protein was not completely suppressed by PEG layers. But, according to the literature, stabilizing effects of a PEG layer on attached proteins were expected. Therefore, in the second part, the covalent immobilization of lysozyme by using PEG acetaldehyde as a spacer molecule was examined with focus on the determination of the influence of immobilization method on biological activity of the attached protein. As shown in scheme 1, ceramic discs were aminosilanized and the surfaces were modified with PEG acetaldehyde to allow for covalent attachment of proteins via the second aldehyde functional group.

#### 3.3.1. Contact angle measurements

Water contact angle measurements of the surfaces were carried out after each subsequent modification step to assess modifications in the chemical composition (Fig. 6). The contact angle of ceramic discs was increased by silanization from  $65^\circ$  to  $70^\circ$  and slightly reduced again after PEGgrafting. After adsorption of lysozyme contact angles for the untreated and silanized ceramics were reduced. The changes in contact angle for the PEGgrafted ceramic discs compared to silanized ceramics were not significant after lysozyme adsorption in any of the experimental groups. Washing with SDS containing buffer further reduced the contact angle in all experimental groups to a level of  $20^\circ$  to  $40^\circ$ .

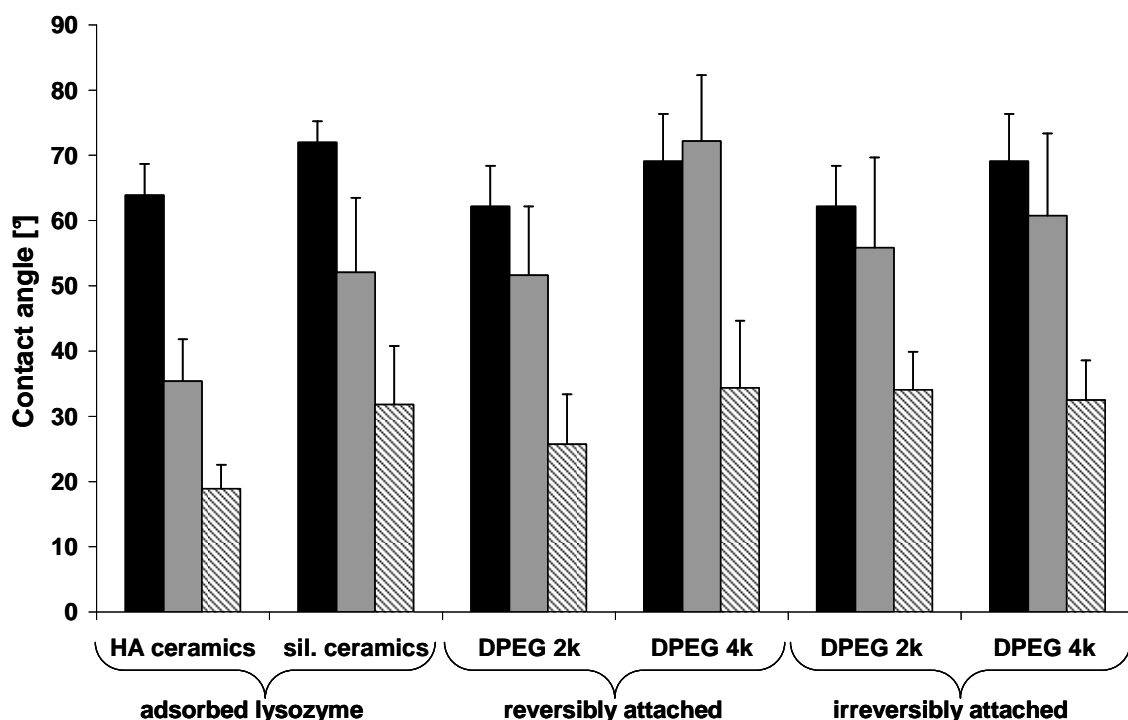


Fig. 6: Contact angle measurements of the surfaces investigated in this study after different modification steps (■ surfaces prior to protein adsorption, ■ surfaces after protein adsorption and ▨ samples after washing with 1% SDS in PBS). DPEG encodes for PEG acetaldehyde, while 2k and 4k correspond to the respective PEG chain length (2000 Da vs. 4000 Da).

### 3.3.2. XPS survey scans after attachment of lysozyme to surfaces modified with PEG acetaldehyde

XPS-survey scans after using PEG acetaldehyde to covalently attach protein revealed that lysozyme was deposited on a PEG dialdehyde ( $M_w = 2000$  Da) grafted ceramic, indicated by the N 1s signal in the inserted spectrum (Fig. 7 a). Unfortunately, after washing the sample with a 1% SDS solution, the protein seemed almost completely desorbed from the surface within the detection limits of the method (Fig. 7 b).

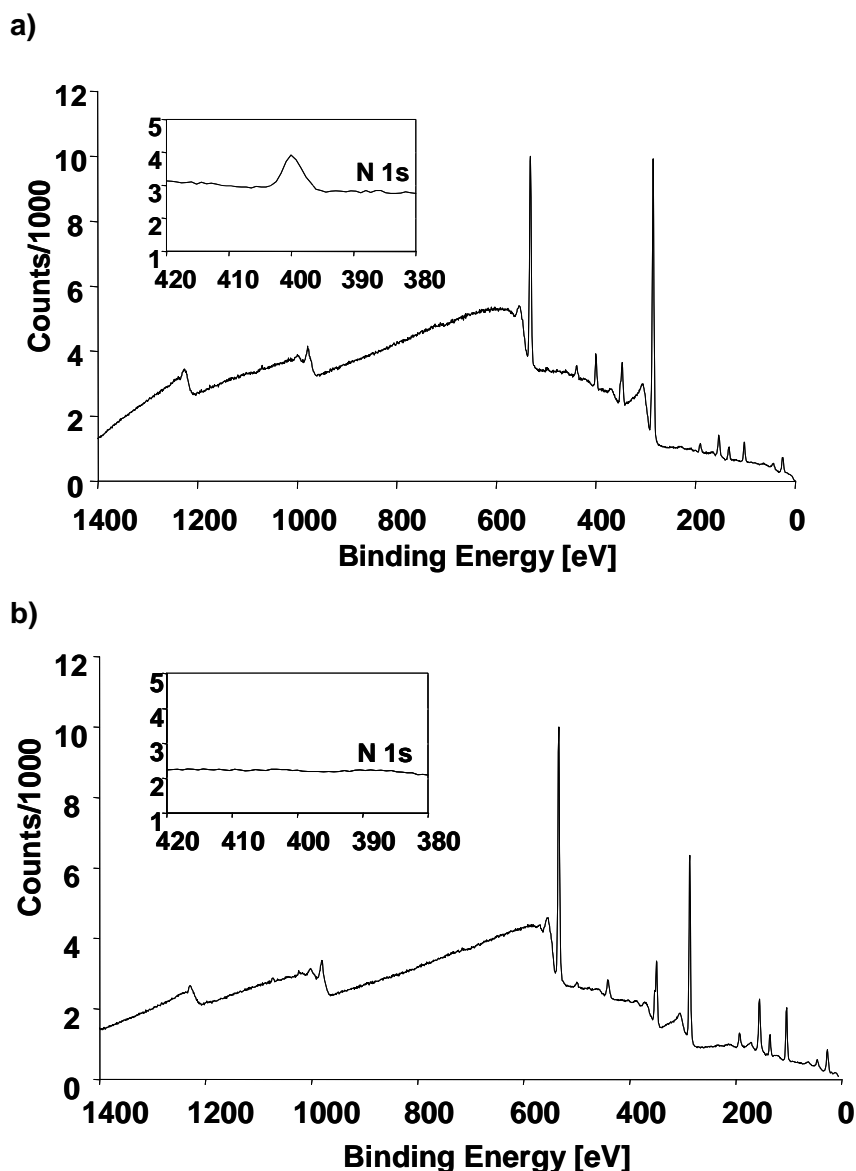


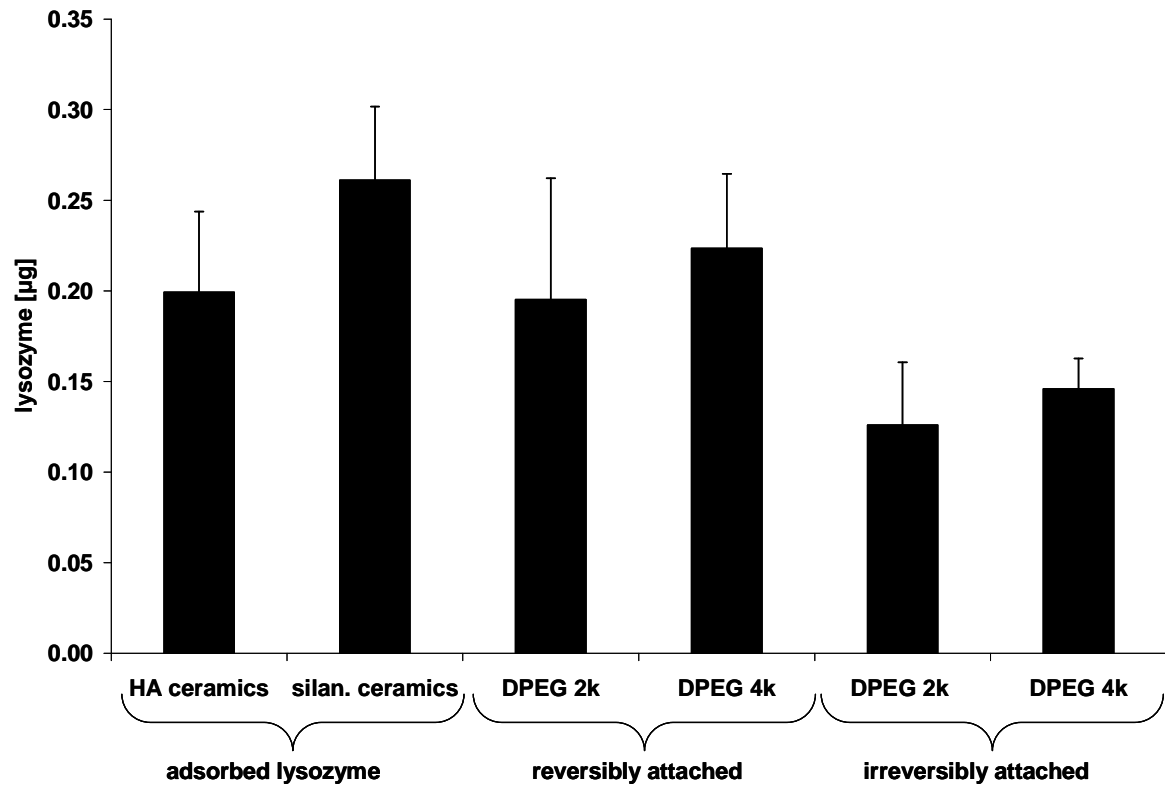
Fig. 7: XPS survey scans for surfaces with covalently attached lysozyme via PEG dialdehyde (2k)-spacers. The peak at binding energies of 550 eV corresponds to the O 1s electron, while the peaks at 350 and 450 eV correspond to the Ca 2p, 400 eV to the N 1s, 250 eV to the C 1s, 200 and 150 eV to the P 2p and 175 and 125 eV to the Si 2p electrons, respectively. Inserted spectra show the nitrogen signal (N 1s) as a measure of protein adsorption at high resolution. **a)** Sample washed with water and **b)** sample washed with water and a solution of 1% SDS in PBS. In Fig. 7a, a clear signal for the N1s electrons can be observed, which indicates that lysozyme adsorbed or was immobilized. As shown in Fig. 7b it can completely be removed by SDS (within the detection limits of the method).

### 3.3.3. Immobilization of $^{125}\text{I}$ -lysozyme on PEGgrafted ceramic discs

To overcome the limitations of the XPS study with regard to the determination of the amount of protein that was deposited on the differently treated ceramic discs, experiments with radiolabeled lysozyme were carried out (Fig. 8). After immersion into a protein solution over night, the deposited amount of lysozyme was ranging from 0.1 to 0.3  $\mu\text{g}$  for the individual surfaces which corresponds to 0.05 to 0.15  $\mu\text{g}/\text{cm}^2$ . The highest amount was detected on the silanized ceramic discs. After PEGgrafting, the mass of protein on the surface was decreased in all cases but the reduction was only significant for the groups with covalently bound protein. As observed in the contact angle measurements, the results for the PEGgrafted surfaces displayed again high standard deviations indicating an inhomogeneous structure of the surfaces (Fig. 8 a). After washing the samples with 1% SDS in PBS to remove reversibly bound protein, the remaining amount was considered to be the “immobilized” mass of the protein (Fig. 8 b).

By treating the samples with surfactant, the mass of protein was reduced to below 0.1  $\mu\text{g}$  per sample which is equal to app. 0.05  $\mu\text{g}/\text{cm}^2$ . Based on the assumption that 1.5  $\mu\text{g}/\text{cm}^2$  represent a monolayer of lysozyme [27;28], this shows that 3.4 % of the surface are protein-covered. Again, on the silanized ceramics more protein was detected than on untreated and on PEGgrafted ceramics. But using PEG spacers for covalent attachment, the amount of remaining protein was comparable to silanized ceramics, while on simply PEGgrafted surfaces less protein adsorbed. On silanized ceramics and by covalent attachment the amount of protein was significantly higher than on pure HA ceramic, but the differences between adsorbed and covalently attached protein on PEG grafted surfaces were not significant.

a)



b)

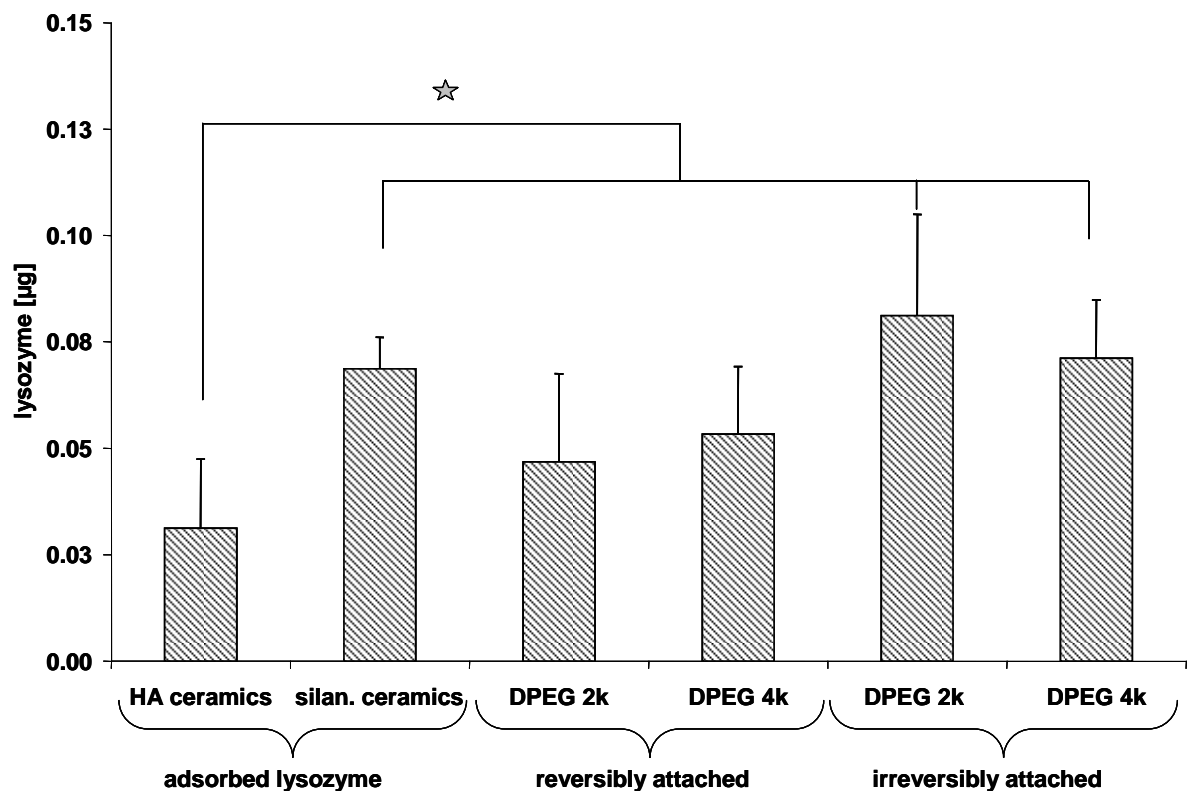
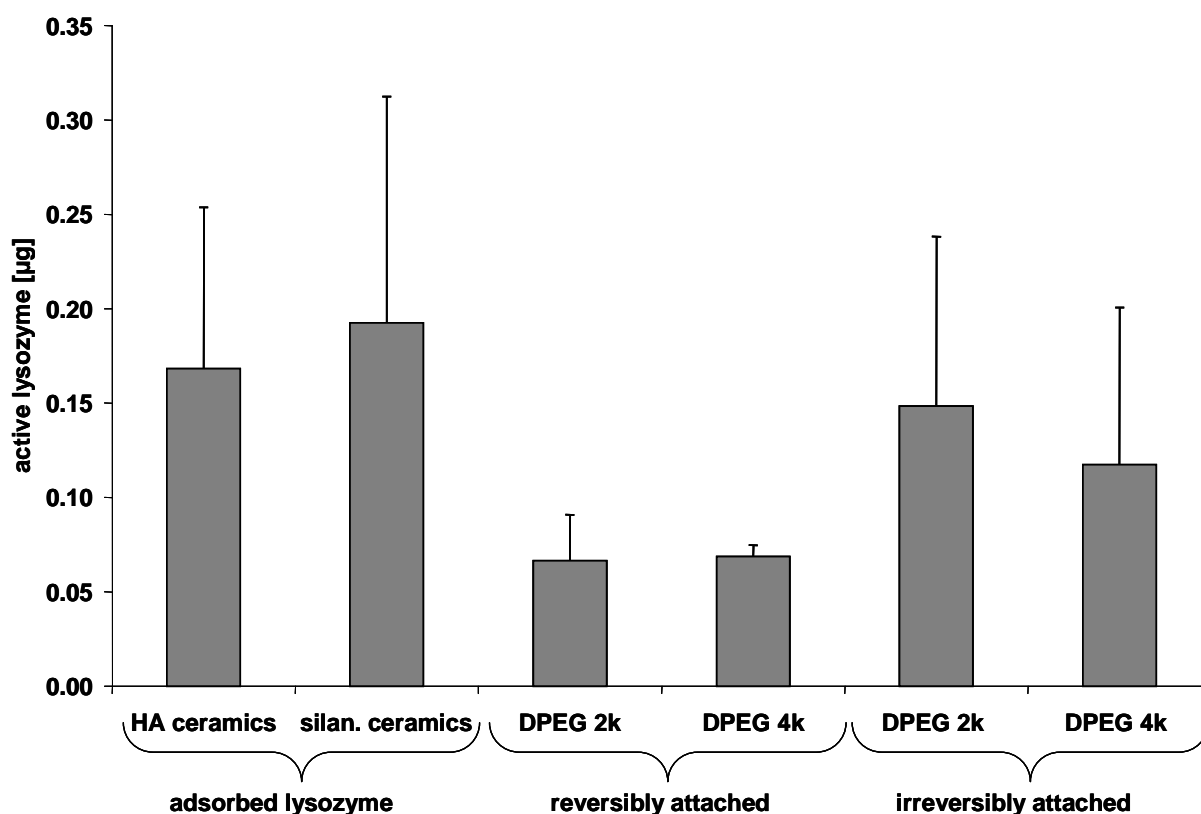


Fig. 8: Adsorption and attachment of  $^{125}\text{I}$ -lysozyme: a) surfaces after protein binding, washed with bidistilled water and b) washed with 1 % SDS in PBS. ☆ indicates significant differences to control (HA ceramics) ( $n=3$ ;  $p<0.05$ ).

## 3.3.4. Enzymatic activity

The enzymatic activity of lysozyme immobilized on the surfaces was investigated. The enzyme activity assay showed again the highest amount of active protein on silanized ceramics, while on all PEGgrafted surfaces the mass of protein was reduced. When grafting conditions were suitable for covalent attachment, the determined lysozyme activity increased again. Results displayed high standard deviations and therefore differences were not statistically significant.



*Fig. 9: Enzymatic activity of adsorbed and immobilized lysozyme after washing the samples with water. Differences were not significant, but in tendency we found, that more active lysozyme was deposited on the surfaces after covalent binding. Nevertheless, activity of covalently attached lysozyme did not exceed the values for lysozyme adsorbed to unmodified and silanized ceramic discs.*

The % share of active lysozyme of total protein was calculated by referring the values for the activity of lysozyme to the mass of protein determined by the experiments with radiolabeled

lysozyme (Tab. 1). On HA ceramics and silanized ceramics at least 74% of lysozyme remained active. The active part of lysozyme that was adsorbed to mPEGgrafted ceramics corresponded to 30% of total protein. When lysozyme was attached via PEGspacers the enzymatic activity of lysozyme 80-100% remained active.

Type of surface	HA ceramics	silanized ceramics	DPEG 2k rev.	DPEG 4k rev.	DPEG 2k irrev.	DPEG 4k irrev.
active lysozyme/ total lysozyme [%]	84 ± 52	74 ± 42	34 ± 7	31 ± 3	117 ± 67	80 ± 53

*Tab. 1: % share of active lysozyme at the surface of the discs after adsorption and reversible (rev.) or irreversible (irrev.) attachment to the surfaces. The active part of the protein determined by the enzymatic activity assay is given relative to the total amount of protein determined by binding experiments with <sup>125</sup>I-lysozyme and removing of weakly bound protein with water.*



## 4. Discussion

The objective of the study was to investigate the suitability of PEGylated HA ceramic discs for the immobilization of a protein and at the same time to achieve selective interactions via the suppression of unspecific adsorption. In general, by PEGylation of surfaces three main purposes are followed: First of all, bioinert surfaces can be created by complete suppression of protein adsorption [8]. Another aim is the creation of surfaces suitable only for a specific type of interactions for example selective cell adhesion [3] when the PEG surface is suitable for covalent attachment [29]. Furthermore, PEG tethers are suitable spacers for protein attachment as they are promoting stability of the attached protein [19].

In order to create surfaces that were capable of defined stimulation of attached cells the potential of PEG modified hydroxyapatite ceramic surfaces was investigated. The protein lysozyme was chosen due to similarities in physicochemical properties with some growth factors, the availability, ease of radioactive labeling and well-known mechanism of enzymatic action that allows for the investigation of impact of the immobilization method on protein activity [30].

Lysozyme adsorbed to all the surfaces, unmodified or PEGgrafted, as clearly shown by XPS data (Fig. 2), represented by an increase in nitrogen content of the uppermost surface layers. None of the investigated mPEGs with chain lengths varying from 750 to 5000 Da was capable to prevent protein adsorption completely when attached to the surface. A quantitative comparison of nitrogen content of untreated ceramic, mPEG 750 and mPEG 5000 grafted samples before and after protein adsorption revealed no significant differences in terms of protein adsorption.

In comparison to other proteins lysozyme displayed enhanced adsorption to PEG-coated surfaces, which was explained by the relatively low molecular weight (14600 Da) [31]. Thus, for surface shielding to suppress lysozyme adsorption, PEG layers apparently have to be more densely packed as for the rejection of other proteins. Compared to values reported in the literature, the water contact angles of the PEG grafted surfaces remained relatively high [4;11] indicating an incomplete coverage with hydrophilic polymer. In order to improve the shielding efficacy of the created PEG layer, alternative methods were suggested in literature as “cloud point grafting” [31], the use of branched PEGs [32] and the creation of interpenetrating networks by grafting a copolymer of polyacrylamide and PEG to surfaces [33]. However, preliminary experiments with rat marrow stromal cells (rMSC) have shown, that cell adhesion could be reduced by grafting of mPEG 5000 to HA ceramic discs [34].

As HA ceramics is a material favoring osseointegration and comprising bone bonding properties [21], it is disputable if a complete shielding of the surface is desirable. Additional advantages of the material would vanish by suppression of all unspecific interactions. Hydroxyapatite is known to be efficiently adsorbing many proteins in comparison to other materials relevant for hard-tissue replacement, which is considered to be responsible for the

excellent osseointegration properties [35]. Nevertheless, PEG modification of surfaces has beneficial effects on adsorbed proteins, such as promoting stability and reorganization of adsorbed fibronectin [12]. By the presence of the hydrophilic and uncharged PEG molecules interactions of adsorbed proteins with the surface could be avoided or attenuated [36;37]. Therefore we investigated as a second advantage of PEGylation the stabilizing effect of the PEG layer on attached or adsorbed lysozyme. However, comparing the enzymatic activity of lysozyme adsorbed to unmodified and to PEGgrafted ceramic discs, lysozyme lost enzymatic activity, which was not prevented by PEGylation (Fig. 9).

A third purpose of PEGylation is the application as spacer molecule to the immobilize proteins as a method to retain the protein at the application site and prevent uncontrolled desorption. Therefore, we investigated the suitability of PEG acetaldehyde grafted surfaces for immobilization of lysozyme. PEG acetaldehydes were used as homobifunctional linkers as they were reported to lead to an effective protein-resistant coating [31;38;39] and to efficiently PEGylate lysozyme [23]. The reductive amination was performed following a protocol from the literature described to obtain high yields [24]. However, the mass of protein deposited on all types of surfaces was below the mass of lysozyme that would create a monolayer according to literature [28]. The highest amount was determined on the silanized surfaces, the most hydrophobic ones in our study. The samples were washed with 1% SDS in PBS to distinguish between reversibly and irreversibly attached lysozyme. A significant increase in protein amount deposited on the surface was obtained after irreversibly attaching lysozyme using PEGspacers relative to unmodified ceramics. The chain length of the respective PEG derivative did not influence the amount of protein that was deposited. However, grafting of homobifunctional polymers was reported to lead to the formation of looplike structures, due to reaction of both aldehydes with the surface [40]. To achieve more homogeneously structured surfaces and higher amounts of attached protein, the use of heterobifunctional PEG would be a valuable tool as they would first react with the surface, by one functional group, and then with the protein by another type of reaction.

## **5. Conclusion**

Modifying the surface of HA ceramic discs by grafting of mPEG acetaldehydes with a molecular weight range from 750 to 5000 Da did not completely suppress the adsorption of lysozyme. When using PEG acetaldehyde as a spacer molecule for covalent attachment of lysozyme, protein mass was increased relative to pure ceramics, and in tendency, the protein retained its enzymatic activity to a higher extent compared to adsorbed protein. However, results were not significant, probably due to inhomogeneous structure of the modified surfaces. Additionally, the highest amount of protein was found after adsorption of lysozyme to silanized ceramics, with acceptable enzymatic activity. To conclude, considering the relatively low mass of protein that has been attached more efficient immobilization methods have to be examined.

## **Acknowledgements**

This work was financially supported by the Bayerische Forschungsförderung (Project: ForTePro).

## 6. References

- [1] Castner, D. G. and Ratner, B. D. (2002): "Biomedical surface science: Foundations to frontiers"; *Surface Science* (500) p.28-60
- [2] Nath, N., Hyun, J., Ma, H., and Chilkoti, A. (2004): "Surface engineering strategies for control of protein and cell interactions"; *Surface Science* (570) p.98-110
- [3] Lieb, E., Hacker, M., Tessmar, J., Kunz-Schughart, L. A., Fiedler, J., Dahmen, C., Hersel, U., Kessler, H., Schulz, M. B., and Goepferich, A. (2005): "Mediating specific cell adhesion to low-adhesive diblock copolymers by instant modification with cyclic RGD peptides"; *Biomaterials* (26) p.2333-2341
- [4] Zdyrko, B., Varshney, S. K., and Luzinov, I. (2004): "Effect of molecular weight on synthesis and surface morphology of high-density poly(ethylene glycol) grafted layers"; *Langmuir* (20) p.6727-6735
- [5] Du, H., Chandaroy, P., and Hui, S. W. (1997): "Grafted poly(ethylene glycol) on lipid surfaces inhibits protein adsorption and cell adhesion"; *Biochimica et Biophysica Acta* (1326) p.236-248
- [6] Unsworth, L. D., Sheardown, H., and Brash, J. L. (2005): "Protein resistance of surfaces prepared by sorption of end-thiolated poly(ethylene glycol) to gold: effect of surface chain density"; *Langmuir* (21) p.1036-1041
- [7] Archambault, J. G. and Brash, J. L. (2004): "Protein repellent polyurethane-urea surfaces by chemical grafting of hydroxyl-terminated poly(ethylene oxide): effects of protein size and charge"; *Colloids and Surfaces B: Biointerfaces* (33) p.111-120
- [8] Kingshott, P. and Griesser, H. J. (1999): "Surfaces that resist bioadhesion"; *Current Opinion in Solid State and Materials Science* (4) p.403-412
- [9] Jeon, S. I., Lee, J. H., Andrade, J. D., and De Gennes, P. G. (1991): "Protein-surface interactions in the presence of polyethylene oxide. I. Simplified theory"; *Journal of Colloid and Interface Science* (142) p.149-158
- [10] Jeon, S. I. and Andrade, J. D. (1991): "Protein-surface interactions in the presence of polyethylene oxide. II. Effect of protein size"; *Journal of Colloid and Interface Science* (142) p.159-166
- [11] Thom, V. H., Altankov, G., Groth, T., Jankova, K., Jonsson, G., and Ulbricht, M. (2000): "Optimizing cell-surface interactions by photografting of poly(ethylene glycol)"; *Langmuir* (16) p.2756-2765
- [12] Altankov, G., Thom, V., Groth, T., Jankova, K., Jonsson, G., and Ulbricht, M. (2000): "Modulating the biocompatibility of polymer surfaces with poly(ethylene glycol): effect of fibronectin"; *Journal of Biomedical Materials Research* (52) p.219-230
- [13] Lieb, E., Tessmar, J., Hacker, M., Fischbach, C., Rose, D., Blunk, T., Mikos, A. G., Goepferich, A., and Schulz, M. B. (2003): "Poly(D,L-lactic acid)-poly(ethylene glycol)-monomethyl ether diblock copolymers control adhesion and osteoblastic differentiation of marrow stromal cells"; *Tissue Engineering* (9) p.71-84
- [14] Otsuka, H., Nagasaki, Y., and Kataoka, K. (2004): "Characterization of aldehyde-PEG tethered surfaces: Influence of PEG chain length on the specific biorecognition"; *Langmuir* (20) p.11285-11287
- [15] Yongli, C., Xiufang, Z., Yandao, G., Nanming, Z., Tingying, Z., and Xinqi, S. (1999): "Conformational changes of fibrinogen adsorption onto hydroxyapatite and titanium oxide nanoparticles"; *Journal of Colloid and Interface Science* (214) p.38-45
- [16] Bentz, H., Schroeder, J. A., and Estridge, T. D. (1998): "Improved local delivery of TGF- $\beta$ 2 by binding to injectable fibrillar collagen via difunctional polyethylene glycol"; *Journal of Biomedical Materials Research* (39) p.539-548
- [17] Mann, B. K., Schmedlen, R. H., and West, J. L. (2001): "Tethered-TGF- $\beta$  increases extracellular matrix production of vascular smooth muscle cells"; *Biomaterials* (22) p.439-444
- [18] DeLong, S. A., Moon, J. J., and West, J. L. (2005): "Covalently immobilized gradients of bFGF on hydrogel scaffolds for directed cell migration"; *Biomaterials* (26) p.3227-3234

- [19] Kuhl, P. R. and Griffith-Cima, L. G. (1996): "Tethered epidermal growth factor as a paradigm for growth factor-induced stimulation from the solid phase."; *Nature Medicine* (New York) (2) p.1022-1027
- [20] Puleo, D. A. and Nanci, A. (1999): "Understanding and controlling the bone-implant interface"; *Biomaterials* (20) p.2311-2321
- [21] Hench, L. L. (1991): "Bioceramics: From concept to clinic"; *Journal of the American Ceramic Society* (74) p.1487-1510
- [22] Luginbuehl, V., Meinel, L., Merkle, H. P., and Gander, B. (2004): "Localized delivery of growth factors for bone repair"; *European Journal of Pharmaceutics and Biopharmaceutics* (58) p.197-208
- [23] Bentley, M. D., Roberts, M. J., and Harris, J. M. (1998): "Reductive amination using polyethylene glycol acetaldehyde hydrate generated in situ: Applications to chitosan and lysozyme"; *Journal of Pharmaceutical Sciences* (87) p.1446-1449
- [24] Hermanson, G. T. (1996): "Bioconjugate Techniques"; Academic Press, San Diego CA
- [25] Fischbach, C., Tessmar, J., Lucke, A., Schnell, E., Schmeer, G., Blunk, T., and Gopferich, A. (2001): "Does UV irradiation affect polymer properties relevant to tissue engineering?"; *Surface Science* (491) p.333-345
- [26] Klaeger, A. J., Cevallos, V., Sherman, M. D., Whitcher, J. P., and Stephens, R. S. (1999): "Clinical application of a homogeneous colorimetric assay for tear lysozyme"; *Ocular Immunology and Inflammation* (7) p.7-15
- [27] Daly, S. M., Przybycien, T. M., and Tilton, R. D. (2003): "Coverage-Dependent Orientation of Lysozyme Adsorbed on Silica"; *Langmuir* (19) p.3848-3857
- [28] Daly, S. M., Przybycien, T. M., and Tilton, R. D. (2005): "Adsorption of poly(ethylene glycol)-modified lysozyme to silica"; *Langmuir* (21) p.1328-1337
- [29] Tessmar, J., Mikos, A. G., and Gopferich, A. (2003): "The use of poly(ethylene glycol)-*block*-poly(lactic acid) derived copolymers for the rapid creation of biomimetic surfaces"; *Biomaterials* (24) p.4459-4473
- [30] Puleo, D. A., Kissling, R. A., and Sheu, M.-S. (2002): "A technique to immobilize bioactive proteins, including bone morphogenetic protein-4 (BMP-4), on titanium alloy"; *Biomaterials* (23) p.2079-2087
- [31] Kingshott, P., Thissen, H., and Griesser, H. J. (2002): "Effects of cloud point grafting, chain length and density of PEG layers on competitive adsorption of ocular proteins"; *Biomaterials* (23) p.2043-2056
- [32] Lee, J. H., Jeong, B. J., and Lee, H. B. (1997): "Plasma protein adsorption and platelet adhesion onto comb-like PEO gradient surfaces"; *Journal of Biomedical Materials Research* (34) p.105-114
- [33] Bearinger, J. P., Castner, D. G., Golledge, S. L., Rezanian, A., Hubchak, S., and Healy, K. E. (1997): "P(AAm-co-EG) Interpenetrating Polymer Networks Grafted to Oxide Surfaces: Surface Characterization, Protein Adsorption, and Cell Detachment Studies"; *Langmuir* (13) p.5175-5183
- [34] Schuessle, A., Volk, B., Mayr, H., Blunk, T., Schulz, M. B. and Gopferich, A. (2005): "Surface modification of hydroxyapatite ceramic to modulate cell adhesion and improve tissue generation"; in "Proceedings of the 9th meeting and seminar on ceramics, cells and tissues" (A.Ravaglioli and A.Krajewski; Eds.), Faenza, Italy
- [35] Kilpadi, K. L., Chang, P. L., and Bellis, S. L. (2002): "Hydroxylapatite binds more serum proteins, purified integrins, and osteoblast precursor cells than titanium or steel"; *Journal of Biomedical Materials Research* (57) p.258-267
- [36] Roach, P., Farrar, D., and Perry, C. C. (2005): "Interpretation of Protein Adsorption: Surface-Induced Conformational Changes"; *Journal of the American Chemical Society* (127) p.8168-8173
- [37] Peng, Z. G., Hidajat, K., and Uddin, M. S. (2004): "Adsorption and desorption of lysozyme on nano-sized magnetic particles and its conformational changes"; *Colloids and Surfaces B: Biointerfaces* (35) p.169-174
- [38] Kingshott, P., McArthur, S., Thissen, H., Castner, D. G., and Griesser, H. J. (2002): "Ultrasensitive probing of the protein resistance of PEG surfaces by secondary ion mass spectrometry"; *Biomaterials* (23) p.4775-4785

- [39] Kingshott, P., Wei, J., Bagge-Ravn, D., Gadegaard, N., and Gram, L. (2003): "Covalent Attachment of Poly(ethylene glycol) to Surfaces, Critical for Reducing Bacterial Adhesion"; *Langmuir* (19) p.6912-6921
- [40] Gong, X., Dai, L., Griesser, H. J., and Mau, A. W. H. (2000): "Surface immobilization of poly(ethylene oxide): structure and properties"; *Journal of Polymer Science, Part B: Polymer Physics* (38) p.2323-2332

# **Chapter 5**

## **A novel method for protein immobilization on hydroxyapatite ceramic surfaces using bisphosphonates**

Submitted to Journal of Biomedical Materials Research Part A

A. Schuessele<sup>1</sup>, H. Mayr<sup>2</sup>, J. Tessmar<sup>1</sup>, A. Goepferich<sup>1</sup>

<sup>1</sup>Department of Pharmaceutical Technology, University of Regensburg, Germany

<sup>2</sup>Friedrich-Baur-Research Institute for Biomaterials, Bayreuth, Germany

**Abstract**

The immobilization of biomolecules on biomaterial surfaces allows for the control of their localization and retention. In numerous studies, proteins have been simply adsorbed to enhance the biological performance of various materials *in vivo*. We investigated the potential of immobilized proteins compared to adsorbed proteins on hydroxyapatite (HA) ceramic discs in an *in vitro* approach. A novel method for protein immobilization was evaluated using the aminobisphosphonates pamidronate and alendronate, as anchors and was compared to the established silanization technique. Lysozyme and bone morphogenetic protein-2 (BMP-2) were used to assess the suitability of the two methods for protein immobilization with regard to the enzymatic activity of lysozyme and to the capacity of BMP-2 to stimulate the osteoblastic differentiation of C2C12 mouse myoblasts. After immobilization, a 2.5 fold increase in enzymatic activity of lysozyme was observed compared to the control. The alkaline phosphatase activity per cell stimulated by immobilized BMP-2 was 2.5 fold higher [ $9 \times 10^{-6}$  I.U.] than the adsorbed growth factor [ $2-4 \times 10^{-6}$  I.U.]. With regard to the increase in protein activity, both immobilization procedures lead to equivalent results. Thus, the bisphosphonate-based surface modification represents a safe and easy alternative for covalent attachment of proteins to HA surfaces.



## 1. Introduction

To ensure the long-term success of an endosseous implant, it is mandatory to obtain and maintain a stable bone-biomaterial interface [1]. With the goal of creating biomimetic materials that are capable of defined interactions with cells [2], interest in surface modification methods to stimulate cell function and tissue formation at the interface has increased in recent years [3]. The delivery of growth factors directly to the bone-implant interface, for example using coating techniques or drug delivery devices, represents a promising strategy to influence and control healing and fixation of implants [4]. Among others, bone morphogenetic protein-2 (BMP-2) has gained significant interest as a prominent factor in bone repair, due to its strong osteoinductive capacity in vivo both in orthotopic and ectopic sites [5;6].

During the last 5 years, in vivo studies have revealed that the osseointegration of implants is strongly accelerated and improved when BMP-2 is adsorbed on the surface of titanium or hydroxyapatite ceramics [7-9], incorporated by mixing with biomaterials such as in a self-setting bone-cement [10], or applied as a coating formed by co-precipitation of BMP-2 with calcium phosphate crystals [11]. More sophisticated approaches, which avoid subjecting the protein to aqueous environments during processing, include the incorporation of BMP-2 in biodegradable polymers such as poly (lactic acid) (PLA) and poly (lactic-co-glycolic acid) (PLGA) either as coatings on titanium screws [12], gelatin sponges [13], or as microparticles in a calcium phosphate cement [14].

Although in vivo studies have demonstrated the enormous benefit of biomimetic coatings on the osseointegration process, proteins, when adsorbed or incorporated, may suffer from uncontrolled release and risk of degradation. This has been clearly demonstrated through in vivo and vitro release studies of various growth factors - including BMP-2 - that were preadsorbed to different materials including ceramics, polymers, and composite materials [15;16]. Covalent immobilization of the protein on the material surface may overcome these drawbacks and achieve prolonged retention of the growth factors at their site of action. Chemically immobilized BMP-2, including BMP-2 either adsorbed or covalently attached to aminosilanized titanium implants, induced new bone formation more efficiently than pure titanium in the presence of soluble BMP-2 in adult rabbits [17]. Recently, a chitosan membrane with immobilized BMP-2 was shown to induce a dramatic increase in alkaline phosphatase activity in the mouse osteoblastic MC3T3 cell line in an in vitro study [18].

The issues outlined above are of significant concern in the modification of hydroxyapatite (HA) ceramics. HA ceramics are particularly interesting biomaterials for bone replacement and have been used as a coating on devices and as the inorganic part of composite materials, due to their similarity to the inorganic phase of bone, osteoconductive properties, mechanical stability, and ease of processing into scaffolds of various types and shapes [19;20]. A hinderance to the creation of biomimetic surfaces by the immobilization of growth

factors, HA ceramics suffer from a lack of functional groups. This chemical inflexibility can usually be overcome, however, through aminosilanization techniques that provide aminogroups needed for the covalent attachment of peptides and proteins [21;22]. Unfortunately, the formation of the silane layer alters the material surface properties, potentially diminishing the beneficial effects on osseointegration [23;24]. Therefore, we were looking for alternative methods for the covalent immobilization of proteins on hydroxyapatite surfaces. Bisphosphonates seemed to be a promising tool for the modification of hydroxyapatite ceramic surfaces as they show a high affinity for calcified tissues [25], which can be utilized to guide conjugated proteins to bone mineral [26;27], and beneficial effects on the proliferation and maturation of osteoblasts in vitro [28;29]. It is well-established that the structure of two phosphonates linked by a single carbon atom is responsible for the high binding affinity to bone mineral via the formation of highly stable complexes [30]. Derivatives with amine groups can furthermore be used for tethering proteins and peptides to coated surfaces. In addition, surface immobilized bisphosphonates stimulated bone formation around tibia implants and improved the mechanical fixation of stainless-steel screws in vivo [31;32].

The main objective of our study was to evaluate the potential of bisphosphonates to provide amine groups to immobilize proteins on hydroxyapatite ceramic surfaces. Two aminobisphosphonates, pamidronate and alendronate, were used to assess the suitability of the approach in comparison to the well-established aminosilanization technique. Hydroxyapatite ceramic discs served as model surfaces and lysozyme was used as a model protein for BMP-2, due to its similar physico-chemical characteristics [33], availability, and the convenience of radioactive labeling. Finally, BMP-2 was immobilized by both methods and its biological activity assessed using C2C12 mouse myoblasts.

## 2. Materials and Methods

### 2.1. Materials

Hydroxyapatite (HA) ceramic discs were provided by the Friedrich-Baur-Research Institute for Biomaterials (Bayreuth, Germany). The ceramic discs had a density of 99% of the theoretical density and consisted of phase pure HA of high crystallinity.

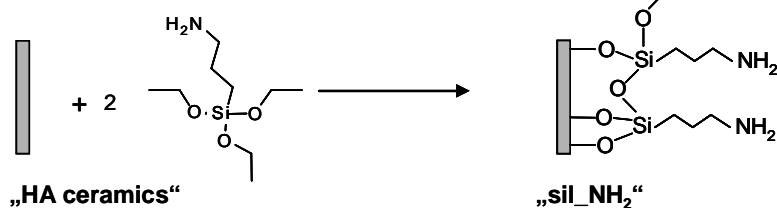
Sodium pamidronate was obtained from Ofichem (Ter Apel, Netherlands). Alendronate was purchased from Sigma-Aldrich (Steinheim, Germany). Aminopropyltriethoxysilane (APTES) was purchased from Sigma-Aldrich (Steinheim, Germany) and freshly distilled prior to use. Toluene was purchased from Merck (Darmstadt, Germany) and dried by azeotropic distillation prior to use. 1-ethyl-3-(3-dimethylaminopropyl) carbodiimide (EDAC), sulfo-N-hydroxysuccinimide (sulfo-NHS), succinic anhydride, sodium hydrogen phosphate, sodium dihydrogen phosphate, N-morpholinoethanesulfonate (MES), sodium cyanoborohydride, dimethyl sulfoxide (DMSO), sodium citrate, and lysozyme (50,000 units/mg) were bought from Sigma-Aldrich (Steinheim, Germany). 0.1 M hydrochloric acid, sodium tetra borate decahydrate, sodium carbonate, and chloramine T were purchased from Merck (Darmstadt, Germany). Iodine-125 - as an alkaline solution of NaI (37 MBq/ml) - and PD 10 columns were purchased from Amersham Biosciences (Freiburg, Germany). Sodium dodecylsulfate (SDS) and phosphate-buffered saline (PBS) were obtained from Invitrogen (Karlsruhe, Germany). P-nitrophenyl penta-N-acetyl- $\beta$ -chitopentaoside (PNP-(GlcNAC)<sub>5</sub>) was purchased from Seikagaku Corp. (Tokyo, Japan).  $\beta$ -N-acetylglucoaminidase from Jack Beans was purchased from Sigma-Aldrich (Steinheim, Germany). C2C12 mouse myoblasts were obtained from DSZM (Dt. Sammlung für Zellkulturen und Mikroorganismen, Braunschweig, Germany). Dulbecco's modified Eagle medium (DMEM; low glucose) was purchased from Sigma (Steinheim, Germany). Fetal bovine Serum (FBS) and antibiotics (Penicillin G/Streptomycin) were purchased from Invitrogen (Karlsruhe, Germany). Bone Morphogenetic Protein-2 (BMP-2) was produced by Scil Proteins (Halle, Germany). Water was of double distilled quality. All reagents were of analytical grade and used as received unless otherwise noted.

### 2.2. Surface modification of HA ceramics

#### 2.2.5. Aminosilanization

HA ceramic discs were washed with ethanol immediately prior to use. The aminosilanization of the discs was carried out in dry toluene. Briefly, 12 ceramic discs (diameter 15 mm) were placed in a reaction vessel, 40 ml of dry toluene were added, and the temperature was increased to 120°C. Freshly distilled aminopropyltriethoxysilane (APTES) was then added to a 1.5% (v/v) concentration and the reaction was held at 120°C for 4 hours in argon atmosphere. After 4 hours, the samples were thoroughly rinsed with toluene and chloroform and dried under vacuum (Scheme 1).

- Aminosilanization of HA ceramic discs in toluene (120°C, argon atm.)

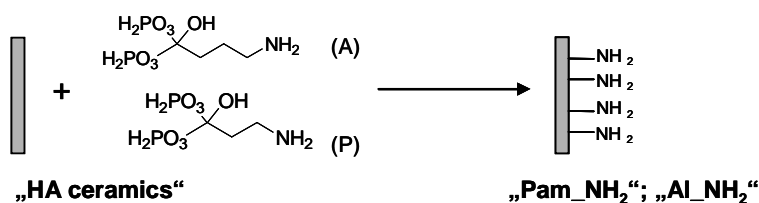


*Scheme 3: Creation of amino-groups at the surface of HA ceramics by the formation of an aminosilane layer that would allow for further conjugation steps.*

#### 2.2.6. Adsorption of aminobisphosphonates

HA ceramic discs were placed in beakers containing an aqueous solution of pamidronate or alendronate of a concentration of 1 mg/ml (3 ceramic discs per 10 ml bisphosphonate solution). The beakers were shaken at room temperature for 4 hours on an orbital shaker (Edmund Bühler GmbH, Tübingen, Germany) set at 20 rpm. The samples were washed three times with distilled water, dried, and stored under vacuum until further use (Scheme 2).

- Adsorption of alendronate (A) or pamidronate (P) to HA ceramic from aqueous solutions



*Scheme 4: Creation of amino-groups at the surface of HA ceramic that would allow for further conjugation steps by the adsorption of the aminobisphosphonates pamidronate and alendronate from aqueous solutions.*

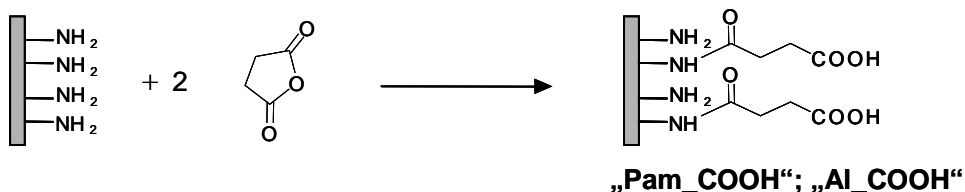
#### 2.2.7. Attachment of sulfo-N-hydroxysuccinimide (s-NHS)

The amino-functionalized ceramic discs were activated for covalent binding of proteins following a protocol described by Puleo et al. [33] with some modifications (Scheme 3). First, the amino groups were transferred to carboxylate groups by the reaction with succinic anhydride. To this end, 3-8 ceramic discs were placed in a beaker containing 30 ml of sodium phosphate buffer (0.1 M; pH 7.4). Succinic anhydride was dissolved in DMSO and added to the ceramic discs. The reagent was used in a 10-fold excess of the number of amino groups that, according to the literature, represents a monolayer on the silanized ceramic [33] and reacted over 3 hours. Discs were rinsed with water and dried.

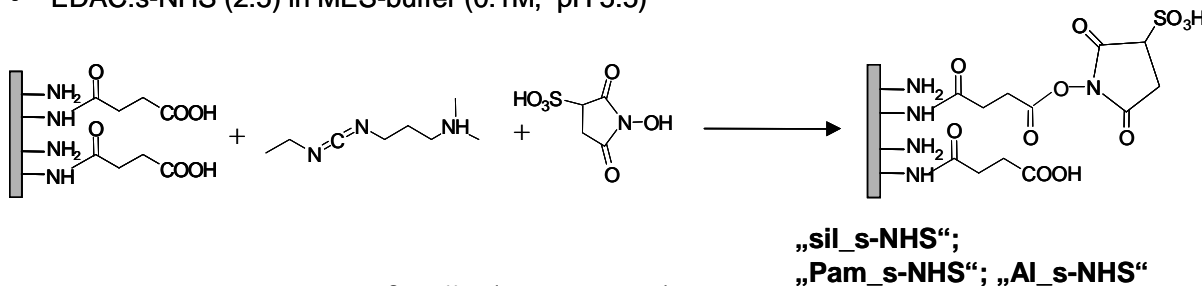
In a second step, 3-8 discs were placed in a beaker containing 30 ml of MES-buffer (0.1 M; pH 5). The activation of the carboxylate-groups with EDAC and sulfo-NHS in a molar ratio of 2:5 was carried out over 4 hours. EDAC was used in 10-fold excess to the number of amino

groups that represents a monolayer on the silanized ceramics according to the literature [33]. The discs were washed with distilled water, dried, and stored under vacuum until further use.

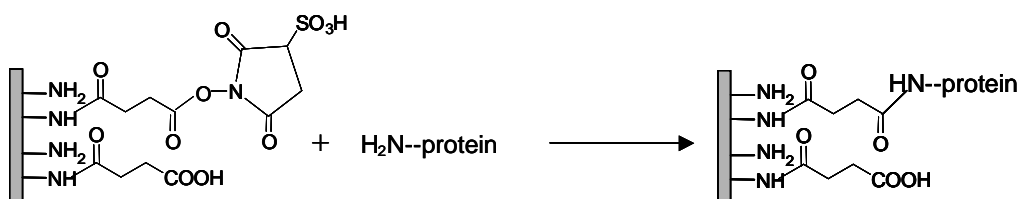
- Reaction with succinic anhydride in phosphate-buffer (0.1 M, pH 7)



- EDAC:s-NHS (2:5) in MES-buffer (0.1M, pH 5.5)



- Reaction with protein in MES-buffer (0.1 M; pH 5.5)



*Scheme 5: Surface modification of aminated HA ceramic surfaces by carbodiimide coupling chemistry. For protein immobilization, surface amino groups were reacted with succinic anhydride and the resulting carboxyl groups were transferred to succinic active esters (sil\_s-NHS; Pam\_s-NHS; Al\_s-NHS).*

### 2.3. Radioactive labeling of lysozyme with $^{125}\text{I}$

Lysozyme was labeled using the chloramine T method. For the preparation of a 1 mg/ml lysozyme solution, 2  $\mu\text{l}$   $\text{Na}^{125}\text{I}$  (1.5-2 MBq) were added to 1 ml of a 1 mg/ml solution of lysozyme in PBS. After the addition of 100  $\mu\text{l}$  of a 0.2 mg/ml chloramine T solution, the mixture was shaken for 10 minutes. In order to stop the reaction, 100  $\mu\text{l}$  of a 4 mg/ml sodium metabisulfite solution was mixed and shaken with the lysozyme solution for 2 minutes. The resulting solution was purified using a PD-10 column containing Sephadex G-25 M and lysozyme was eluted with PBS (pH 7.4). The resulting solution was a 700  $\mu\text{g/ml}$   $^{125}\text{I}$ -lysozyme solution in PBS (pH 7.4) with a specific activity > 95%, which was used at different dilutions for all adsorption and binding experiments.

## **2.4. Immobilization of lysozyme at HA ceramic surfaces**

The reaction of the Sil<sub>s</sub>-NHS coupled ceramic discs with lysozyme was performed in MES buffer (0.1 M; pH 5). The protein was used at a concentration of 10 or 20 µg/ml. The discs were washed with water and a solution of 1% sodium dodecylsulfate (SDS) in PBS. Discs with radiolabeled lysozyme were submitted to scintillation to determine the amount of protein bound, while discs with non-labeled lysozyme were used to investigate the enzymatic activity.

The samples were placed in polyvials (Zinsser Analytik, Frankfurt, Germany) and submitted to scintillation using a NaI(Tl) Scintillation Detector (Ortec, Oak Ridge, USA). The GammaVision-32 software package (Version 5.2, Ortec, Oak Ridge, USA) was used for data analysis.

## **2.5. Enzymatic activity of lysozyme**

The enzymatic activity was assessed using a method described by Klaeger et al. [34]. The ceramic discs were immersed in a 10 µg/ml solution of lysozyme in 0.1 M MES buffer (pH 5.5) and allowed to react overnight. The samples were rinsed thoroughly with water and placed in 24 well plates. The enzymatic activity was assessed by the coupled reaction of lysozyme and β-N-acetylglucosaminidase to cleave the sugar residues from (PNP-(GlcNAc)<sub>5</sub>) resulting in free p-nitrophenol. Samples were incubated at 37°C and allowed to react for 5 hours until a considerable amount of the substrate was cleaved. A standard curve was recorded and the amount of released p-nitrophenolate was measured with a microplate reader (CS 9301, Shimadzu) at 405 nm.

## **2.6. Contact angle measurements**

To assess changes in surface wettability, the surface water contact angles were measured before protein adsorption/immobilization and after the subsequent washing steps. The measurements were performed on OCA 15 (dataphysics, Filderstadt, Germany), using the sessile drop method with 1 µl drops of ddH<sub>2</sub>O.

## **2.7. Cell culture**

C2C12 cells were thawed and expanded once in growth media (Dulbecco's modified eagle medium (DMEM), 15% fetal bovine serum (FBS), and antibiotics (100 U/ml of Penicillin G and 100 µg/ml of Streptomycin)). Aliquots of 300,000 cells were frozen in DMEM containing 20% FBS and 10% DMSO.

For the BMP-2 testing experiment, protocols described by Katagiri et al. were followed [35]. Briefly, aliquots of cells were thawed and maintained in growth media at 37°C in a humidified atmosphere of 5% CO<sub>2</sub> in air (Figure 1). To examine the effects of BMP-2 and ceramic surface modifications, cells were seeded at a density of  $2 \times 10^4$  cells/cm<sup>2</sup> and cultured in

growth media. On day 1, the growth medium was replaced by low mitogen media (DMEM, 5% FBS, and antibiotics) with various concentrations of BMP-2. Cells were kept in low mitogen media for a total of 6 days. Media was changed every second day. BMP-2 was supplemented either only on day 1 or with every media change. On day 6, cell culture media was removed; the cells were washed with PBS and stored at -21°C until the samples were analyzed.

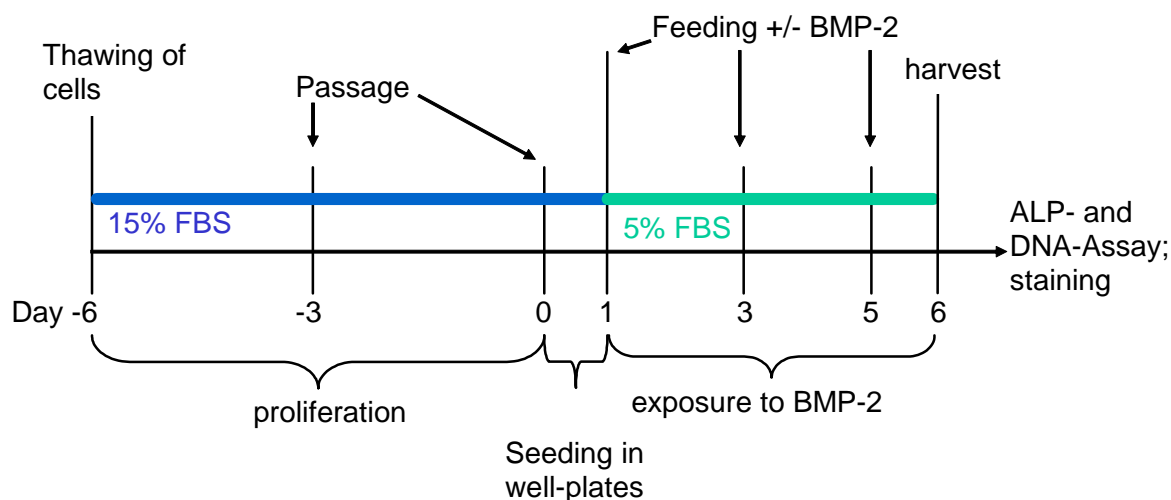


*Fig. 1: Cell culture of C2C12 mouse myoblasts. Experimental setup to examine the effects of BMP-2 supplemented to cell culture medium and various surface treatments of HA ceramic on the osteoblastic differentiation of C2C12 cells.*

## 2.8. Von Kossa staining

To assess the mineralization of the C2C12 mouse myoblasts after 6 days of supplementation with BMP-2, von Kossa staining was performed. Cells were fixed for 12 hours with 10% formaldehyde in PBS. After rinsing with water, cells were incubated with a 5% aqueous silver nitrate solution and exposed to natural light. After rinsing thoroughly with water and a 5% aqueous sodium thiosulfate solution, cells were counterstained with a 0.5% Safranin O solution for 30 seconds. Images of stained cells were taken with a digital camera (DS-U1, Nikon; Düsseldorf, Germany).

## 2.9. DNA assay

To measure the total amount of DNA per sample and subsequently determine the cell number, a fluorometric assay was performed (DNA-QF, Sigma). For the assay, the frozen samples were kept on ice and cells were scraped off the surface with disposable cell scrapers (Biochrom, Germany). Cells were dispersed in 0.8 ml of EDTA-solution (10 mM, pH 12.3). After sonication in an ice bath for 10 min, 0.2 ml of a  $\text{KH}_2\text{PO}_3$  solution (1 M) were added to each sample. The DNA assay was performed as described in the protocol provided by Sigma. For individual DNA measurements, 2 ml of a Hoechst 33258 dye solution (100

ng/ml) and 30  $\mu$ l of sample were used. DNA standards (calf thymus, Sigma) and cell standards were prepared and examined in parallel. A conversion factor of 19 pg DNA/cell was determined and used to determine cell number. Samples were measured on a RF-1501 Spectrofluorimeter (Shimadzu, Munich, Germany).

### **2.10. Alkaline phosphatase assay**

For the determination of alkaline phosphatase activity, a protocol described by Lieb et al. [36;37] was followed with minor modifications. The frozen samples were kept on ice and scraped off the surface using disposable cell scrapers. Cells were dispersed in 1 ml Tris (hydroxymethyl) aminomethane buffer (1 M, pH 8.0). The collected cell suspensions were sonicated in an ice bath for ten minutes and stored on ice until analysis. 0.5 ml of cell lysate were added to 0.5 ml of 2-amino-2-methyl-1-propanol-buffer (1.5 M, pH 10.3) and 0.5 ml of p-nitrophenyl phosphate (pNP) solution (4 mg/ml). Samples were incubated at 37°C for 30 minutes. Alkaline phosphatase converted the colorless pNP to the yellow-colored p-nitrophenolate. The enzymatic reaction was stopped with 10 ml of a 0.05 N sodium hydroxide solution. The hydrolyzed pNP was measured with a photometer (Uvikon 941, Kontron Instruments, Munich, Germany) at 405 nm and the amount of enzyme was quantified by comparison with a standard curve. Alkaline phosphatase levels were normalized to the cell number using the cell counts determined by the DNA assay.

### **2.11. Statistical analysis**

All measurements were collected (n=3 for radiolabeled lysozyme, n=3 for enzyme activity of lysozyme, n=3 for DNA, and n = 4 for ALP) and expressed as means  $\pm$  standard deviation (SD). Single factor analysis of variance (ANOVA) was used in conjunction with a multiple comparison test (Tukey test) to assess the statistical significance.



### 3. Results

Several authors correlated surface water contact angles with cell response and protein adsorption [38-40]. Therefore, we first assessed the wettability of surfaces after the subsequent modification steps (Figure 2).

#### 3.1. Water contact angles on HA surfaces

The contact angle of untreated ceramic discs (60°) was significantly increased (up to 70°) after silanization, indicating the formation of a hydrophobic layer on the surface. It remained at the same level after activation with sulfo-NHS (sil\_s-NHS). After adsorption of lysozyme, contact angles of all groups decreased to about 30-45° and remained in the same range after reversibly bound protein was removed from the surface by washing with a 1% SDS solution. After SDS washing, the lowest contact angle value of 30° was measured on unmodified ceramic discs, while the silanized and sil\_s-NHS modified surfaces maintained significantly higher contact angles (50°). These results indicate that the silane layer remained intact.

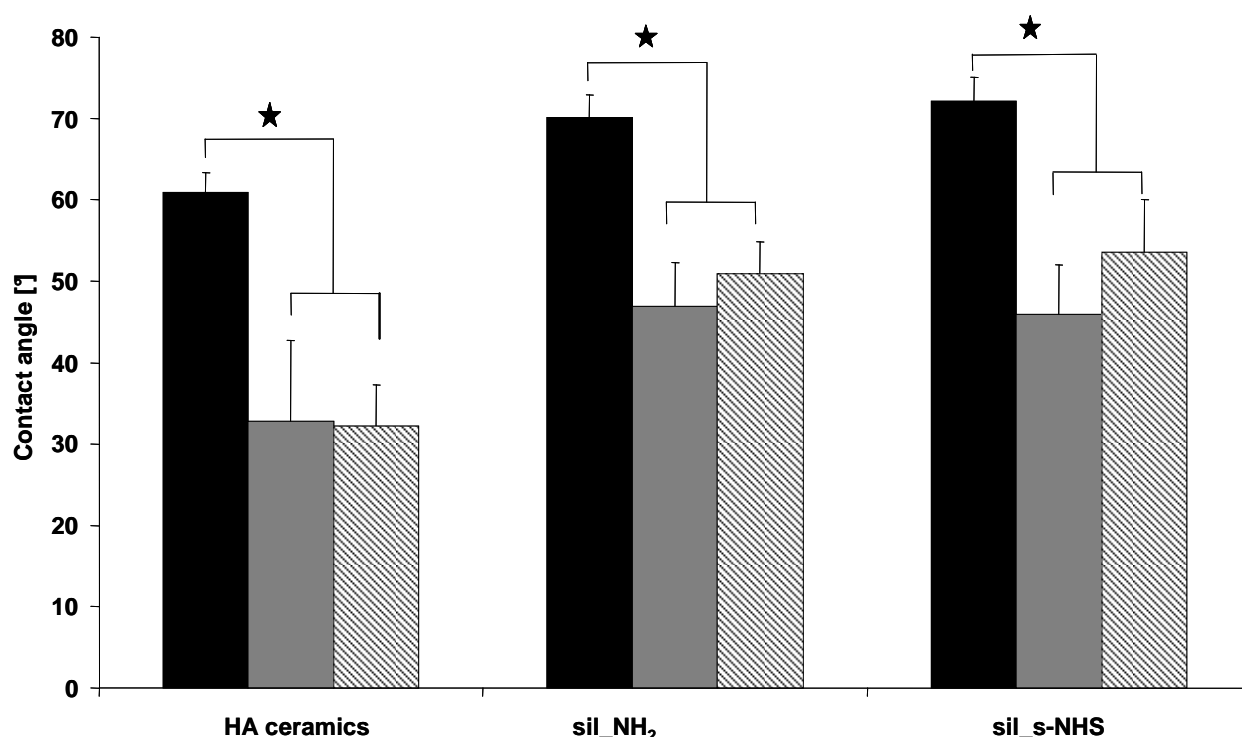


Fig. 2: Water contact angles for untreated surfaces and surfaces after adsorption/binding of lysozyme at a concentration of 10 µg/ml. ■ untreated surfaces; ■ after adsorption/binding of lysozyme; ▨ after washing the samples with 1% SDS in PBS. ★ indicates significant differences ( $p < 0.05$ ;  $n = 15$ ).

In contrast, the adsorption of the two aminobisphosphonates, pamidronate and alendronate, from aqueous solutions and the subsequent activation by carbodiimide chemistry lead to extremely hydrophilic surfaces: Contact angles were reduced from 60° for the unmodified HA ceramic to 20° and 30° for the pamidronate and alendronate modified samples, respectively (Figure 3).

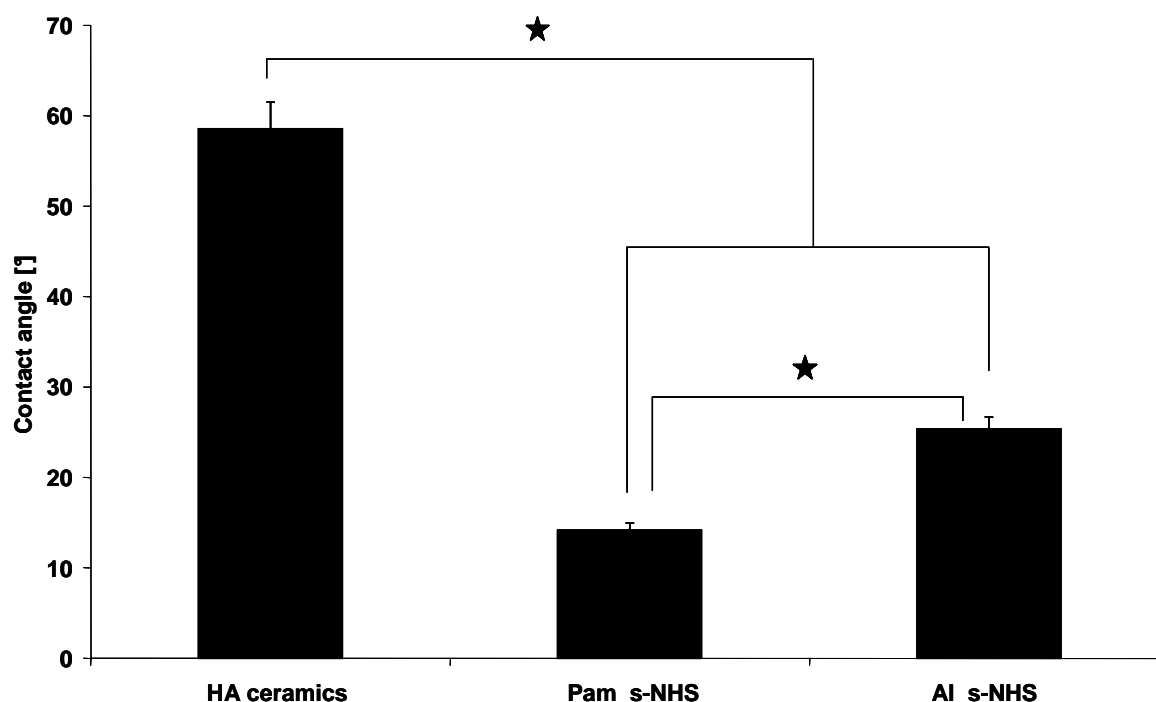


Fig. 3: Water contact angles of untreated ceramic discs and activated discs modified by adsorption of pamidronate and alendronate. Significant differences are indicated by ★ ( $p < 0.05$ ;  $n = 5$ ).

### 3.2. Immobilization of $^{125}\text{I}$ -lysozyme on HA ceramic surfaces

To investigate the potential of the amine-functionalized HA ceramic to immobilize proteins, lysozyme was used as a model protein. 10  $\mu\text{g/ml}$  and 20  $\mu\text{g/ml}$  lysozyme solutions were used and the protein was allowed to adsorb or react overnight. After washing with distilled water, the discs treated with 20  $\mu\text{g/ml}$  of protein maintained higher amounts per sample than the 10  $\mu\text{g/ml}$  discs, indicating an incomplete coverage of the surface with protein when treating with 10  $\mu\text{g/ml}$  or the formation of multilayers after immersion in a 20  $\mu\text{g/ml}$  solution [33;41] (Figure 4a). On the silanized ceramic, less protein was found compared to pure ceramic and sil\_s-NHS activated ceramic. The significant increase in protein mass from silanized to activated ceramic suggests a covalent attachment of protein to the disc surfaces.

After washing with SDS, a total mass of 200 ng lysozyme remained on the activated discs (sil\_s-NHS), irrespective of whether a 10  $\mu\text{g/ml}$  or 20  $\mu\text{g/ml}$  solution of lysozyme was used (Figure 4b). The mass of protein that remained on the samples after washing with the surfactant solution was considered the immobilized protein. When a concentration of 10  $\mu\text{g/ml}$  was used, the adsorption of lysozyme to HA ceramic and silanized ceramic resulted in significantly lower amounts of protein than the covalent attachment. The same tendency was observed for protein immobilization from a 20  $\mu\text{g/ml}$  solution.

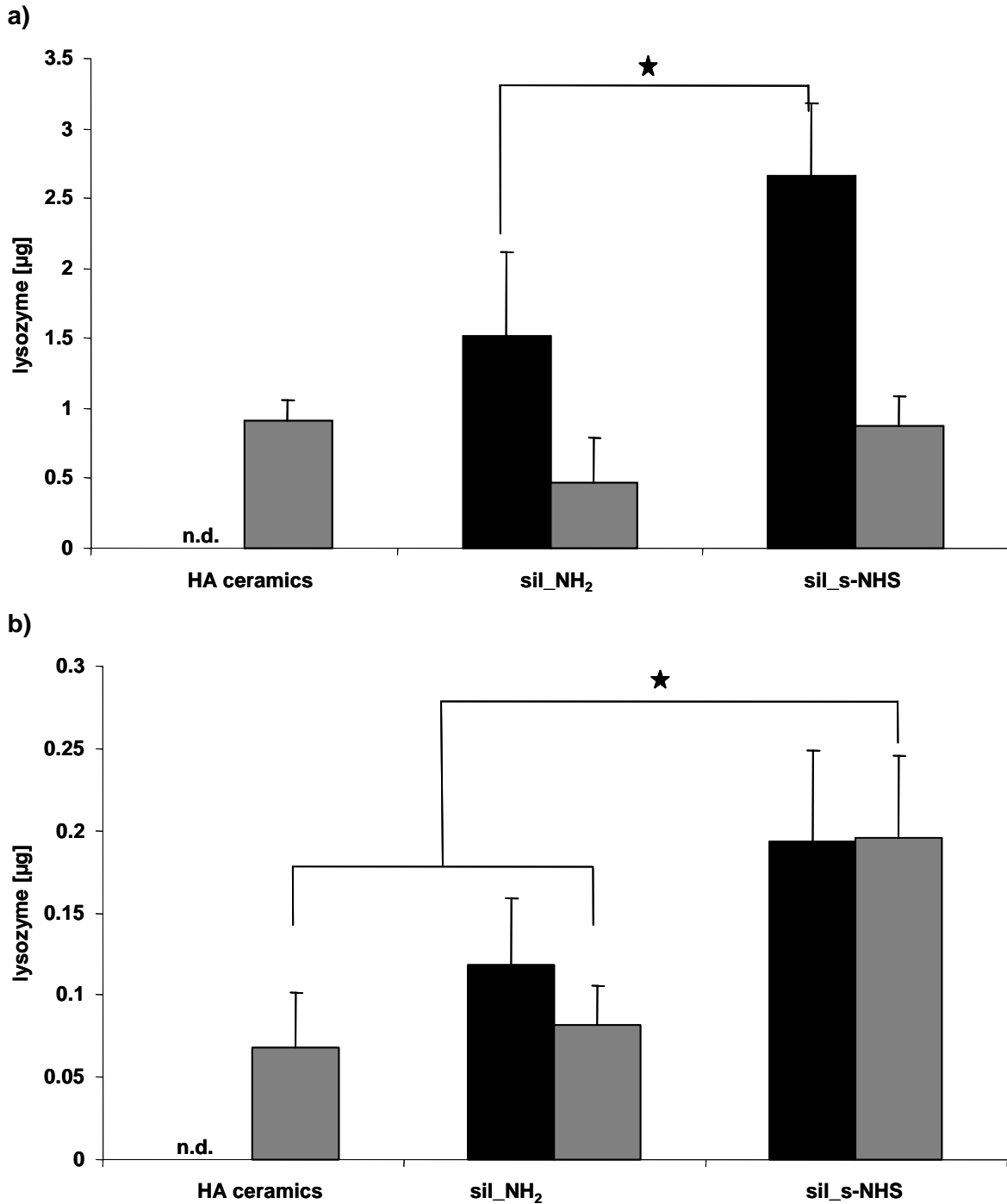
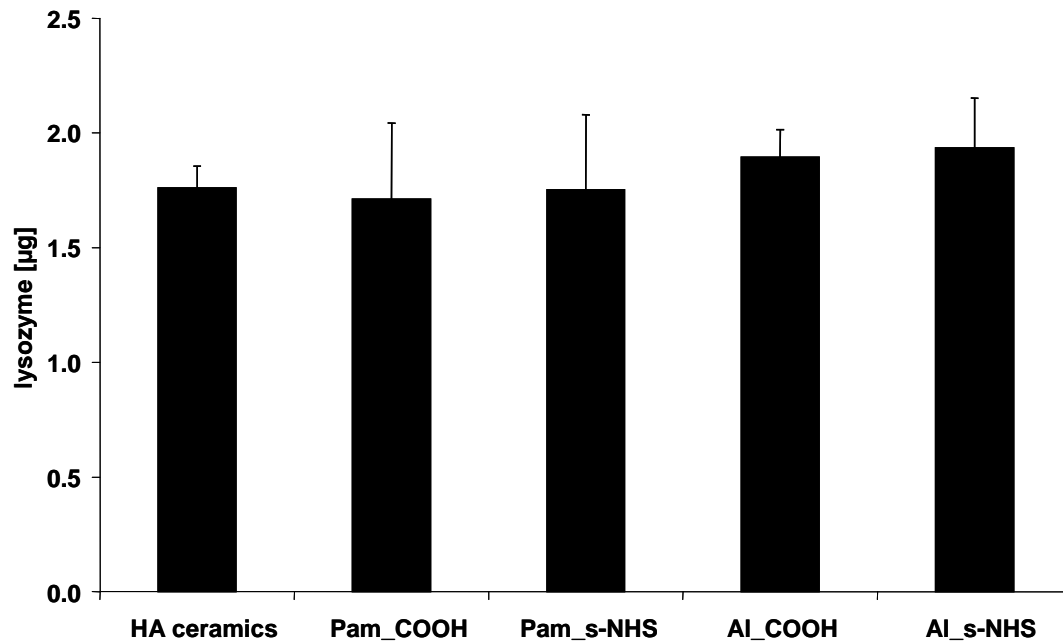


Fig. 4: HA ceramics activated by aminosilanization: Adsorption and binding of  $^{125}$ I-lysozyme. a) Adsorbed and immobilized lysozyme using two different concentrations (■ 20 µg/ml and ▒ 10 µg/ml) after washing the samples with distilled water. Significant differences (indicated by ★;  $p < 0.05$ ;  $n = 3$ ) were measured among the samples incubated with 20 µg/ml. The same tendency was observed between the samples incubated with 10 µg/ml. b) Adsorbed and immobilized lysozyme using two different concentrations (■ 20 µg/ml and ▒ 10 µg/ml) after washing the samples with 1% SDS in PBS. ★ indicates significant differences ( $p < 0.05$ ;  $n = 3$ ). The total amount of immobilized lysozyme is about 200 ng per sample. Adsorption of lysozyme (20 µg/ml) to HA ceramics was not determined (n.d.)

a)



b)

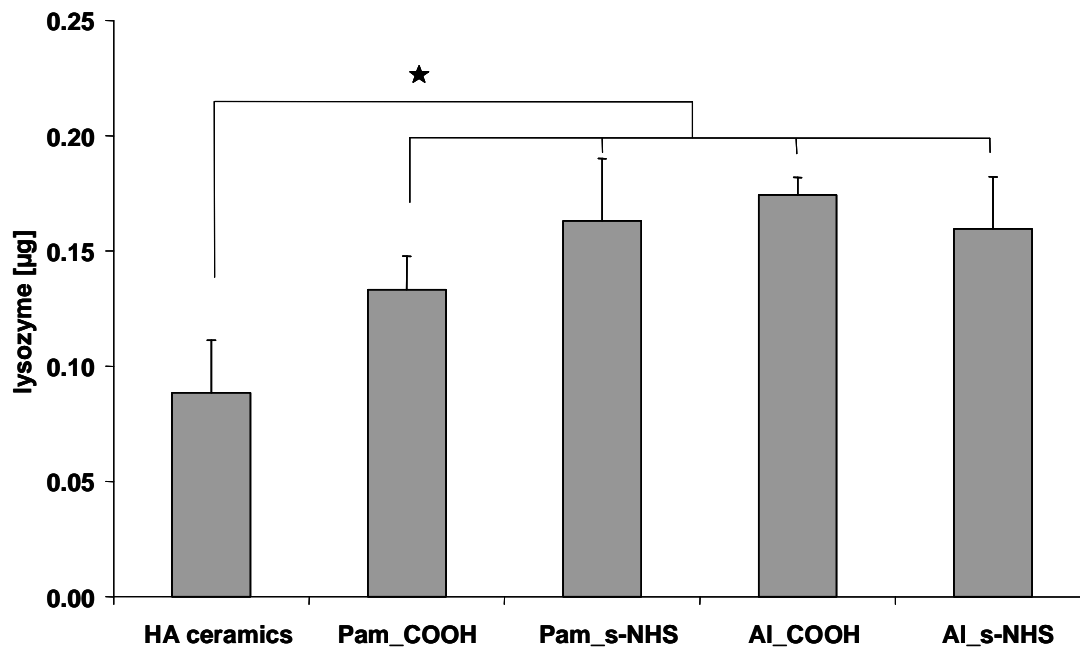


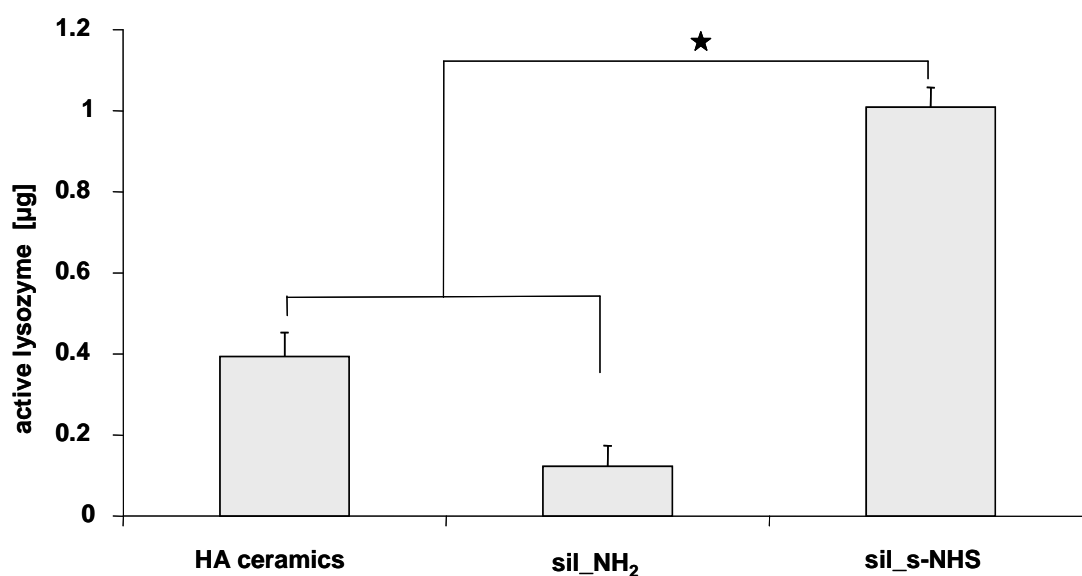
Fig. 5: Surface modifications of HA ceramics by the use of aminobisphosphonates:  
a) Adsorption and binding experiments of  $^{125}$ I-lysozyme to unmodified and bisphosphonate-modified HA ceramic discs. Significant differences were not detected, equivalent amount of the protein adsorbed to all the discs.  
b) Lysozyme deposited on the discs after washing with 1% SDS in PBS. Significant differences are indicated by ★ ( $p < 0.05$ ;  $n = 3$ ).

Using aminobisphosphonates to activate ceramic surfaces for covalent attachment, comparable amounts of lysozyme was deposited on the variously modified ceramic discs (Figure 5a). After washing the samples with a surfactant-containing buffer, the amount of protein on the pure HA surface was significantly lower than on the discs that have been activated for covalent attachment (Figure 5b). Again the mass of lysozyme that was considered immobilized on the Pam\_s-NHS and Al\_s-NHS samples was about 200 ng per disc.

### 3.3. Enzymatic activity of lysozyme immobilized on the surfaces

The enzymatic activity of lysozyme on the surfaces was investigated after immobilization and subsequent washing with water (Figure 6) and compared to the quantitative measurements of radioactively labeled protein (Table 1). Lysozyme was completely inactivated by treatment with SDS, so no results were obtained for the activity of the immobilized protein (data not shown). The activity of covalently attached lysozyme was significantly higher than the activity on surfaces loaded by adsorption, regardless of whether it was bound after silanization or with a bisphosphonate.

a)



*To be continued next page*

b)

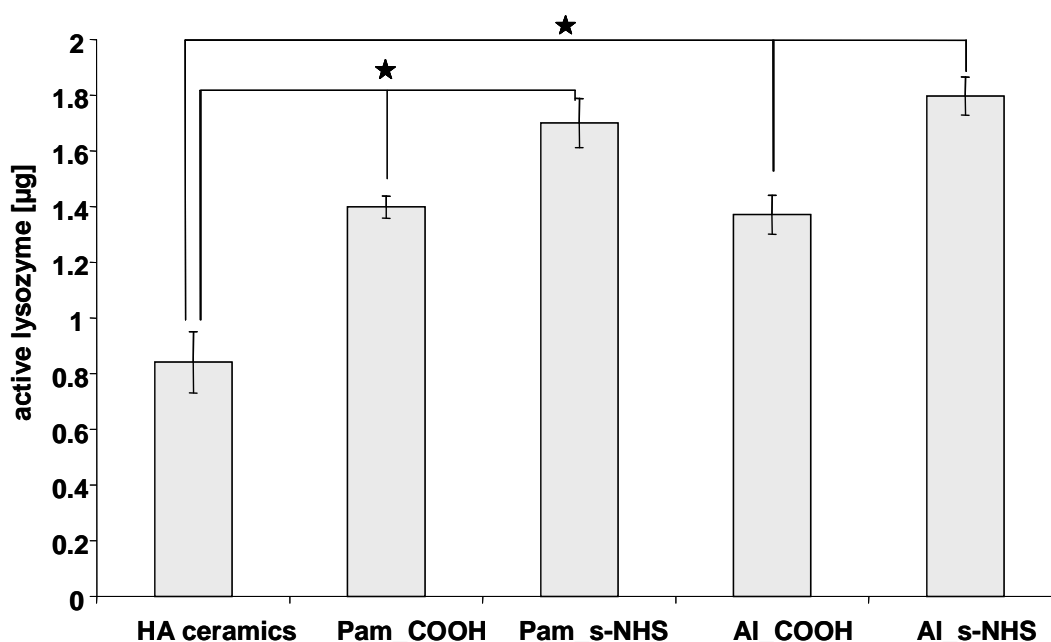


Fig. 6: Enzymatic activity assay of surface immobilized lysozyme.

a) Surface modification by aminosilanization: the protein deposited on the sil\_s-NHS was significantly more active compared to HA ceramic and silanized ceramic ( $p < 0.01$ ;  $n = 3$ ; indicated by ★).

b) Surface modification with aminobisphosphonates: highest activity compared to controls was demonstrated by immobilized lysozyme (Pam\_s-NHS; Al\_s-NHS). Significant differences are indicated by ★ ( $p < 0.01$ ;  $n = 3$ ).

The percent share of active lysozyme in total protein was calculated by dividing the values for the activity of lysozyme by the mass of protein determined by the radioactive binding experiments (Table 1). These results suggest that the protein layer on samples activated by aminosilanization for covalent attachment remained almost completely active, while the activity on surfaces that allow only for adsorption is decreased to 43% for untreated ceramics and 26% for the silanized ceramics. Immobilization by the two aminobisphosphonates lead to approximately 100% active protein, while on untreated ceramic discs only 43% was active and on the discs coupled with inactivated succinic acid ("Pam\_COOH"; "Al\_COOH") 82% and 72% active protein was determined, respectively.

*Table 2: The active part of the immobilized lysozyme relative to the total amount of protein determined by radioactive measurements. When immobilized, the active part of lysozyme corresponds to approx. 100% of the protein that was deposited on the samples.*

	HA ceramics	Sil_NH <sub>2</sub>	Sil_s-NHS	Pam_ COOH	Pam_ s-NHS	Al_COOH	Al_s-NHS
Active lysozyme/ total lysozyme [%]	43 ± 9	26 ± 10	116 ± 46				
	43 ± 2			82 ± 15	97 ± 22	72 ± 6	93 ± 13

### 3.4. Effect of BMP-2 on the osteoblastic differentiation of C2C12 cells

As the experiments with lysozyme have demonstrated that the bisphosphonate-based surface modification method is suitable to bind proteins to HA surfaces and even preserves the protein activity to a higher extent than by simple adsorption, we intended to elucidate whether these positive effects would also hold for the immobilization of BMP-2, a growth factor widely used for surface coatings to improve the osseointegration of implants.

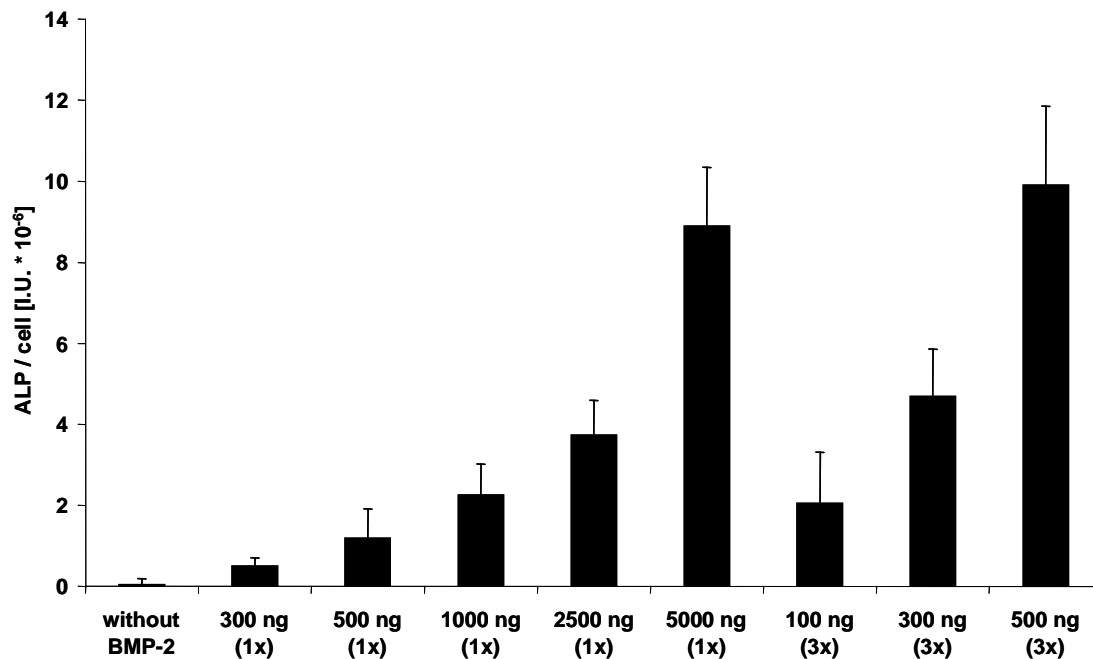


*Fig. 7: Dose-dependent increase of alkaline phosphatase activity per cell after supplementation of BMP-2 to C2C12 mouse myoblasts either on day 1 („1x“) or on day 1 and following with every media change („3x“).*

Alkaline phosphatase activity was taken as a measure for different amounts of active BMP-2 [42;43]. When applied as a solution to cells in polystyrene well-plates, a clearly dose

dependent effect in alkaline phosphatase activity per cell was observed after 6 days of supplementation of different concentrations of BMP-2 to the cell culture media (Figure 7). This dose-dependency was found for a one-time application of BMP-2 on day 1 as well as for a continuous cultivation with BMP-2 in cell culture media over 6 days. In our study, comparably high levels of alkaline phosphatase activity of  $10 \times 10^{-6}$  I.U./cell were reached either by the supplementation of 5000 ng once or 500 ng three times. However, even a single dose of 300 ng or continuous supplementation with 100 ng in the media over 6 days led to a significant increase of ALP activity compared to the control. Von Kossa staining revealed that the supplementation of the lowest doses in the study was sufficient to cause a change in cell morphology (Figure 8). While C2C12 mouse myoblasts grew in parallel bundles, the supplementation of BMP-2 led to the formation of cobblestone-like patterns.

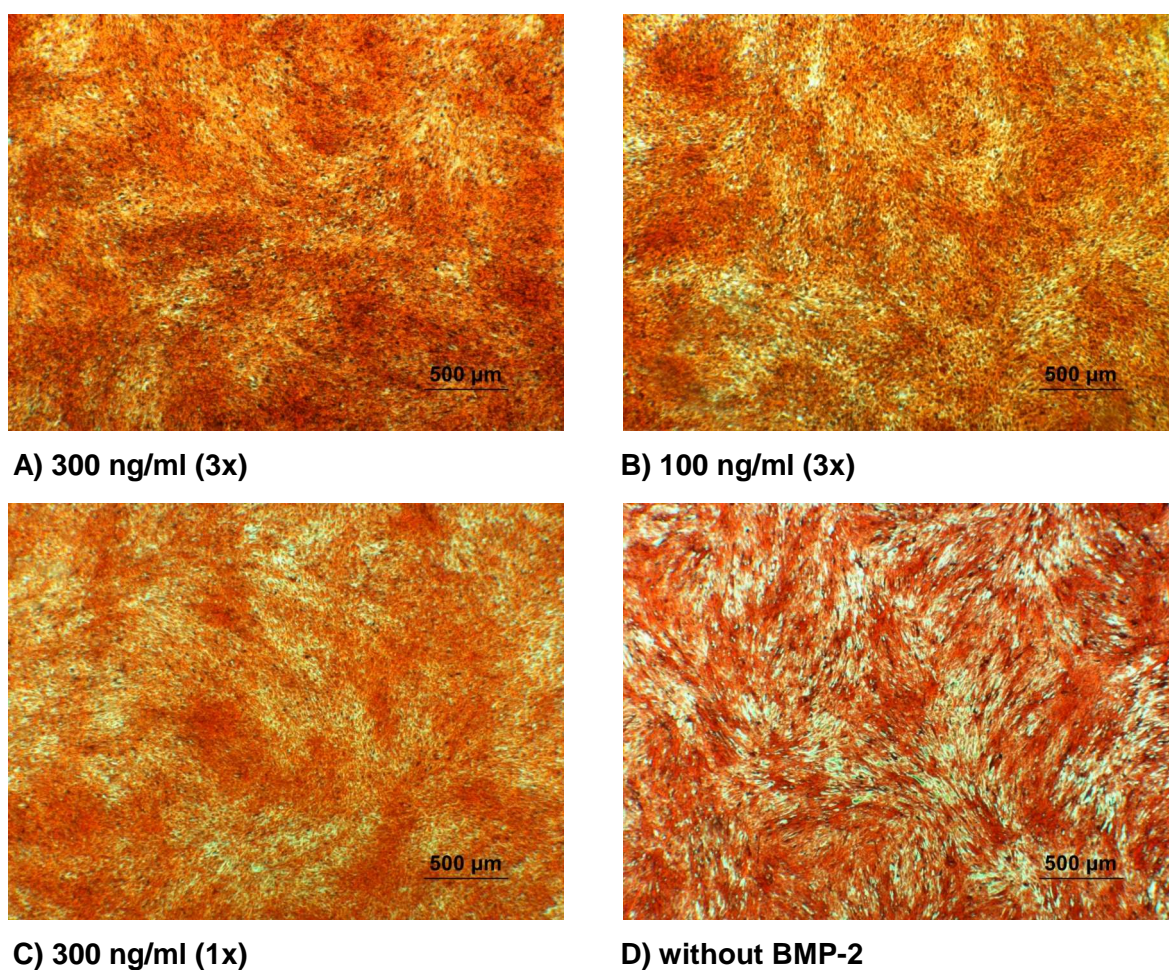


*Fig. 8: Von Kossa staining of C2C12 mouse myoblasts cultured for 6 days with various concentrations of BMP-2. Mineralization (bone nodules) was not observed after this period of time, but cell morphology changed from the formation of parallel bundles (D) to cobblestone-like patterns (A, B and C).*



### 3.5. Effect of HA ceramics on the osteoblastic differentiation of C2C12 cells

Cells were seeded on untreated ceramic discs to investigate if the material itself had an impact on the level of alkaline phosphatase activity of the cells. C2C12 cells on cell culture plastic (TCPS) did not express ALP after 6 days of culture and unmodified HA ceramic surfaces were not capable of inducing an expression of the marker of osteoblastic differentiation (Figure 9). While cells on both surfaces showed increased ALP activity with the supplementation of BMP-2 in the cell culture medium (300 ng, 3x), the cells responded equally on both types of surfaces.

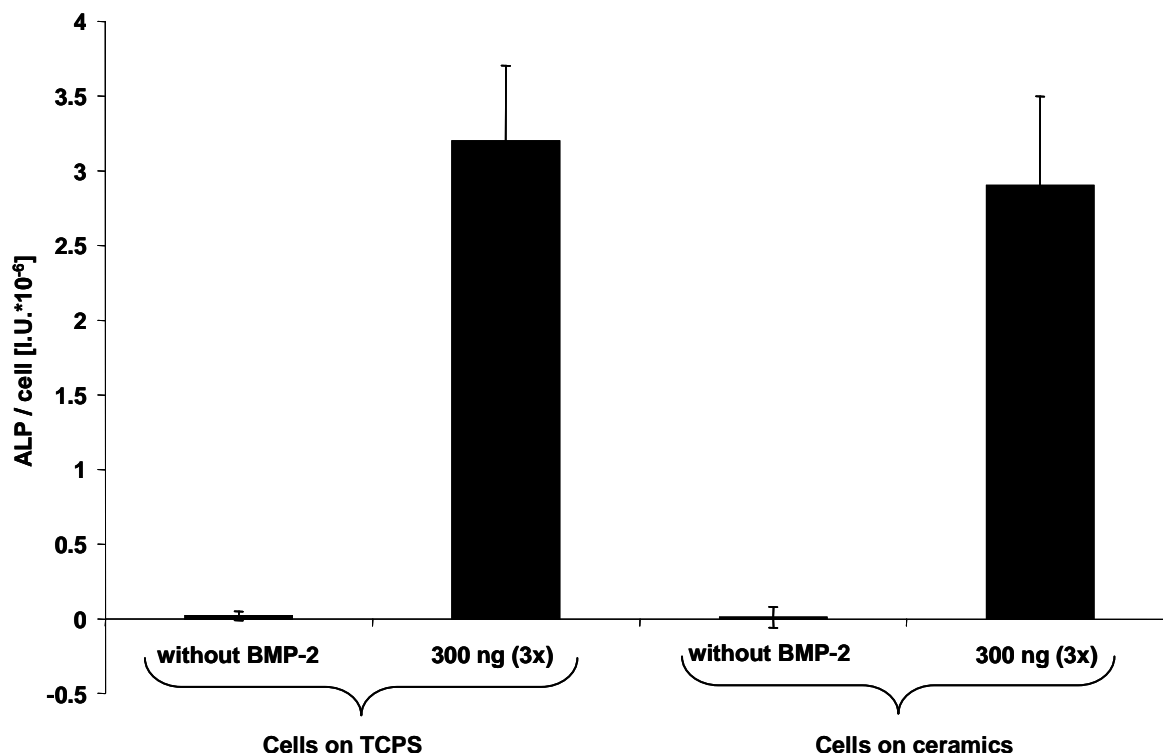


Fig. 8: Comparison of ALP activity on day 6 of cells cultured on TCPS and HA ceramic. The cells on ceramic responded to a supplementation of 300 ng BMP-2 in solution in an equivalent manner while neither the cultivation on TCPS nor on pure HA ceramic lead to a significant expression of the differentiation marker.

### 3.6. Alkaline phosphatase activity stimulated by adsorbed and immobilized BMP-2

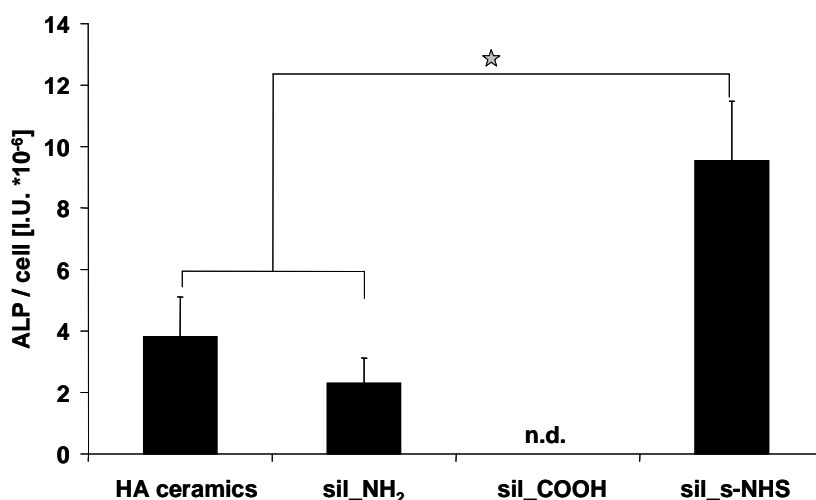
C2C12 cells were cultivated for 6 days on ceramic discs coated with BMP-2 using the two different surface modification techniques. Immobilization of the growth factor led to a dramatic increase in alkaline phosphatase activity (Figure 10 a-c). On day 6 alkaline phosphatase activity per cell reached values of  $10 \cdot 10^{-6}$  I.U. after stimulation by covalently-bound BMP-2, irrespective of the immobilization technique that had been applied. Simply adsorbing BMP-2 to the samples was not as effective as covalent attachment. Surface functionalization by aminosilanization and by aminobisphosphonates was comparably efficient with regard to the stimulation of osteoblastic differentiation of C2C12 cells.

After protein immobilization by the silanization procedure, ALP values were 2.5 fold higher than stimulated from simply adsorbed protein on unmodified or silanized HA surfaces. BMP-2 adsorbed to silanized ceramics had the lowest capacity to stimulate alkaline phosphatase expression. These results correlate perfectly with the results for the enzyme activity of lysozyme.

Comparable results for BMP-2 and lysozyme were also found when aminobisphosphonates were used for surface modification. Again a 2.5 fold increase in ALP expression was obtained by immobilizing BMP-2. Modification by either pamidronate or alendronate lead to an increase of protein activity when adsorbing to samples modified with bisphosphonate and subsequent reaction with succinic acid anhydride ("Pam\_COOH"; "Al\_COOH") relative to absorption to the unmodified ceramics, although the effect was only significant in the case of pamidronate.

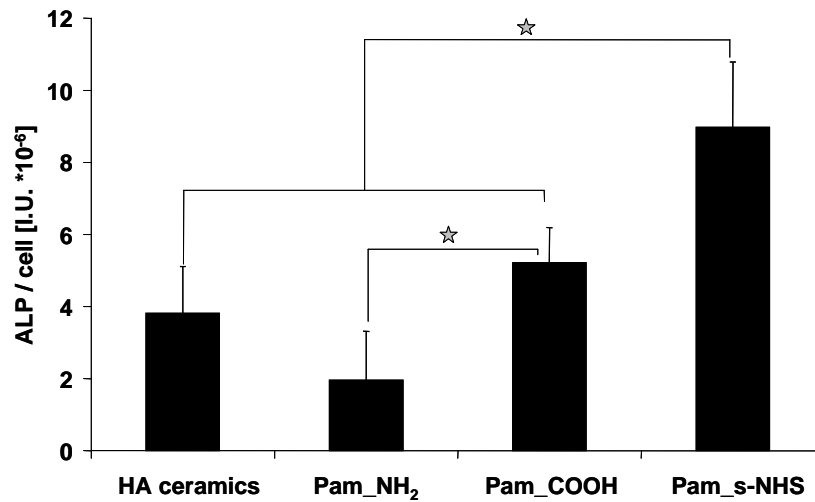
An influence of surface modification on the proliferation of C2C12 cells was not detected; cell numbers for the different experimental groups were equivalent to the values obtained for unmodified hydroxyapatite ceramics (data not shown), which is well in accordance with the literature [35].

a)



*To be continued next page*

b)



c)

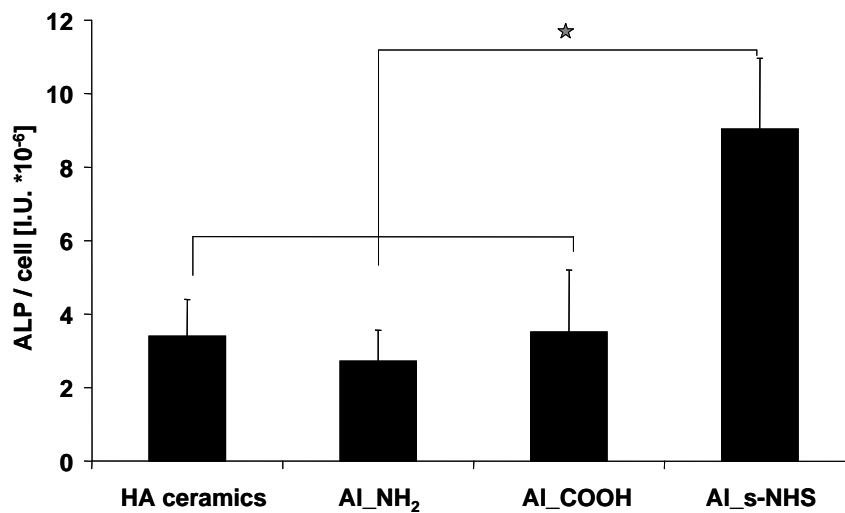


Fig. 10: Alkaline phosphatase activity of C2C12 mouse myoblasts cultured for 6 days on samples with immobilized BMP-2. a) BMP-2 immobilized after aminosilanization. b) BMP-2 immobilized by pamidronate (Pam) and c) BMP-2 immobilized by alendronate (Al) as an anchoring molecule. Immobilized BMP-2 by any of the investigated methods performed superiorly compared to simply adsorbed protein. Significant differences are indicated by ★ ( $p < 0.05$ ).

## 4. Discussion

The main goal of this study was to evaluate the potential of a novel surface modification technique for Ca-rich ceramics using bisphosphonates. This novel approach was compared with the well-established silanization technique [21].

Regarding the manufacturing process, the surface modification with aminobisphosphonates provides several advantages over the silanization procedure: The bisphosphonate modification can be performed at room temperature in aqueous solutions, which is a clear advantage with regard to toxicity concerns or sterilization of the excipients, and would particularly simplify the production of biomimetic surfaces under aseptic conditions. For the covalent immobilization of lysozyme and BMP-2, a two-step zero-length cross-linking strategy has been applied [44], where only one component, in our case the amino-functionalized ceramic discs, had to be exposed to the cross-linker (Scheme 3). After modification, ceramic samples could be stored under dry conditions and growth factors attached immediately prior to cell seeding or implantation (Scheme 3: “Sil\_s-NHS”, “Pam\_s-NHS”; “Al\_s-NHS”).

By measuring the water contact angles of the ceramic samples, we assessed changes in surface composition that might influence the adsorption behavior of proteins. As demonstrated in Figures 2 and 3, both aminosilanization and adsorption of aminobisphosphonates clearly changed the contact angle of the surfaces compared to the unmodified ceramics. However, a correlation between contact angle and the amount of adsorbed or immobilized protein was not discernable, as demonstrated by the experiments with  $^{125}\text{I}$ -lysozyme (Figures 4a and 5a).

When determining the amount of attached lysozyme, the samples suited for covalent immobilization (“Sil\_s-NHS”, “Pam\_s-NHS”, and “Al\_s-NHS”) displayed highest values (Figures 4a and 5a). However, a significant increase compared to unmodified ceramic was not detected. The samples were then washed with a 1% SDS solution in PBS, to remove reversibly bound protein and to determine the mass of immobilized protein. The total mass of lysozyme was reduced to approximately 200 ng, indicating a high amount of adsorbed lysozyme. But the residual amount of lysozyme on discs suited for covalent immobilization (“Sil\_s-NHS”, “Pam\_s-NHS” and “Al\_s-NHS”) was significantly increased compared to control (“HA ceramics”) for both modification procedures (Figures 4b and 5b).

As a well-studied enzyme, whose structure and mechanisms of action are known [45], lysozyme allows for an examination of the effects of immobilization on biological activity. The enzyme activity assay clearly demonstrated that protein activity was not reduced by covalent immobilization by either modification principle: silanization or bisphosphonate-based functionalization. Relating lysozyme activity to amount of protein, an improved stability and performance of immobilized compared to adsorbed protein was found (Table 1). As lysozyme

had been used as model protein for BMPs before [33;46], both techniques were found promising for immobilization of BMP-2 with retention of its biological activity.

The biological activity of immobilized BMP-2 was assessed by the well-established stimulation of the osteoblastic differentiation of C2C12 mouse myoblasts [35]. Their response in terms of alkaline phosphatase expression to different doses of BMP-2 was the basis for measuring the biological efficacy of the growth factor. While in most studies a continuous exposure to BMP-2 over the whole culture period of 6 days was applied, we have shown that a single dose of BMP-2 on day one could induce similar values of alkaline phosphatase per cell (Figure 7). However, the required doses were 10 fold higher to reach comparable levels of ALP by single stimulation.

An enhanced stimulation of ALP activity per cell by immobilized BMP-2 compared to adsorbed BMP-2 was observed after modifying the surfaces both by silanization and using bisphosphonate anchors.

Several reasons could explain this observation: First, more protein could have been deposited on the surface after covalent attachment, as our results have demonstrated that stimulation by a single, but higher, dose lead to similar expression of ALP as continuous supplementation. Second, the covalently attached BMP-2 could function more effectively than the adsorbed protein. This is in accordance with the results for lysozyme and might be explained by a directed presentation of the growth factor after covalent attachment, whereas adsorbed protein would be randomly oriented. Third, the ceramic discs, silanized or bisphosphonate-modified, could serve as a drug release system for the protein with continuous release into the cell culture medium. This is of particular interest as a sustained (pseudo-zero order) release of BMP-2 from gelatin coatings was demonstrated to be the most effective inducer of the differentiation of bone marrow cells when several time-dependent release profiles were compared [47]. In any case, the stimulation of alkaline phosphatase expression was profoundly enhanced by using the conditions for immobilizing BMP-2 to the surfaces.

In previous studies, the beneficial effects of hydroxyapatite on osteoblastic differentiation of bone marrow cells in vitro and bone ingrowth in vivo have been demonstrated [48-51] and bisphosphonates have been shown to lead to increased expression of ALP in osteoblasts [28;29;52;53]. However, in the experiments presented here, the level of alkaline phosphatase expression of C2C12 cells was not stimulated or increased by the ceramic surfaces (Figure 9), or by the bisphosphonate coating (Figure 10 b, c).

To summarize, we have shown that lysozyme and BMP-2 were successfully immobilized on the surface of HA ceramic discs and, in addition to the well-known silanization procedure, the immobilization by aminobisphosphonates as a novel principle was demonstrated and displayed equivalent efficacy.

## 5. Conclusion

By the use of aminobisphosphonates as anchoring molecules a novel method for the immobilization of proteins to HA ceramic surfaces has been investigated and compared to the well-known aminosilanization procedure. We have shown that pamidronate and alendronate allowed for the immobilization of proteins on hydroxyapatite ceramic surfaces by the use of carbodiimide-coupling chemistry. Although for lysozyme no striking effect on the amount of immobilized protein was found, the performance of immobilized protein was superior compared to adsorbed protein in terms of the enzymatic activity of lysozyme and stimulation of osteoblastic differentiation of C2C12 cells by BMP-2. Therefore, we suggest the use of aminobisphosphonates as a novel and simple principle for surface functionalization towards the design of biomimetic coatings for hydroxyapatite that might also be applied to other Ca-rich inorganic or composite materials. Furthermore, for in vivo use, the implant integration process could be supported by the pharmacological effects of the bisphosphonates on osteoblasts and osteoclasts, which would have to be substantiated by additional experiments.

## Acknowledgements

We would like to thank Allison Dennis, Georgia Institute for Technology, Atlanta, USA, for careful revision of the manuscript. Parts of this work were financially supported by the Bayerische Forschungsstiftung (Project: ForTePro).

## 6. References

- [1] Puleo, D. A. (2004): "Bone-implant interface"; Encyclopedia of Biomaterials and Biomedical Engineering (1) p.190-198; Marcel Dekker, Inc., New York
- [2] Shin, H., Jo, S., and Mikos, A. G. (2003): "Biomimetic materials for tissue engineering"; Biomaterials (24) p.4353-4364
- [3] Hench, L. L. and Polak, J. M. "Third-generation biomedical materials"; Science (295) p.1014-1017
- [4] Luginbuehl, V., Meinel, L., Merkle, H. P., and Gander, B. (2004): "Localized delivery of growth factors for bone repair"; European Journal of Pharmaceutics and Biopharmaceutics (58) p.197-208
- [5] Ripamonti, U. and Duneas, N. (1998): "Tissue morphogenesis and regeneration by bone morphogenetic proteins"; Plastic and reconstructive surgery (101) p.227-239
- [6] Chen, D., Zhao, M., and Mundy, G. R. (2004): "Bone Morphogenetic Proteins"; Growth Factors (22) p.233-241
- [7] Jennissen, H. P. (2002): "Accelerated and improved osteointegration of implants bio-coated with bone morphogenetic protein 2 (BMP-2)"; Annals of the New York Academy of Sciences (961) p.139-142
- [8] Akazawa, T., Itabashi, K., Murata, M., Sasaki, T., Tazaki, J., Arisue, M., Kobayashi, M., and Kanno, T. (2005): "Osteoinduction by Functionally Graded Apatites of Bovine Origin Loaded with Bone Morphogenetic Protein-2"; Journal of the American Ceramic Society (88) p.3545-3548
- [9] Sachse, A., Wagner, A., Keller, M., Wagner, O., Wetzel, W. D., Layher, F., Venbrocks, R. A., Hortschansky, P., Pietraszczyk, M., and Wiederanders, B. (2005): "Osteointegration of hydroxyapatite-titanium implants coated with nonglycosylated recombinant human bone morphogenetic protein-2 (BMP-2) in aged sheep"; Bone (37) p.699-710
- [10] Niedhart, C., Maus, U., Redmann, E., Schmidt-Rohlfing, B., Niethard, F. U., and Siebert, C. H. (2003): "Stimulation of bone formation with an in situ setting tricalcium phosphate/rhBMP-2 composite in rats"; Journal of Biomedical Materials Research (65A) p.17-23
- [11] Liu, Y., Hunziker, E. B., de Groot, K., and Layrolle, P. (2003): "Introduction of ectopic bone formation by BMP-2 incorporated biomimetically into calcium phosphate coatings of titanium-alloy implants"; Key Engineering Materials (240-242) p.667-670
- [12] Schmidmaier, G., Wildemann, B., Cromme, F., Kandziora, F., Haas, N. P., and Raschke, M. (2002): "Bone morphogenetic protein-2 coating of titanium implants increases biomechanical strength and accelerates bone remodeling in fracture treatment: a biomechanical and histological study in rats"; Bone (30) p.816-822
- [13] Kokubo, S., Fujimoto, R., Yokota, S., Fukushima, S., Nozaki, K., Takahashi, K., and Miyata, K. (2003): "Bone regeneration by recombinant human bone morphogenetic protein-2 and a novel biodegradable carrier in a rabbit ulnar defect model"; Biomaterials (24) p.1643-1651
- [14] Ruhe, P. Q., Boerman, O. C., Russel, F. G. M., Spauwen, P. H. M., Mikos, A. G., and Jansen, J. A. (2005): "Controlled release of rhBMP-2 loaded poly(dl-lactic-co-glycolic acid)/calcium phosphate cement composites in vivo"; Journal of Controlled Release (106) p.162-171
- [15] Uludag, H., D'Augusta, D., Palmer, R., Timony, G., and Wozney, J. (1999): "Characterization of rhBMP-2 pharmacokinetics implanted with biomaterial carriers in the rat ectopic model"; Journal of Biomedical Materials Research (46) p.193-202
- [16] Ziegler, J., Mayr-Wohlfart, U., Kessler, S., Breitig, D., and Gunther, K. P. (2002): "Adsorption and release properties of growth factors from biodegradable implants"; Journal of Biomedical Materials Research (59) p.422-428
- [17] Voggenreiter, G., Hartl, K., Assenmacher, S., Chatzinikolaidou, M., Rumpf, H. M., and Jennissen, H. P. (2001): "Assessment of the biological activity of chemically immobilized rhBMP-2 on titanium surfaces in vivo"; Materialwissenschaft und Werkstofftechnik (32) p.942-948

- [18] Park, Y. J., Kim, K. H., Lee, J. Y., Ku, Y., Lee, S. J., Min, B. M., and Chung, C. P. (2006): "Immobilization of bone morphogenetic protein-2 on a nanofibrous chitosan membrane for enhanced guided bone regeneration"; *Biotechnology and Applied Biochemistry* (43) p.17-24
- [19] Hench, L. L. (1991): "Bioceramics: From concept to clinic"; *Journal of the American Ceramic Society* (74) p.1487-1510
- [20] Sampathkumaran, U., De Guire, M. R., and Wang, R. (2001): "Hydroxyapatite coatings on titanium"; *Advanced Engineering Materials* (3) p.401-405
- [21] Durrieu, M. C., Pallu, S., Guillemot, F., Bareille, R., Amedee, J., Baquey, C., Labrugere, C., and Dard, M. (2004): "Grafting RGD containing peptides onto hydroxyapatite to promote osteoblastic cells adhesion"; *Journal of Materials Science: Materials in Medicine* (15) p.779-786
- [22] Schuessele, A., Volk, B., Mayr, H., Blunk, T., Schulz, M. B., and Goepferich, A. (2005): "Surface modification of hydroxyapatite ceramic to modulate cell adhesion and improve tissue generation"; in: *Proceedings of the 9<sup>th</sup> meeting and seminar on ceramics, cells and tissues* (A. Ravaglioli, A. Krajewski, Eds.), Faenza, Italy; p.87-94
- [23] de Groot, K. (1998): "Carriers that concentrate native bone morphogenetic protein in vivo"; *Tissue Engineering* (4) p.337-341
- [24] Rosengren, A., Pavlovic, E., Oscarson, S., Krajewski, A., Ravaglioli, A., and Piancastelli, A. (2002): "Plasma protein adsorption pattern on characterized ceramic biomaterials"; *Biomaterials* (23) p.1237-1247
- [25] Lin, J. H. (1996): "Bisphosphonates: A review of their pharmacokinetic properties"; *Bone* (18) p.75-85
- [26] Uludag, H., Kousinioris, N., Gao, T., and Kantoci, D. (2000): "Bisphosphonate conjugation to proteins as a means to impart bone affinity"; *Biotechnology Progress* (16) p.258-267
- [27] Uludag, H., Gao, T., Wohl, G. R., Kantoci, D., and Zernicke, R. F. (2000): "Bone affinity of a bisphosphonate-conjugated protein in vivo"; *Biotechnology Progress* (16) p.1115-1118
- [28] Giuliani, N., Pedrazzoni, M., Negri, G., Passeri, G., Impicciatore, M., and Girasole, G. (1998): "Bisphosphonates stimulate formation of osteoblast precursors and mineralized nodules in murine and human bone marrow cultures in vitro and promote early osteoblastogenesis in young and aged mice in vivo"; *Bone* (22) p.455-461
- [29] Im, G. I., Qureshi, S. A., Kenney, J., Rubash, H. E., and Shanbhag, A. S. (2004): "Osteoblast proliferation and maturation by bisphosphonates"; *Biomaterials* (25) p.4105-4115
- [30] Nancollas, G. H., Tang, R., Phipps, R. J., Henneman, Z., Gulde, S., Wu, W., Mangood, A., Russell, R. G. G., and Ebetino, F. H. (2006): "Novel insights into actions of bisphosphonates on bone: Differences in interactions with hydroxyapatite"; *Bone* (38) p.617-627
- [31] Kajiwar, H., Yamaza, T., Yoshinari, M., Goto, T., Iyama, S., Atsuta, I., Kido, M. A., and Tanaka, T. (2005): "The bisphosphonate pamidronate on the surface of titanium stimulates bone formation around tibial implants in rats"; *Biomaterials* (26) p.581-587
- [32] Tengvall, P., Skoglund, B., Askendal, A., and Aspenberg, P. (2004): "Surface immobilized bisphosphonate improves stainless-steel screw fixation in rats"; *Biomaterials* (25) p.2133-2138
- [33] Puleo, D. A., Kissling, R. A., and Sheu, M.-S. (2002): "A technique to immobilize bioactive proteins, including bone morphogenetic protein-4 (BMP-4), on titanium alloy"; *Biomaterials* (23) p.2079-2087
- [34] Klaeger, A. J., Cevallos, V., Sherman, M. D., Whitcher, J. P., and Stephens, R. S. (1999): "Clinical application of a homogeneous colorimetric assay for tear lysozyme"; *Ocular Immunology and Inflammation* (7) p.7-15
- [35] Katagiri, T., Yamaguchi, A., Komaki, M., Abe, E., Takahashi, N., Ikeda, T., Rosen, V., Wozney, J. M., Fujisawa-Sehara, A., and Suda, T. (1994): "Bone morphogenetic protein-2 converts the differentiation pathway of C2C12 myoblasts into the osteoblast lineage"; *Journal of Cell Biology* (127) p.1755-1766



- [36] Lieb, E., Milz, S., Vogel, T., Hacker, M., Dauner, M., and Schulz, M. B. (2004): "Effects of transforming growth factor b1 on bonelike tissue formation in three-dimensional cell culture I. culture conditions and tissue formation"; *Tissue Engineering* (10) p.1399-1413
- [37] Lieb, E., Vogel, T., Milz, S., Dauner, M., and Schulz, M. B. (2004): "Effects of transforming growth factor b1 on bonelike tissue formation in three-dimensional cell culture II: Osteoblastic differentiation"; *Tissue Engineering* (10) p.1414-1425
- [38] Kaelble, D. H. and Moacanin, J. (1977): "A surface energy analysis of bioadhesion"; *Polymer* (18) p.475-482
- [39] Vogler, E. A. (1998): "Structure and reactivity of water at biomaterial surfaces"; *Advances in Colloid and Interface Science* (74) p.69-117
- [40] Norde, W. and Lyklema, J. (1991): "Why proteins prefer interfaces"; *Journal of Biomaterials Science, Polymer Edition* (2) p.183-202
- [41] Daly, S. M., Przybycien, T. M., and Tilton, R. D. (2003): "Coverage-dependent orientation of lysozyme adsorbed on silica"; *Langmuir* (19) p.3848-3857
- [42] Lieb, E., Tessmar, J., Hacker, M., Fischbach, C., Rose, D., Blunk, T., Mikos, A. G., Goepferich, A., and Schulz, M. B. (2003): "Poly(D,L-lactic acid)-poly(ethylene glycol)-monomethyl ether diblock copolymers control adhesion and osteoblastic differentiation of marrow stromal cells"; *Tissue Engineering* (9) p.71-84
- [43] Gopferich, A., Peter, S. J., Lucke, A., Lu, L., and Mikos, A. G. (1999): "Modulation of marrow stromal cell function using poly(DL-lactic acid)-block-poly(ethylene glycol)-monomethyl ether surfaces"; *Journal of Biomedical Materials Research* (46) p.390-398
- [44] Grabarek, Z. and Gergely, J. (1990): "Zero-length crosslinking procedure with the use of active esters"; *Analytical Biochemistry* (185) p.131-135
- [45] Chipman, D. M. and Sharon, N. (1969): "Mechanism of lysozyme action"; *Science* (165) p.454-465
- [46] Scheufler, C., Sebald, W., and Hulsmeier, M. (1999): "Crystal structure of human bone morphogenetic protein-2 at 2.7 Å resolution"; *Journal of Molecular Biology* (287) p.103-115
- [47] Raiche, A. T. and Puleo, D. A. (2004): "Cell responses to BMP-2 and IGF-I released with different time-dependent profiles"; *Journal of Biomedical Materials Research* (69A) p.342-350
- [48] Cook, S. D., Thomas, K. A., Dalton, J. E., Volkman, T. K., Whitecloud, T. S., III, and Kay, J. F. (1992): "Hydroxylapatite coating of porous implants improves bone ingrowth and interface attachment strength"; *Journal of Biomedical Materials Research* (26) p.989-1001
- [49] Ozawa, S. and Kasugai, S. (1996): "Evaluation of implant materials (hydroxyapatite, glass-ceramics, titanium) in rat bone marrow stromal cell culture"; *Biomaterials* (17) p.23-29
- [50] Stephenson, P. K., Freeman, M. A., Revell, P. A., Germain, J., Tuke, M., and Pirie, C. J. (1991): "The effect of hydroxyapatite coating on ingrowth of bone into cavities in an implant"; *Journal of Arthroplasty* (6) p.51-58
- [51] Vasudev, D. V., Ricci, J. L., Sabatino, C., Li, P., and Parsons, R. (2004): "In vivo evaluation of a biomimetic apatite coating grown on titanium surfaces"; *Journal of Biomedical Materials Research* (69A) p.629-636
- [52] Yoshinari, M., Oda, Y., Ueki, H., and Yokose, S. (2001): "Immobilization of bisphosphonates on surface modified titanium"; *Biomaterials* (22) p.709-715
- [53] Reinholz, G. G., Getz, B., Pederson, L., Sanders, E. S., Subramaniam, M., Ingle, J. N., and Spelsberg, T. C. (2000): "Bisphosphonates directly regulate cell proliferation, differentiation, and gene expression in human osteoblasts"; *Cancer Research* (60) p.6001-6007



# **Chapter 6**

## **Pamidronate-based surface modification of hydroxyapatite particles: adsorption and co-precipitation**

A. Schuessele<sup>1</sup>, A. Goeperich<sup>1</sup>

<sup>1</sup>Department of Pharmaceutical Technology, University of Regensburg, Germany

**Abstract**

Hydroxyapatite is widely used in bone replacement as coating on materials for hard tissue repair or inorganic phase of composite materials. Methods for the functionalization of hydroxyapatite surfaces are of particular interest to immobilize molecules at the bone-implant interface or achieve covalent bonding of organic to inorganic phase of composite materials. The aminobisphosphonate pamidronate was adsorbed to hydroxyapatite powders to obtain particles with amino groups on the surface that were accessible for further conjugation steps. Furthermore, an adsorption study was carried out revealing that within a range of 0-20 mmol/L the number of amino groups on the surface can be controlled by the concentration of the bisphosphonate solution. The adsorption of pamidronate cannot be described by the Langmuir type of adsorption. After removing reversibly bound pamidronate by washing the samples, the amount of bisphosphonate levels at  $1.3 \mu\text{mol}/\text{m}^2$ . As alternative route to surface functionalization, particles were obtained by precipitation in the presence of pamidronate. X-ray diffraction patterns revealed that particles were composed of brushite ( $\text{CaHPO}_4 \cdot 2 \text{H}_2\text{O}$ ) and these particles were suitable for further conjugation steps. However, the precipitation process needs further optimization towards the control of particle size and type of calcium phosphate. By adsorption and co-precipitation particles were obtained with amino groups on the surface that were accessible for the attachment of the amine-reactive model compound TNBS.

## 1. Introduction

Selective drug delivery to the skeletal system becomes very important in certain bone related diseases such as osteoporosis, bone fractures and infections [1]. Hydroxyapatite (HA) is a particularly interesting material as drug carrier or for bone replacement as it resembles the natural inorganic phase of bone [2-4]. Due to their similarity to the mineral phase of bone, HA particles were used as solid part of composite materials for hard tissue repair in combination with synthetic or natural polymers [5]. The interface between organic filler material and inorganic part of such composites influences the stability of the construct [6]. To improve the properties of the composite the interfacial bond strength was increased by modifying hydroxyapatite surfaces to allow for their covalent attachment to the polymeric filler [7-11]. Furthermore, hydroxyapatite particles have been used as drug carriers for local delivery of drugs after adsorption or incorporation, such as antibiotics [12], proteins [13-15], or bisphosphonates [16]. In certain cases, covalent attachment of drugs to HA surfaces would be favorable for the delivery of drugs to bone or the bone-implant interface favoring a prolonged retention at the site of action [17;18]. In order to enable covalent attachment of drugs, HA surfaces have been modified using silane-coupling chemistry and hexamethylene diisocyanates, methods that are limited in stability of the created bonds, poor control of the reaction and toxicity concerns of the educts, respectively [9;10;19-21]. Therefore, alternatives were searched allowing additionally for a control of the number of functional groups per surface area. This possibility of controlling the number of binding sites is of particular interest for the attachment of adhesive peptides [22].

Bisphosphonates, well-known as inhibitors of bone resorption [23], accumulate in bone and calcified tissues as a consequence of their high affinity to hydroxyapatite [24;25]. Depending on the structure of the bisphosphonate derivative, bi- or tridentate interactions with hydroxyapatite are observed [26]. Due to the strong affinity of bisphosphonates to hydroxyapatite, it was hypothesized that adsorbed amino-bisphosphonates can serve as a platform for covalent attachment to HA surfaces. In this study, the adsorption of the aminobisphosphonate pamidronate (Fig. 1) was investigated as a novel method for the creation of functional groups on HA surfaces. The dye trinitrobenzenesulfonic acid (TNBS) was attached as a model compound to prove the suitability of pamidronate modified hydroxyapatite for further conjugation steps. The type of adsorption was determined and the number of amino groups accessible for covalent attachment of molecules was measured by the ninhydrin method.

As an alternative route to functionalized particles the precipitation of HA in the presence of pamidronate was investigated. By this approach, we additionally aimed for the control of particle size, morphology and degree of crystallinity, as bisphosphonates were shown to inhibit the growth of HA crystals [27] and enable variations in zeta potential depending on the adsorbed derivative [28]. The particles were characterized by X-ray diffraction (XRD) to

determine phase composition and crystallinity, and scanning electron microscopy (SEM) to examine particle size and morphology. Finally, the suitability for covalent attachment of the HA/pamidronate co-precipitate was assessed by attachment of TNBS as a model compound.

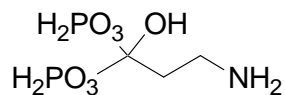


*Fig. 1: The aminobisphosphonate pamidronic acid.*

## 2. Materials and Methods

### 2.1. Materials

Hydroxyapatite (HA) powder was a gift from Merck Biomaterials (Darmstadt, Germany). Disodium 3-amino-1-hydroxypropylidene-1,1-bisphosphonate (disodium pamidronate) was obtained from Ofichem (Ter Apel, the Netherlands). Trinitrobenzenesulfonic acid (TNBS), 2,2'-dihydroxy-2,2'-biindan-1,1',3,3'-tetrone (hydrindantin), ammonium peroxodisulfate, calcium hydroxide and 1,2,3-indanetrione (ninhydrin) were purchased from Sigma-Aldrich (Steinheim, Germany). Dimethylene sulfoxide (DMSO), di-sodium tetra-borate decahydrate, potassium chloride, Titriplex III, sodium heptamolybdate, lithium hydroxide, hydrazinium sulfate, acetic acid, phosphoric acid and tin (II) chloride dihydrate were purchased from Merck (Darmstadt, Germany). 6-Amino hexanoic acid was purchased from CARL Roth GmbH (Karlsruhe, Germany). For all experiments double distilled water (ddH<sub>2</sub>O) was used. All chemicals were of analytical grade.

### 2.2. Specific surface area of hydroxyapatite powder

Analysis of the surface area of the powders was performed according to the method of Brunauer-Emmet-Teller (BET) using the Accelerated Surface Area and Porosimetry System ASAP 2010 of Micromeritics Instrument Corp. (Norcross, USA). 100 mg of the powder sample were analyzed using nitrogen as adsorptive. A surface area of  $67.16 \pm 0.04 \text{ m}^2/\text{g}$  was determined. This value was used for further calculations.

### 2.3. Attachment of a model compound: TNBS-Assay

To investigate the presence of amino groups at the surface of HA powders after adsorption of pamidronate, a colorimetric assay described in the literature was used [29]. NH<sub>2</sub> groups on the surfaces were determined by the reaction with 2,4,6-trinitrobenzenesulfonic acid (TNBS). Samples of 100 mg were incubated in Eppendorf cups with 1.5 ml of a 0.1 % solution of TNBS in 3% sodium borate solution at 70°C for 15 min. The suspensions were centrifuged at 12000 rpm (Centrifuge 5415R; Eppendorf, Hamburg, Germany). The supernatant was discarded and replaced by 1.5 ml distilled water. After shaking, the samples were centrifuged again. The washing procedure was repeated 5 times until the rinsing water was colorless. Photographs of the resulting colored powders were taken for documentation.

### 2.4. Adsorption study

Sodium pamidronate was dissolved in distilled water in concentrations ranging from 0.05 mmol/L up to 100 mmol/L. 150 mg hydroxyapatite powder and 1.5 ml of the pamidronate solution were added to a glass vessel and the suspension was shaken overnight at room temperature on an orbital shaker (Edmund Bühler GmbH, Tübingen, Germany) set at 20 rpm. The HA suspension was centrifuged at 12000 rpm (Centrifuge

5415R; Eppendorf, Hamburg, Germany) and aliquots of the supernatant were processed as described in 2.5. (pamidronate assay). The amount of remaining free bisphosphonate in the supernatant was determined by the pamidronate assay and the amount of adsorbed pamidronate was calculated. The hydroxyapatite samples loaded with pamidronate were dried and aliquots were used for TNBS and ninhydrin assay.

## **2.5. Determination of organic phosphates - pamidronate assay**

The method of Ames et al. for the determination of total phosphate content in samples of organic origin was used with some modifications [30]. An aliquot of the supernatant solutions of 2.4 was added to 400  $\mu$ l of a 4% (w/v) aqueous ammonium peroxodisulfate solution in a glass vessel. The samples were reduced to ashes at 200°C over night. The ashes were dissolved in 500  $\mu$ l of an aqueous solution of potassium chloride (0.02 M) and EDTA (0.3 M). Ammonium heptamolybdate was dissolved in a 3.5% sulfuric acid to gain a 1% (w/v) solution. 120  $\mu$ l of the molybdate reagent were added to the phosphate solution. The resulting heteropolyoxomolybdate was reduced to a blue colored product by adding 120  $\mu$ l of a hydrazinium sulfate/ tin (II) chloride solution in 3% sulfuric acid. Samples were checked for inorganic phosphate dissolved from hydroxyapatite by preparing the assay without the oxidation step and values were subtracted from the absorbance of the samples after oxidation. The whole process was checked for free phosphate, e.g. from glass vessels, by analyzing distilled water. A calibration curve was prepared starting with solutions of known pamidronate concentration. The absorbance of samples was read in microtest-plates with a microplate reader (CS-9301 PC, Shimadzu, Munich, Germany) at 700 nm. In order to determine the resulting number of amino groups per area dependent on the initially used concentration of pamidronate the initial concentrations were plotted against the resulting number of pamidronate molecules per  $m^2$ .

## **2.6. Quantification of surface amino groups – ninhydrin assay**

The hydroxyapatite powders loaded with pamidronate from the adsorption study (2.4.) were washed with 1.5 ml of bidistilled water. The powder was separated by centrifugation and dried under vacuum. For each sample 20.0 mg of HA (n=3 per experimental group) were immersed in a vial of a parallel synthesis block (synthesis 1, Heidolph, Germany). The ninhydrin reagent was prepared as follows: 2.4 g of ninhydrin and 0.36 g of hydrindantin were dissolved in 90 ml DMSO and mixed with 30 ml of a lithium acetate buffer (4 M, pH 5.2) [31]. 5 ml of this reagent were added to each sample. The reaction mixture was heated to 105°C and shaken at 800 rpm. The reaction of ninhydrin with primary amines results in a violet color. The samples were filtrated, diluted with 10 ml of ethanol (50% v/v) and the absorbance was read on a Photometer (Uvikon 941, Kroton Inst., Munich, Germany) at 570 nm. A calibration curve was prepared using 6-amino-hexanoic acid as a standard.



### 2.7. Calculation of adsorbed pamidronate and plotting of isotherm

The amount of pamidronate (mmol) adsorbed per m<sup>2</sup> on HA powder (Q) was calculated by the difference between the initial (C<sub>1</sub>) and the equilibrium (C<sub>eq</sub>) pamidronate concentration (mmol/L) using equation (1):

$$Q = [(C_1 - C_{eq}) \times V] / (W \times S) \quad (1)$$

Where V is the volume of the solution (1.5 ml), W is the mass of the adsorbent (HA; 150mg), and S is the specific surface area of the adsorbent.

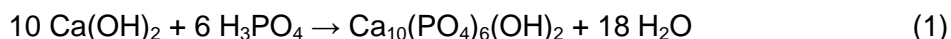
To determine if the isotherm followed a Langmuir type of adsorption, the equilibrium concentrations (C<sub>eq</sub>) were plotted against the resulting number of pamidronate molecules per cm<sup>2</sup> and the quotient of C<sub>eq</sub>/Q was plotted against the equilibrium concentration C<sub>eq</sub>. This plot results in a straight line if the adsorption isotherm fits the Langmuir model of adsorption [32;33].

### 2.8. Calculation of the surface area covered by pamidronate

To estimate the surface area covered by pamidronate the size of a pamidronate molecule was determined with the software package SYBYL (version 7.1; Tripos GmbH, Munich, Germany). Reports from literature were followed stating that the phosphonates and the hydroxyl function are oriented towards the surface (PPO) [26], or the phosphonates and the amino group are involved in surface binding (PPN) as described in [34]. The area of the triangle formed by these functional groups was computed as an estimation of the area covered by a pamidronate molecule.

### 2.9. Precipitation of HA particles

Hydroxyapatite particles were prepared by a wet chemical precipitation method following reaction (1) proposed in the literature [35]:



0.74 g Ca(OH)<sub>2</sub> were dissolved in 20 ml water (0.5 mol/l) and stirred on a magnetic stirrer at 400 rpm (Heidolph MR 3001K; Nürnberg, Germany). The solution was heated to 40 °C or 60 °C and thermostated in a water bath. 20 ml of dilute phosphoric acid (0.3 mol/l) were added dropwise under stirring.

In a third reaction, particles were precipitated in the presence of pamidronate at a concentration of 0.7 mg/ml at 40 °C. The resulting particle suspensions were centrifuged, the supernatant was decanted and the precipitates were dried under vacuum.

## **2.10. Characterization of particles**

### **2.10.1 Light microscopy**

The resulting suspensions were analyzed by light microscopy (Axiovert, Zeiss, Germany). Images were taken with a digital camera (DS-U1, Nikon; Düsseldorf, Germany). The TNBS reaction was performed on the samples to determine if there were amino groups present on the surface as described in 2.3.

### **2.10.2 Scanning electron microscopy**

The morphology of particles was investigated by scanning electron microscopy (SEM). The particles were mounted on aluminum stubs using conductive carbon tape (LeitTape; Plannet GmbH; Wetzlar, Germany) and coated with a layer of 1.4 nm gold-palladium (SEM auto-coating unit E2500; Polaron Equipment Ltd.; Watford, UK). The micrographs were obtained at 5.0 kV on a scanning electron microscope (JSM 840, Jeol; Echting, Germany).

### **2.10.3 X-ray powder diffraction**

The precipitated particles were characterized by X-ray powder diffraction techniques. Flat samples in transmission geometry were analyzed on a STOE STADI-P (STOE, Darmstadt, Germany). Cu- $K_{\alpha 1}$  radiation was used ( $\lambda = 1.5406 \text{ \AA}$ ; Ge monochromatized) and a  $\theta$ -range from 10-90 ° $\theta$  was analyzed. Phase composition of samples was determined by the WinXPow software package (STOE 2000). X-ray diffraction patterns obtained from literature served as reference patterns for hydroxyapatite [36] and brushite [37].

### 3. Results

#### 3.1. Adsorption study of pamidronate

To prove the hypothesis, that by adsorption of aminobisphosphonates amino groups were deposited on hydroxyapatite surfaces that were suitable for further conjugation steps, pamidronate was adsorbed to hydroxyapatite and the amine-reactive dye TNBS was attached. After washing the powders until the water was colorless, the samples showed differences in intensity of yellow color depending on the concentration of pamidronate that had been used for adsorption (Fig. 2). Hydroxyapatite powder that had not been pretreated with pamidronate served as control: After immersion in a TNBS solution and washing, the yellow colored dye was completely removed and the hydroxyapatite powder remained white.



*Fig. 2: TNBS-reaction performed after adsorption of pamidronate from solutions with different concentrations. From left to right the intensity of yellow color is strongly increased with rising amount of pamidronate indicating an increase in functional groups present on the surface.*

To determine the type of adsorption of pamidronate an adsorption study was performed assessing the equilibrium concentration of pamidronate by a pamidronate assay [30]. The adsorption study revealed that the amount of pamidronate and consequently the number of amino groups per surface area was dependent on the concentration of pamidronate within the tested range of concentrations (Fig. 3 A). After washing the samples once with water to remove reversibly bound pamidronate, the ninhydrin assay was performed. By this method, the number of remaining primary amines on the surface was assessed and plotted against the initial concentration of the pamidronate solution (Fig.3 B).

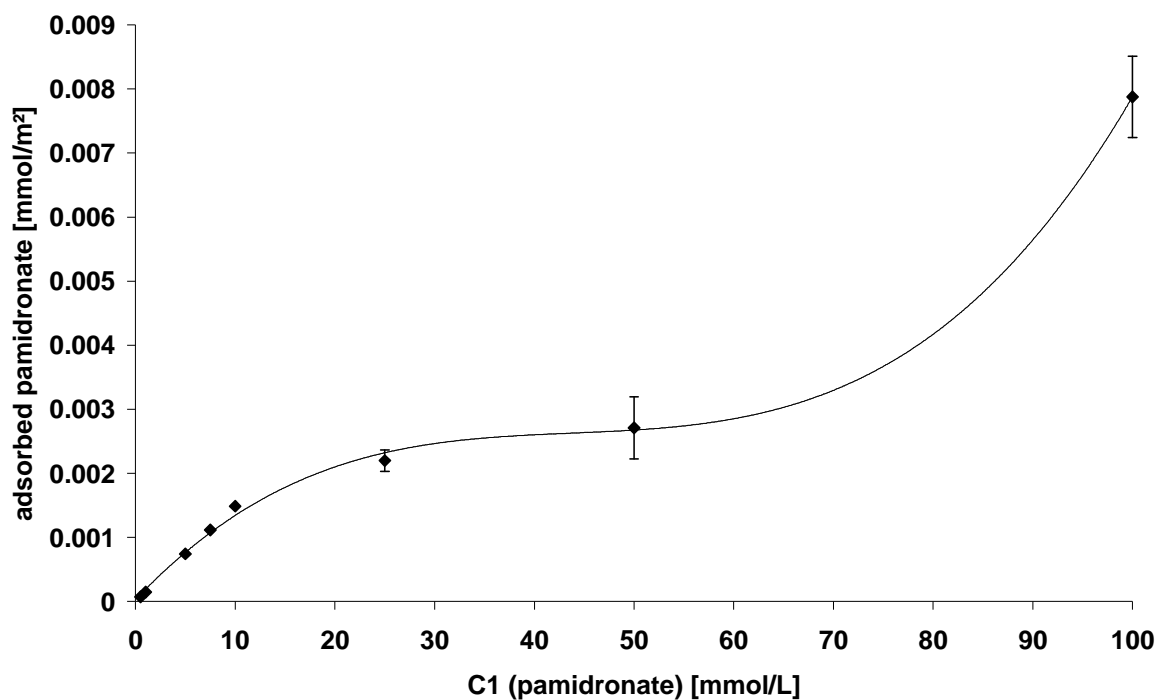
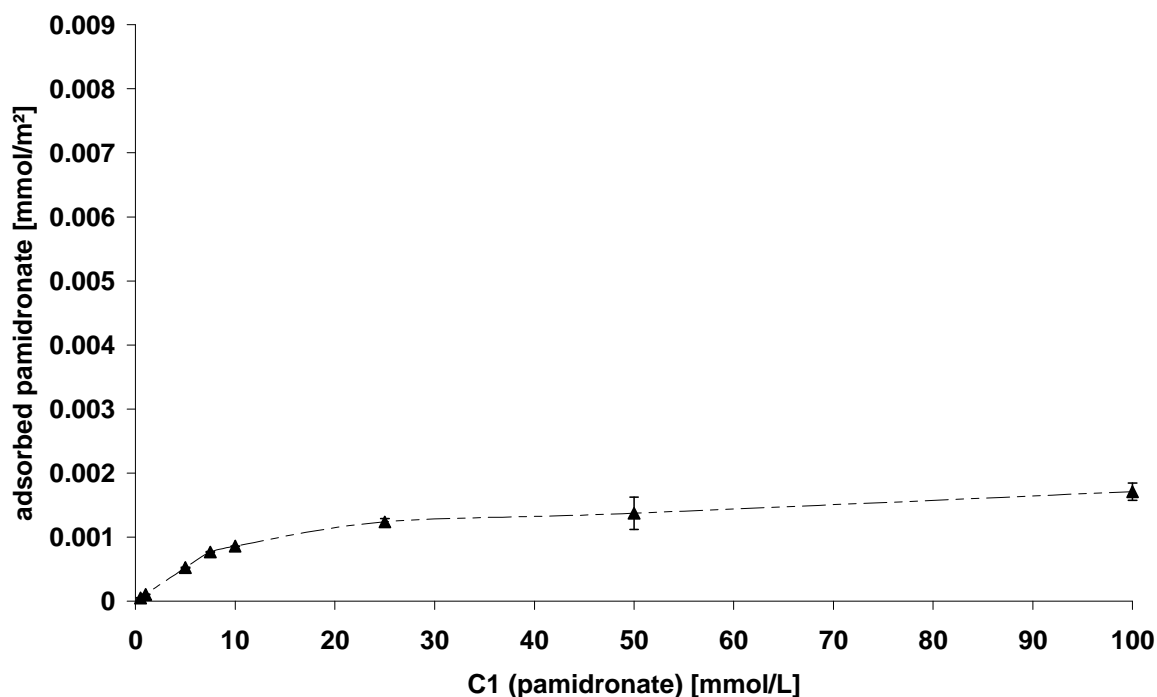
**A****B**

Fig.3: Adsorption study of pamidronate on HA powder: **A)** pamidronate assay: amounts of pamidronate in the supernatant were determined and adsorbed amounts were calculated. **B)** ninhydrin method: determination of remaining primary amines on the surface after washing the HA powders with water.

The results for the adsorption of pamidronate showed that amino groups for covalent attachment can be deposited on the surface of HA. Below initial pamidronate concentrations of 10 mmol/L, the number of surface amino groups was directly proportional to the concentration of the pamidronate solution and pamidronate adsorbed completely to the hydroxyapatite surface.

Using the ninhydrin method, the remaining number of amino groups after washing the samples with distilled water was determined. These remaining pamidronate molecules were regarded as irreversibly attached. The results for the ninhydrin assay displayed clearly that by washing the number of pamidronate molecules per area was reduced compared to the initially adsorbed amount and leveled at  $1.3 \mu\text{mol}/\text{m}^2$ .

To determine if the adsorption of pamidronate would fit the Langmuir model of adsorption, which is based on the assumption that adsorption cannot proceed beyond monolayer coverage [33] data were plotted as described in [32]. Obviously, the type of adsorption did not fit the Langmuir type of isotherm as the plot  $C_{\text{eq}}$  versus  $Q$  did not reach a plateau (Fig. 4 A) and the plot  $C_{\text{eq}}$  versus  $C_{\text{eq}}/Q$  did not result in a linear correlation (Fig. 4 B).

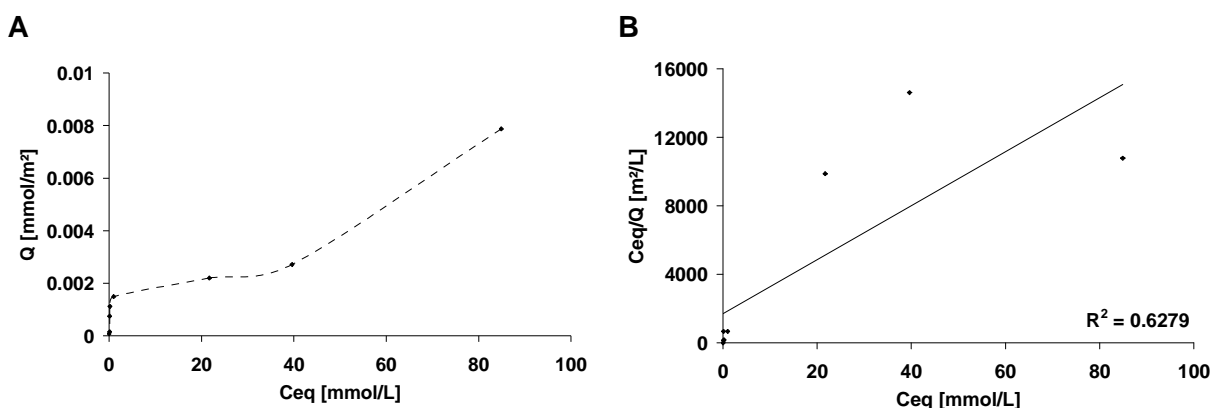


Fig.4: The isotherm was plotted to determine if it followed a Langmuir type of adsorption isotherm as described in [32].

The degree of surface coverage was estimated by calculations using the two different orientations of pamidronate towards hydroxyapatite surfaces that were described in the literature [26;34]. 100 % surface coverage would correspond to  $0.053 \text{ mmol}/\text{m}^2$  when pamidronate adsorbed with the two phosphonates and the hydroxyl function.  $0.04 \text{ mmol}/\text{m}^2$  would represent a monolayer when additionally the amino group is oriented towards the surface (Table 1). The maximum surface concentration of pamidronate determined by the pamidronate assay was  $0.008 \text{ mmol}/\text{m}^2$ . This would correspond to a surface coverage of 15 or 20 %, respectively.

*Table 1: The area covered by pamidronate was determined using the different orientations towards the surface that are described in literature. These values were used to compute the % surface coverage at the maximum adsorption of pamidronate as determined by the pamidronate and the ninhydrin assay.*

Orientation of pamidronate to HA surface	Area covered by 1 mmol pamidronate	Amount to cover 1 m <sup>2</sup>	% surface coverage pamidronate assay (C <sub>1</sub> = 100 mmol/L)	% surface coverage ninhydrin assay (C <sub>1</sub> = 100 mmol/L)
PPO* [26]	19 m <sup>2</sup> /mmol	0.053 mmol	15 %	3.2 %
PPN** [34]	25 m <sup>2</sup> /mmol	0.04 mmol	20 %	4.3 %

\* pamidronate oriented towards the hydroxyapatite surface with the phosphonates and the hydroxyl function (PPO)

\*\* pamidronate oriented towards the hydroxyapatite surface with the phosphonates and the amino group (PPN)

### 3.2. Precipitation of particles

As advanced route to obtain functionalized hydroxyapatite surfaces, the precipitation of calcium phosphate particles was investigated aiming to influence particle characteristics additionally. In contrast to literature [35], the precipitation did not result in particles of nanometer size. Light microscopy revealed differences in particle morphology (Fig. 5 A-C): the particles precipitated at 40 °C appeared amorphous (Fig. 5 A) while particles precipitated at 60 °C appeared as needle-shaped crystals (Fig. 5 B). Particle precipitation in the presence of pamidronate at 40 °C resulted in crystalline particles that were smaller than the particles precipitated at 40 and 60 °C (Fig. 5 C).

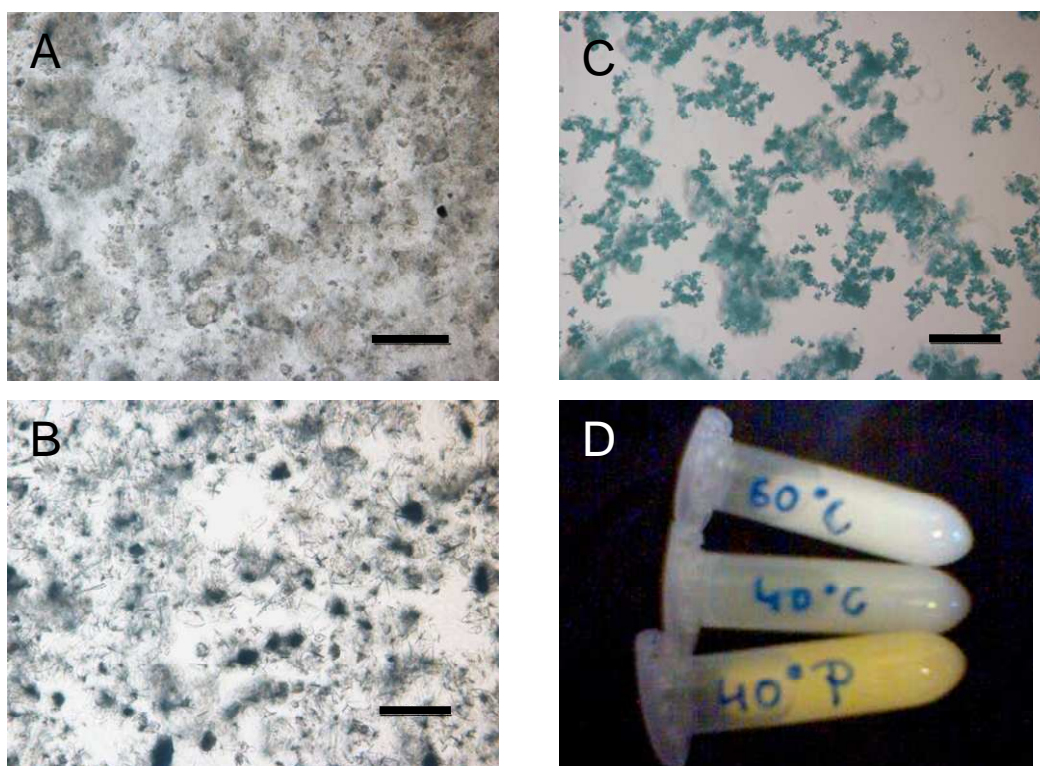


*Fig. 5: Light microscopy images of calcium phosphate particles precipitated under different conditions: A) 40 °C B) 60 °C C) 40 °C in the presence of pamidronate. Scale bars represent 200  $\mu$ m. D) TNBS-reaction performed with particles A, B and C.*

The TNBS reaction was performed on all three samples (Fig. 5 D). The particles that were precipitated in the presence of pamidronate were suitable for attachment of the dye TNBS indicating the presence of primary amines at the particle surfaces.

Particles were further characterized by scanning electron microscopy (SEM) (Fig. 6). The observations of light microscopy were confirmed. Particles precipitated at 40 °C were amorphous (Fig. 6 a, b). By precipitation at 60 °C (Fig. 6 c, d) and precipitation in the presence of pamidronate (Fig. 6 e, f), particles of needle-like shapes were formed. The particles that were formed in the presence of pamidronate were smaller than the other two samples. All samples formed aggregates.

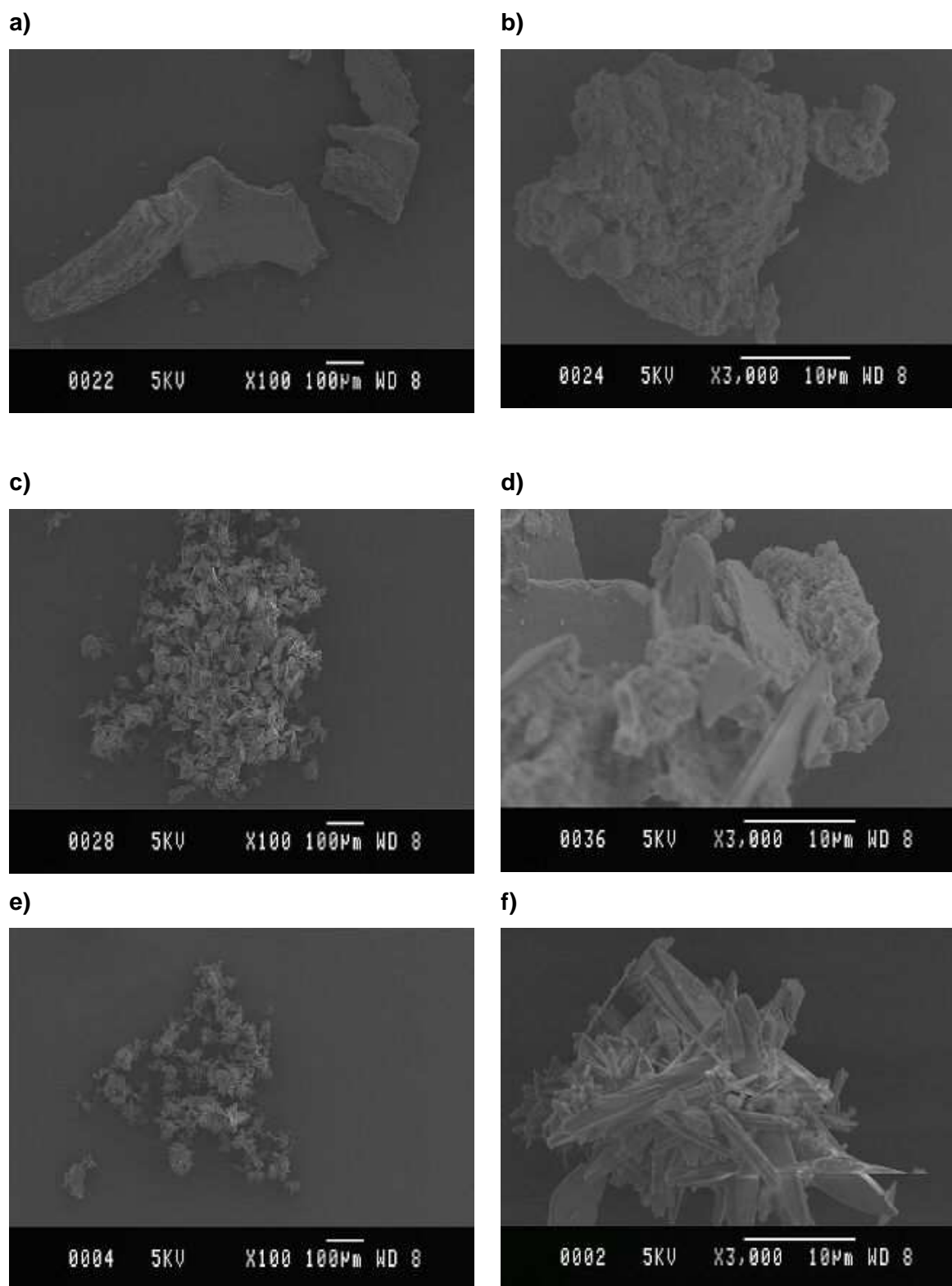


*Fig. 6: Scanning electron microscopy images of particles: a) and b) precipitated at 40 °C; c) and d) precipitated at 60 °C and e) and f) precipitated at 40 °C in the presence of pamidronate. Images in the left column were recorded in 100x magnification while images in the right column were recorded in 3000x magnification.*

X-ray diffraction patterns of the samples revealed that the particles precipitated at 40 °C resembled the X -ray diffraction pattern of hydroxyapatite ( $\text{Ca}_{10}(\text{OH})_2(\text{PO}_4)_6$ ) (Fig. 7), whereas the particles precipitated at 60 °C were in good accordance with the pattern of brushite



( $\text{CaHPO}_4 \cdot 2\text{H}_2\text{O}$ ) (Fig. 8). In the X-ray diffraction patterns, the observation that particles precipitated at 40 °C were less crystalline than particles precipitated at 60 °C was confirmed as indicated by the broad reflexes in the pattern of the 40 °C sample.

The precipitation in the presence of pamidronate was performed at 40 °C as these conditions have led to the formation of hydroxyapatite. Again the X-ray diffraction pattern of the particles resembled the pattern of brushite (Fig. 9). When compared to the pattern of the particles precipitated at 60 °C, additional reflexes or differences due to the incorporation of pamidronate into the structure of the calcium phosphate modification were not observed.

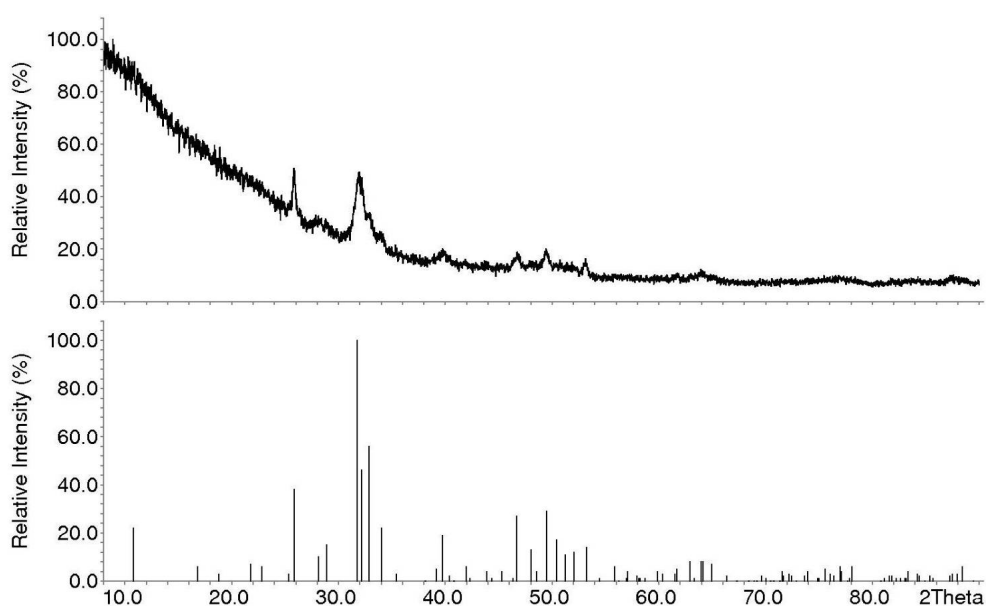


*Fig .7: X-ray diffraction pattern of particles precipitated at 40 °C and reference pattern of hydroxyapatite according to literature [36].*

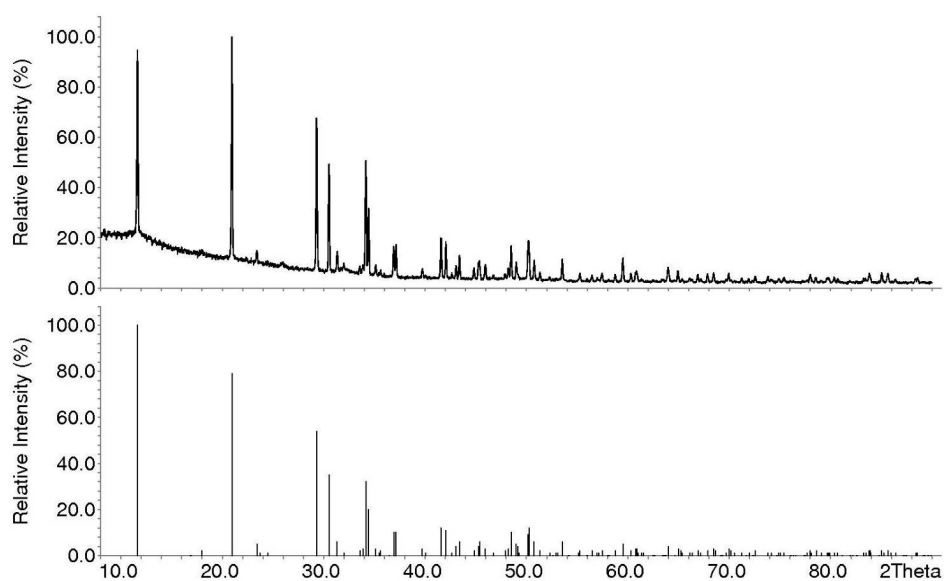


*Fig. 8: X-ray diffraction pattern of particles precipitated at 60 °C and reference pattern of brushite derived from literature [37].*

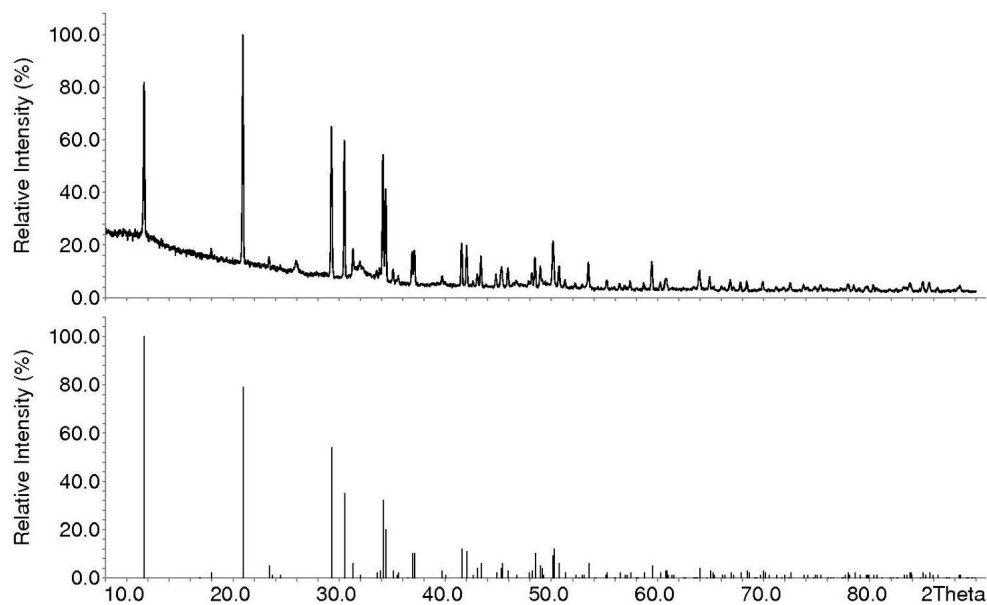


*Fig. 9: X-ray diffraction pattern of particles precipitated at 40 °C in the presence of pamidronate and reference pattern of brushite from literature [37].*

## 4. Discussion

The objective of this study was to investigate the functionalization of hydroxyapatite particles by the aminobisphosphonate pamidronate towards covalent attachment of molecules. The creation of functional groups that would allow for further conjugation steps on the surface of hydroxyapatite particles is therefore useful for strengthening the interface between organic and inorganic part of composite materials. Additionally, covalent attachment provides a possibility to retain drugs delivered to the bone-implant interface at their site of action. Two methods for the functionalization were compared: the adsorption of the amino-bisphosphonate pamidronate to the surface of HA particles and the co-precipitation of hydroxyapatite in the presence of pamidronate.

The adsorption isotherm of the aminobisphosphonate pamidronate was determined to estimate the maximum loading of particles with the bisphosphonate and the possibility of controlling the number of amino groups on the surface that were accessible for further conjugation steps. The adsorption of pamidronate did not follow the Langmuir model of adsorption as indicated by the lack of linear correlation in Fig. 4 B. Following the Langmuir isotherm [33], adsorption cannot proceed beyond monolayer coverage [38]. A determination of the irreversibly bound pamidronate after washing the powders using the ninhydrin method revealed that the surface concentration of pamidronate leveled at  $1.3 \mu\text{mol}/\text{m}^2$ . The number of amino groups was reduced relative to the results for the pamidronate assay indicating that parts of the bisphosphonate were reversibly attached. Furthermore, this suggests that a saturation of binding sites on the surface of hydroxyapatite occurs at  $1.3 \mu\text{mol}/\text{m}^2$ . Further adsorption may be due to the formation of multilayers on the surface. However, by theoretical calculations based on different conformations of pamidronate described in the literature when neighboring hydroxyapatite surfaces [26;34], a maximum surface coverage of 15 % to 20 % was determined. A model exceeding the Langmuir type of adsorption is provided by the Frumkin isotherm, stating that interactions such as attraction or repulsion can occur between adsorbed species [38;39]. But, from the data presented here, further conclusions concerning the type of adsorption and the model of isotherm can not be drawn.

However, the adsorption study clearly demonstrated that the number of amino groups is proportional to the initially used concentration of pamidronate within a certain range of concentrations (0-10 mmol/L). The results of the ninhydrin assay, performed after washing the samples, demonstrated clearly that amino groups remained on the surface of the HA powder and that they were accessible for covalent attachment of amine-reactive molecules. Both methods, pamidronate and ninhydrin assay, demonstrated that within a certain range of concentrations (0-20 mmol/L) the number of primary amines created on the surface can be controlled thus enabling the control of surface density of attached molecules.

The precipitation of HA particles intended to obtain particles with structural, morphological and compositional characteristics suitable for their potential application in the biomedical

field. The presence of bisphosphonates during precipitation has recently been demonstrated to influence particle properties such as size and zeta potential [28]. The particles obtained under varied conditions were clearly different in morphology, degree of crystallinity and particle size. X-ray diffraction revealed that amorphous forms of hydroxyapatite were obtained at 40 °C, whereas brushite ( $\text{CaHPO}_4 \cdot 2\text{H}_2\text{O}$ ) was formed when particles were precipitated at 60 °C or in the presence of pamidronate. Brushite one of the possible intermediate phases in the process of precipitation of hydroxyapatite and can be transferred to hydroxyapatite by calcination [40].

However, even though the obtained phase was not hydroxyapatite, the surface of the particles was functionalized by adsorbed pamidronate molecules as indicated by the persisting yellow color of attached TNBS (Fig. 5 D). The X-ray diffraction pattern resembles the brushite phase and does not differ remarkably in reflexes from the pattern of the 60 °C particles. This indicates that pamidronate was solely adsorbed on the surface and not integrated in the 3D-structure of the resulting crystals. Furthermore, the diffraction pattern shows no reflections due to crystalline modifications of pamidronate. Precipitation in the presence of pamidronate resulted in smaller particles as determined by light microscopy and SEM (Fig. 5 and 6), which is in agreement with literature [28].

In order to investigate the particle precipitation and the influences of pamidronate on particle composition, size, morphology, zeta potential, and surface functionalization more deeply, a systematic study with variation of different parameters should be performed. Nevertheless, using the two methods, adsorption and co-precipitation, amine-functionalized particles were obtained that were suitable for the conjugation of model compounds.

## 5. Conclusion

By adsorption of the aminobisphosphonate pamidronate, the surface of hydroxyapatite powder was functionalized. The number of functional groups was directly proportional to the equilibrium concentration of pamidronate within a range of 0-2  $\mu\text{mol}/\text{m}^2$  and they were accessible for the conjugation of a model compound. This is a promising result towards surface grafting of biomolecules, such as cytokines or adhesive peptides, or the creation of a stable interface bonding of organic and inorganic phases in composite materials. By co-precipitation of hydroxyapatite with pamidronate, particles with amino groups on the surface were obtained that were accessible for the immobilization of a model compound. However, the needle-like shape and micrometer-scaled size of the particles might not be advantageous for the application as bone filler or inorganic part of composites. Therefore, the adsorption method is suggested to create functional groups on HA particle surfaces using pamidronate.

## 6. References

- [1] Jain, A. K. and Panchagnula, R. (2000): "Skeletal drug delivery systems"; *International Journal of Pharmaceutics* (206) p.1-12
- [2] Hench, L. L. (1991): "Bioceramics: From concept to clinic"; *Journal of the American Ceramic Society* (74) p.1487-1510
- [3] Queiroz, A. C., Teixeira, S., Santos, J. D., and Monteiro, F. J. (2004): "Production of porous hydroxyapatite with potential for controlled drug delivery"; *Materials Science Forum* (455-456) p.358-360
- [4] Ginebra, M. P., Traykova, T., and Planell, J. A. (2006): "Calcium phosphate cements as bone drug delivery systems: A review"; *Journal of Controlled Release* (113) p.102-110
- [5] Wahl, D. A. and Czernuszka, J. T. (2006): "Collagen-hydroxyapatite composites for hard tissue repair"; *European Cells and Materials* (11) p.43-56
- [6] Wang, M., Bonfield, W., Li, M., and Guiu, F. (1997): "Interphase in composite materials"; *Key Engineering Materials* (127-131) p.583-590
- [7] Liu, Q., de Wijn, J. R., Bakker, D., and van Blitterswijk, C. A. (1996): "Surface modification of hydroxyapatite to introduce interfacial bonding with Polyactive 70/30 in a biodegradable composite"; *Journal of Materials Science: Materials in Medicine* (7) p.551-557
- [8] Deb, S., Wang, M., Tanner, K. E., and Bonfield, W. (1996): "Hydroxyapatite-polyethylene composites: effect of grafting and surface treatment of hydroxyapatite"; *Journal of Materials Science: Materials in Medicine* (7) p.191-193
- [9] Dong, G., Sun, J.-S., Yao, C.-H., Jiang, G.-J., Huang, C.-W., and Lin, F.-H. (2001): "A study on grafting and characterization of HMDI-modified calcium hydrogenphosphate"; *Biomaterials* (22) p.3179-3189
- [10] Liu, Q., de Wijn, J. R., and van Blitterswijk, C. A. (1998): "Composite biomaterials with chemical bonding between hydroxyapatite filler particles and PEG/PBT copolymer matrix"; *Journal of Biomedical Materials Research* (40) p.490-497
- [11] Zhang, S., Luo, Q., Cao, R., and Li, S. (2005): "Molecular modification of hydroxyapatite to introduce interfacial bonding with poly (lactic acid) in biodegradable composites"; *Key Engineering Materials* (288-289) p.227-230
- [12] Kanellakopoulou, K. and Giamarellos-Bourboulis, E. J. (2000): "Carrier systems for the local delivery of antibiotics in bone infections"; *Drugs* (59) p.1223-1232
- [13] Matsumoto, T., Okazaki, M., Inoue, M., Yamaguchi, S., Kusunose, T., Toyonaga, T., Hamada, Y., and Takahashi, J. (2004): "Hydroxyapatite particles as a controlled release carrier of protein"; *Biomaterials* (25) p.3807-3812
- [14] Wang, Y. J., Lin, F. H., Sun, J. S., Huang, Y. C., Chueh, S. C., and Hsu, F. Y. (2003): "Collagen-hydroxyapatite microspheres as carriers for bone morphogenic protein-4"; *Artificial Organs* (27) p.162-168
- [15] Sun, J. S., Lin, F. H., Wang, Y. J., Huang, Y. C., Chueh, S. C., and Hsu, F. Y. (2003): "Collagen-hydroxyapatite/tricalcium phosphate microspheres as a delivery system for recombinant human transforming growth factor-b 1"; *Artificial Organs* (27) p.605-612
- [16] Josse, S., Fauchoux, C., Soueidan, A., Grimandi, G., Massiot, D., Alonso, B., Janvier, P., Laib, S., Pilet, P., and Gauthier, O. (2005): "Novel biomaterials for bisphosphonate delivery"; *Biomaterials* (26) p.2073-2080
- [17] Backer, M. V., Patel, V., Jehning, B. T., Claffey, K. P., and Backer, J. M. (2006): "Surface immobilization of active vascular endothelial growth factor via a cysteine-containing tag"; *Biomaterials* (27) p.5452-5458
- [18] Luginbuehl, V., Meinel, L., Merkle, H. P., and Gander, B. (2004): "Localized delivery of growth factors for bone repair"; *European Journal of Pharmaceutics and Biopharmaceutics* (58) p.197-208
- [19] Durrieu, M. C., Pallu, S., Guillemot, F., Bareille, R., Amedee, J., Baquey, C., Labrugere, C., and Dard, M. (2004): "Grafting RGD containing peptides onto hydroxyapatite to promote osteoblastic cells adhesion"; *Journal of Materials Science: Materials in Medicine* (15) p.779-786

- [20] Furuzono, T., Sonoda, K., and Tanaka, J. (2001): "A hydroxyapatite coating covalently linked onto a silicone implant material"; *Journal of Biomedical Materials Research* (56) p.9-16
- [21] Liu, Q., de Wijn, J. R., and van Blitterswijk, C. A. (1998): "A study on the grafting reaction of isocyanates with hydroxyapatite filler particles"; *Journal of Biomedical Materials Research* (40) p.358-364
- [22] Rezanian, A. and Healy, K. E. (2000): "The effect of peptide surface density on mineralization of a matrix deposited by osteogenic cells"; *Journal of Biomedical Materials Research* (52) p.595-600
- [23] Widler, L., Jaeggi, K. A., Glatt, M., Mueller, K., Bachmann, R., Bisping, M., Born, A. R., Cortesi, R., Guiglia, G., Jeker, H., Klein, R., Ramseier, U., Schmid, J., Schreiber, G., Sellenmeyer, Y., and Green, J. R. (2002): "Highly potent geminal bisphosphonates. From pamidronate disodium (Aredia) to zoledronic acid (Zometa)"; *Journal of Medicinal Chemistry* (45) p.3721-3738
- [24] Lin, J. H. (1996): "Bisphosphonates: A review of their pharmacokinetic properties"; *Bone* (18) p.75-85
- [25] Papapoulos, S. E. (2006): "Bisphosphonate actions: Physical chemistry revisited"; *Bone* (38) p.613-616
- [26] Grossmann, G., Grossmann, A., Ohms, G., Breuer, E., Chen, R., Golomb, G., Cohen, H., Hagele, G., and Classen, R. (2000): "Solid-state NMR of bisphosphonates adsorbed on hydroxyapatite"; *Magnetic Resonance in Chemistry* (38) p.11-16
- [27] Cohen, H., Solomon, V., Alferiev, I. S., Breuer, E., Ornoy, A., Patlas, N., Eidelman, N., Hagele, G., and Golomb, G. (1998): "Bisphosphonates and tetracycline: experimental models for their evaluation in calcium-related disorders"; *Pharmaceutical Research* (15) p.606-613
- [28] Nancollas, G. H., Tang, R., Phipps, R. J., Henneman, Z., Gulde, S., Wu, W., Mangood, A., Russell, R. G. G., and Ebetino, F. H. (2006): "Novel insights into actions of bisphosphonates on bone: Differences in interactions with hydroxyapatite"; *Bone* (38) p.617-627
- [29] Puleo, D. A. (1995): "Activity of enzyme immobilized on silanized Co-Cr-Mo"; *Journal of Biomedical Materials Research* (29) p.951-957
- [30] Ames, B. N. (1966): "Assay of inorganic phosphate, total phosphate, and phosphatases"; *Methods in Enzymology* (8) p.115-118
- [31] Moore, S. (1968): "Amino Acid Analysis: Aqueous Dimethyl Sulfoxide as solvent for the Ninhydrin-Reaction"; *the Journal of Biological Chemistry* (243) p.6281-6283
- [32] Bouropoulos, N. and Moradian-Oldak, J. (2004): "Analysis of hydroxyapatite surface coverage by amelogenin nanospheres following the Langmuir model for protein adsorption"; *Calcified Tissue International* (74) p.124-125
- [33] Langmuir, I. (1918): "The adsorption of gases on plane surfaces of glass, mica and platinum"; *Journal of the American Chemical Society* (40) p.1361-1402
- [34] Neves, M., Gano, L., Pereira, N., Costa, M. C., Costa, M. R., Chandia, M., Rosado, M., and Fausto, R. (2002): "Synthesis, characterization and biodistribution of bisphosphonates Sm-153 complexes: correlation with molecular modeling interaction studies"; *Nuclear Medicine and Biology* (29) p.329-338
- [35] Bouyer, E., Gitzhofer, F., and Boulos, M. I. (2000): "Morphological study of hydroxyapatite nanocrystal suspension"; *Journal of Materials Science: Materials in Medicine* (11) p.523-531
- [36] Posner, A. S., Perloff, A., and Diorio, A. F. (1958): "Refinement of the hydroxyapatite structure"; *Acta Crystallographica* (11) p.308-309
- [37] Curry, N. A. and Jones, D. W. (1971): "Crystal structure of brushite, calcium hydrogen orthophosphate dihydrate. Neutron-diffraction investigation"; *Journal of the Chemical Society [Section] A: Inorganic, Physical, Theoretical* p.3725-3729
- [38] Doerfler, H.-D. (1994): "Grenzflächen- und Kolloidchemie"; VCH Verlagsgesellschaft mbH, Weinheim, Germany

- [39] Frumkin, A. (1925): "Surface tension curves of the higher fatty acids and the equation of condition of the surface layer"; Zeitschrift für physikalische Chemie (116) p.466-484
- [40] Johnsson, M. S. and Nancollas, G. H. (1992): "The role of brushite and octacalcium phosphate in apatite formation"; Critical Reviews in Oral Biology and Medicine (3) p.61-82



# **Chapter 7**

## **Confocal microscopy for monitoring uptake and distribution of nanoparticles in a three-dimensional cell culture model**

A. Schuessele<sup>1</sup>, W. Eder<sup>2</sup>, L. A. Kunz-Schughart<sup>2</sup>, T. Blunk<sup>1</sup>, J. Tessmar<sup>1</sup>, A. Goepferich<sup>1</sup>

<sup>1</sup>Department of Pharmaceutical Technology, University of Regensburg

<sup>2</sup>Department of Pathology, University of Regensburg

**Abstract**

Drug and nanoparticle transport in tissues *in vivo* is hindered by many obstacles thus limiting therapeutic efficacy. For a deeper understanding of the key factors, models for the *in vitro* testing of novel therapeutic approaches, such as drug delivery devices, are of particular interest. To improve the formulation of nanoparticles, i.e. for cancer therapy, there is a need for simple *in vitro* cell culture models mimicking a three-dimensional cellular context and analytical techniques to rapidly monitor drug and particle uptake and distribution throughout tissues.

Therefore, confocal microscopy was evaluated to determine nanoparticle interactions with cells in 2D and 3D cell culture. Spheroids of the human colon carcinoma cell line HCT-116 were used. 500 cells were initiated to reach a diameter of app. 400  $\mu\text{m}$  after 4 days of culture. The growth rate of these spheroids was determined to be 100  $\mu\text{m}$  in diameter per 24 hours. Fluorescent nanoparticles of 100 and 200 nm served as model colloids. Fluorescence measurements revealed an increase of cell-associated particles over a period of 4 hours in 2D cell culture, while observations with confocal microscopy revealed that particles were hardly internalized by the cells in monolayer culture. The use of confocal microscopy for the analysis of spheroids is limited by the optical density of the spheroid tissue that allows only for gathering information of the outer layers of the spheroid (30-50  $\mu\text{m}$  penetration depth). However, differences in particle penetration inside the outer layer of the spheroids were determined as 200 nm particles proceeded faster than 100 nm particles. To conclude, confocal microscopy would be a valuable tool for the comparison of tissue penetration rates of various particle formulations in spheroids with a slower growth rate.

## 1. Introduction

In the treatment of cancer, surgical resection of tumors offers the best chance for cure. In order to improve survival rates and for the treatment of tumors that are not accessible for surgery, radiotherapy and chemotherapy are adjuvants [1]. Chemotherapy can be significantly improved by using suitable drug delivery strategies [2]. Numerous *in vivo* investigations have shown that biodistribution profiles of anticancer drugs can be controlled by their entrapment in colloidal carriers such as nanoparticles [3]. In general, drug delivery to tumors by nanoparticles has a variety of advantages: Due to the enhanced permeation and retention effect, the particles accumulate in the tumor, leading to significantly higher drug concentrations in the neoplastic tissue [3]. Nanoparticles can furthermore increase the half-life of a drug compared to drug solutions. The prolonged release of a drug from the particles at the site of action might lead to a continuous and more effective inhibition of tumor growth. For particular drugs, such as paclitaxel, the problem of poor solubility in aqueous solutions can be overcome by using nanoparticles. Additionally, for some drugs toxic side effects can be avoided: encapsulated doxorubicin, for example, is less nephrotoxic than the free drug in solution [4].

Most of the *in vitro* cell culture studies for drug delivery systems for cancer therapy are carried out in monolayer cell culture. As it is becoming more and more apparent that monolayer cultures of tumor cells cannot completely represent the characteristics of a three-dimensional solid tumor [5], there is a need for alternative culture systems for rapid and easy *in vitro* testing of novel tumor therapies [6]. The similarity of multicellular tumor spheroids (MCTS) with the initial avascular growth stage of malignancies makes them a suitable model for the testing of new anti-tumor drugs [7]. Drug distribution inside a spheroid is limited by diffusion, which mimics the *in vivo* situation and might be one explanation for the fact that the drug response of a spheroid differs from the drug response of a monolayer culture [8]. The investigation of nanoparticles as drug delivery system in MCTS would provide a better *in vitro* model to study uptake and distribution of the particles in a three-dimensional cell formation. Therefore, we monitored the uptake of fluorescent nanoparticles as a model system by spheroids using confocal laser scanning microscopy (CLSM). Our spheroids were made of transfected cells of the human colon carcinoma cell line HCT-116 expressing the green fluorescent protein (GFP). This allowed using confocal microscopy as a technique for rapid characterization of nanoparticle penetration to identify parameters critical for particle formulation.

To characterize the interactions of fluorescent nanoparticles with spheroids particles with a negative surface charge were chosen intending to prevent uptake inside the cells and investigate passive diffusion inside tissue only [9;10]. Particles of 100 nm and 200 nm size were chosen as model colloids [11-14]. The interactions of nanoparticles with cells in two and

three dimensional cell culture were investigated with confocal microscopy and fluorescence spectrometry. In addition to this non-invasive approach, cryo-sections of spheroids were prepared.

## **2. Materials and Methods**

### **2.1. Materials**

Agarose “for routine use” was bought from Sigma-Aldrich (Steinheim, Germany). Fluorescent nanoparticles (Fluospheres®; carboxylate-modified nanospheres;  $\lambda_{\text{ex}}$  540 nm,  $\lambda_{\text{em}}$  560 nm) were obtained from Molecular Probes (Invitrogen, Karlsruhe, Germany). Particle sizes were 100 and 200 nm and zeta potential was of -55 mV. Particles were supplied as 2% solids in aqueous dispersion. Dulbecco’s modified eagle media (DMEM) and fetal bovine serum (FBS) were purchased from PAN Biotech (Aidenbach, Germany). Triton X-100, sodium hydroxide (NaOH) and sodium chloride (NaCl) were obtained by Merck (Darmstadt, Germany). Phosphate-buffered saline (PBS) and antibiotics (Penicillin G/Streptomycin) were purchased from Invitrogen (Karlsruhe, Germany). Killik frozen section media was obtained by Bioptica (Milan, Italy). Cell culture flasks (T75, T25) were bought from Sarstedt AG (Nürnberg, Germany) and 96-well plates were purchased from Becton Dickinson Labware (Heidelberg, Germany). Water was of double distilled quality. All reagents were of analytical grade and used as received unless something different is stated.

### **2.2. Cell line and cell culture**

The human colon carcinoma cell line HCT-116 GFP was obtained from ATCC. HCT-116 cells expressing the green fluorescent protein (HCT-116 GFP) were obtained from Dr. Rachel Cowen and Dr. Alain Pluen, School of Pharmacy, University of Manchester, UK. Cells were cultured in Dulbecco’s modified eagle media (DMEM), 10% fetal bovine serum (FBS) and antibiotics (100 U/ml of Penicillin G and 100 µg/ml of Streptomycin) and maintained at 37 °C in a humidified atmosphere of 5 % CO<sub>2</sub> in air. Cells were passaged every 3-4 days and seeded in a density of 16000 cells/cm<sup>2</sup>. No more than 20 passages were used.

### **2.3. Spheroid cultivation**

HCT-116 spheroids were made applying a liquid overlay technique using agarose-coated 96-well plates (50 µl 1.5% (w/v) agarose/well), and 500-2000 exponentially growing tumor cells per well in a total volume of 200 µl cell-culture media [15]. After an initiation period of 4 days, 100 µl media was aspirated and replaced by fresh media. Spheroids were harvested on day 4 and used for further experiments.

### **2.4. Spheroid growth**

For the determination of spheroid growth, photographs of spheroids (n=12) were taken every 24 hours starting on day 4 over a period of 5 days totally using a Leica DMIRB microscope (Leica Microsystems, Bensheim, Germany). Pictures of spheroids were taken with a digital camera (DS-U1, Nikon; Düsseldorf, Germany) and analyzed for mean diameter with the EclipseNet software (Version 1.20.0; Laboratory Imaging Ltd., Prague, Czech Republic).

### **2.5. Determination of particle size and zeta potential**

Particle size and zeta potential of model nanoparticles were determined with a Zetasizer HSA (Malvern Instruments GmbH; Herrenberg, Germany). 50 µl of particle suspension were diluted in 2 ml of the respective media (1 mM sodium chloride, PBS buffer, DMEM media without FBS, DMEM with FBS). Refractive index and viscosity of the respective media were determined for the calculation of the results.

### **2.6. Determination of cell-associated fluorescence in monolayer culture**

HCT-116 GFP cells were seeded in 96 well-plates in a density of 50 000 cells per cm<sup>2</sup> and incubated until they formed a confluent monolayer. Having reached confluence, the culture media was replaced by media containing nanoparticles in which the cells were incubated at 37 °C for 1-4 hours (n=6). Different ratios of cells to nanospheres were used for the two particle sizes: a) the same mass of polystyrene per cell, resulting in different ratios of cells to nanospheres: 100 nm 1:500000, 200 nm 1:62500. b) the same ratio of cells to nanospheres (1:5000). The experiment was terminated by washing the cell monolayer three times with phosphate-buffered saline (PBS, pH 7.4) to eliminate excess particles which were not entrapped by the cells. Cell membrane was permeabilized with 0.5% Triton X-100 in 0.2 N aqueous NaOH to expose the internalized nanoparticles for the quantitative measurement. Cell-associated particles were quantified by analyzing the cell lysate in a GENios pro microplate reader (Tecan; Crailsheim, Germany) using an excitation wavelength of 485 nm and an emission wavelength of 590 nm. Uptake was expressed as the percentage of fluorescence associated with cells versus the amount of fluorescence present in the feed solution.

### **2.7. Particle uptake in monolayer culture (2D)**

HCT-116 GFP cells were seeded in chamber coverglasses and allowed to attach over night. The next day, cell culture media was removed, cells were washed once with PBS and then media was added containing fluorescent nanoparticles in a ratio of 5000 particles per cell. To assure constant pH during analysis by microscope, HEPES buffer was added to result in a final concentration of 10 mM. Particle uptake in 2D culture was monitored with confocal microscopy as described in 2.9.

### **2.8. Particle uptake in spheroids (3D)**

Spheroids (500 cells per well) were initiated in a total volume of 200 µl media. After 4 days 100 µl media were aspirated and replaced by 100 µl fresh media supplemented with 1 µl of the nanoparticle suspensions. Media was gently mixed and spheroids were incubated with nanospheres at 37°C. At defined points of time spheroids (n=3) were harvested and analyzed either by confocal microscopy as described in 2.9 or by cryo sections as described in 2.10.

### **2.9. Confocal laser scanning microscopy (CLSM)**

For the CLSM experiments, a Zeiss Axiovert 200M microscope coupled to a Zeiss LSM 510 scanning device was used (Carl Zeiss Co., Ltd., Germany). The inverted microscope was equipped with a Plan – Apochromat 40x, a Plan – Apochromat 63x and a Plan-Neofluar 20x/0.5 objective. An argon laser with 488 nm was used to excite GFP and a Helium Neon laser was used to excite the nanoparticles at 543 nm. The fluorescence was imaged in the multitracking modus using a band-pass filter of 425-525 nm to detect GFP and a long-pass filter of 585 nm to detect nanoparticles fluorescence.

For observations of monolayers, cells were placed in 8-well Lab-Tek™ chambered cover glasses (Nunc GmbH & Co. KG, Germany) at an initial density of 80,000 cells in a volume of 400 µl culture media. For maintaining a pH of 7.4, 20 mM HEPES was supplied. After 18 hours, the media was changed, nanoparticles were added and measurements were directly performed in each well at 37°C. The thickness of the optical sections was between 0.7 and 1.2 µm.

For taking confocal images of spheroids, they were harvested 4 days after initiation, placed on cover glasses with 100 µl of media and measured at 37°C. The z-stack mode was used to investigate the penetration of nanoparticles inside the spheroids. Z-stacks were performed with a thickness of optical sections of 2.1 µm. The permeation depth of nanoparticles was determined by the number of slices displaying nanoparticle fluorescence in the center of the spheroid.

### **2.10. Cryo sections**

Spheroids were harvested and fixed in 2.5% glutaraldehyde in PBS. Spheroids were immersed in a solution containing 15% sucrose (w/v) overnight. 3 to 5 spheroids were placed in a plastic ring (diameter 0.5 cm), water was removed and the ring was then filled with Killik frozen section media. Cylinders with spheroids were shock frozen in liquid nitrogen and stored at -80°C until cutting and analysis. Samples were cryo-sectioned to 15 µm thickness (HM 550 OMP, Microm, Walldorf, Germany). The median slice of a spheroid was analyzed by confocal laser scanning microscopy.

### 3. Results

#### 3.1. Spheroid cultivation and growth

The transfected cell line HCT-116 GFP formed perfectly round spheroids in liquid overlay over a broad range of cell numbers (Fig. 1). 500 cells per well were enough to reach a spheroid diameter of 400  $\mu\text{m}$  4 days after initiation. Below a diameter of 400  $\mu\text{m}$  a central necrosis due to limitations in supply with nutrients is not expected [16]. Therefore spheroids with an initial cell number of 500 cells were used for the experiments with nanospheres.

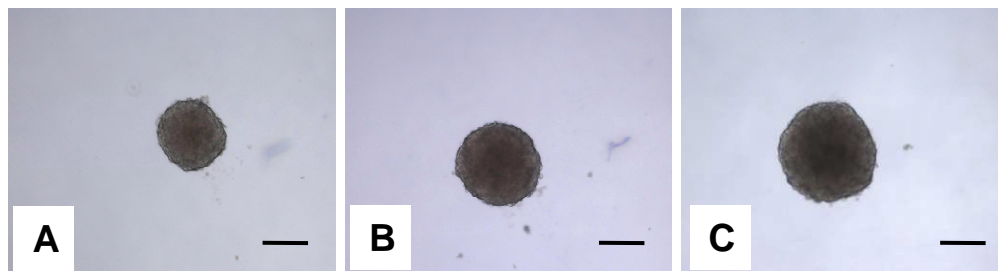


*Fig. 1: HCT-116 GFP spheroids 4 days after initiation: A) 500 cells B) 1000 cells C) 2000 cells were initially seeded per well. Scale bars represent 200  $\mu\text{m}$ .*

The growth of the spheroids was monitored over 5 days (Fig. 2). During this time period the growth proceeded linear and did not reach a plateau. Spheroids with smaller initial cell numbers grew faster than spheroids with higher cell numbers. The addition of fluorescent nanoparticles to the culture media when spheroids were initiated did not affect the growth rate of the spheroids as there were no significant differences in the respective growth curves. The average growth rate for spheroids with an initial cell number of 500 cells was 100  $\mu\text{m}$  in diameter per 24hours



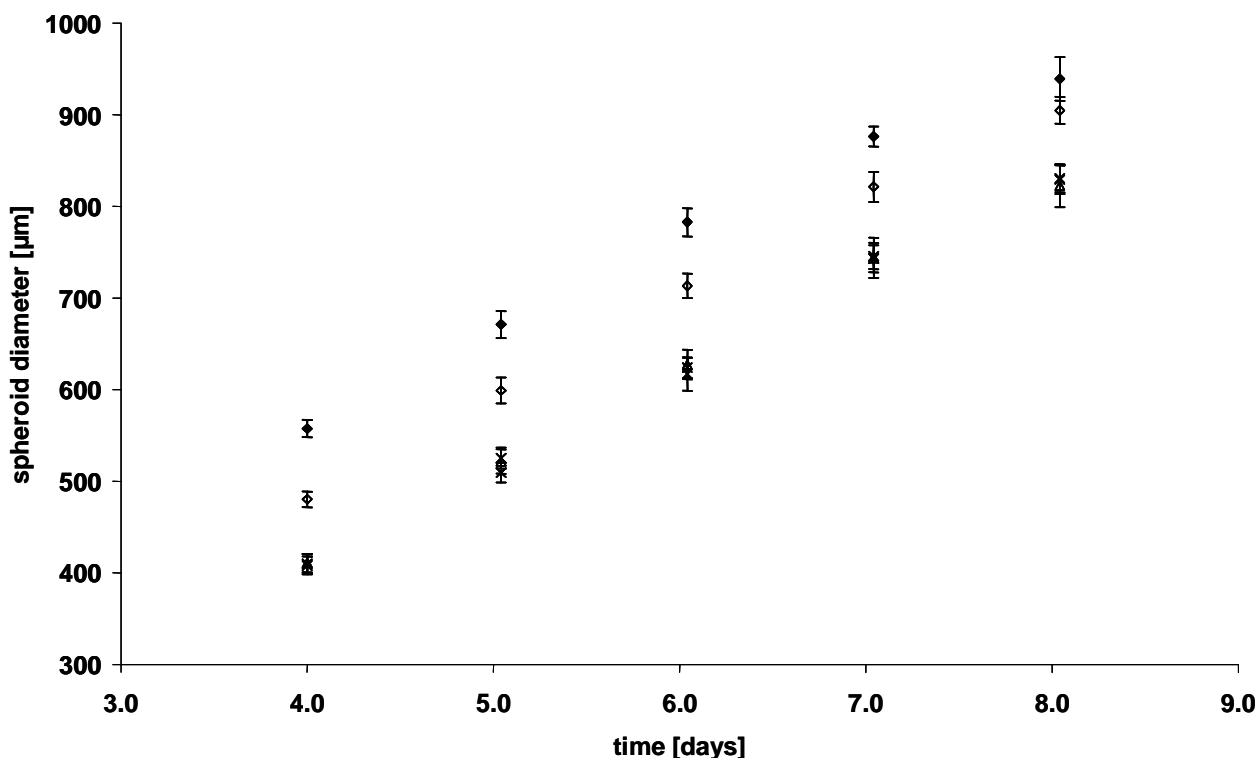


Fig. 2: Growth of HCT-116 GFP spheroids over 5 days ( $n=12$ ). Different cell numbers were initially seeded: ♦ 2000 cells per well ◇ 1000 cells per well and ✱ 500 cells per well. Additionally, fluorescent nanoparticles suspension (1  $\mu$ l) was added to the cell culture media to wells containing 500 cells: ✕ 500 cells and 100 nm particles; △ 500 cells and 200 nm particles. Spheroid growth was not affected by the presence of nanoparticles in the culture media.

### 3.2. Size, size distribution and zeta potential of model nanoparticles

Size and zeta potential of the fluorescent particles were characterized in various media (Tab. 1) as the surface charge was assumed to be an important parameter determining uptake and cell-membrane association of particles [9]. Intending to minimize uptake of particles by cells, negatively charged polystyrene particles were used with a zeta potential of -55 mV according to the manufacturer. Particles of particle size 100 and 200 nm were used, which is a common size range for drug loaded nanoparticles in cancer treatment. Measurements in different media (1 mM NaCl, PBS-buffer and DMEM) affirmed the size and narrow size distribution of the particles as expressed by the polydispersity index. However, in cell culture media containing serum proteins (DMEM + FBS) the size of the particles increased due to the adsorption of serum proteins to the particles' surfaces. Zeta potential of the particles continuously increased with increasing ion content of dispersant (PBS) and further increased in cell culture media (DMEM) to result finally in a zeta potential of -11.2 mV for 100 nm and -8.3 mV for 200 nm particles under the conditions for the experiments with monolayer cell culture and spheroids (DMEM + FBS).

*Table 3: Particle size and zeta potential of fluorescent nanoparticles of a) 100 and b) 200 nm in different media determined by laser light scattering. An increase in particle size and polydispersity index is observed in serum containing media (DMEM + FBS) due to coating of nanoparticles with serum proteins. Zeta potential is decreased by media containing ions, amino acids and proteins from -50-60 mV initially to approximately -10 mV.*

	Mean particle size [nm]	Polydispersity index	Zeta potential [mV]
<b>a) 1 mM NaCl</b>	104.6 ± 0.4	0.04 ± 0.01	-51.9 ± 0.7
<b>PBS-buffer</b>	102.1 ± 0.1	0.03 ± 0.01	-41.5 ± 0.8
<b>DMEM</b>	101.4 ± 1.3	0.03 ± 0.01	-33.3 ± 3.8
<b>DMEM + FBS</b>	152.2 ± 2.8	0.21 ± 0.02	-11.2 ± 4.4
<b>b) 1 mM NaCl</b>	200.7 ± 0.6	0.02 ± 0.01	-58.4 ± 2.2
<b>PBS-buffer</b>	185.7 ± 1.3	0.03 ± 0.01	-44.2 ± 0.1
<b>DMEM</b>	191.2 ± 4.2	0.03 ± 0.01	-40.6 ± 1.3
<b>DMEM + FBS</b>	226.1 ± 0.4	0.1 ± 0.02	-8.3 ± 3.4

### 3.3. Cell-associated particles in monolayer cell culture

To investigate if HCT-116 GFP would internalize the fluorescent model particles, cells were seeded in 96-well plates and incubated at 37 °C with nanospheres. Ratios of cells to nanospheres were calculated to assure the same mass of polystyrene per cell (Fig. 3a) and the same number of particles per cell (Fig. 3b) for both particle sizes.

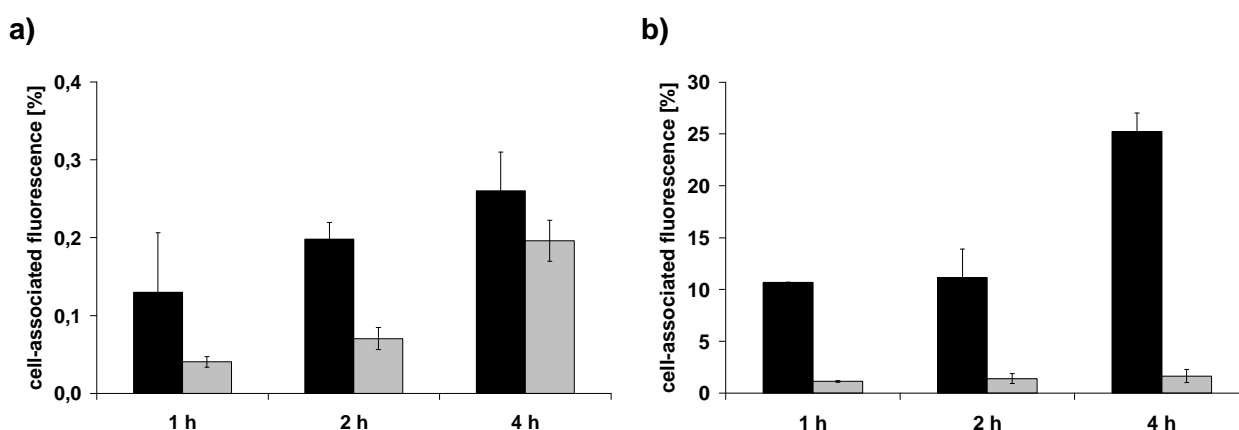


*Fig. 3: The percentage of cell associated particles was determined after incubation of HCT-116 GFP cells with nanoparticles of 100 nm (■) and 200 nm (□) in different ratios cells to nanospheres (n=6): **a)** the same mass of polystyrene per cell was taken resulting in different ratios of cells to nanospheres: 100 nm 1:500000, 200 nm 1:62500. **b)** the same ratio of cells to nanospheres was taken for both particle sizes (1:5000).*

After 4 hours cells in Fig. 3 a) have taken up 28% of the 100nm particles while cells in Fig. 3 b) have taken up only 0.27%. Both values correspond to approximately 1350 particles that were associated to one cell assuming that cell proliferation over a period of 4 hours is negligible and the cells were already confluent when the experiment was started. After 4 hours the cells internalized 0.2% of the 200 nm particles in Fig. 3 a) (initial ratio 1:62500) and 1.65% of the particles in Fig. 3 b) (initial ratio 1:5000). This corresponds to a rate of 125 vs. 82 nanoparticles associated to or internalized by each cell, respectively.

### 3.4. Particle uptake in 2D cell culture monitored by confocal laser scanning microscopy

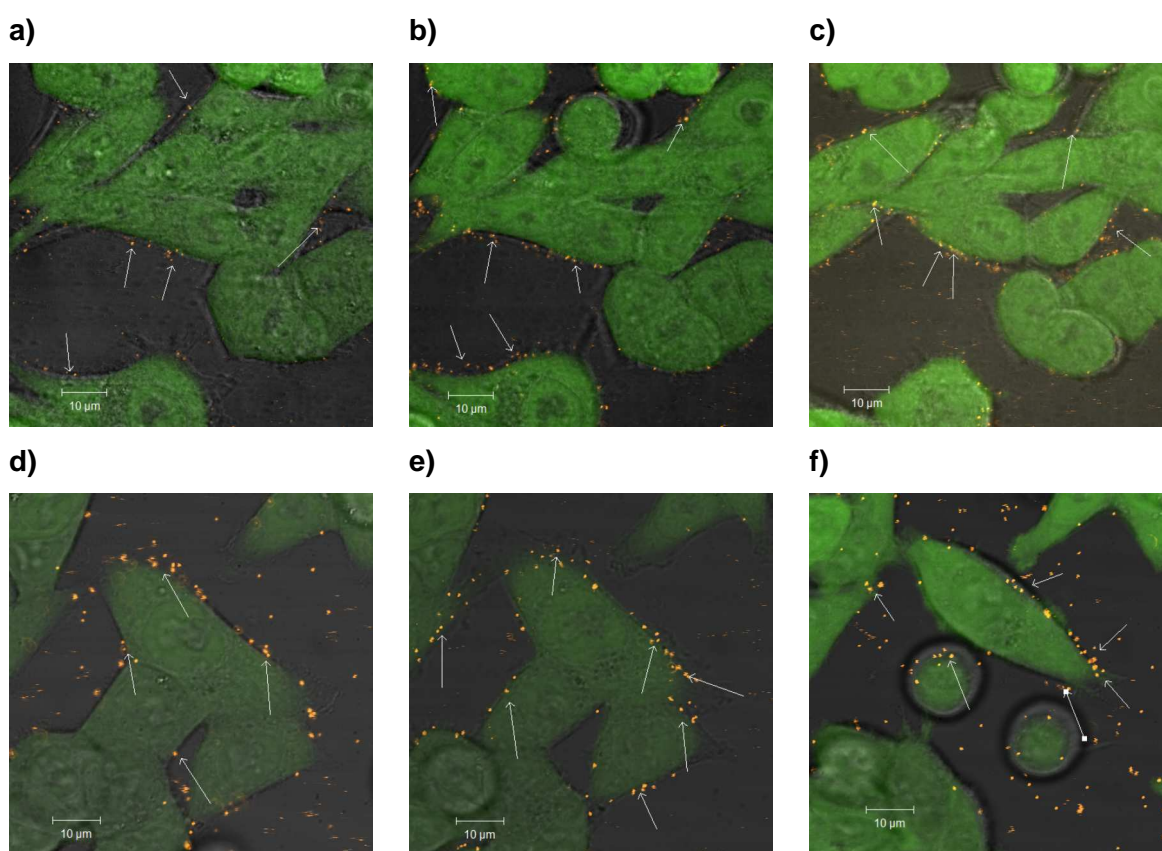


*Fig. 4: Time series of HCT-116 GFP cells with nanospheres (ratio 1:5000) in media monitored by confocal laser scanning microscopy: a) 100nm, 1h b) 100nm, 2h c) 100nm, 4h d) 200 nm, 1h e) 200 nm, 2h and f) 200nm, 4h.*

The increase in cell associated particles over the observation time of 4 hours was confirmed by confocal microscopy pictures (Fig. 4). Particles of 100 and 200 nm were used in a ratio of 5000 particles per cell. The number of particles associated with the cell membranes was increased time-dependently (white arrows). Particles inside cells were rarely detected after 4 hours and mainly observed in the rounded, most likely dead cells.

### 3.5. Uptake and distribution of nanoparticles in 3D cell culture

Uptake and distribution of nanospheres in three dimensional spheroids was monitored with confocal microscopy using the z-stack mode with optical slices of 2.1  $\mu\text{m}$ . Fig. 5 shows z-stacks of the first 30  $\mu\text{m}$  of spheroids incubated with particles of 100 nm (Fig. 5 a,b) and 200 nm (Fig. 5 c,d). The confocal pictures of the nanoparticles (red channel) were overlaid with the transmission pictures to indicate spheroid size. 15 min after starting the incubation (Fig. 5 a,c) the spheroid slices were not colored by the red particles. After 8 hours of incubation (Fig. 5 b,d) the whole cross sectional areas of the individual slices were evenly colored by red nanoparticles, the last image representing a penetration depth of 30  $\mu\text{m}$ .

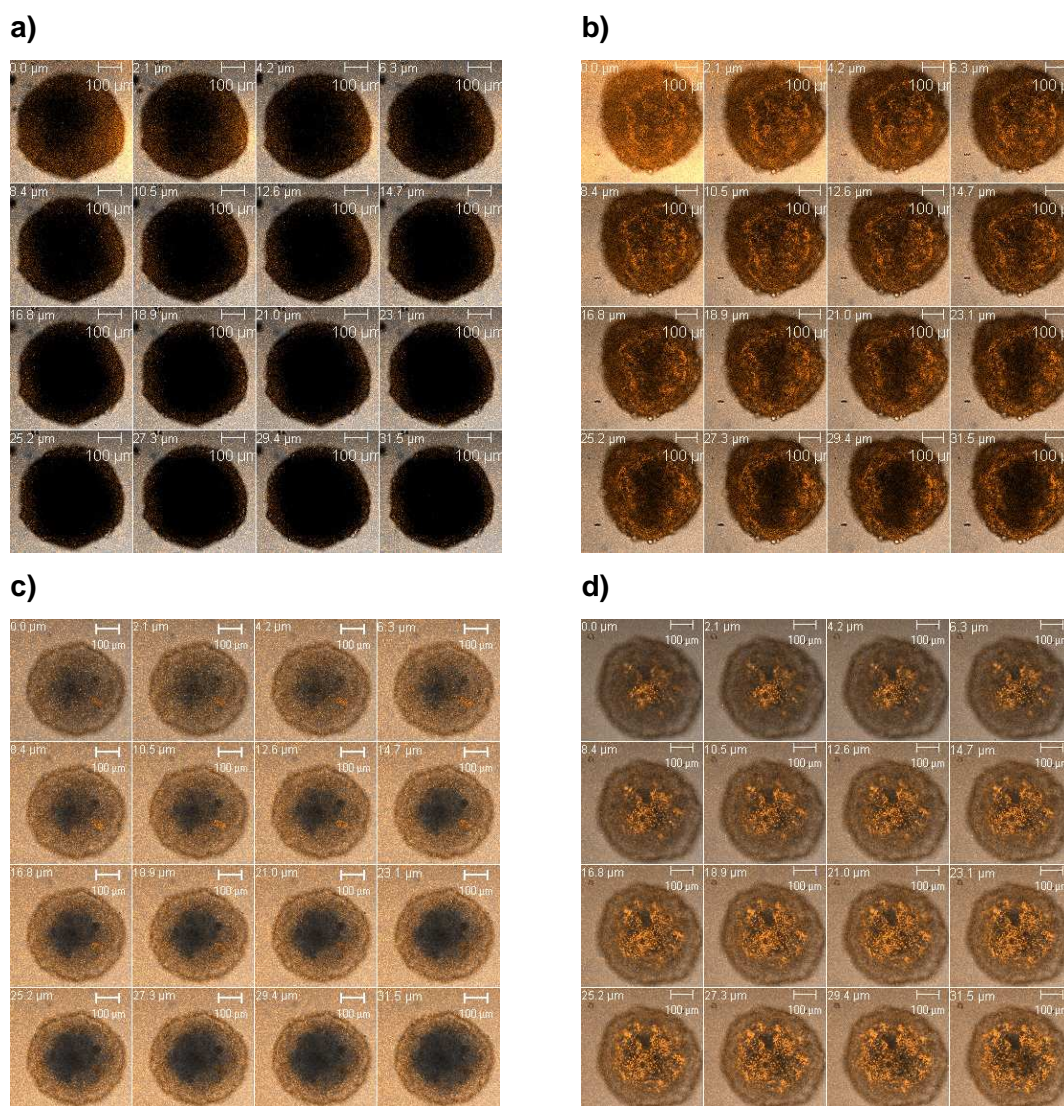


**Fig. 5:** Confocal microscopy images (z-stacks) of spheroids incubated with nanospheres: a) 100 nm particles 15 min; b) 100 nm particles after 8 hours. c) 200 nm particles, 15 min d) 200 nm particles after 8 hours. Optical slices of a thickness of 2.1  $\mu\text{m}$  were shown over 31.5  $\mu\text{m}$  in total.

While the particles of 200 nm filled the outer layers of the spheroid (first 30  $\mu\text{m}$  depth of 400  $\mu\text{m}$  in total) the 100 nm particles did only penetrate as far as 18  $\mu\text{m}$ . The observation that particles of 100 nm penetrated more slowly than particles of 200 nm was followed over the whole period of 8 hours (Fig. 6).

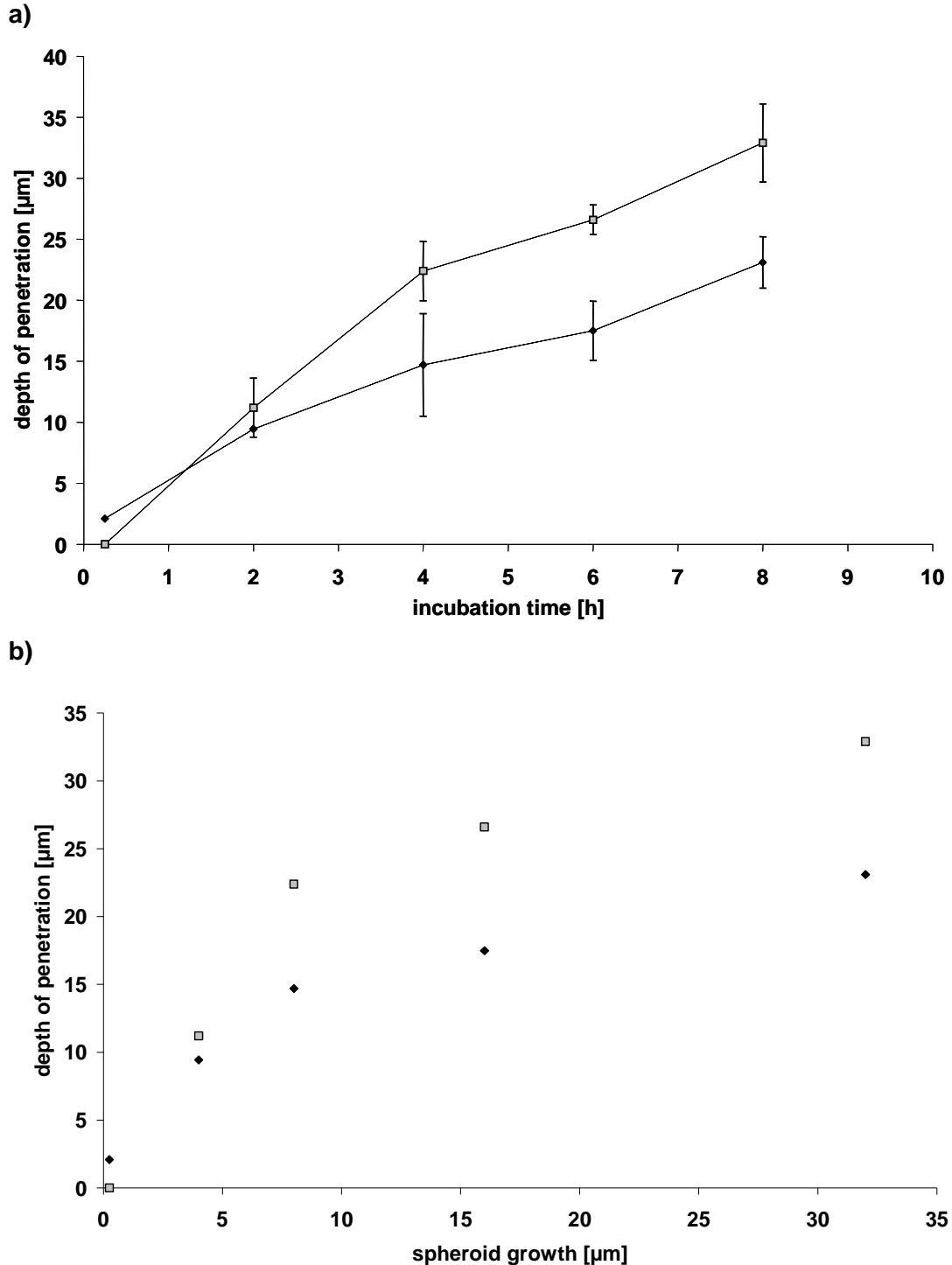


Fig. 6: Penetration of particles in spheroids ( $n=3$ ):  $\blacklozenge$  100 nm  $\blacksquare$  200 nm. **a)** depth of penetration of particles vs. incubation time. **b)** depth of penetration of particles vs. spheroid growth during 8 hours. The penetration of 200 nm particles seems to proceed faster than the uptake of 100 nm particles.

When penetration depth was plotted vs. time it became clearly visible that 200 nm particles proceeded faster into the spheroid. When penetration depth was plotted vs. growth a profile with two phases was detected: for the first 4 hours penetration proceeded faster than growth, then spheroid growth proceeded faster than particle uptake.

### 3.6. Cryo sections

To verify the observations of confocal microscopy and to gather further information on particle penetration inside spheroids, cryo sections of spheroids were prepared after incubating spheroids with nanospheres for different time periods. In preliminary experiments a method for cryo sectioning was established to preserve the cellular structure of the spheroids and the fluorescence of GFP at the same time. Cryo sections were prepared of spheroids that were initiated with nanospheres in cell culture media and of spheroids that were incubated with nanospheres for 15 min and for 8 hours.

Fig. 7 shows cryo sections of spheroids that were incubated with particles of 100 nm size. Pictures in the left column are taken with 20fold magnification and show only the red channel (nanoparticle fluorescence) while pictures in the right column are taken with 63fold magnification and represent an overlay of red channel (nanoparticle fluorescence) and green channel (GFP, cells). The even red color of the sections in the right column is due to artefacts of the preparation technique. Therefore, nanoparticles can only be observed in Fig. 7 a) as brighter areas. In the higher magnification nanoparticles are visible as small yellow dots and are clearly distributed over the first 50  $\mu\text{m}$  from the edge towards the center that are shown in the picture. However, in the sections of spheroids that have been incubated with particles for 15 min or 8 hours not a single particle was detected.

In contrast, when 200 nm particles were used, particles were clearly visible over the whole cross section of spheroids that were initiated with particles in culture media (Fig. 8 a). A higher concentration of particles at the edge of the section is observed. After incubation for 15 min no particles were visible but after 8 hours incubation time a ring of particles is visible around the edge of the spheroid section. However, particles did not penetrate deeper inside a spheroid than 20  $\mu\text{m}$ .



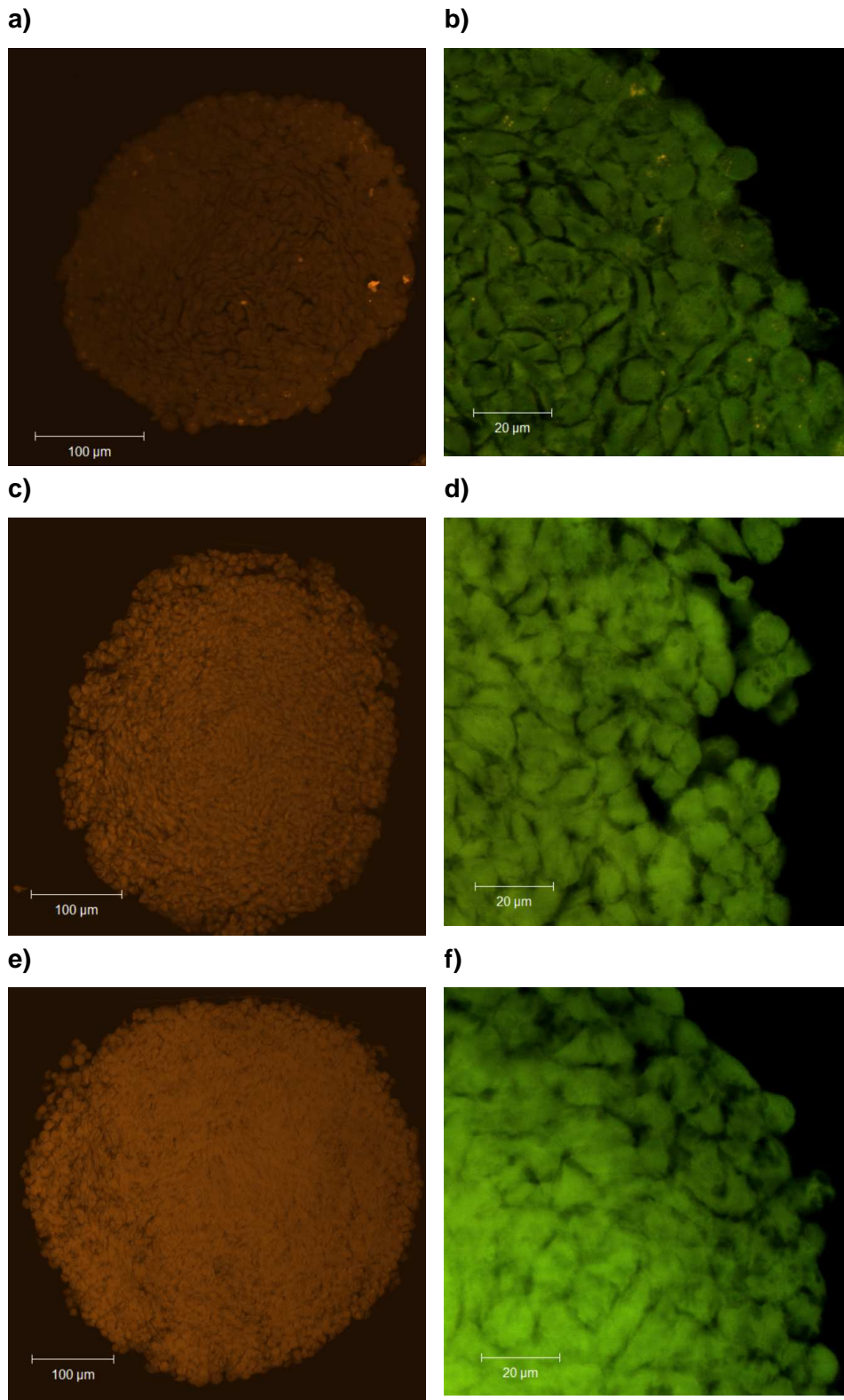


*Fig. 7: Cryosections of spheroids incubated with nanospheres (100 nm). a,b) Particles in cell culture media when spheroids were initiated. c,d) spheroids 15 min in contact with particle solution. e,f) spheroids 8 hours in contact with particle solution. a,c,e) the red channel with the particle fluorescence is shown (20x magnification); b,d,f) overlay of red and green channel are shown (63x magnification).*

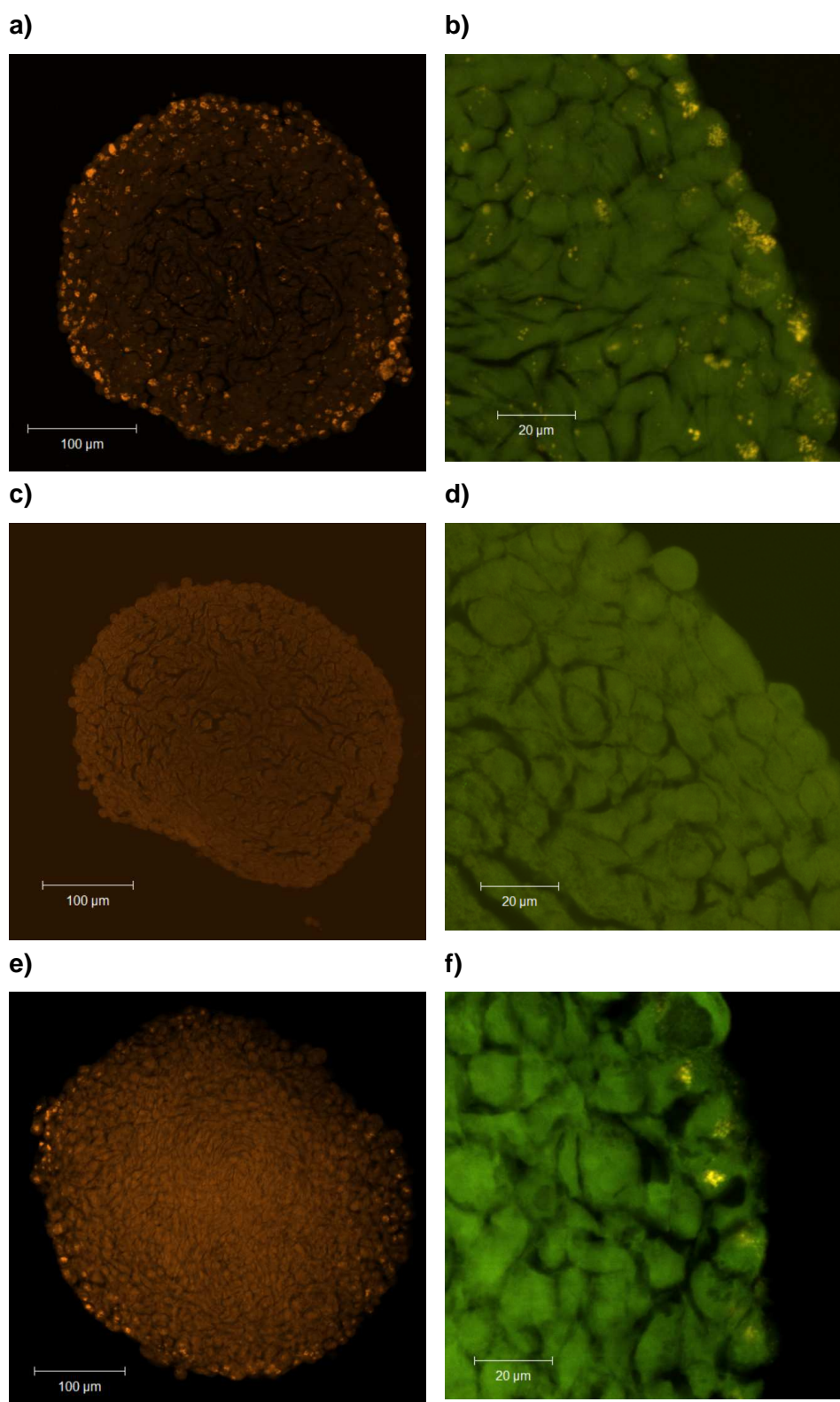


*Fig. 8: Cryosections of spheroids incubated with nanospheres (200 nm). a,b) Particles in cell culture media when spheroids were initiated. c,d) spheroids in contact with particle solution for 15 min. e,f) spheroids in contact with particle solution for 8 hours. a,c,e) the red channel with the particle fluorescence is shown (20x magnification); b,d,f) overlay of red and green channel are shown (63x magnification).*



## 4. Discussion

To elucidate the suitability of multicellular tumor spheroids for in vitro investigation of anti-tumor drug delivery systems we investigated the interactions of fluorescent nanoparticles with monolayers and spheroids of the human adenocarcinoma cell line HCT-116. As we intended to use confocal laser scanning microscopy for the elucidation of particle diffusion processes into spheroids transfected cells expressing green fluorescent protein as a marker were used. As model nanoparticles carboxylate-modified polystyrene nanospheres with a negative surface charge were used intending to minimize particle internalization and adhesion to negatively charged cell membranes. However, under the conditions of the cell culture experiments, particles were coated with serum proteins as clearly shown by laser light scattering and zeta potential increased to approximately -10 mV. Therefore, internalization of the particles or interactions with the cell membranes can not be excluded. The particle uptake by cell monolayers was investigated by fluorescence measurements of cell lysates and by confocal microscopy. Assessing the cell-associated fluorescence after incubation of a cell monolayer with nanospheres the 100 nm particles were internalized to a higher extent than the 200 nm particles. In these experiments, the percent uptake of particles by cells was strongly dependent on the size of particles. Although different ratios of cells to particles were used, the absolute number of particles internalized per cell was constant for each particle size. A time-dependent saturation of cells with particles might be the explanation, which has to be substantiated by further experiments to clarify if there is a maximum of possible uptake of particles of a defined size per cell. In addition to the high rate of cell-associated particles determined by fluorescence measurements, in confocal microscopy a strong increase in particles that were assembled at the cell membrane over 4 hours was detected. However, hardly any particles were observed inside the cells by confocal microscopy.

The investigation of particle diffusion inside three-dimensional cell agglomerates was performed with spheroids initiated with 500 cells and having reached a diameter of 400  $\mu\text{m}$  after 4 days in culture. Spheroids of HCT-116 GFP initiated with 500 cells per well grew 100  $\mu\text{m}$  in diameter per 24 hours and this growth rate was not affected by the addition of nanoparticles to the cell culture media. Over the observation time of nanoparticle diffusion into the spheroid of 8 hours the spheroids grew 33  $\mu\text{m}$  in diameter. This means that we look at a new layer of cells at every point of the observation with confocal microscopy. Due to limitations of the microscope, pictures can only be detected up to a maximum depth of 50  $\mu\text{m}$  while a cross section through the center of the spheroid can not be analyzed. In the upper layers, the 200 nm particles proceeded faster than the 100 nm particles. To gain information about the interior of a spheroid and how far particles would penetrate cryo sections were prepared. Although the chemical fixation method leads to a good preservation of the cells, it

can not be excluded that the preparation method influenced the profile of nanoparticles distribution inside a spheroid. During the incubation steps particles might be washed out or the diffusion into the spheroid might continue. However, only 200 nm particles were internalized in cells on the outer layers of the spheroid while 100 nm particles were not detected in the respective cryo-sections. This is in accordance with the faster proceeding of 200 nm particles into the spheroid that was observed by confocal microscopy. Reasons for this result have to be elucidated by further experiments.

Confocal microscopy would be a suitable method for monitoring diffusion processes at least in the uppermost layers of slowly growing spheroids or tissue objects. However, to elucidate the diffusion process in spheroids of fast growing cell lines there is a strong need for alternative methods, for example the preparation of cryo-sections with optimal preservation of the diffusion profile and the cellular structure at the same time. The search for the optimal method continues to gain information about particle distribution in the extracellular matrix or gaps between the cells of a spheroid. The preparation method applied here provides information about intracellular particles and it can be hypothesized that the 200 nm particles were internalized in cells on the outer layer of a spheroid.

## **5. Conclusions**

Confocal microscopy is a suitable means for rapid monitoring of diffusion processes of nanoparticles inside slowly growing spheroids at least in the outer layers of the cell agglomerates. However, spheroids of the fast growing cell line HCT-116 GFP grew more rapidly than particles were transported into the interior of a spheroid. In the outer layers of the spheroid particles were incorporated into the structure either by internalization or simple embedding in the growing cell structure. When monolayers of HCT-116 were observed, particles were hardly internalized. To elucidate diffusion processes in fast growing spheroids alternative methods such as the time-consuming cryo-sections have to be used. Cryo-sections of spheroids showed that particles were present inside the cells. A preparation method to gain information about particle distribution outside the cells has to be established.

## **6. Acknowledgements**

The German Federal Ministry of Education and Research (BMBF) for financial support (Grant: 31P3183).

## 7. References

- [1] Seiwert, T. Y. and Cohen, E. E. W. (2005): "State-of-the-art management of locally advanced head and neck cancer"; *British Journal of Cancer* (92) p.1341-1348
- [2] Moses, M. A., Brem, H., and Langer, R. (2003): "Advancing the field of drug delivery: Taking aim at cancer"; *Cancer Cell* (4) p.337-341
- [3] Brigger, I., Dubernet, C., and Couvreur, P. (2002): "Nanoparticles in cancer therapy and diagnosis"; *Advanced Drug Delivery Reviews* (54) p.631-651
- [4] Brannon-Peppas, L. and Blanchette, J. O. (2004): "Nanoparticle and targeted systems for cancer therapy"; *Advanced Drug Delivery Reviews* (56) p.1649-1659
- [5] Santini, M. T. and Rainaldi, G. (1999): "Three-dimensional spheroid model in tumor biology"; *Pathobiology* (67) p.148-157
- [6] Kunz-Schughart, L. A., Freyer, J. P., Hofstaedter, F., and Ebner, R. (2004): "The use of 3-D cultures for high-throughput screening: the multicellular spheroid model"; *Journal of Biomolecular Screening* (9) p.273-285
- [7] Mueller-Klieser, W. (1997): "Three-dimensional cell cultures: from molecular mechanisms to clinical applications"; *American Journal of Physiology* (273) p.C1109-C1123
- [8] Lankelma, J. (2002): "Tissue transport of anti-cancer drugs"; *Current Pharmaceutical Design* (8) p.1987-1993
- [9] Foged, C., Brodin, B., Frokjaer, S., and Sundblad, A. (2005): "Particle size and surface charge affect particle uptake by human dendritic cells in an in vitro model"; *International Journal of Pharmaceutics* (298) p.315-322
- [10] Yin Win, K. and Feng, S. S. (2005): "Effects of particle size and surface coating on cellular uptake of polymeric nanoparticles for oral delivery of anticancer drugs"; *Biomaterials* (26) p.2713-2722
- [11] Dong, Y. and Feng, S. S. (2006): "Nanoparticles of poly(D,L-lactide)/methoxy poly(ethylene glycol)-poly(D,L-lactide) blends for controlled release of paclitaxel"; *Journal of Biomedical Materials Research, Part A* (78A) p.12-19
- [12] Steinhauser, I., Spaenkuch, B., Strebhardt, K., and Langer, K. (2006): "Trastuzumab-modified nanoparticles: Optimisation of preparation and uptake in cancer cells"; *Biomaterials* (27) p.4975-4983
- [13] Xu, P., Van Kirk, E. A., Murdoch, W. J., Zhan, Y., Isaak, D. D., Radosz, M., and Shen, Y. (2006): "Anticancer efficacies of cisplatin-releasing pH-responsive nanoparticles"; *Biomacromolecules* (7) p.829-835
- [14] Liang, H. F., Chen, C. T., Chen, S. C., Kulkarni, A. R., Chiu, Y. L., Chen, M. C., and Sung, H. W. (2006): "Paclitaxel-loaded poly(g-glutamic acid)-poly(lactide) nanoparticles as a targeted drug delivery system for the treatment of liver cancer"; *Biomaterials* (27) p.2051-2059
- [15] Kunz-Schughart, L. A., Doetsch, J., Mueller-Klieser, W., and Groebe, K. (2000): "Proliferative activity and tumorigenic conversion: impact on cellular metabolism in 3-D culture"; *American Journal of Physiology* (278) p.C765-C780
- [16] Mueller-Klieser, W. "Tumor biology and experimental therapeutics"; *Critical Reviews in Oncology/Hematology* (36) p.123-139

# **Chapter 8**

## **Summary and Conclusions**

## 1. Summary

With the goal of controlling the events at the bone-implant interface, it was the main objective of this thesis to provide a basis for the conjugation of cell stimulating molecules or targeting motifs to the surface of hydroxyapatite ceramic discs and particles. To this end, several methods for surface functionalization have been investigated for the attachment of biomolecules.

First, a method was established to modify the surfaces of hydroxyapatite ceramic discs by using aminopropyltriethoxysilane (APTES) to create an amino group-containing layer that would allow for further conjugation steps. As the suppression of non-specific cell adhesion, commonly achieved by surface grafting of uncharged and hydrophilic polymers such as poly(ethylene glycol) (PEG), is a prerequisite for inducing specific interactions, a synthesis protocol for PEG acetaldehyde was adopted from the literature, leading to a storable intermediate (PEG acetaldehyde diethylacetal) and compounds of varying molecular weight were synthesized. The mPEG derivatives were covalently attached to the amino groups present at the silanized ceramic surface and surfaces were characterized by water contact angle and XPS measurements. Depending on the molecular weight of the respective polymer, the mPEG-grafted surfaces performed differently with regard to hydrophobicity and adhesion of rat marrow stromal cells (rMSCs). The longer the PEG chain, the more hydrophilic were the surfaces. Cell adhesion was reduced after PEGylation with mPEG acetaldehyde of 5000 Da, but not completely suppressed (**Chapter 2**).

In order to investigate protein immobilization on the surfaces, a procedure was established for the radiolabeling of lysozyme with  $^{125}\text{I}$ iodine. By using the labeled compound, relative quantitative measurements of small amounts of protein on the surface of HA ceramic discs were possible. A washing procedure to distinguish between reversibly bound and strongly adsorbed lysozyme was established. This experimental set up allowed for the investigation and comparison of different strategies for protein immobilization on the surfaces. Despite reports in the literature, labeling of BMP-2 was not successful (**Chapter 3**).

The immobilization of the protein lysozyme by the use of PEG spacers intended to utilize several advantages that are described for PEG modified surfaces, including the suppression of non-specific adsorption and the support of protein stability and biological activity. HA ceramic discs were modified by grafting mPEG acetaldehydes with a molecular weight range from 750 to 5000 Da. The adsorption of lysozyme was not completely suppressed by PEGylation as determined by XPS measurements. When using PEG acetaldehyde (2000 and 4000 Da) as a spacer molecule for the covalent attachment of lysozyme, more protein was deposited by immobilization relative to adsorption to HA ceramics. In general, the immobilized protein retained its enzymatic activity to a higher extent compared to adsorbed protein. However, the amounts of immobilized protein were relatively low and the results

were not significant, probably due to the inhomogeneous structure of the modified surfaces (**Chapter 4**).

As the immobilization via PEG tethers did not result in satisfying amounts of immobilized lysozyme, the attachment to aminosilanized ceramic surfaces using carbodiimide coupling chemistry was investigated. Additionally, the aminobisphosphonates pamidronate and alendronate were used as anchoring molecules as a novel method for the immobilization of proteins to HA ceramic surfaces and compared to the well-known aminosilanization procedure. Lysozyme was successfully immobilized by employing both principles and the enzymatic activity of immobilized protein was significantly increased compared to adsorbed lysozyme. Therefore, the potential of the amine-functionalized HA surfaces to immobilize BMP-2 was investigated. In a cell culture study, the biological activity of immobilized BMP-2 compared to adsorbed BMP-2 was elucidated. Immobilized BMP-2 significantly increased the expression of ALP in C2C12 cells. The novel bisphosphonate-based method was found to be as efficient as the well-established aminosilanization (**Chapter 5**).

To gain deeper insight into the adsorption behavior of the aminobisphosphonate pamidronate on hydroxyapatite surfaces, an adsorption study was performed. Using adsorption techniques, the number of functional groups on the surface could be controlled within a range of 0-2  $\mu\text{mol}/\text{cm}^2$ . As alternative route to functionalized surfaces, particles were precipitated in the presence of pamidronate. By adsorption and by co-precipitation of hydroxyapatite with pamidronate, functionalized particles were obtained that were accessible for the immobilization of a model compound (**Chapter 6**).

In order to elucidate particle transport and diffusion processes in cells and tissues, we investigated the use of confocal microscopy for rapid monitoring of uptake and distribution of nanoparticles in multicellular tumor spheroids. Confocal microscopy provided information about particle transport into the outer layers of a spheroid (30-50  $\mu\text{m}$ ). Fluorescent model nanoparticles were incorporated or embedded into the outer layers of the growing spheroids of the cell line HCT-116. The transport of particles inside a spheroid was monitored over a time period of 8 hours. 200 nm particles proceeded faster than 100 nm particles (**Chapter 7**).

## 2. Conclusions

In conclusion, this thesis contributed to the development of surface modification methods for Ca-rich inorganic materials in order to achieve a selective cell response.

Although PEGylation with PEG acetaldehyde did not suppress cell adhesion or lysozyme adsorption completely, a modulation of the surface properties was achieved. The shielding efficacy of the PEG layer might further be improved by alternative methods that have been suggested in the literature [1-3]. Although lysozyme was immobilized by PEG tethers, particular advantages in terms of the amount or increased stability of the immobilized protein were not determined. By varying grafting conditions, these results may be further optimized and more homogeneously structured surfaces might be obtained.

By employing smaller spacer molecules, such as succinic acid, larger amounts of protein were attached. Carbodiimide coupling chemistry was shown to attach proteins to HA ceramic surfaces with retention of their biological activity. It was clearly demonstrated that the biological performance of immobilized protein was superior to adsorbed protein both for lysozyme and BMP-2 in terms of the enzymatic activity of lysozyme and stimulation of osteoblastic differentiation of C2C12 cells by BMP-2. In addition to the well-established silanization procedure, proteins were immobilized using the bisphosphonates pamidronate and alendronate with equivalent efficacy. This novel method combines three approved and effective principles for enhanced osseointegration of implants: hydroxyapatite coating, surface-immobilized bisphosphonates, and localized delivery of BMP-2. Further investigations should focus on a deeper understanding of the stability of the bisphosphonate binding and a quantification of the functional groups as well as the attached BMP-2.

The bisphosphonate-based surface modification method is also applicable to other calcium phosphates, such as brushite, and allows for a control of functional groups within a certain concentration range. For a control of particle size, morphology, and zeta potential the precipitation procedure of the particles has to be improved. However, hydroxyapatite or calcium phosphate particles have a potential for many applications including composite materials for hard tissue replacement, drug delivery, and gene delivery. Nanophase materials are of particular interest as they resemble the inorganic phase of bone that consists of nanocrystals.

A tool for rapid monitoring of diffusion processes of fluorescent nanoparticles inside a three-dimensional cell culture model is provided by confocal microscopy. The spheroid model is perfectly suited for these investigations due to its well-defined geometry. However, to elucidate diffusion processes in fast growing spheroids, alternative methods, such as the time-consuming cryo-sections, have to be used. To compare diffusion profiles of particles of different characteristics, the use of spheroids of slowly growing cell lines is suggested.



### **3. Outlook**

Delivery strategies for growth factors will play a major role in the field of bone tissue engineering [4] with a focus on biomaterials that additionally act as delivery devices for cell stimulators [5]. Interesting future research approaches for surface modifications include the use of sulfated polysaccharides, such as heparin [6] for attachment of growth factors, such as BMP-2, by their heparin binding site [7]. The use of DNA encoding for growth factors will be of key interest, intending to let cells at the interface produce the adequate growth factors for osteoblastic differentiation [8]. A potential application for hydroxyapatite nanoparticles might be the delivery of DNA [9]. All these improvements represent steps towards the goal of “smart materials” that are capable of reacting upon external stimuli like natural bone [10].

## 4. References

- [1] Kingshott, P., Thissen, H., and Griesser, H. J. (2002): "Effects of cloud point grafting, chain length and density of PEG layers on competitive adsorption of ocular proteins"; *Biomaterials* (23) p.2043-2056
- [2] Lee, J. H., Jeong, B. J., and Lee, H. B. (1997): "Plasma protein adsorption and platelet adhesion onto comb-like PEO gradient surfaces"; *Journal of Biomedical Materials Research* (34) p.105-114
- [3] Bearinger, J. P., Castner, D. G., Golledge, S. L., Rezaei, A., Hubchak, S., and Healy, K. E. (1997): "P(AAm-co-EG) interpenetrating polymer networks grafted to oxide surfaces: Surface characterization, protein adsorption, and cell detachment studies"; *Langmuir* (13) p.5175-5183
- [4] Chen, R. R. and Mooney, D. J. (2003): "Polymeric growth factor delivery strategies for tissue engineering"; *Pharmaceutical Research* (20) p.1103-1112
- [5] Vasita, R. and Katti, D. S. (2006): "Growth factor-delivery systems for tissue engineering: a materials perspective"; *Expert Review of Medical Devices* (3) p.29-47
- [6] Takada, T., Katagiri, T., Ifuku, M., Morimura, N., Kobayashi, M., Hasegawa, K., Ogamo, A., and Kamijo, R. (2003): "Sulfated polysaccharides enhance the biological activities of Bone Morphogenetic Proteins"; *Journal of Biological Chemistry* (278) p.43229-43235
- [7] Nickel, J., Dreyer, M., and Sebald, W. (2002): "Deciphering the binding code of BMP-receptor interaction"; in "Bone Morphogenetic Proteins" (Vukicevic, S. and Sampath, K. T.; Eds.), p.61-85, Birkhaeuser Verlag, Basel, Switzerland
- [8] Ono, I., Yamashita, T., Jin, H. Y., Ito, Y., Hamada, H., Akasaka, Y., Nakasu, M., Ogawa, T., and Jimbow, K. (2004): "Combination of porous hydroxyapatite and cationic liposomes as a vector for BMP-2 gene therapy"; *Biomaterials* (25) p.4709-4718
- [9] Zhu, S. H., Huang, B. Y., Zhou, K. C., Huang, S. P., Liu, F., Li, Y. M., Xue, Z. G., and Long, Z. G. (2004): "Hydroxyapatite nanoparticles as a novel gene carrier"; *Journal of Nanoparticle Research* (6) p.307-311
- [10] Hench, L. L. and Polak, J. M. (2002): "Third-generation biomedical materials"; *Science* (295) p.1014-1017

# Appendices

## Abbreviations

AFM	Atomic force microscopy
APTES	Aminopropyl-triethoxysilane
ATP	Adenosine triphosphate
BET	Brunauer-Emmet-Teller
BMP	Bone morphogenetic protein
BMP-2	Bone morphogenetic protein-2
BP	Bisphosphonate
BSA	Bovine serum albumine
CDCl <sub>3</sub>	Deuterated chloroform
CLSM	Confocal laser scanning microscopy
2D	Two dimensional
3D	Three dimensional
Da	Dalton
DMEM	Dulbecco's modified eagle medium
DMSO	Dimethylene sulfoxid
DMSO-d <sub>6</sub>	Deuterated dimethylene sulfoxid
DNA	Deoxyribonucleic acid
DPEG	Poly(ethylene glycol) acetaldehyde
ECM	Extracellular matrix
EDAC	1-ethyl-3-(3-dimethylaminopropyl)carbodiimide
EDTA	Ethylenediaminetetraacetic acid
EGF	Epidermal growth factor
EPR-effect	Enhanced permeation and retention effect
ESI-MS	Electrospray ionization – mass spectrometry
FGF	Fibroblast growth factor
FBS	Fetal bovine serum
GFP	Green fluorescent protein
GPC	Gel permeation chromatography
HA	Hydroxyapatite
HCl	Hydrochloric acid
HEPES	N-(2-Hydroxyethyl)piperazine-N'-(2-ethanesulfonic acid) hemisodium salt
<sup>1</sup> H-NMR	<sup>1</sup> H nuclear magnetic resonance spectroscopy

HPLC-MS	High performance liquid chromatography combined with a mass spectroscopy detector
IGF	Insulin-like growth factor
I.U.	International Units
$\lambda_{em}$	Emission wavelength of a fluorescent dye
$\lambda_{ex}$	Excitation wavelength of a fluorescent dye
m/z	Mass per charge ratio
Maldi-ToF	Matrix assisted laser desorption/ionization time of flight mass spectroscopy
MCTS	Multicellular tumor spheroid
MDR	Multidrug resistance
mPEG	Poly(ethylene glycol) monomethylether
mPEGAc	Poly(ethylene glycol) monomethylether acetaldehyde
MPS	Mononuclear phagozyte system
$M_w$	Molecular weight
$Na_2SO_4$	Sodium sulfate
N-BP	Aminobisphosponate
NCE	New chemical entities
PBS	Phosphate-buffered saline
PEG	Poly(ethylene glycol)
PI	Polydispersity index
R.F.U	Relative fluorescence units
RGD	Arginine-glycin-aspartic acid
rMSC	Rat marrow stromal cells
SD	Standard deviation
SDS	Sodium dodecylsulfate
SEC	Size exclusion chromatography
SEM	Scanning electron microscopy
s-NHS	Sulfo-N-Hydroxysuccinimide
T-25 flask	25-cm <sup>2</sup> flask
TCP	Tricalcium phopshate
TGF	Transforming growth factor
TGF- $\beta$	Transforming growth factor – $\beta$
TMS	Tetramethylsilane
TNBS	Trinitrobenzenesulfonic acid

Tris buffer	Tris(hydroxymethyl)aminomethane buffer
VEGF	Vascular endothelial growth factor
XPS	X-ray photoelectron spectroscopy
XRD	X-ray diffraction

## Curriculum Vitae

### Persönliche Daten:

Name: Andrea Schüssele  
Beruf: Apothekerin  
Geburtsdatum: 13. April 1976  
Geburtsort: Freiburg i. Br., Deutschland  
Staatsangehörigkeit: deutsch  
Familienstand: ledig

### Schule:

1982-1986 Schwarzenberg-Grundschule in 79183 Waldkirch  
1986-1995 Geschwister-Scholl-Gymnasium in 79183 Waldkirch

### Studium und Berufspraxis:

10/1995 - 04/2000 Pharmaziestudium an der Albert-Ludwigs-Universität, Freiburg i. Br.  
  
03/1998 1. Staatsexamen  
  
04/2000 2. Staatsexamen  
  
05 - 11/2000 Pharmaziepraktikum in der Anker-Apotheke in Lübeck-Travemünde.  
  
11/2000 – 04/2001 Pharmaziepraktikum bei der Bayer AG in Leverkusen;  
Abteilung: galenische Entwicklung.  
  
06/2001 3. Staatsexamen, Approbation als Apothekerin.  
  
07 – 12/2001 Wissenschaftliche Mitarbeiterin am Pharmazeutischen Institut der  
Universität Tromsø, Nordnorwegen;  
  
04/2002 – 06/2006 Promotion am Lehrstuhl für Pharmazeutische Technologie der  
Universität Regensburg bei Prof. Dr. A. Göpferich. Projekte:  
1. „Knochenneubildung“ im Forschungsverbund „ForTePro“, gefördert  
von der Bayerischen Forschungstiftung, 04/2002 - 02/2005.  
2. „Spheroïd-based screen: Aufbau einer technologischen Plattform  
zum Einsatz eines 3D-Zellkultur-Modells im industriellen Antitumor-  
Wirkstoff-Screening“, gefördert vom BMBF, 03/2005 – 12/2005.  
  
ab 09/2006 Grünenthal GmbH, Aachen.

## List of Publications

### Publications

A. Schuessele, B. Volk, H. Mayr, T. Blunk, M. B. Schulz and A. Goepferich

„Surface modification of Hydroxyapatite ceramics to modulate cell adhesion and improve tissue generation“

Proceedings of the 9<sup>th</sup> meeting and seminar on ceramics, cells and tissues  
„Materials for Tissue Engineering: Chemistry and Microstructure- the Role for Ceramics“,  
p. 87-94

Editors: A. Ravaglioli und A. Krajewski, ISTEC-CNR, Faenza, Italy, 2005

**(Chapter 2)**

A.Schuessele, H. Mayr, M. B. Schulz and A. Goepferich

“Adsorption and immobilization of lysozyme on PEGylated hydroxyapatite ceramic surfaces”

To be submitted to Journal of Colloid and Interface Science **(Chapter 4)**

A. Schuessele, H. Mayr, J. Tessmar and A. Goepferich

“A novel method for protein immobilization on hydroxyapatite ceramic surfaces using bisphosphonates”

submitted to Journal of Biomedical Materials Research Part A **(Chapter 5)**

A. Schuessele and A. Bauer-Brandl

„Note on the measurement of flowability according to the European Pharmacopeia“

International Journal of Pharmaceutics 257 (2003) 301-304



## Conference Abstracts

A. Schuessele, H. Mayr, M.B. Schulz, J. Tessmar, T. Blunk and A. Goepferich:

„Immobilized BMP-2 on hydroxyapatite surfaces improves the osteoblastic differentiation of C2C12 cells”

Controlled Release Society, 33th Annual meeting, Wien, Juli 2006

A. Schuessele, H. Mayr, M.B. Schulz, T. Blunk and A. Goepferich:

„Immobilization of a model protein to hydroxyapatite ceramic surfaces by adsorption and covalent coupling“

Dt. Gesellschaft für Biomaterialien, Jahrestagung 2005, Würzburg, Oktober 2005

BIOMaterialien 6 (3) 2005, p. 248

A. Schuessele, B. Volk, H. Mayr, T. Blunk, M.B. Schulz and A. Goepferich:

„Surface modification of Hydroxyapatite ceramics to modulate cell adhesion and improve tissue generation“

Ceramics, cells and tissues, Faenza, Italy, Oktober 2004

A. Schuessele, B. Volk, H. Mayr, F. Skofitsch, M.B. Schulz and A. Goepferich:

„PEGylation of Hydroxyapatite ceramics by reductive amination“

Strategies in Tissue Engineering, Würzburg, Juni 2004,

Cytotherapy 6 (3) 2004, p. 284

A. Schuessele, B. Volk, U. Deisinger, F. Stenzel, A. Goepferich and M.B. Schulz:

„PEGgrafted inorganic surfaces for the control of stem cell adhesion“

Proc. International Meeting on Pharmaceutics, Biopharmaceutics and Pharmaceutical Technology, p. 365-366, Nürnberg, März 2004

A. Schuessele, A. Bauer-Brandl:

„The European Pharmacopoeia test of flowability of powders – a critical remark”

Proc. International Meeting on Pharmaceutics, Biopharmaceutics and Pharmaceutical Technology, p.43-44, Nürnberg, März 2004

## Danksagung

Die vorliegende Arbeit wurde von April 2002 bis Juni 2006 am Lehrstuhl Pharmazeutische Technologie der Universität Regensburg angefertigt. Viele haben zum Gelingen dieser Arbeit beigetragen.

Mein besonderer Dank gilt deshalb:

- Herrn Prof. Dr. Achim Göpferich für die Überlassung der Themen, viele wissenschaftliche Anregungen und die Möglichkeit zur Teilnahme an Konferenzen im In- und Ausland, die eine besondere Bereicherung für die Arbeit waren.
- Dr. Torsten Blunk und Dr. Jörg Teßmar für die Diskussionen und Anregungen im Rahmen der „PEG-und BMBF-Meetings“.
- Prof. Dr. M.B. Schulz, Karl-Franzens-Universität, Graz, für eineinhalb Jahre Betreuung.
- Der Bayerischen Forschungsförderung und dem Bundesministerium für Bildung und Forschung für finanzielle Unterstützung der Projekte „Knochenneubildung“ (ForTePro) und „spheroid-based screen – Aufbau einer technologischen Plattform zum Einsatz eines 3D-Zellkulturmodells im industriellen Antitumor-Wirkstoff-Screening-Prozess“.
- Den Mitgliedern des AK Prof. Korber, anorganische Chemie, v.a. Dr. Thomas Roßmeier und Christof Suchentrunk, für die Einarbeitung beim Arbeiten unter Schutzgas.
- Dr. Johann Vancea, Lehrstuhl für Oberflächenphysik, für die Durchführung der ESCA-Messungen.
- Dr. Rainer Müller, Lehrstuhl für Physikalische Chemie, für wichtige Anregungen zur Oberflächenmodifizierung und die Durchführung der BET-Messungen.
- Dem Team des Friedrich-Baur-Forschungsinstituts für Biomaterialien, Bayreuth, für die gute Zusammenarbeit auf dem ForTePro-Projekt; Dipl.-Ing. Ulrike Deisinger für die Möglichkeit zur Nutzung von Messgeräten in Bayreuth und Dipl. Min. Helmar Mayr für die Bereitstellung der Hydroxylapatit-Keramiken.
- Dr. Benjamin Stölcker, Institut für Pathologie, für Hilfe am Fluoreszenzmikroskop.
- Dr. Breda Vogel für die gute Zusammenarbeit bei der Testung der PEGylierten Keramik.
- Dr. T. Burgemeister, Zentrale Analytik, für Hilfestellung bei  $^1\text{H}$ -NMR-Spektroskopie.
- Dr. Josef Kiermeier, Zentrale Analytik, für die HPLC-MS-Analytik von jodiertem Lysozym.
- Dr. Robert Schupfner, Dr. Gerald Haas, Erika Treml, Markus Eder, Zentrales Radio-Nuklidlaboratorium, für die Hilfe beim Etablieren der radioaktiven Analytik von Lysozym.
- PD Dr. Klaus Höcherl, Lehrstuhl für Pharmakologie, für das unkomplizierte Schaffen einer Ausweichmöglichkeit für radioaktives Arbeiten während der Asbestsanierungen.
- PD Dr. Leoni Kunz-Schughart und Dr. Wolfgang Eder, Institut für Pathologie, für die freundliche Aufnahme in die Arbeitsgruppe und viele Anregungen zum Sphäroidprojekt. Frank van Rey für die geduldige Einführung in die Sphäroidzellkultur.

- Hendrik Preuß, Lehrstuhl für Pharmazeutische Chemie, für die Unterstützung beim „Pamidronat-Modelling“.
- Dr. Thomas Bernert und Dr. Martina Andratschke, AK Prof. Pfitzner, Inst. für anorganische Chemie, für die Durchführung der XRD-Messungen.
- David Matipa und Veronika Rödl für tatkräftige Unterstützung im Labor im Rahmen ihrer Ausbildung zum/zur CTA.
- Albert Weingart und Stefan Kolb für diverse Spezialanfertigungen und Reparaturen.
- Lydia Frommer und Liane Öttl für ihre Hilfe bei Verwaltungsangelegenheiten.
- Angelika Berié für die Durchführung von Maldi-Tof-Untersuchungen und das Anfertigen von elektronenmikroskopischen Aufnahmen.
- Edith Schindler, Angelika Berié, Renate Liebl und Andrea Blaimer für die Erledigung vieler Routine-Aufgaben, ohne die ein reibungsloser Ablauf der Arbeit im Labor kaum möglich wäre.
- Allison Dennis, Georgia Institute for Technology, Atlanta, USA, für die sorgfältige Korrektur der englischen Manuskripte, die sich nicht nur auf sprachliche Anmerkungen beschränkte, sondern wertvolle inhaltliche Vorschläge einschloss.
- Den Mitdoktoranden am Lehrstuhl danke ich für die gute Zusammenarbeit, viele Diskussionen und ihre Hilfsbereitschaft bei allerlei Schwierigkeiten im Labor. Namentlich erwähnt seien: Dr. Sigrid Drotleff für die Durchführung von GPC-Messungen, Stephanie Könnings für Starthilfe bei der Lysozym-Analytik, Barbara Weiser für viele Tipps aus ihrem reichen Zellkultur-Erfahrungsschatz, Barbara Weiser und Dr. Daniela Eyrich für's gelegentliche „Zellen sitzen“, Dr. Uta Lungwitz für die unermüdliche Erweiterung der Laborgeräteausstattung und Christian Becker für seinen schwarzen Humor. Allen „bitsandbytes“ ein großes Dankeschön für oft zeitaufwändige Hilfe bei Computer- und Netzwerkproblemen. Besonders danke ich den Kollegen für die faire Aufteilung von Gemeinschaftsaufgaben, gerade im Praktikum, die von den allermeisten mitgetragen wurde. Nicht zuletzt danke ich allen, die dafür gesorgt haben, dass Uni und Forschungsergebnisse ab und zu in der Priorität zurückgestuft wurden.
- Ganz besonders möchte ich mich bei Uta und Christof bedanken, ohne deren Motivation, Diskussionsbereitschaft und Unterstützung in allen Lebenslagen diese Arbeit vielleicht nicht entstanden wäre.

